Author:
Linton, C. M

Title:
Wave reflection by submerged bodies in water of finite depth

Wave Reflection by Submerged Bodies in Water of Finite Depth

by

Christopher M. Linton

A dissertation submitted for the degree of Doctor of Philosophy in the School of Mathematics, University of Bristol.

September 1988

ACKNOWLEDGEMENTS

I would like to thank Professor D.V. Evans for his constant help, guidance and encouragement during the three years in which I have been preparing the subject matter for this thesis. I would also like to thank Dr. J.P. Davis for his assistance in the experimental work.

The financial support of the Science and Engineering Research Council (MTD) through grant no. GR/E/0697.8 is gratefully acknowledged.

I would also like to thank Mr. P. Shiarly for his help in the preparation of the text.

MEMORANDUM

The work in this dissertation was carried out in the Department of Mathematics, University of Bristol with the exception of some wave tank experiments which were carried out in the Civil Engineering Department, University of Bristol and has not been submitted for any other degree or diploma of any examining body. All the work in this dissertation is the original work of the author except where otherwise acknowledged in the text.

C. M. Linton

C.M. Linton

Abstract

The main theme of this thesis is that of wave reflection. All the problems that will be examined will be based on linear inviscid water wave theory and for the most part the problems will be two-dimensional. In chapters 2,3 and 4 the effects that various obstacles have on an incident wave will be discussed. A distinction is made between passive devices, devices that are fixed, and active ones, devices that are allowed to move subject to a restoring force in response to the incident wave.

In chapter 2 the shallow water approximation is used to examine the qualitative reflection properties of submerged blocks. A comparison of results with those of other authors who have looked at similar problems shows that fixed submerged obstacles are not particularly good at reflecting waves.

If a body is allowed to move in response to an incident wave then perfect reflection can be achieved and this problem is looked at in detail in chapters 3 and 4. Chapter 3 contains the general theory for this situation together with some applications of its use whilst in chapter 4 one particular shape of body is singled out for detailed study: a horizontal circular cylinder. Results, both theoretical and experimental, show that such devices can be very efficient wave reflectors.

The final two chapters are not concerned with wave reflection but are further examples of applications of the techniques used in solving the problems in previous chapters. Both chapters are concerned with spherical geometries.

In chapter 5 the problem of a submerged sphere making forced periodic oscillations in water of finite depth is considered using techniques introduced in chapter 4. In chapter 6 a related technique is used to examine the problem of water in motion inside a hemisphere.

CONTENTS

CHAPTER 1

Introduction

1.1 Historical Review

This thesis is concerned with problems arising from the interaction of surface gravity waves and rigid bodies. Surface gravity waves are extremely familiar to most people as they are the type of waves that one observes on the surface of seas and lakes. They are mainly generated by the action of the wind on the water surface and as their name suggests the main restoring force involved is gravity. Surface gravity waves have been the subject of extensive research over the last one and a half centuries and many excellent texts exist including Lamb (1932), Stoker (1957) and Whitham (1974).

The mathematical study of wave-body interactions also has a long history, beginning over a century ago with the pioneering work of W. Froude and A.N. Krylov. It is only in the last few decades however that interest in the subject has become widespread. One reason for the increased interest in this area has been the need of offshore engineers and ship designers to be able to predict accurately the forces that will be exerted on structures placed in the sea by the waves.

One method for calculating forces on structures due to waves is the semi-empirical formula known as Morison's equation (Morison et al. 1950). The major drawback of this method is that it takes no account of the fact that when a body is placed in a wave field it diffracts the field. This effect becomes more noticeable the larger the body is and

many structures, like ships or oil rigs, are big enough to make Morison's equation invalid.

Not surprisingly the solution of the general problem of waves incident on a body which is moving in response to the waves is extremely difficult even if the geometry of the body is very simple. In order to simplify the problem one assumes that the fluid is inviscid and incompressible (these are very good approximations in the case of water waves) and that the flow is irrotational so that potential theory can be used. Furthermore it is usual to assume that the amplitude of the waves is much smaller than the wavelength and then to linearise the equations of motion and the boundary conditions of the problem. With these assumptions progress can be made. A fundamental simplification arises from the fact that due to the linearity of the resulting problem we can decompose the general problem of waves incident on a moving body into two much simpler problems; the radiation of waves by a body oscillating in a forced manner in otherwise still water and the diffraction (or scattering) of waves by a fixed obstacle. As will be shown in §1.2 these problems are not independent but are linked in many ways.

A rigid body in three dimensions has six degrees of freedom and thus six possible modes of motion. The three translational modes are referred to as sway, surge and heave while the three rotational modes are referred to as pitch, roll and yaw. This is illustrated in figure (1.1.1).

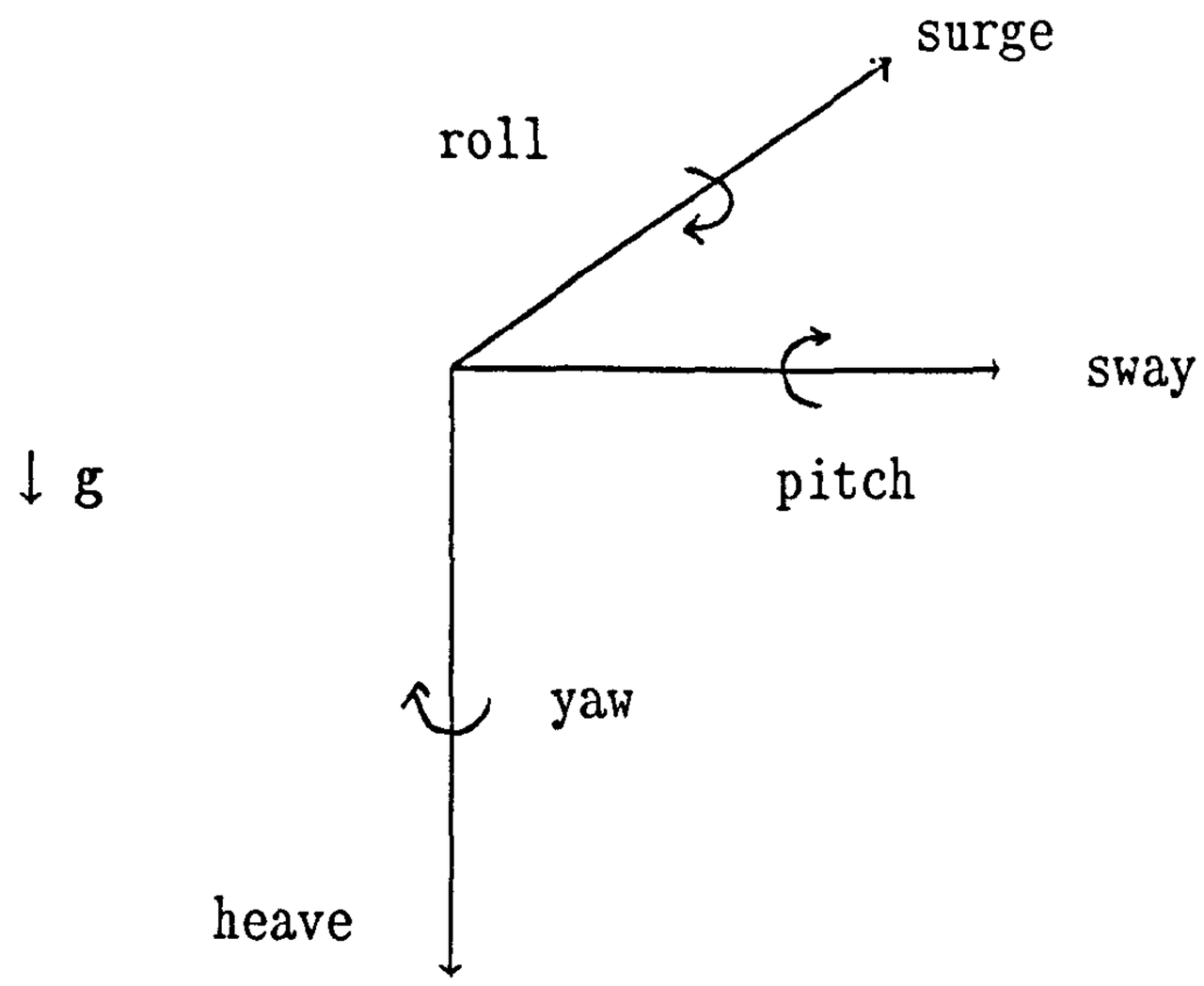

Figure 1.1.1

Thus the solution of a problem in which a wave is incident on a body which is completely free to move requires the solution of seven separate problems; six radiation problems corresponding to the six different modes of motion and a scattering problem.

In two dimensions there are only three possible modes of motion; sway, heave and roll which provides some simplification. Another simplification arises from the fact that in two dimensions outgoing waves have constant amplitude as they travel away from a wave source whereas in three dimensions the amplitude decays like $r^{-1/2}$, where r is the horizontal distance from the wave source. This allows us to define reflection and transmission coefficients for the problem of waves incident on a body in two dimensions. They are the ratios of the amplitude of the reflected wave to that of the incident wave and the amplitude of the transmitted wave to that of the incident wave respectively. The general scattering problem in two dimensions was first looked at by Kreisel (1949).

In order to make any progress analytically, simple geometries must be considered and in this thesis we will only be concerned with two

dimensional problems or problems with a spherical geometry. Another approach is to consider more complicated structures and to develop a numerical technique for the solution of wave body interaction problems. This is an area of extensive research at present but will not concern us here. A review of numerical methods in use in this area can be found in Mei (1978).

In 1929 Havelock solved the so called 'wavemaker' problem and provided formulas from which the velocity potential could be calculated if the horizontal fluid velocity was known on a vertical line (in two dimensions) or a vertical circular cylinder (in three dimensions). This provided the starting point for work carried out in the latter half of the 1940's by Dean (1945) and Ursell (1947) on the interaction of waves and vertical plates. Since then many problems involving waves and plates have been studied. One case that has not been considered previously is the two-dimensional problem of a vertical plate, hinged at the sea bed, not extending to the free surface and performing rolling oscillations about its hinge. This problem is solved in chapter 3 using the method of matched eigenfunction expansions.

The next geometry to receive attention was that of a horizontal circular cylinder in two dimensions. Much use will be made of this geometry in this thesis and so a detailed account of the history of problems involving waves and horizontal circular cylinders will be given here.

The most remarkable result concerning horizontal circular cylinders in two dimensions was discovered by Dean (1948) who used a conformal mapping technique to solve the problem of wave scattering by a submerged cylinder with the approximation that the water was infinitely deep. He showed that such a body reflects no waves! The effect of finite depth on this result will be discussed in chapter 4. Ursell (1950) studied the same problem in a more rigorous fashion and supplied a uniqueness

proof for the solution. The method used by Ursell was that of multipole expansions which will be used throughout chapters 4 and 5 of this thesis. Multipoles are singular solutions of Laplace's equation which satisfy the free surface and bottom boundary conditions and behave like outgoing waves far from the singular point. Ursell generated these multipoles by repeated differentiation of a wave source with respect to the source point. Thorne (1953) provided an alternative technique for generating multipoles using complex integration.

Prior to this work Ursell (1949) solved the problem of the radiation of waves by a half-immersed cylinder oscillating in heave (i.e. vertically) in infinitely deep water. The method of solution here was similar to the multipole method discussed above but instead of using multipoles, which behave like outgoing waves far from the source point, he used a combination of a single wave source and a set of wave free potentials, which as their name suggests make no contribution far from the source point. Work, both analytic and experimental, on the scattering of waves by a half immersed cylinder was performed by Dean and Ursell (1959). Yu and Ursell (1961) extended the work of Ursell (1949) to solve the problem of radiation of waves by a half-immersed cylinder in finite depth.

Ogilvie (1963) extended the work of Ursell (1950) to calculate the first order and mean second order forces on a submerged cylinder. This paper also provided the impetus for Evans et al. (1979) who investigated the possibility of using a submerged cylinder as a wave energy device.

Levine (1965) investigated whether or not the phenomenon of zero reflection, discovered by Dean (1948), was still true if the wave was obliquely incident on the cylinder and he found, using an integral equation technique, that it was not. The same method was used by Schnute (1971) to examine the scattering of waves by two fixed parallel

cylinders (with different radii and immersion depths), again in infinitely deep water.

Some of the complications that arise when considering two cylinder problems can be simplified by assuming that the cylinders are identical in both radius and immersion depth, a case which is clearly relevant to catamaran-type hulls. Wang and Wahab (1971) used multipole expansions to examine the heaving of two half-immersed cylinders and, more recently, Wang (1981) solved the problem of the radiation of waves by two identical submerged cylinders oscillating in both sway and heave. The more general problem of the radiation of waves by a group of any number of cylinders, with different radii and immersion depths, was solved by McIver (1985) using the multipole method.

In all the work on cylinders discussed so far, except that of Yu and Ursell, the water depth has been assumed to be infinite. The extension to the finite depth case of the work of Ursell (1950) and Wang (1981) is presented in chapter 4. Some results for the scattering of waves by a single submerged cylinder in finite depth are given in Naftzger and Chakrabarti (1979) who used a numerical technique based on the boundary element method developed by John (1950). In their paper they also showed results for the scattering of waves by a half immersed cylinder in finite depth and by a semicircular hump on the bottom.

Another geometry for which progress can be made is a spherical one. Havelock (1955) solved the problem of the radiation of waves by a half-immersed sphere in infinite depth making small vertical oscillations. The method of solution is similar to that used by Ursell (1949) for the half-immersed cylinder. Hulme (1982) gave a much improved solution based on the same method and also extended the results to include the case of sway. In an appendix to a paper on wave-power absorption by a submerged sphere Srokosz (1979) solves the problem of the radiation of waves by a submerged sphere in infinite depth in both

the heave and sway cases using the multipole expansion method. The extension of this work to finite depth is presented in chapter 5. Hulme (1985) has also solved the problem of wave radiation by a submerged torus making heaving oscillations.

The scattering of waves by two-dimensional rectangular obstacles, both on the bottom or immersed through the free surface, has been looked at by Newman (1965), who assumed that the obstacle was long compared to wavelength, Mei et al. (1969), who used a variational technique, and McIver (1985) who used the method of matched eigenfunction expansions to solve the full linear problem. Black et al. (1971) used the same techniques as Mei et al. (1969) to solve the problem of wave radiation by such obstacles. They also considered the three-dimensional problem of the radiation of waves by oscillating vertical cylinders. The method of McIver (1985) is used in chapter 3 to solve the full linear problem of wave radiation by a block on the bottom in heave and in sway. The heaving of a vertical cylinder was solved using the same method in McIver and Evans (1984), following ideas in Thomas (1981) who considered a vertical cylindrical duct as a wave-power absorber.

In general the problems discussed in chapters 2,3 and 4 are not looked at from the point of view of being able to predict wave forces acting on fixed bodies, but rather from the point of view of examining the wave reflection properties of the bodies in question. Thus we will be primarily interested in the reflection and transmission coefficients. However one of the simplest ways to calculate these coefficients is to solve two radiation problems, one for heave and one for sway, and then use the Newman relations, Newman (1975), which connect the radiation and scattering problems. These relations are discussed in §1.2 below. Thus much of the work will involve the solution of radiation problems and the calculation of wave forces on bodies due to their own motion. The wave force on a body due to its own motion is conventionally decomposed into

two components, one in phase with the velocity of the body called the damping coefficient and one in phase with the acceleration called the added mass coefficient (or added inertia in the case of rotational motion). These quantities will also be necessary in calculating the reflection and transmission properties of a tethered buoyant cylinder in §4.6.

There has been a continued interest in wave reflection for many years due to the need to protect coastal or offshore installations or to limit wave motions in harbours by the design of suitable breakwaters. Many different types of wave reflector have been considered. Most obvious is a solid wall extending from the sea bed through the free surface which clearly reflects all the incoming waves. Such a construction is often not feasible due to cost or water depth and it is often undesirable since it does not allow the passage of vessels over it and may cause unwanted environmental effects such as the build up of sediment in a harbour. The effect of other fixed obstacles, such as trenches or blocks on the bottom or naturally ocurring sandbars, have been considered by other authors, for example Kirby and Dalrymple (1983), Mei et al. (1969), Mei et al. (1988) and Davies (1982). These fixed obstacles, while not suffering from the drawbacks of the wall breakwater mentioned above, turn out to be not very good at reflecting waves, though at certain resonant frequencies a group of sandbars can produce strong reflection.

In this thesis we look at the possibility of using devices which are allowed to move in response to the waves, while subject to a restoring force, as wave reflectors. This is the subject of chapter 3 and a further application is given in §4.6. The idea for this work came from Guevel et al. (1985) who were in fact looking at the reflection of waves from a fixed submerged horizontal plate. However in order to solve this problem they formulated it as if the water under the plate was simply

oscillating back and forth and this led them to consider the problem of wave reflection by moving bodies. The general theory for this problem is given in §3.2 and it is subsequently applied to three different obstacles; a vertical plate hinged at the sea bed and not extending to the free surface, a rectangular block on the bottom and a submerged circular cylinder. Leach et al. (1985) solved the problem of wave reflection by a vertical plate hinged at the bottom subject to a restoring force but in their case the plate extended through the free surface.

All the problems considered so far concern bodies placed in water and their interaction with waves. Many of the techniques that can be used to solve such problems can also be used to examine the problem of the wave motion of fluids inside containers. The problem here is to work out the natural frequencies of oscillation of fluid in a partially filled container. This is another area that has received extensive study over the years. Most of the early results on the subject can be found in Lamb (1932). Interest in the problem grew after the second world war as the problem of transportation of fluids became more important. During the 1960's NASA did a lot of research into the problem to aid the design of rocket fuel containers. A comprehensive review of the subject is provided by Moiseev (1964), Moiseev and Petrov (1965) and Fox and Kuttler (1983). Most of the container geometries that have been studied analytically in the past have been two-dimensional where complex analysis can be used, see for example Craggs and Duck (1978).

In chapter 6 methods which are the internal equivalent of those used by Hulme (1982) for the heaving half-immersed sphere are used to solve the problem of the sloshing of fluid inside a sphere in the case when the sphere is half full. The sloshing of fluid inside a sphere has been considered previously by Budiansky (1960) who used an integral equation

method and more recently by McIver (1988) who uses a sophisticated integral equation technique and gives results for various fill depths. The method of solution used in chapter 6 is much simpler but is only applicable to a half full sphere.

The lowest modes (i.e. modes with the lowest frequency) of oscillation of a fluid in a tank are the most easily observed and are the most significant in terms of effect. The higher modes can often be obtained with sufficient accuracy by using short wave asymptotics. Methods developed by Alker (1974) and Davis (1974) for the two-dimensional case of the semicircular canal have been used by Davis (1975) to provide asymptotic values for the natural modes of oscillation of a half-full sphere.

1.2 Hydrodynamic Relations for Wave Body Interactions

Cartesian coordinates x,y,z are chosen with x,z horizontal and y vertically downwards, with the undisturbed free surface corresponding to $y = 0$. Fluid occupies the region $0 < y < h$. The fluid is assumed to be inviscid and incompressible. Under the assumptions of linearised, irrotational water wave theory there exists a velocity potential $\Phi(x,t)$ satisfying

$$\nabla^2\Phi = 0 \qquad \text{in the fluid} \qquad (1.2.1)$$

$$\frac{\partial\Phi}{\partial y} = 0 \qquad \text{on} \quad y=h \qquad (1.2.2)$$

$$\frac{\partial H}{\partial t} = \frac{\partial\Phi}{\partial y} \qquad \text{on} \quad y=0 \qquad (1.2.3)$$

where $H(x,t)$ is the free surface elevation measured downwards from

$y = 0$, and

$$\rho \frac{\partial \Phi}{\partial t} - \rho g H = -p_a \qquad \text{on } y=0 \tag{1.2.4}$$

where p_a is the pressure just above the free surface. The terms on the left hand side of equation (1.2.4) represent the dynamic and hydrostatic pressure respectively.

If the motion is assumed to be simple harmonic in time with angular frequency ω then this boundary-value problem can be simplified by introducing time-independent quantities ϕ and η defined by

$$\begin{aligned} \Phi(x,t) &= \mathrm{Re}[\phi(x)e^{i\omega t}] \\ H(x,t) &= \mathrm{Re}[\eta(x)e^{i\omega t}]. \end{aligned} \tag{1.2.5}$$

It is further assumed that p_a is a constant and thus, by incorporating this term into Φ, it can be replaced by zero. Then

$$\nabla^2 \phi = 0 \qquad \text{in the fluid} \tag{1.2.6}$$

$$\frac{\partial \phi}{\partial y} = 0 \qquad \text{on } y=h \tag{1.2.7}$$

$$\frac{\partial \phi}{\partial y} + K\phi = 0 \qquad \text{on } y=0 \tag{1.2.8}$$

where $K = \omega^2/g$. The dynamic pressure is given by equation (1.2.4):

$$p(x) = -i\rho\omega\phi(x). \tag{1.2.9}$$

A simple two-dimensional solution of these equations describing a progressive wave travelling in the ±x direction is

$$\eta = A\ e^{\mp i\kappa x} \qquad (1.2.10)$$

where κ is the real positive solution of

$$K = \kappa \tanh \kappa h. \qquad (1.2.11)$$

This corresponds to a velocity potential

$$\phi(x,y) = ig\frac{A}{\omega}\ \frac{\cosh\ \kappa(y\ -\ h)}{\cosh\ \kappa h}\ . \qquad (1.2.12)$$

The general problem to be considered is that of a wave incident upon a body. The body will diffract the incident wave to produce a scattered wave field and it will also be set in motion by the wave, resulting in a radiated wave field. These will be represented by the time-independent potentials ϕ_S and ϕ_R respectively.

The equation of motion of the body will be assumed to be linear and boundary conditions on the body will be applied on the fixed equilibrium position of the body, S_B. For the case of the scattered potential this condition is simply

$$\frac{\partial\phi_S}{\partial n} = 0 \qquad \text{on} \quad S_B. \qquad (1.2.13)$$

The most general motion of a rigid body in three dimensions involves six degrees of freedom. In order to simplify the following discussion we will write $x_1 = x$, $x_2 = y$, $x_3 = z$. Sway, heave and surge correspond to motions along the x,y,z axes respectively, whilst pitch, yaw and roll correspond to rotations about these axes.

The normal velocity of a point on the surface of the body is

$$V_n = Re\{[(U_1,U_2,U_3) + (\Omega_1,\Omega_2,\Omega_3)\times r].n\ e^{i\omega t}\} \qquad (1.2.14)$$

where U_1,U_2,U_3 are the components of the sway, heave and surge and $\Omega_1,\Omega_2,\Omega_3$ are the components of pitch, yaw and roll. The vector r is the position vector of the point on the surface with the origin at the centre of rotation and n is the unit normal. If we write

$$U_i = \Omega_i \qquad i=4,5,6$$

$$n_i = \cos(n,x_i) \qquad i=1,2,3 \quad \text{(direction cosines)}$$

$$n_i = (r \times n)_i \qquad i=4,5,6$$

the body boundary condition becomes

$$\frac{\partial \phi_R}{\partial n} = \sum_{i=1}^{6} U_i n_i \qquad \text{on } S_B. \qquad (1.2.15)$$

If ϕ_R is decomposed into six potentials, one for each mode of motion, by

$$\phi_R = \sum_{i=1}^{6} U_i \phi_i \qquad (1.2.16)$$

then equation (1.2.15) becomes

$$\frac{\partial \phi_i}{\partial n} = n_i \qquad \text{on } S_B. \qquad (1.2.17)$$

The force on a body in waves is made up of two components. The first is the hydrostatic force which is extremely important in the case of floating bodies. Since we will only be considering submerged bodies

in this thesis where the hydrostatic forces are irrelevant these forces will not be discussed here. The reader is referred to Newman (1977) for a description of hydrostatic forces and their role in wave-body interactions. The second component of the force is that due to the wave motion, the so-called hydrodynamic force. The generalised hydrodynamic force on the body in the ith direction is, with n pointing into the body,

$$F_i(t) = \mathrm{Re}[X^{(1)} e^{i\omega t}] \tag{1.2.18}$$

where

$$X^{(1)} = -i\rho\omega \int_{S_B} \phi \, n_i \, dS \, . \tag{1.2.19}$$

(For $i = 4,5,6$ this is clearly a moment.) Decomposing $X^{(1)}$ in the obvious way gives

$$X_S^{(1)} = -i\rho\omega \int_{S_B} \phi_S \, n_i \, dS \tag{1.2.20}$$

$$X_R^{(1)} = \sum_{j=1}^{6} U_j T_{ji} \tag{1.2.21}$$

where

$$T_{ji} = -i\rho\omega \int_{S_B} \phi_j \, n_i \, dS. \tag{1.2.22}$$

The complex matrix $\underline{T}$ can be divided into two real matrices, one in phase with the acceleration of the body which is called the added mass matrix $\underline{M}$ and one in phase with the velocity which is called the radiation damping matrix $\underline{B}$:

$$\underline{T} = -(\underline{B} + i\omega\underline{M}) . \tag{1.2.23}$$

These matrices are frequency dependent but independent of the velocity of the body. In many cases it is convenient to non-dimensionalise $\underline{B}$ and $\underline{M}$ to give the matrices $\underline{\mu}$ and $\underline{\nu}$ respectively. If m is a typical mass then

$$\underline{B} + i\omega\underline{M} = im\omega(\underline{\mu} - i\underline{\nu}). \qquad (1.2.24)$$

Green's theorem can be used to derive various relations between the hydrodynamic quantities discussed above. If ϕ and ψ are harmonic in the volume V surrounded by the surface S then

$$\int_S \left[\phi \frac{\partial\psi}{\partial n} - \psi \frac{\partial\phi}{\partial n}\right] dS = 0. \qquad (1.2.25)$$

For our purpose S is taken to be the free surface, S_F, the body surface, S_B, the sea bed, y = h, and a large vertical cylinder, S_∞, far enough from the body for the far field asymptotic behaviour of the potentials to be applied. In two-dimensional problems S_∞ is replaced by two vertical lines.

Because of the boundary conditions on S_F and y = h equation (1.2.25), when applied to any of the potentials discussed above, reduces to

$$\int_{S_B} \left[\phi \frac{\partial\psi}{\partial n} - \psi \frac{\partial\phi}{\partial n}\right] dS = -\int_{S_\infty} \left[\phi \frac{\partial\psi}{\partial n} - \psi \frac{\partial\phi}{\partial n}\right] dS. \qquad (1.2.26)$$

In three dimensions any radiation potential, that is, one which represents an outgoing wave far away from the body, satisfies the Sommerfeld radiation condition

$$r^{\nu 2} \left[\frac{\partial\phi}{\partial r} + i\kappa\phi\right] \longrightarrow 0 \quad \text{as} \quad r \longrightarrow \infty \qquad (1.2.27)$$

where $r = (x^2 + z^2)^{1/2}$. The equivalent condition in two dimensions is

$$\frac{\partial \phi}{\partial |x|} + i\kappa\phi \longrightarrow 0 \quad \text{as} \quad |x| \longrightarrow \infty. \tag{1.2.28}$$

(See Mei (1983) §7.4.1). In this case the integral over S_∞ can then be simplified by replacing $\frac{\partial \phi}{\partial n}$ by $i\kappa\phi$. By choosing both ϕ and ψ to be radiation potentials this integral vanishes and we are left with

$$\int_{S_B} \phi_i \, n_j \, dS = \int_{S_B} \phi_j \, n_i \, dS.$$

It follows that the matrices $\underline{B}$ and $\underline{M}$ are symmetric. If we choose ϕ to be a radiation potential and take $\psi = \bar{\phi}$, its complex conjugate, we can derive the relation

$$B_{ij} = \rho\omega\kappa \int_{S_\infty} \phi_i \bar{\phi}_j \, dS. \tag{1.2.29}$$

In two dimensions a radiation potential, ϕ, can be assumed to satisfy

$$\phi \sim A^{\pm} \, e^{\mp i\kappa x} \frac{\cosh \kappa(y - h)}{\cosh \kappa h} \quad \text{as} \quad x \longrightarrow \pm\infty \tag{1.2.30}$$

for some $A^{\pm}$. Equation (1.2.29) can then be written

$$B_{ij} = \frac{\rho\omega^2 c_g}{g} (A_i^- \bar{A}_j^- + A_i^+ \bar{A}_j^+). \tag{1.2.31}$$

Here c_g is the group velocity given by

$$c_g = \frac{\omega}{2\kappa} \left[1 + \frac{2\kappa h}{\sinh 2\kappa h}\right].$$

As a special case

$$B_{11} = \frac{\rho\omega^2 c_g}{g} (|A^-|^2 + |A^+|^2). \tag{1.2.32}$$

A physical interpretation of the damping coefficient is thus straightforward; it is a measure of the wavemaking ability of the body. More specifically, for a single mode of motion, the damping coefficient is proportional to the energy in the waves radiated away from the body and is never negative.

The added mass coefficient has no such simple physical interpretation. For deeply submerged bodies it can be interpreted as the fluid mass accelerated by the body and is positive, but for bodies close to the free surface the effect of the free surface can be such that the added mass is negative over a range of frequencies as in McIver and Evans (1984).

For the remainder of this section we will confine our attention to the two-dimensional case. If $\phi^{(1)}$ and $\phi^{(2)}$ are both scattering potentials we have

$$\int_{S_\infty} \left[\phi^{(1)} \frac{\partial \phi^{(2)}}{\partial n} - \phi^{(2)} \frac{\partial \phi^{(1)}}{\partial n} \right] dS = 0. \qquad (1.2.33)$$

The potentials $\phi^{(1)}$ and $\phi^{(2)}$ can be characterised, using a notation due to Kreisel (1949), by

$$\phi^{(1)} = \{A_1, B_1; C_1, D_1\}$$

indicating that

$$\begin{aligned} \phi^{(1)} &\sim (A_1 e^{-i\kappa x} + B_1 e^{i\kappa x}) \frac{igA}{\omega} \frac{\cosh \kappa(y - h)}{\cosh \kappa h} \quad \text{as} \quad x \longrightarrow -\infty \\ &\sim (C_1 e^{-i\kappa x} + D_1 e^{i\kappa x}) \frac{igA}{\omega} \frac{\cosh \kappa(y - h)}{\cosh \kappa h} \quad \text{as} \quad x \longrightarrow +\infty. \end{aligned} \qquad (1.2.34)$$

Equations (1.2.33) and (1.2.34) then give, after some simple algebra,

$$A_1B_2 - B_1A_2 = C_1D_2 - D_1C_2. \tag{1.2.35}$$

The scattering of a plane wave from $x = +\infty$ is characterised by

$$\{1,R_1;T_1,0\} \equiv \phi^{(1)} \tag{1.2.36}$$

whilst if the wave is from $x = -\infty$ we have

$$\{0,T_2;R_2,1\} \equiv \phi^{(2)}. \tag{1.2.37}$$

We can apply the result given by equation (1.2.35) to these two potentials, giving

$$T_1 = T_2 \tag{1.2.38}$$

showing that the direction of the incident wave has no effect on the transmitted wave regardless of the shape of the body. If, instead of $\phi^{(2)}$ as given by equation (1.2.37), $\bar{\phi}^{(1)}$ is used the equation

$$|R_1|^2 + |T|^2 = 1 \tag{1.2.39}$$

is obtained. Equation (1.2.39) is an expression of the conservation of energy. Similarly, using $\phi^{(2)}$ and $\bar{\phi}^{(2)}$, we can derive the equation

$$|R_2|^2 + |T|^2 = 1$$

which in turn shows that

$$|R_1| = |R_2| . \qquad (1.2.40)$$

If ϕ is a radiation potential whose behaviour at $\pm\infty$ is given by equation (1.2.30) then $\phi^{(2)} \equiv \phi - \bar{\phi}$ is a scattering potential characterised by

$$\{A^-, -\bar{A}^-; A^+, -\bar{A}^+\}.$$

Equation (1.2.33) can then be applied to this potential and another given by either equation (1.2.36) or (1.2.37). This results in the Newman relations (Newman (1975)) :

$$A^- + R_1\bar{A}^- + T\bar{A}^+ = 0 \qquad (1.2.41)$$

$$A^+ + R_2\bar{A}^+ + T\bar{A}^- = 0. \qquad (1.2.42)$$

If the body is symmetric and is making symmetric oscillations then $R_1 = R_2$ and $A^+ = A^-$ which implies that

$$R + T = -A^+/\bar{A}^+ . \qquad (1.2.43)$$

If a symmetric body is making antisymmetric oscillations the relation between the complex amplitudes of the radiated waves at $\pm\infty$ is then $A^+ = -A^-$ and so, in this case,

$$R - T = -A^+/\bar{A}^+ . \qquad (1.2.44)$$

Finally if ϕ and ψ in equation (1.2.26) are chosen to be a scattering potential due to an incident wave from $x = +\infty$ and a

radiation potential for a particular mode then it can be shown from equation (1.2.20) that the exciting force, $X_s^{(1)}$, is given by

$$X_s^{(1)} = 2\rho\omega A A_i^{\dagger} c_g. \qquad (1.2.45)$$

This result is known as the Haskind relation (Haskind (1959)).

In this section we have examined the general theory of wave body interactions and in particular some of the consequences of equation (1.2.26). For a more complete discussion, including the extension to three dimensions of many of the results, see, for example, Mei (1983) chapter 7, or Newman (1976).

CHAPTER 2

Wave reflection from fixed submerged obstacles

2.1 Introduction

Before considering the problem of wave reflection from bodies which move in response to the incident wave, the problem of reflection by passive devices, devices which are fixed, will be considered. The main reason for doing this is to get an idea of the sort of reflection and transmission coefficients that can be achieved just by inserting some fixed obstacle into the water.

A fixed barrier stretching from the free surface to the sea bed reflects all the incoming waves but does not allow boats to pass over it. A compromise is necessary and for this reason, whatever device is being considered, a reasonable clearance will be left above it.

Another restriction that will be imposed is that the depths far upstream and downstream of the device are the same. Thus situations like flow over a step will not be considered.

Newman (1965) considered the problem of the reflection and transmission of waves past long obstacles, i.e. long compared with wavelength. One result shown in his paper corresponds to experiments performed by Takano (1960). The obstacle considered is a rectangular block of length $8.86h_o$ where h_o is the water depth above the block. The water on either side of the block is assumed to be infinitely deep. Even though the obstacle is very large the transmission coefficients that are achieved are all in the range $0.7 < |T| < 1$.

These sort of values for $|T|$ are fairly typical of other passive devices. Mei and Black (1969) and Black, Mei and Bray (1971) looked at the full linear problem of radiation and scattering by rectangular blocks, both on the sea bed and immersed through the free surface, using a variational technique. This problem will be looked at in detail in chapter 3. Here we just note that the values obtained for the transmission coefficient for small to moderately large blocks are again all above about 0.7.

A different sort of fixed obstacle was considered by Kirby and Dalrymple (1983). Here, instead of a block, a trench was considered. In the case of waves normally incident on the trench the results are similar to those for the block for obstacles of approximately the same dimensions. For obliquely incident waves much greater reductions in transmission can be achieved, say $|T| \simeq 0.1$, if the trench-parallel wavenumber component exceeds the wavenumber for freely propagating waves in a trench. This three dimensional effect is important but not relevant to the present study.

In this chapter one particular sort of device will be considered: the rectangular block. The full linear problem is solved in chapter 3; here the problem of waves incident on a rectangular block in shallow water will be examined. This problem is much simpler than the full linear problem and the results can be used to look at the situation with two rectangular obstacles on the sea bed separated by a gap. The use of the shallow water approximation for problems with depth discontinuities is not likely to give very accurate results as was originally pointed out by Lamb (1932) §176 so in §3.5 the shallow water theory is compared to the full linear theory to see how applicable it is in these circumstances.

2.2 Rectangular Obstacle, Shallow Water Theory

One of the simplest configurations that can be examined is that of a wave incident on a rectangular obstacle under the assumption of shallow water theory. The basic assumption of this theory can be expressed in three equivalent forms: the pressure is hydrostatic, the horizontal velocity does not vary with depth, or the depth is much smaller than the wavelength (see Stoker 1957). A rigorous derivation of the shallow water equations can be found in, for example, Peregrine (1972). Here we will anticipate the final dispersion relation and assume that

$$Kh \ll 1 \ . \qquad (2.2.1)$$

To see how this assumption affects the boundary value problem given by equations (1.2.6)-(1.2.8) it is convenient to non-dimensionalise the independent variables by

$$Kx = x' \ ; \ Ky = y' . \qquad (2.2.2)$$

Then

$$\nabla'^2\phi = 0 \qquad (2.2.3)$$

$$\frac{\partial\phi}{\partial y'} = 0 \qquad \text{on} \quad y'=Kh \qquad (2.2.4)$$

$$\frac{\partial\phi}{\partial y'} + \phi = 0 \qquad \text{on} \quad y'=0. \qquad (2.2.5)$$

Equation (2.2.3) implies that

$$\frac{1}{Kh}\int_0^{Kh}\left[\frac{\partial^2\phi}{\partial x'^2} + \frac{\partial^2\phi}{\partial y'^2}\right] dy' = 0 \ .$$

Since the horizontal fluid velocity, $\frac{\partial\phi}{\partial x}$, is assumed to be independent

of y this is equivalent to

$$\frac{\partial^2 \phi}{\partial x'^2} + \frac{1}{Kh} \left[\frac{\partial \phi}{\partial y'}\right]_0^{Kh} = 0 \ . \qquad (2.2.6)$$

Using equations (2.2.4) and (2.2.5) gives

$$\frac{\partial^2 \phi}{\partial x'^2} + \frac{1}{Kh} \phi(x',0) = 0 \ . \qquad (2.2.7)$$

Taylor's theorem implies that if $0 \leq y' \leq Kh$

$$\phi(x',y') = \phi(x',0) + O(Kh) \ .$$

Thus, for small Kh, ϕ can be regarded as a function of x' alone satisfying the simple ordinary differential equation

$$\frac{d^2 \phi}{dx'^2} + \frac{1}{Kh} \phi = 0 \ .$$

In terms of the dimensional variables this is

$$\frac{d^2 \phi}{dx^2} + \kappa^2 \phi = 0 \qquad (2.2.8)$$

where $$\kappa^2 h = K \equiv \omega^2/g \ .$$

Thus if $Kh \ll 1$ it follows that $\kappa h \ll 1$ and so $h \ll \lambda$, which is the condition for shallow water theory.

Solutions for ϕ are thus of the form

$$\phi = Ae^{i\kappa x} + Be^{-i\kappa x} \ . \qquad (2.2.9)$$

A progressive wave travelling in the $\pm x$ direction is given by

$$\phi = Ae^{\mp i\kappa x} \ .$$

The problem of interest here is that of a wave incident, say from $x = -\infty$, on a rectangular obstacle. The problem is most easily described by means of a diagram:

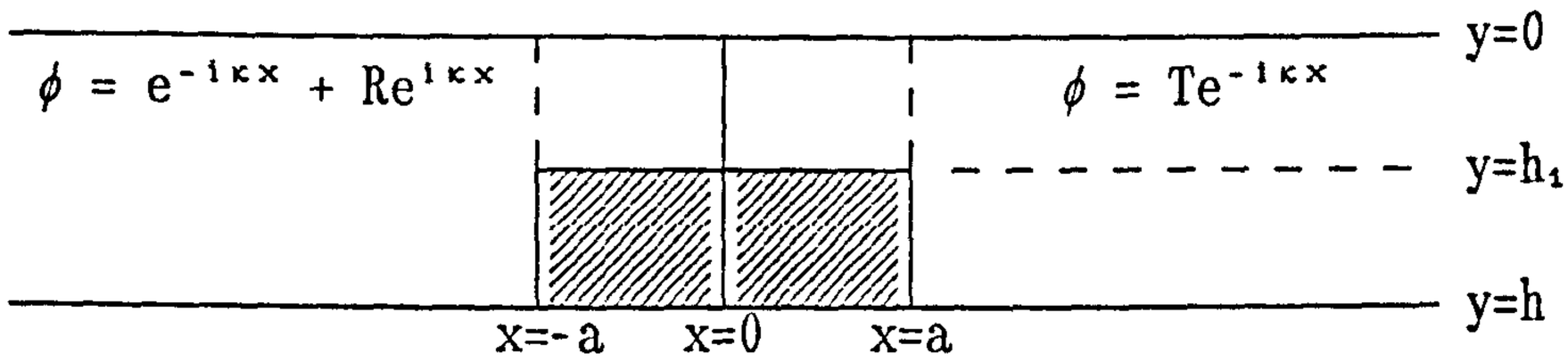

Figure 2.2.1

A solution of this problem requires the solution of four simultaneous equations corresponding to matching pressure and mass flux on $x = \pm a$ which is straightforward, if lengthy. It is more instructive to use a trick which can greatly simplify the algebra for such problems.

The trick relies on the fact that the problem described by figure (2.2.1) is just the 'sum' of the symmetric and antisymmetric problems defined by figures (2.2.2) and (2.2.3).

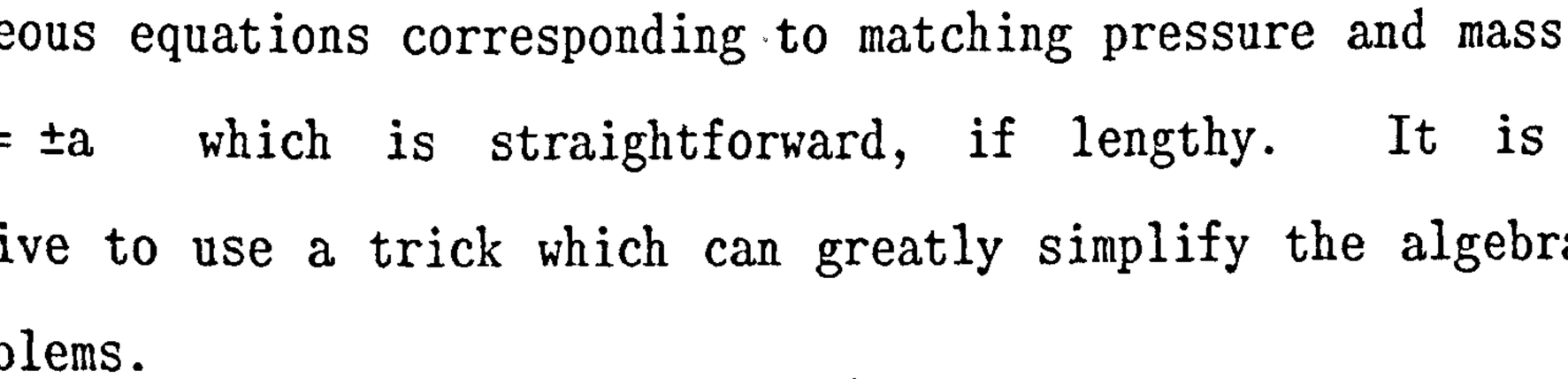

Figure 2.2.2

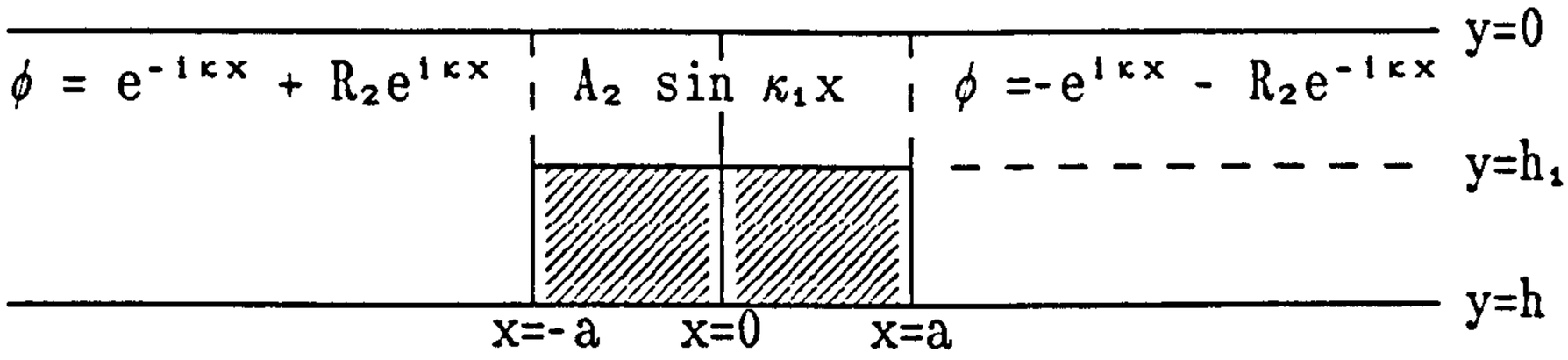

Figure 2.2.3

The wavenumber κ_1 satisfies $\kappa_1^2 h_1 = K$. A comparison with the original problem shows that

$$R = \tfrac{1}{2}(R_1 + R_2) \quad ; \quad T = \tfrac{1}{2}(R_1 - R_2) \ . \tag{2.2.10}$$

The solution to each of these problems requires the solution of a pair of simultaneous equations since we need only consider half the fluid domain, say $x > 0$. In the symmetric case, corresponding to figure (2.2.2) these equations, which ensure the conservation of pressure and mass flux across $x = \pm a$, are

$$A_1 \cos \kappa_1 a = e^{i\kappa a} + R_1 e^{-i\kappa a} \tag{2.2.11}$$

$$-\kappa A_1 \sin \kappa_1 a = i\kappa_1 (e^{i\kappa a} - R_1 e^{-i\kappa a}) \ . \tag{2.2.12}$$

The fact that $\kappa_1^2 h_1 = \kappa^2 h \equiv K$ has been used here and is used hereafter in order to remove h and h_1 from the equations. Equations (2.2.11) and (2.2.12) can be solved for R_1 to give

$$R_1 = e^{2i\kappa a} \frac{i\kappa_1 \cot \kappa_1 a + \kappa}{i\kappa_1 \cot \kappa_1 a - \kappa} \ . \tag{2.2.13}$$

In a similar manner the antisymmetric case leads to

$$R_2 = e^{2i\kappa a} \frac{i\kappa_1 \tan \kappa_1 a - \kappa}{i\kappa_1 \tan \kappa_1 a + \kappa} . \qquad (2.2.14)$$

It is convenient to define

$$D = 2i\kappa\kappa_1 \cos 2\kappa_1 a - (\kappa^2 + \kappa_1^2) \sin 2\kappa_1 a$$

so that R and T can be written, using equation (2.2.10),

$$R = (\kappa^2 - \kappa_1^2) \sin 2\kappa_1 a \, e^{2i\kappa a} / D \qquad (2.2.15)$$

$$T = 2i\kappa\kappa_1 \, e^{2i\kappa a} / D . \qquad (2.2.16)$$

It is a simple matter to check that these values satisfy the conservation of energy condition, $|R|^2 + |T|^2 = 1$.

The reflection and transmission coefficients can be considered to be defined by figure (2.2.1) in which a wave with velocity potential $e^{-i\kappa x}$ is incident on the block. The position of the block on the x-axis is thus important as the phase of the incoming wave relative to the block will be altered if the block is in a different position. A simple coordinate transformation shows that if, instead of lying between $x = -a$ and $x = a$, the obstacle lies between $x = b$ and $x = b+2a$ the new reflection and transmission coefficients, $\tilde{R}$ and $\tilde{T}$, are given by

$$\tilde{R} = Re^{-2i\kappa(b+a)} \qquad (2.2.17)$$

$$\tilde{T} = T . \qquad (2.2.18)$$

where R and T are given by equations (2.2.15) and (2.2.16).

2.3 Two Rectangular Obstacles, Shallow Water Theory

The following configuration will be considered:

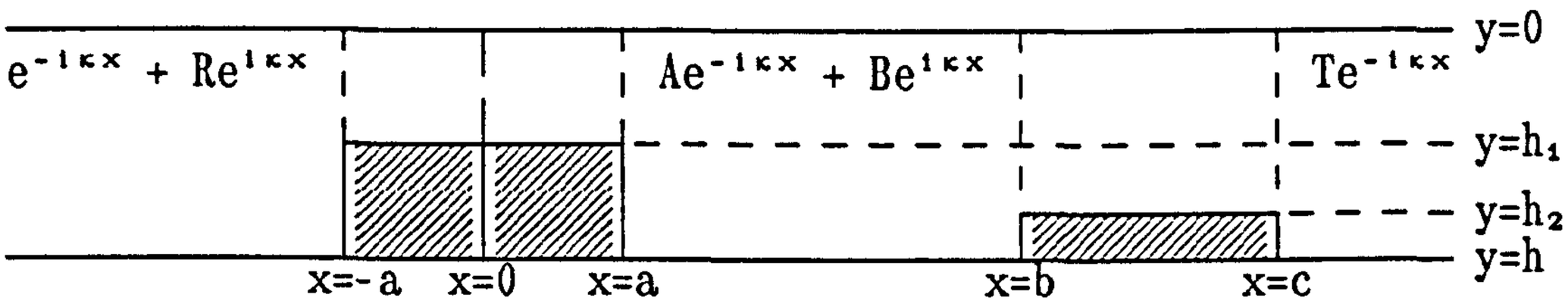

Figure 2.3.1

In order to solve the problem of two rectangular obstacles using shallow water theory we could proceed by defining five potentials corresponding to the five different regions of the problem and then match pressure and mass flux across the lines $x = -a$, $x = a$, $x = b$ and $x = c$. This would lead to an 8 x 8 system of equations which would require a lot of effort to solve.

It is much simpler however, to relate the wave amplitudes in the three regions with depth h to the reflection and transmission coefficients for the single obstacles, say R_1, T_1 and R_2, T_2 . Note that T_1 and T_2 are equally applicable to waves incident on the obstacles from either side (see equation (1.2.38)), whereas R_1 and R_2 refer to waves incident from $x = -\infty$. The coordinate system is chosen with the first obstacle symmetric about $x = 0$ so that R_1 is also the reflection coefficient for the first obstacle for waves incident from $x = +\infty$.

There are two waves incident on the first obstacle: the incident wave, $e^{-i\kappa x}$, from $x = -\infty$ and $Be^{i\kappa x}$ from the right. These give rise to two waves radiating from the body, $Re^{i\kappa x}$ to the left and $Ae^{-i\kappa x}$

to the right. Thus

$$R = R_1 + BT_1 \qquad (2.3.1)$$

$$A = T_1 + BR_1 \ . \qquad (2.3.2)$$

Similarly for the second obstacle

$$B = AR_2 \qquad (2.3.3)$$

$$T = AT_2 \ . \qquad (2.3.4)$$

Solving these four equations gives

$$R = \frac{R_1 - R_2(R_1^2 - T_1^2)}{1 - R_1R_2} \qquad (2.3.5)$$

$$T = \frac{T_1T_2}{1 - R_1R_2} \ . \qquad (2.3.6)$$

2.4 Results

In this chapter the shallow water approximation has been used to examine the reflection of waves from either one or two rectangular obstacles on the sea bed. The solutions to both of these problems therefore assume (see §2.2) that

$$Kh \ll 1 \ .$$

It is not clear how stringent this condition is or indeed how valid the results are for values of Kh which clearly violate this condition. In §3.5 results for a single obstacle in shallow water will be compared

with results from the full linear theory where it will be seen that agreement is not that good. However at this stage it is instructive to plot the results for these shallow water approximations over quite a wide range of values of Kh as this gives a good indication of the qualitative properties of the results.

Figure (2.4.1) shows the transmission coefficient as a function of non-dimensional wavenumber, Kh, for various single obstacles. The figure shows that, as one would expect, reflection is increased if the obstacle is larger, though even when the obstacle has a height equal to 4/5 of the depth the transmission coefficient never drops below 0.75. The figure also shows a comparison with an obstacle twice as long and still with a height of 0.8 times the depth. This is simply equivalent to a scaling of the x coordinate and so in this case the Kh axis appears to have been squashed up. (Doubling lengths is equivalent to dividing Kh by four since $Kh = \kappa^2 h^2 = 4\pi^2 h^2/\lambda^2$.)

If two identical blocks are spaced apart on the bottom then, as is shown in figure (2.4.2), the transmission coefficient is lower than in the case of a single obstacle. It should be noted however that in the long wave region, i.e. small Kh, where the shallow water theory is expected to be most accurate the performance of the double obstacle as a reflector is, if anything, worse than that of the single obstacle.

A noticeable feature of figure (2.4.1) is that the curves for the two obstacles of different lengths but the same height seem to complement each other, i.e. where one has a maximum in transmission the other has a minimum. It is clear, by scaling the x coordinate, that a block three times the length of the original will not increase the maximum reflection but the complementary nature of the obstacles with lengths h and 2h suggests placing these spaced apart by some distance. The results are shown in figure (2.4.3) for various gap

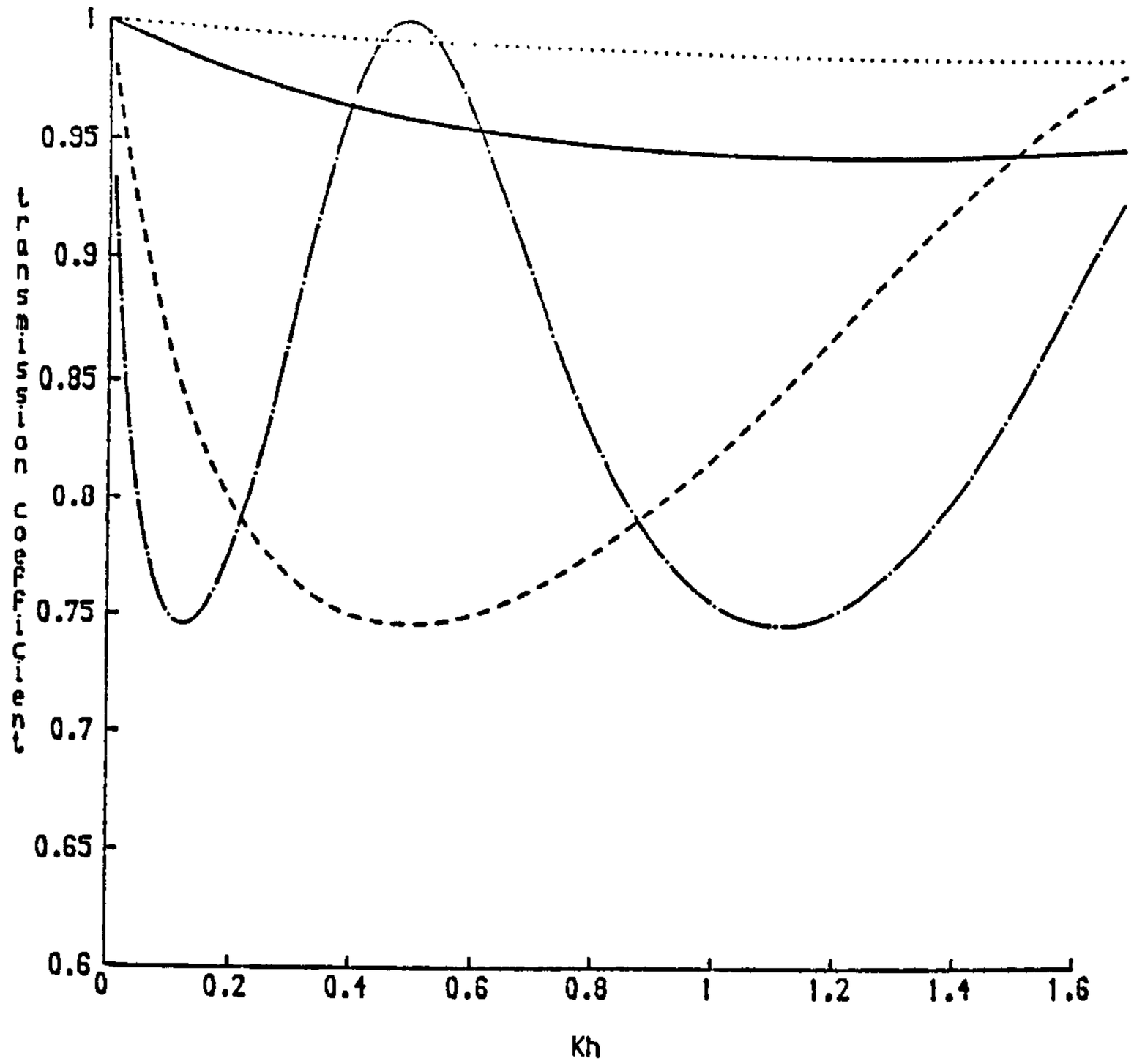

Figure 2.4.1. |T| plotted against Kh for 4 single blocks. ····· $h_1/h=0.7$, $a/h=0.5$; ——— $h_1/h=0.5$, $a/h=0.5$; – – – $h_1/h=0.2$, $a/h=0.5$; –·–·– $h_1/h=0.2$, $a/h=1$.

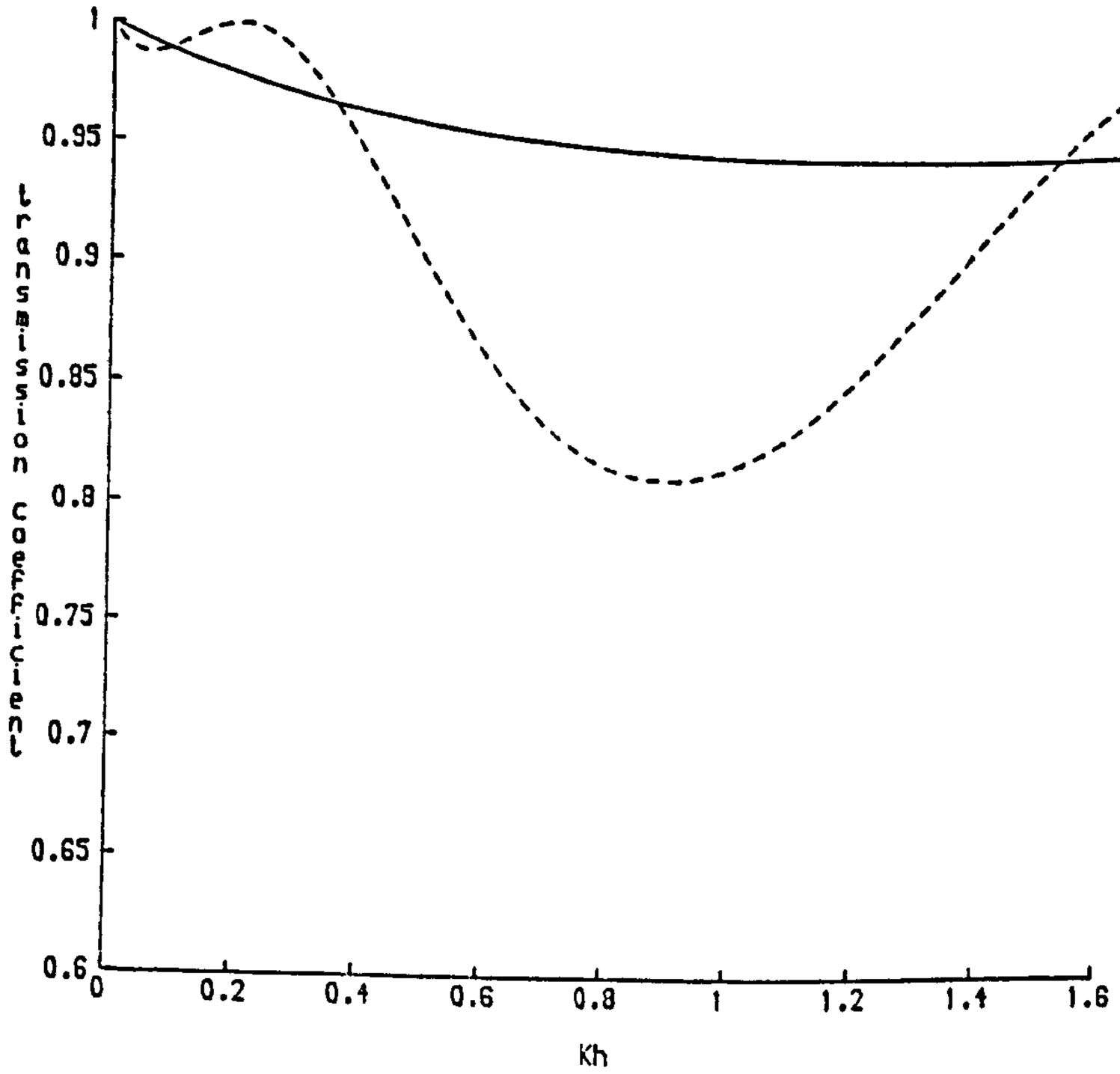

Figure 2.4.2. |T| plotted against Kh. ——— single block, $h_1/h=0.5$, $a/h=0.5$; – – – two blocks, $h_1/h=h_2/h=0.5$, $a/h=0.5$, $b/h=2.5$, $c/h=3.5$.

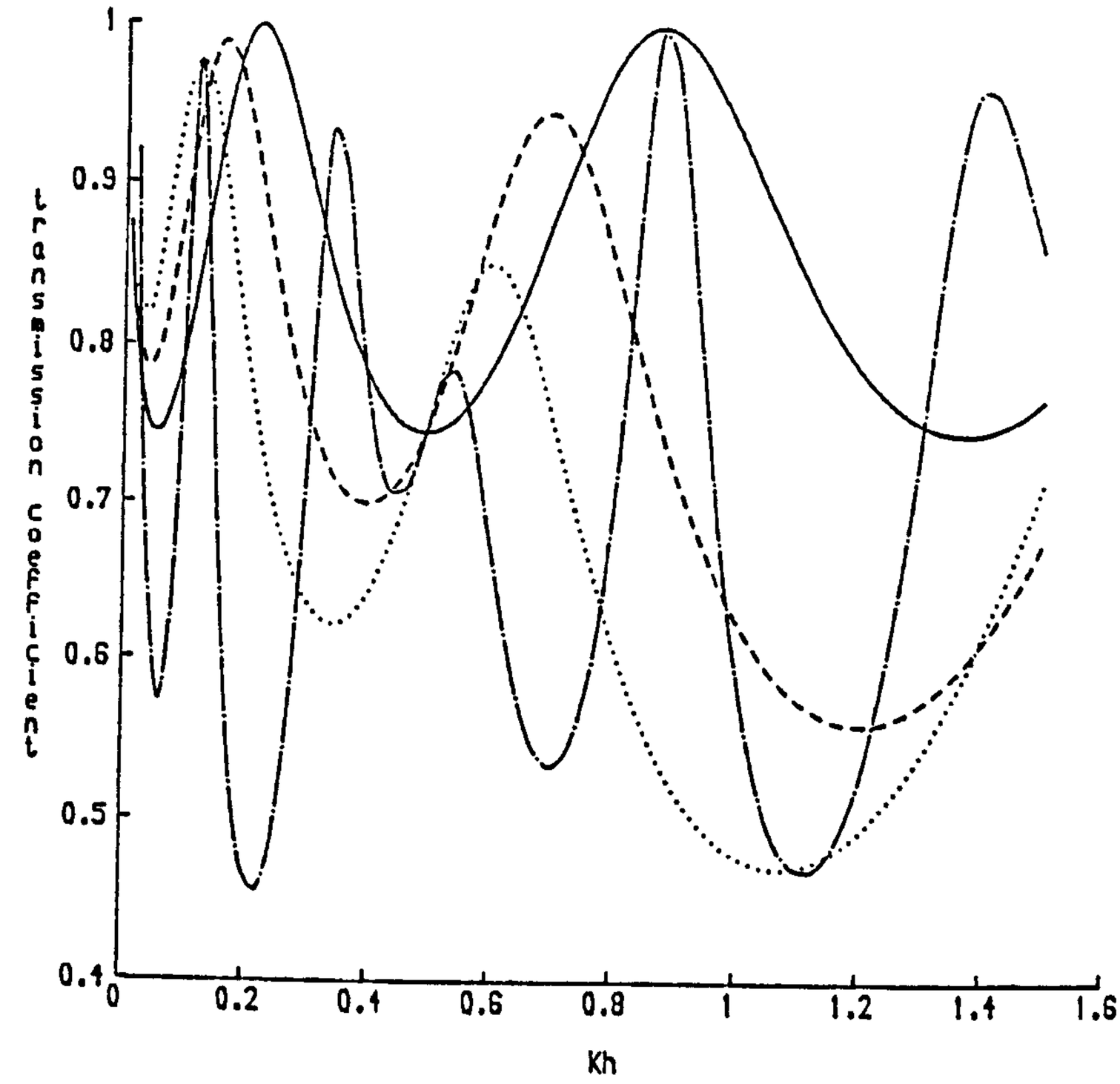

Figure 2.4.3. |T| plotted against Kh for two blocks, of length h and 2h, with 4 different gap widths. In all cases $h_1/h=h_2/h=0.2$. ——— gap/h=0; – – – gap/h=0.5; ····· gap/h=1; –·–·– gap/h=10.

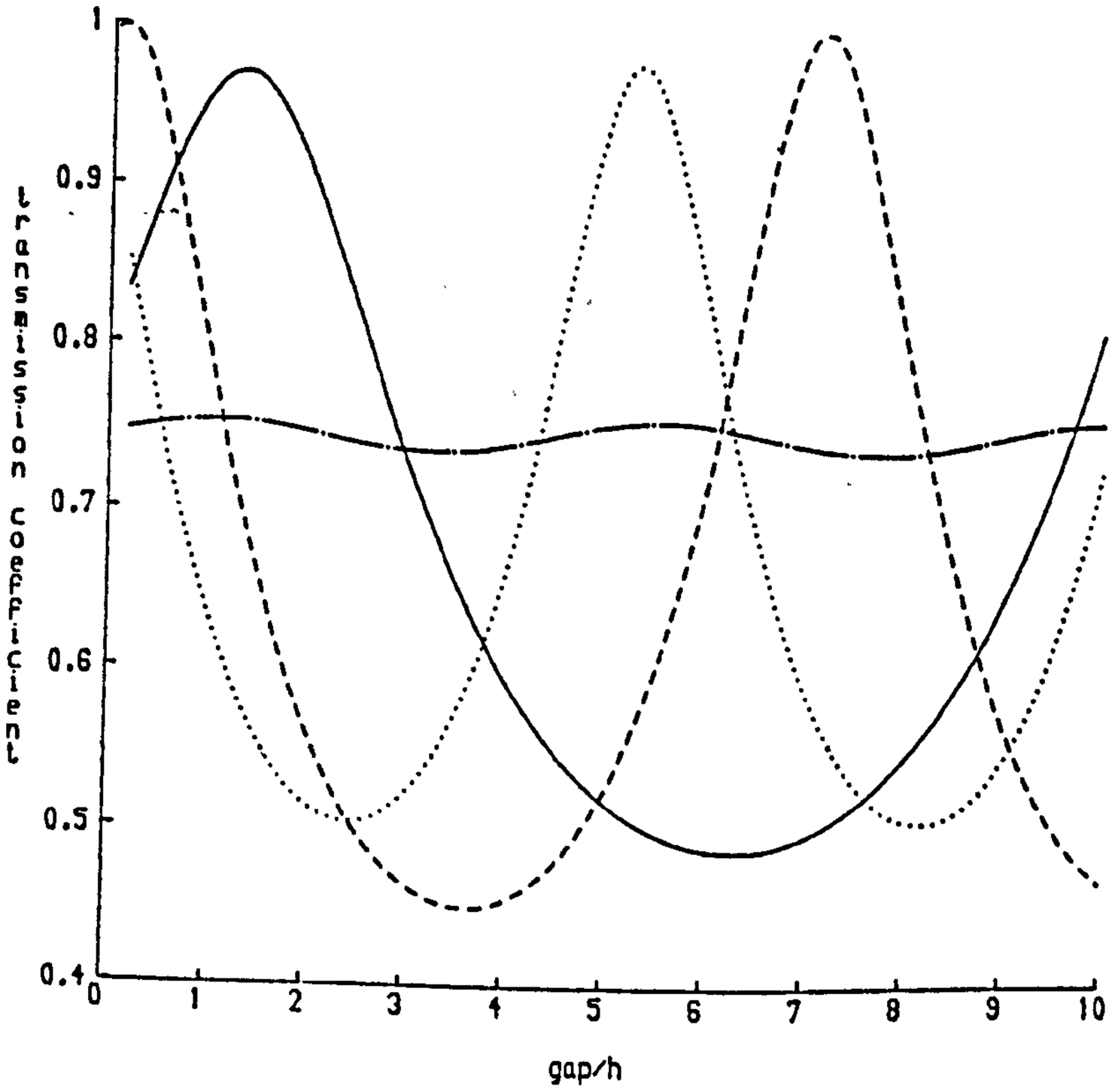

Figure 2.4.4. |T| plotted against gap/h for two blocks, of length h and 2h, at 4 different frequencies. In all cases $h_1/h=h_2/h=0.2$. ——— Kh=0.1; – – – Kh=0.2; ····· Kh=0.3; –·–·– Kh=0.5.

widths and it is clear that by incorporating this gap we have substantially improved the reflective properties. The optimal gap width is clearly a function of Kh and figure (2.4.4) shows the variation of transmission coefficient with non-dimensional gap width for various values of Kh. The figure shows that the gap width is more important for some wavenumbers than for others and for this configuration it hardly matters at all when Kh = 0.5.

2.5 Conclusion

The simplest way in which to obtain wave reflection is to place some fixed obstacle in the water. This problem has been briefly addressed in this chapter, in particular the question of whether large reductions in transmission can be achieved with reasonably small obstacles has been considered.

In order to get some qualitative idea of how fixed obstacles might perform as wave reflectors the shallow water approximation was used to solve the problem of wave incident on one or two rectangular obstacles on the sea bed. The results for a single block show that such an obstacle is not a good wave reflector. This is in agreement with previous work on rectangular obstacles, whether blocks or trenches, see §2.1.

A device consisting of two blocks separated by a gap was shown to perform slightly better as a wave reflector though even with two large blocks (4/5 of the depth in height) transmission coefficients of less than $\frac{1}{2}$ are only obtained at a very few frequencies.

CHAPTER 3

Wave reflection from submerged obstacles that are allowed to move in response to the waves

3.1 Introduction

In this chapter, and again in chapter 4, the two-dimensional problem of wave reflection by submerged bodies moving in response to an incident wave subject to a restoring force is considered. The general theory has recently been developed by D.V. Evans using an approach similar to that used in Evans (1976) for the problem of wave energy absorption by a damped oscillating body. In that paper it was shown that a submerged horizontal circular cylinder could be highly efficient as a wave power absorber. Problems concerning circular cylinders will be looked at in detail in chapter 4.

Here the general theory will be summarised in §3.2 and then, in §§3.3 and 3.4, applied to two simple cases.

In §3.3 the problem of a completely submerged vertical plate, hinged at the sea bed, is analysed. The hydrodynamic characteristics of such a system are found using the method of matched eigenfunction expansions. A similar problem has been solved by Leach et al. (1985), the difference being that in their work the plate extends through the free surface.

In §3.4 the problems of a rectangular block on the bottom oscillating in sway and in heave are considered and again the method of matched eigenfunction expansions is used.

Results for these simple cases are discussed in §3.6 and it is noted that there is a vast improvement in the reflective properties over fixed

devices. It is also found that the vertical hinged plate not extending to the free surface can, with an appropriate restoring force, reflect more waves than the hinged plate considered by Leach et al. (1985) even though the latter extends through the free surface.

As will be shown in the next section, in order to calculate the properties of a moving body in waves it is necessary to know the characteristics of the same body when fixed in those waves. In the case of the block this will allow results obtained in §2.2 for the shallow water case to be compared with the full linear solution. The reflection and transmission coefficients for a rectangular block on the bottom have been calculated by McIver (1985) who solved the scattering problem by the method of matched eigenfunction expansions. Here these quantities will be obtained from the solution of two radiation problems, one symmetric and one antisymmetric, via the Newman relations. This is done in §3.5.

In §3.7 it is indicated how the general theory can be extended to cover incoming wave fields having a frequency spectrum rather than just a single frequency.

A discussion of the conclusions that can be drawn from the work presented in this section is given in §3.8.

3.2 General Theory

The material in this section is based on ideas due to D.V. Evans and together with material from §§4.2-4.7 forms part of a joint paper by Evans and Linton to be published in Applied Ocean Research. An approach is used which follows closely that of Evans (1976) for the wave power absorption problem in order to solve the general problem of wave reflection by moving bodies in two dimensions.

We consider a single body spanning a narrow wave tank and constrained to oscillate at the same frequency as the incident waves in a single mode of motion, either heave, sway, or roll. Its motion is opposed by an external force proportional to its (small) displacement. For example this could be regarded as the hydrostatic restoring force for a surface-piercing body, or a mooring force.

As described in §1.2 there exists a velocity potential

$$\Phi(x,y,t) = \mathrm{Re}[\phi(x,y)e^{i\omega t}] \qquad (3.2.1)$$

where the time independent potential $\phi(x,y)$ satisfies

$$\nabla^2\phi = 0 \quad \text{in the fluid} \qquad (3.2.2)$$

$$K\phi + \frac{\partial\phi}{\partial y} = 0 \quad \text{on } y = 0, \quad K = \omega^2/g \qquad (3.2.3)$$

$$\frac{\partial\phi}{\partial y} = 0 \quad \text{on } y = h \qquad (3.2.4)$$

$$\frac{\partial\phi}{\partial n} = \mathbf{U}.\mathbf{n} \quad \text{on the body.} \qquad (3.2.5)$$

As $x \longrightarrow +\infty$ we assume

$$\phi \sim \frac{gA}{\omega}\,\frac{\cosh\,\kappa(y-h)}{\cosh\,\kappa h}\,(e^{i\kappa x} + R_1 e^{-i\kappa x}) \qquad (3.2.6)$$

with A real, whilst as $x \longrightarrow -\infty$

$$\phi \sim \frac{gA}{\omega}\,\frac{\cosh\,\kappa(y-h)}{\cosh\,\kappa h}\,T_1 e^{i\kappa x}\ . \qquad (3.2.7)$$

Here κ is the real positive root of

$$K = \kappa \tanh \kappa h \ . \tag{3.2.8}$$

It is clear from equations (3.2.6), (3.2.7), and the equation

$$\eta(x) = -i\omega g^{-1} \phi(x,0) \tag{3.2.9}$$

for the time-independent surface elevation, that ϕ describes a wave of amplitude A incident upon the body and giving rise to reflected and transmitted waves of amplitude $A|R_1|$ and $A|T_1|$ respectively.

It is convenient to separate ϕ into two potentials, so that

$$\phi = \phi_S + U\phi_R \ . \tag{3.2.10}$$

Thus ϕ_S is a scattering potential which satisfies all the previous conditions satisfied by ϕ but with the body held fixed and then U, the time-independent velocity (or angular velocity in roll) of the body is zero and R_1, T_1 in equations (3.2.6) and (3.2.7) become R, T respectively.

On the other hand ϕ_R is a radiation potential satisfying equations (3.2.2)-(3.2.4) and

$$\frac{\partial \phi_R}{\partial n} = (U.n)/U \quad \text{on the body} \tag{3.2.11}$$

whilst for $x \to \pm\infty$

$$\phi_R \sim \frac{A^{\pm} \cosh k(y-h)}{\cosh kh} e^{\mp ikx} \ . \tag{3.2.12}$$

describing waves radiating away from the body.

It is clear that the combination given by equation (3.2.10) satisfies all the conditions of the problem. Furthermore we have

$$R_1 = R + \frac{\omega U}{gA} A^+, \quad T_1 = T + \frac{\omega U}{gA} A^- \ . \tag{3.2.13}$$

At this stage we shall restrict the body and its motion to be symmetric in the sense that in heave, $A^+ = A^- = A_s$, say, and in sway or roll, $A^+ = -A^- = A_s$.

Now if we require the induced motion of the body to create a wave which cancels the downstream wave, we require

$$T \pm \frac{\omega U}{gA} A_s = 0 \tag{3.2.14}$$

where the upper sign refers to heave, the lower to sway or roll. If we substitute this optimal value of U determined from equation (3.2.14) into the expression for R_1 in equation (3.2.13) we obtain

$$R_1 = R \pm T, \quad T_1 = 0 \ . \tag{3.2.15}$$

But for symmetric bodies it follows directly from the Newman relations (Newman (1975), see equation (3.2.21) below) that $|R + T| = |R - T| = 1$. It follows that not only does U, chosen to satisfy equation (3.2.14), eliminate the downstream wave but no work needs to be fed in or taken out of the system in the process since the incident wave is totally reflected. This result was first pointed out by Guevel (1985).

We turn next to the external force on the body and, in the light of the previous result, choose a form which is non-dissipative. We denote time-independent forces by X, their actual value being $\mathrm{Re}[Xe^{i\omega t}]$.

Thus we shall assume the external force to be

$$X_{ex} = i\lambda\omega^{-1}U, \quad \lambda \text{ real}, \tag{3.2.16}$$

that is, proportional to the oscillatory displacement of the body and hence its time-independent velocity U. With λ real it is clear that the mean power over a cycle, $\frac{1}{2}\mathrm{Re}[\bar{X}_{ex}U]$, is zero. (Here a bar denotes a complex conjugate).

Similarly we denote the exciting force on the fixed body, corresponding to the potential ϕ_s, by X_s and the radiation force, corresponding to the potential $U\phi_R$, by X_R. This latter force is conveniently separated into a term in phase with the acceleration of the body and a term in phase with the velocity.

Thus

$$X_R = -(B + i\omega M)U \tag{3.2.17}$$

where B, M are the frequency-dependent radiation damping and added-mass coefficients for the body in question, and can be assumed known.

The relations amongst the various quantities we have introduced which were proved in chapter 1 will be used to simplify the subsequent work. Thus for the symmetric problem being considered we have from equation (1.2.45)

$$X_s = 2\rho\omega A A_s c_g \quad \text{(Haskind)} \tag{3.2.18}$$

and from equation (1.2.32)

$$B = 2\rho\omega^2 g^{-1}|A_s|^2 c_g \tag{3.2.19}$$

whilst from equation (1.2.39)

$$|R|^2 + |T|^2 = 1 \qquad \text{(conservation of energy)} \qquad (3.2.20)$$

and from equations (1.2.43) and (1.2.44)

$$R \pm T = -A_s/\bar{A}_s \qquad \text{(Newman)}. \qquad (3.2.21)$$

The equation of motion for the body is

$$X_{ex} + X_R + X_S = i\omega IU \qquad (3.2.22)$$

where I is the mass (heave, sway) or moment of inertia (roll) of the body. This can be written, using equations (3.2.16) and (3.2.17), as

$$B(1 + iC)U = X_S \qquad (3.2.23)$$

where

$$C = \{(M + I)\omega^2 - \lambda\}/B\omega$$

which determines the motion of the body in terms of the constant λ.

It follows from equations (3.2.13), (3.2.21) and (3.2.23) that

$$R_1 = (CR \pm iT)/(C - i) \qquad (3.2.24)$$

$$T_1 = (CT \pm iR)/(C - i). \qquad (3.2.25)$$

It is easily verified that

$$|R_1|^2 + |T_1|^2 = 1 \qquad (3.2.26)$$

and that

$$R_1 \pm T_1 = \frac{(C + i)}{(C - i)} (R \pm T) \ . \qquad (3.2.27)$$

This in turn implies that $|R_1 \pm T_1| = |R \pm T|$ since C is real.

Now since $|R + T| = |R - T| = 1$ it follows that $Re[R/T] = 0$ provided $T \neq 0$. Thus we may write $R/T = i\chi$ where χ is real and one-signed provided $R \neq 0$ at any frequency.

Thus

$$T_1 = T(C \mp \chi)/(C - i) \qquad (3.2.28)$$

$$R_1 = R(C \pm \chi^{-1})/(C - i). \qquad (3.2.29)$$

The condition for $T_1 = 0$ is

$$C = \pm\chi \quad \text{or} \quad \lambda = (M + I)\omega^2 \mp B\omega\chi \qquad (3.2.30)$$

whilst the condition for $R_1 = 0$ is

$$C = \pm\chi^{-1} \quad \text{or} \quad \lambda = (M + I)\omega^2 \pm B\omega\chi^{-1} \ . \qquad (3.2.31)$$

It would appear therefore that it may be possible to 'tune' a body to reflect all the incident waves, so that $T_1 = 0$, at a given frequency, by a suitable choice of 'spring' constant λ satisfying equation (3.2.30).

With λ_o fixed, equation (3.2.28) gives T_1 as a function of wave frequency, vanishing if and when

$$C = \pm\chi \quad \text{or} \quad \lambda_o = (M + I)\omega^2 \mp B\omega\chi. \qquad (3.2.32)$$

In order to demonstrate the theory we will apply it to two simple cases. In the next section the problem of a vertical plate hinged at the sea bed is considered and then the problem of a rectangular block on the sea bed will be considered in §3.4.

Equation (3.2.28) gives T_1 as a function of a number of parameters. Before we can use this equation to work out the reflecting properties of a body a method for calculating the non-dimensional added mass and radiation damping coefficients together with the reflection and transmission coefficients for the scattering problem must be found.

3.3 Vertical Plate Hinged at the Sea Bed

Here we will solve the radiation problem for the vertical hinged plate by using the method of matched eigenfunction expansions. The geometry of the problem is indicated in figure (3.3.1).

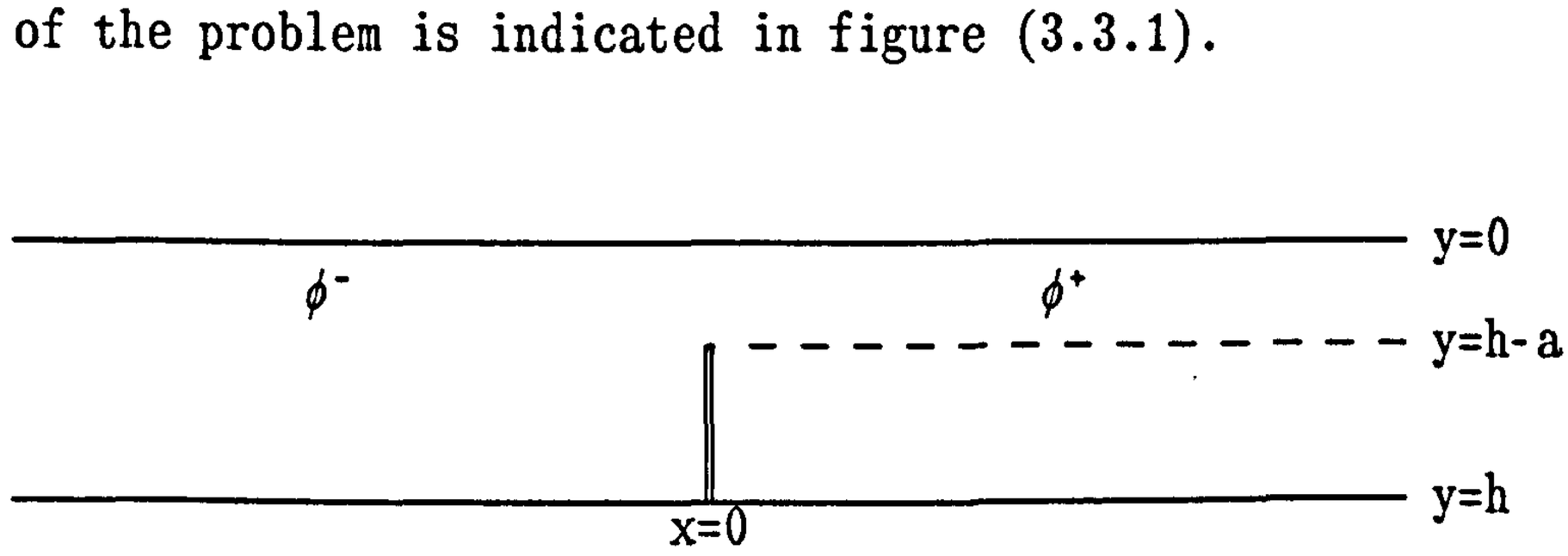

Figure 3.3.1

Once again the starting point for the solution is the velocity potential $\Phi(x,y,t)$. The time independent velocity potential $\phi(x,y)$, defined by equation (3.2.1), is the solution of the boundary-value problem given by equations (3.2.2)-(3.2.5) with a radiation condition imposed at $x = \pm\infty$. The fluid region will be divided into two parts : let the potential in $x < 0,\ 0 < y < h$ be ϕ^- and in $x > 0,\ 0 < y < h$

be ϕ^+. Then

$$\nabla^2 \phi^- = 0 \qquad x < 0$$
$$\nabla^2 \phi^+ = 0 \qquad x > 0 \tag{3.3.1}$$

$$\phi^{\pm} \sim A^{\pm} \frac{\cosh \kappa(h-y)}{\cosh \kappa h} e^{\mp i\kappa x} \quad \text{as} \quad x \to \pm\infty. \tag{3.3.2}$$

Continuity of pressure and velocity across $x = 0$ give the conditions

$$\phi^- = \phi^+ \qquad x = 0,\ 0 < y < h-a \tag{3.3.3}$$

$$\frac{\partial \phi^-}{\partial x} = \frac{\partial \phi^+}{\partial x} \qquad x = 0,\ 0 < y < h-a \tag{3.3.4}$$

and if the plate is hinged at the bottom we then have

$$\frac{\partial \phi^-}{\partial x} = \frac{\partial \phi^+}{\partial x} = U\left[\frac{h-y}{a}\right] \quad x = 0,\ h-y < y < h. \tag{3.3.5}$$

where U can be taken to be an arbitrary complex number (see equations (1.2.14)-(1.2.17)).

We will use the complete orthogonal functions, (see Mei (1983) pp 304-306),

$$f_n \equiv N_n^{-1/2} \cos k_n(h-y)$$

where

$$N_n = \tfrac{1}{2}\left[1 + \frac{\sin k_n h}{2k_n h}\right] \qquad n = 0,1,\ldots \ .$$

Here k_n $n = 0,1,\ldots$ are the solutions of

$$K + k_n \tan k_n h = 0 \tag{3.3.6}$$

and it can be assumed without loss of generality that $\mathrm{Re}(k_n) \geq 0$ $n = 0,1,2,\ldots$. Note that the $n = 0$ equation is just equation (3.2.8) with $\kappa = -ik_o$ and so

$$f_o = N_o^{-1/2} \cosh \kappa(h-y)$$

where

$$N_o = \tfrac{1}{2}\left[1 + \frac{\sinh 2\kappa h}{2\kappa h}\right] .$$

Writing $k_n h = z \equiv x + iy$ reduces equation (3.3.6) to $Kh + z \tan z = 0$. The imaginary part of this equation reduces to

$$\frac{\sin 2x}{2x} = \frac{\sinh 2y}{2y}$$

which has no solution except in the limit $(x,y) \longrightarrow (0,0)$. It follows that all the remaining solutions to equation (3.3.6), i.e. k_n $n \geq 1$, are real and it is easy to show that there are an infinite number of them. The functions f_n satisfy

$$\frac{1}{h}\int_0^h f_n(y)\, f_m(y)\, dy = \delta_{mn} \qquad m,n = 0,1,\ldots \quad . \qquad (3.3.7)$$

The first step in solving the problem is to write down eigenfunction expansions of ϕ^- and ϕ^+. Thus

$$U^{-1}\ \phi^-(x,y) = B_o^-\, f_o\, e^{i\kappa x} + \sum_{n=1} B_n^-\, f_n \exp(k_n x) \qquad (3.3.8)$$

$$U^{-1}\ \phi^+(x,y) = B_o^+\, f_o\, e^{-i\kappa x} + \sum_{n=1}^{\infty} B_n^+\, f_n \exp(-k_n x). \qquad (3.3.9)$$

A comparison with equation (3.3.2) immediately gives

$$A^{+} = N_0^{-1/2} B_0^{+} \cosh \kappa h \quad ; \quad A^{-} = N_0^{-1/2} B_0^{-} \cosh \kappa h \tag{3.3.10}$$

From equations (3.3.8) and (3.3.9) it follows that

$$U^{-1} \left. \frac{\partial \phi^{\pm}}{\partial x} \right|_{x=0} = \mp i\kappa B_0^{\pm} f_0 \mp \sum_{n=1}^{\infty} k_n B_n^{\pm} f_n. \tag{3.3.11}$$

The boundary conditions on $x = 0$ then imply that $B_0^{-} = -B_0^{+}$ and $B_n^{-} = -B_n^{+}$ which is clear on physical grounds due to the antisymmetry of the problem.

The problems for ϕ^{-} and ϕ^{+} can now be simplified to just one problem, say for ϕ^{+}, with the extra condition that

$$\phi^{+}(0,y) = 0 \qquad 0 < y < h-a. \tag{3.3.12}$$

This condition is equivalent to

$$\sum_{n=0}^{\infty} B_n^{+} f_n(y) = 0 \qquad 0 < y < h-a \tag{3.3.13}$$

and equation (3.3.5) is equivalent to

$$\sum_{n=0}^{\infty} k_n B_n^{+} f_n(y) = \frac{y-h}{a} \qquad h-a < y < h. \tag{3.3.14}$$

To convert these two equations into a single infinite system the

following method is used.

$$\text{Let} \qquad F(y) = \begin{cases} \alpha \sum_{n=0}^{\infty} B_n^+ \, f_n(y) & 0 < y < h-a \\ \beta \left[\sum_{n=0}^{\infty} k_n a \, B_n^+ \, f_n(y) + \quad (h-y) \right] & h-a < y < h \end{cases} \tag{3.3.15}$$

where $\alpha, \beta \neq 0$. Then

$$F(y) \equiv 0 \qquad 0 < y < h. \tag{3.3.16}$$

Therefore

$$\frac{1}{h} \int_0^h F(y) \, f_m(y) \, dy = 0 \qquad m = 0,1,\ldots \quad . \tag{3.3.17}$$

It follows from equation (3.3.7) that

$$\frac{1}{h} \int_{h-a}^{h} f_n(y) \, f_m(y) \, dy = \delta_{mn} - \frac{1}{h} \int_0^{h-a} f_n(y) \, f_m(y) \, dy \tag{3.3.18}$$

and so equation (3.3.17) implies that

$$\sum_{n=0}^{\infty} B_n^+ \, [\, \alpha \, D_{mn} + \beta \, k_n a \, (\delta_{mn} - D_{mn}) \,] = \beta \int_{h-a}^{h} \frac{y-h}{h} \, f_m(y) \, dy \tag{3.3.19}$$

where

$$D_{mn} = \frac{1}{h} \int_0^{h-a} f_n(y) \, f_m(y) \, dy. \tag{3.3.20}$$

The constants α and β are arbitrary but non-zero. By varying these parameters the convergence properties of the final system of equations will be altered. It was found however that the effect of altering either parameter was slight and so from now on it will be assumed that $\alpha = \beta = 1$ since this keeps the algebra as simple as

possible. Then, putting

$$C_n = - B_n^+ k_n a/h \qquad (3.3.21)$$

equation (3.3.19) becomes

$$\sum_{n=0}^{\infty} C_n \left[\delta_{mn} + D_{mn} \left(\frac{1}{k_n a} - 1\right) \right] = \int_{h-a}^{h} \frac{h-y}{h^2} f_m(y)\, dy. \qquad (3.3.22)$$

Evaluating the right hand side gives

$$\sum_{n=0}^{\infty} C_n \left[\delta_{mn} + D_{mn} \left(\frac{1}{k_n a} - 1\right) \right] = N_m^{-1/2} \left[\frac{a}{h} \frac{\sin k_m a}{k_m h} - \frac{1 - \cos k_m a}{(k_m h)^2}\right]$$

$$m = 0,1,\ldots \quad . \qquad (3.3.23)$$

Equation (3.2.23) represents an infinite system of equations for the unknowns C_n $n = 0,1,\ldots$. It is more convenient to have the indices n and m running from 1 rather than from 0 and so we write equation (3.3.23) as

$$\sum_{n=1}^{\infty} M_{mn} X_n = Y_m \qquad m=1,2,\ldots \qquad (3.3.24)$$

where

$$M_{mn} = \delta_{mn} + D_{m-1,n-1} \left(\frac{1}{k_{n-1} a} - 1\right) \qquad m = 1,2,\ldots$$
$$n = 2,3,\ldots$$

$$M_{m1} = \delta_{m1} + D_{m-1,0} \left(\frac{1}{i\kappa a} - 1\right)$$
$$= \delta_{m1} - D_{m-1} - i\, D_{m-1,0}/(\kappa a) \qquad m = 1,2,\ldots$$

$$X_n = C_{n-1} \qquad n = 1,2,\ldots$$

$$Y_n = N_{m-1}^{-1/2} \left[\frac{a}{h} \frac{\sin k_{m-1} a}{k_{m-1} h} - \frac{1 - \cos k_{m-1} a}{(k_{m-1} h)^2}\right] \qquad m = 2,3,\ldots$$

$$Y_1 = N_0^{-\nu/2} \left[\frac{a}{h} \frac{\sinh \kappa a}{\kappa h} - \frac{1 - \cosh \kappa a}{(\kappa h)^2}\right] .$$

Equation (3.3.24) represents an infinite system of equations in an infinite number of unknowns. For the purpose of computation equation (3.3.24) is truncated to an $N \times N$ system and approximations are calculated to the finite set of coefficients X_n $n = 1,2,\ldots,N$ (and hence C_n). By increasing the value of N the convergence of the method can be checked and providing the method does converge, i.e. the values obtained for the coefficients X_n tend to some limiting value as $N \longrightarrow \infty$, greater accuracy can be achieved at the expense of computing time. In this example taking $N = 50$ was found to give an accuracy of about 1%, though greater values of N are required when a/h is small. The values of the coefficients C_n can thus be assumed known and $\phi^{\pm}$ can be calculated from

$$\phi^{+}(x,y) = -\phi^{-}(x,y) = -Uh \sum_{n=0}^{\infty} \frac{C_n f_n(y)}{k_n a} \exp(-k_n x). \qquad (3.3.25)$$

The moment, f, on the plate is given by integrating the moment of the pressure around the plate and is therefore given by

$$f = -2\rho\omega i \int_{h-a}^{h} (y-h)\, Uh \sum_{n=0}^{\infty} \frac{C_n f_n(y)}{k_n a}\, dy \qquad (3.3.26)$$

and so the added inertia and damping coefficients, non-dimensionalised with respect to the quantity $\rho a^3 U\omega$, μ and ν, are given by

$$\mu - i\nu = 2 \left[\frac{h}{a}\right]^3 \sum_{n=0}^{\infty} \frac{C_n}{k_n a} N_n^{-\nu/2} \left[\frac{a}{h} \frac{\sin k_n a}{k_n h} - \frac{1 - \cos k_n a}{(k_n h)^2}\right] \qquad (3.3.27)$$

$$= 2\,\frac{h}{a}\sum_{n=1}^{\infty}\frac{C_n}{k_n a}\,N_n^{-\nu 2}\left[\frac{\sin k_n a}{k_n a}-\frac{1-\cos k_n a}{(k_n a)^2}\right]$$

$$-\,2i\,\frac{h}{a}\,\frac{C_o}{\kappa a}\,N_o^{-\nu 2}\left[\frac{\sinh \kappa a}{\kappa a}+\frac{1-\cosh \kappa a}{(\kappa a)^2}\right]. \qquad (3.3.28)$$

Some curves of μ and ν, plotted against non-dimensional frequency, Ka, are shown in figures (3.3.2) and (3.3.3).

Standard theorems connecting the far field behaviour with the damping coefficient can now be used as a check on the results. Comparing equations (3.3.2) and (3.3.25) we see that the amplitudes of the waves in the far field are proportional to $|A^{\pm}|$ where the $A^{\pm}$ are given by

$$|A^{\pm}|^2 = |C_o|^2\,\frac{\cosh^2\kappa h}{N_o\,\kappa^2}\left[\frac{h}{a}\right]^2 = |C_o|^2\,\frac{4}{\kappa^2}\,\frac{\kappa h\,\cosh^2\kappa h}{2\kappa h+\sinh 2\kappa h}\left[\frac{h}{a}\right]. \qquad (3.3.29)$$

The damping coefficient, ν, and these amplitudes are connected by equation (1.2.32), thus

$$\nu\rho\omega a^2 = \frac{\rho\omega^2 c_g}{g}\left(|A^+|^2+|A^-|^2\right) \qquad (3.3.30)$$

where c_g is the group velocity and is given by $\frac{\omega}{2\kappa}\left[1+\frac{2\kappa h}{\sinh 2\kappa h}\right]$. This can be simplified to

$$\nu = |C_o|^2\,\frac{2}{\kappa a}\left[\frac{h}{a}\right]^3 \qquad (3.3.31)$$

where the dispersion relation, equation (3.2.8), has been used.

The Newman relations, equations (1.2.41)-(1.2.44), connecting the reflection and transmission coefficients for the scattering problem with the far field behaviour of the radiation problem, can now be used to

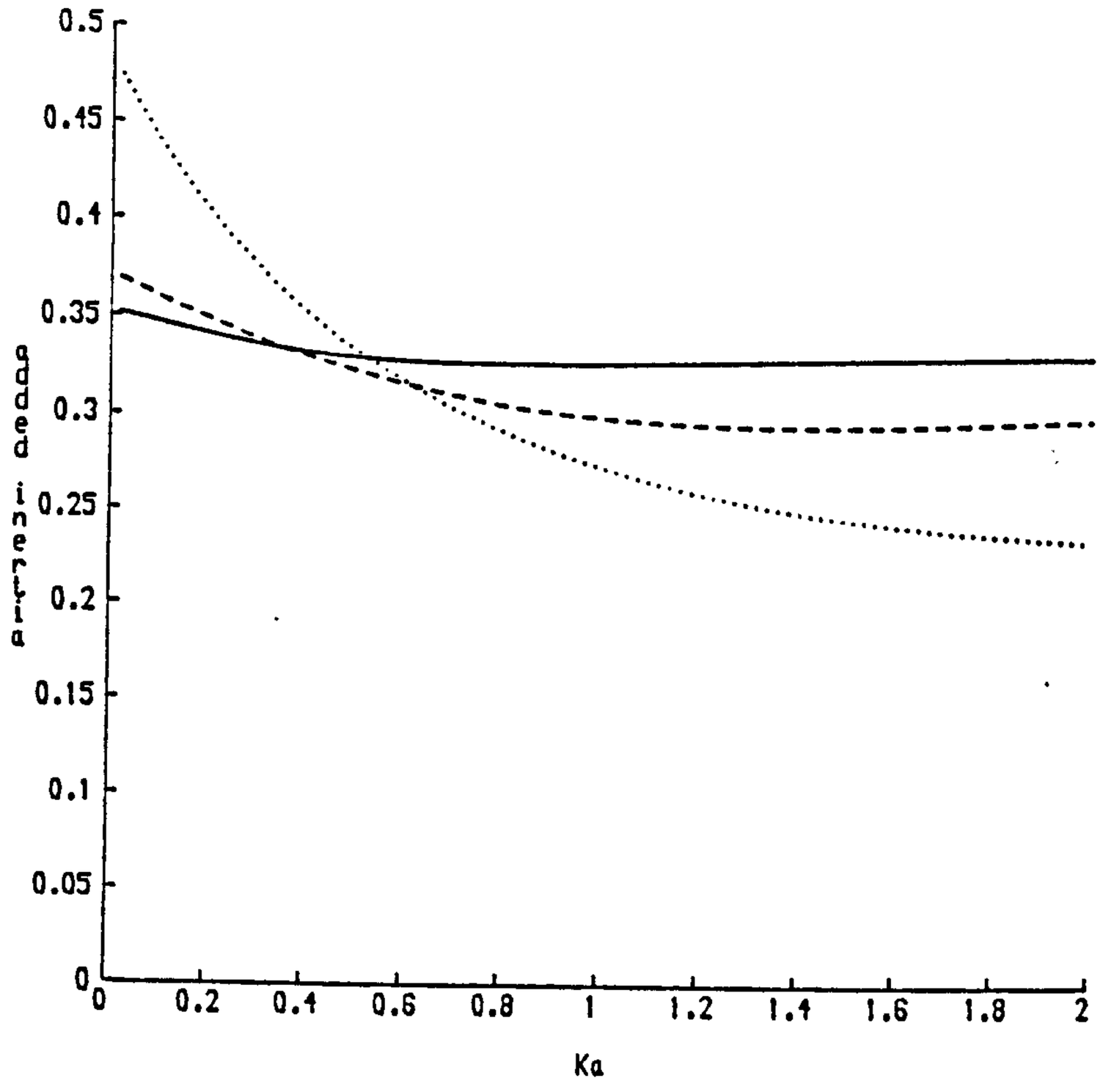

Figure 3.3.2. μ plotted against Ka for three vertical hinged plates. ——— a/h=0.3; – – – a/h=0.5; ····· a/h=0.8.

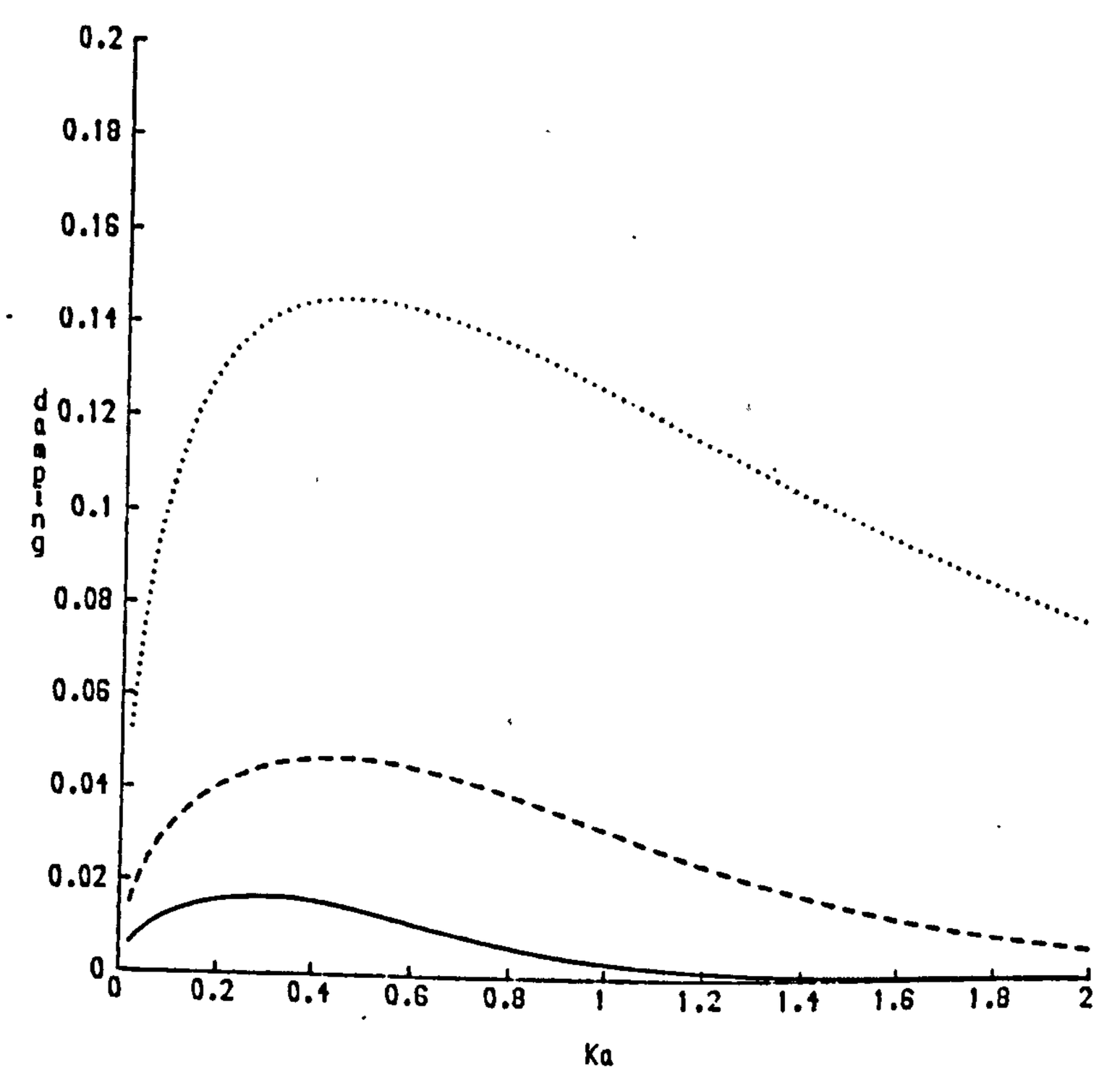

Figure 3.3.3. ν plotted against Ka for three vertical hinged plates. ——— a/h=0.3; – – – a/h=0.5; ····· a/h=0.8.

show that

$$R - T = C_o/\bar{C}_o. \tag{3.3.32}$$

In order to find expressions for R and T separately we must solve a symmetric problem as well as the antisymmetric problem solved here. Before this is done the case a = h will be examined, which should check with the simple wavemaker solution due to Havelock (1929).

If a = h then $D_{mn} = 0 \ \forall$ m,n so that M is the identity matrix. Therefore $X_n = Y_n$ and the coefficients C_n are given by

$$C_o = N_o^{-1/2}\left[\frac{\sinh \kappa h}{\kappa h} + \frac{1 - \cosh \kappa h}{(\kappa h)^2}\right]$$

$$C_n = N_n^{-1/2}\left[\frac{\sin k_n h}{k_n h} - \frac{1 - \cos k_n h}{(k_n h)^2}\right]. \qquad n = 1,2,... \tag{3.3.33}$$

It is straightforward to check that this solution is the same as the solution to the wavemaker problem. In this case the coefficients C_n n = 0,1,... are all real.

The quantities μ and ν in this case can be calculated using equation (3.3.28) with the values for C_n those given by equation (3.3.33). As the C_n's are all real the damping coefficient is given exactly by

$$\nu = 4(\kappa h)^{-1}\left[1 + \frac{\sinh 2\kappa h}{2\kappa h}\right]^{-1}\left[\frac{\sinh \kappa h}{\kappa h} + \frac{1 - \cosh \kappa h}{(\kappa h)^2}\right]^2$$

which shows that $\nu \sim (2\kappa h)^{-1}$ as $\kappa h \longrightarrow 0$. Figure (3.3.3) shows that the damping coefficient is not unbounded in this limit if a/h < 1 and thus the hydrodynamic characteristics of the plate must change dramatically as the plate approaches the free surface. This is not particularly surprising considering the fact that when a small gap

exists above a rolling plate it is likely that a substantial oscillatory flow will be generated above the plate. However when $a/h = 1$ this can no longer exist. A similar situation arises when a submerged cylinder approaches the bottom and this will be discussed in some detail in §4.4. Figures (3.3.4) and (3.3.5) show the change in μ and ν as $a/h \longrightarrow 1$.

As mentioned above it is necessary to solve a symmetric problem in order to be able to calculate R and T. Here a symmetric problem is one where the potentials $\phi^+(x,y)$ and $\phi^-(x,y)$ satisfy

$$\phi^+(x,y) = \phi^-(-x,y) \tag{3.3.34}$$

The symmetric problem that will be solved will be a boundary value problem for ϕ^+ :

$$\nabla^2 \phi^+ = 0 \qquad x > 0 \tag{3.3.35}$$

$$\phi^+ \sim A_s \frac{\cosh \kappa(h-y)}{\cosh \kappa h} e^{-i\kappa x} \qquad \text{as} \quad x \to \infty \tag{3.3.36}$$

$$\left.\frac{\partial \phi^+}{\partial x}\right|_{x=0} = \begin{cases} 0 & 0 < y < h-a \\ (h-y)\,\dfrac{U}{a} & h-a < y < h \end{cases} . \tag{3.3.37}$$

This problem can be solved explicitly using simple wavemaker theory as developed by Havelock (1929). The only value that is of interest is that of A_s which is given by

$$A_s = \frac{i \cosh \kappa h}{\kappa N_o} \left[\frac{\sinh \kappa a}{\kappa h} + \frac{1 - \cosh \kappa a}{\kappa a \, \kappa h} \right] \tag{3.3.38}$$

which is pure imaginary. It follows from the Newman relations that $R + T = 1$ and then equation (3.3.32) gives

$$R = \tfrac{1}{2}\,(1 + C_o/\bar{C}_o) \quad ; \quad T = \tfrac{1}{2}\,(1 - C_o/\bar{C}_o) \, . \tag{3.3.39}$$

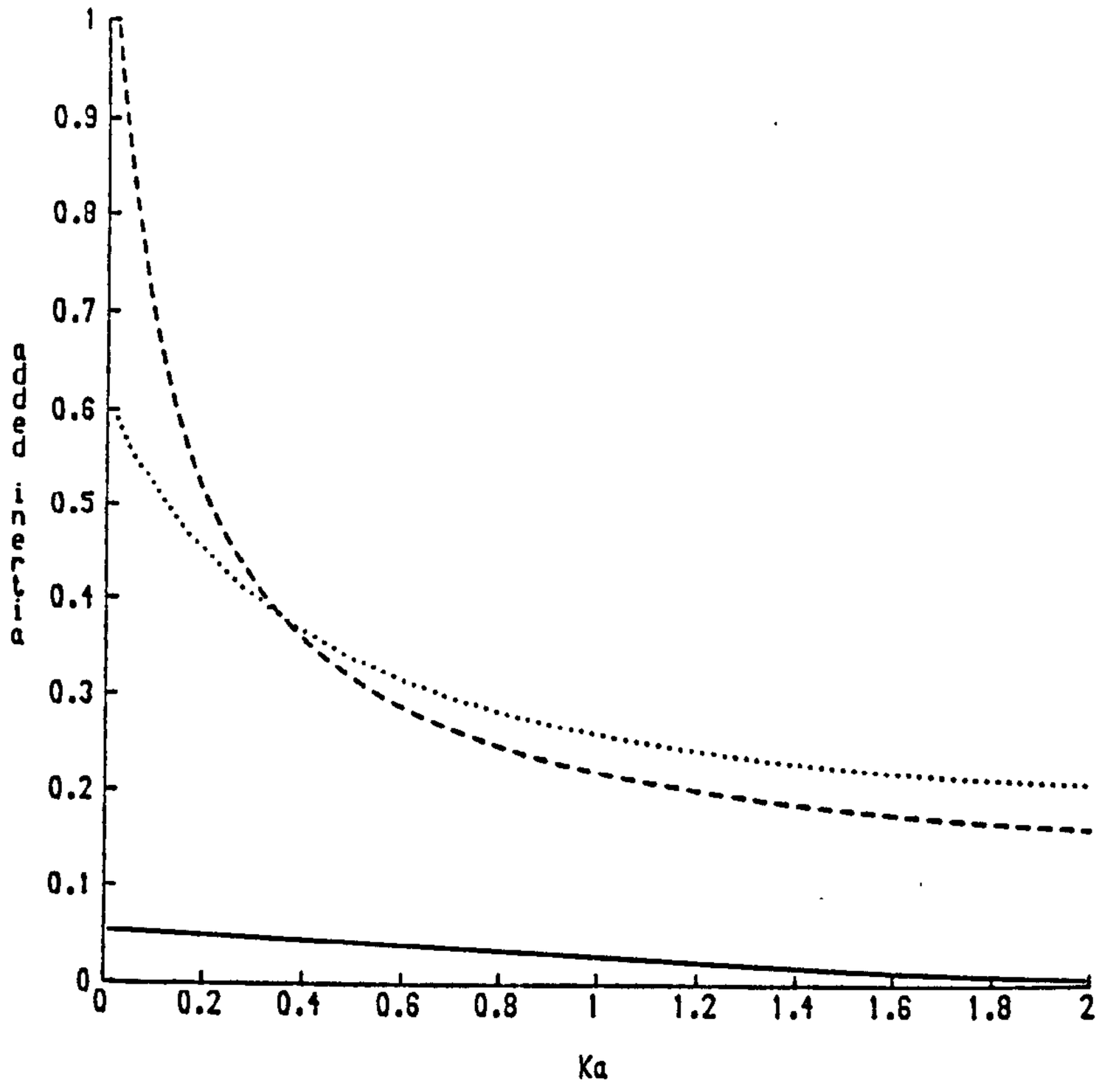

Figure 3.3.4. μ plotted against Ka for three vertical hinged plates. ····· a/h=0.9; – – – a/h=0.98; ——— a/h=1.

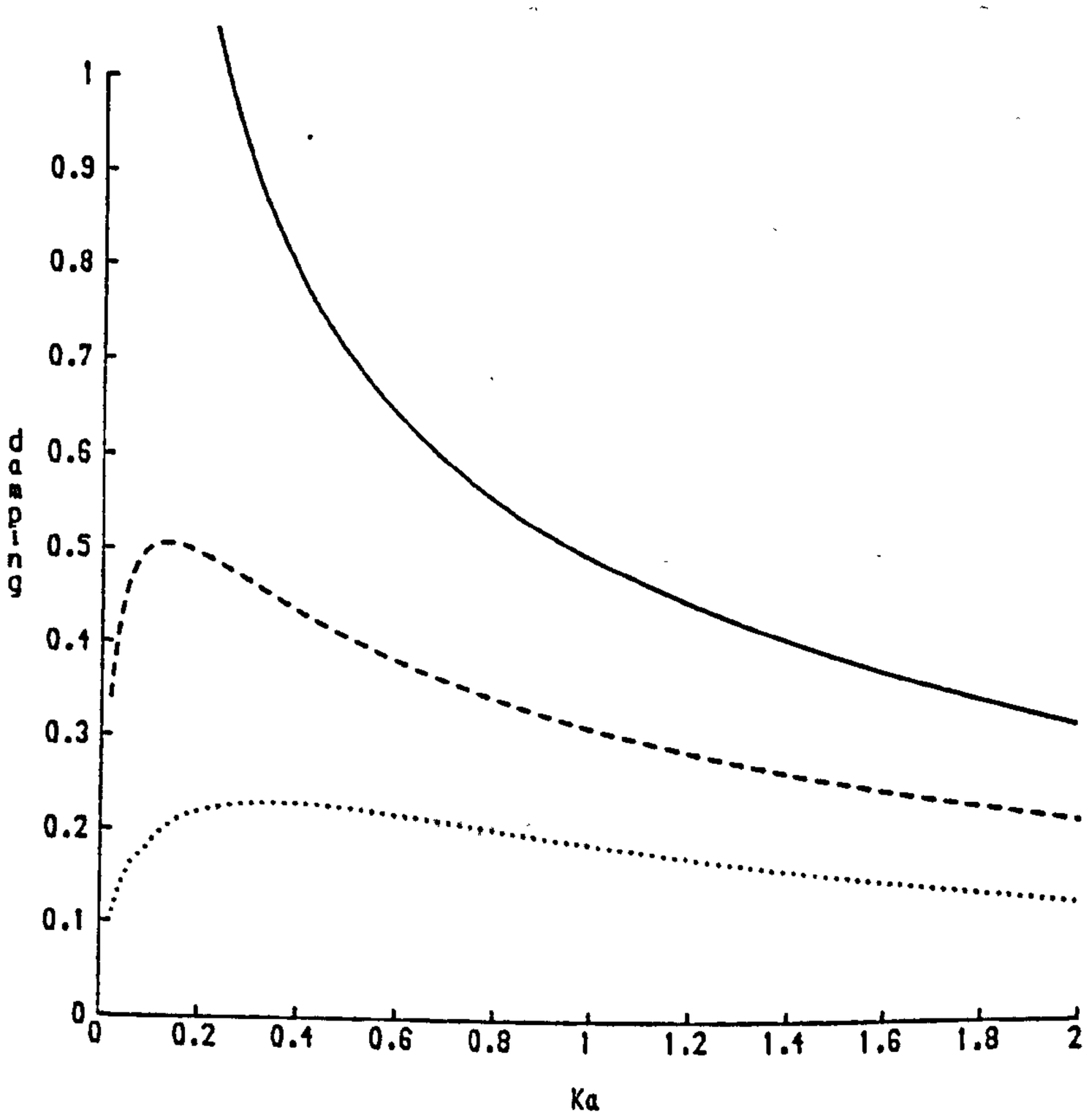

Figure 3.3.5. ν plotted against Ka for three vertical hinged plates. ····· a/h=0.9; – – – a/h=0.98; ——— a/h=1.

Figure (3.3.6) shows a curve of $|T|$ against Ka for three plates of different heights, the largest having a height equal to $4/5$ of the depth. The curve shows that as a fixed device a vertical plate not extending to the free surface is a poor reflector of waves.

3.4 Rectangular Block on the Sea Bed

In this section, as in the previous section, the method of matched eigenfunction expansions is used to solve a radiation problem. This time the problem concerned is that of a rectangular obstacle on the sea bed. Due to the symmetry of the obstacle it is only necessary to work in the region $x > 0$ with a suitable condition on $x = 0$.

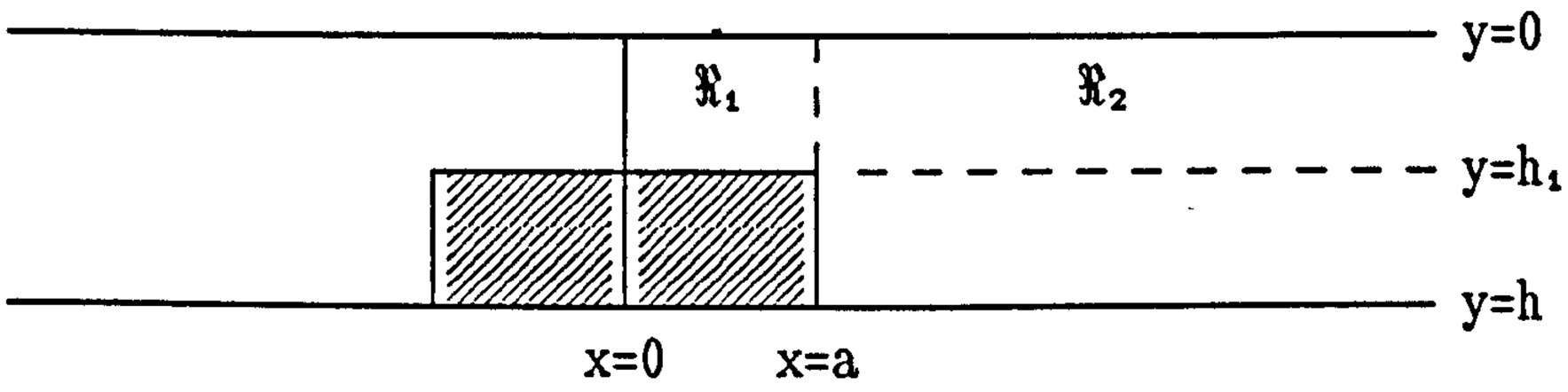

Figure 3.4.1

The problems of heave and sway will be considered simultaneously. Bracketed superscripts will be used to distinguish between the two problems with $^{(1)}$ referring to sway and $^{(2)}$ to heave. The fluid domain of interest is divided into two regions :

$$\Re_1 : 0<x<a,\ 0<y<h_1 \quad \text{and} \quad \Re_2 : a<x,\ 0<y<h\ .$$

The time-independent potential in $\Re_1$ will be written as $\phi_1^{(j)}$ $j = 1,2$ and that in $\Re_2$ as $\phi_2^{(j)}$ $j = 1,2$. The two boundary-value problems

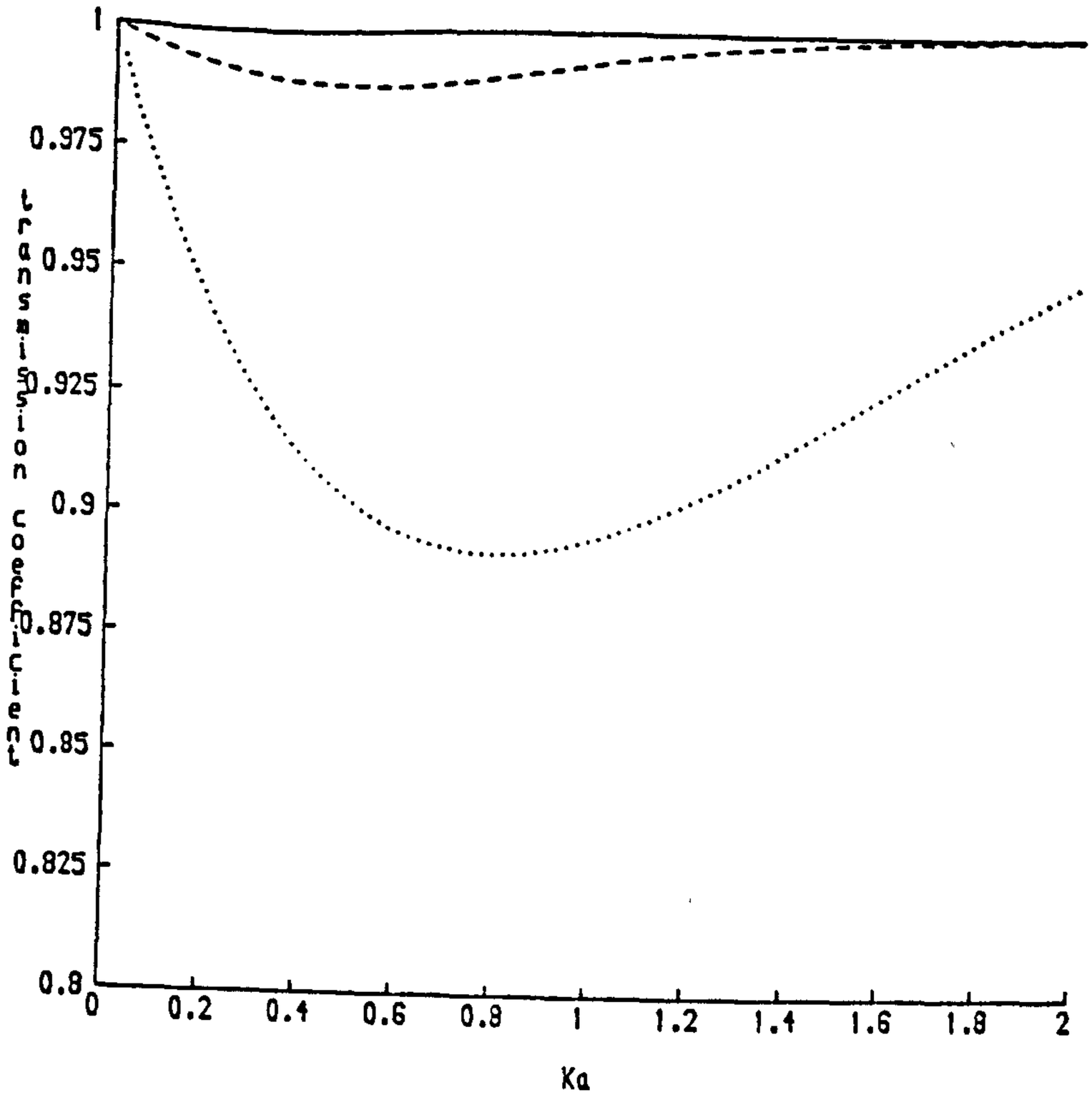

Figure 3.3.6. |T| plotted against Ka for three fixed vertical plates. ——— a/h=0.3; - - - a/h=0.5; ····· a/h=0.8.

are then given by

$$\nabla^2 \phi_i^{(j)} = 0 \qquad \text{in } \Re_1 \quad i,j=1,2 \tag{3.4.1}$$

$$K\phi_i^{(j)} + \frac{\partial \phi_i^{(j)}}{\partial y} = 0 \qquad \text{on } y=0 \quad i,j=1,2 \tag{3.4.2}$$

$$\frac{\partial \phi_2^{(j)}}{\partial y} = 0 \qquad \text{on } y=h, \ a<x \quad j=1,2 \tag{3.4.3}$$

$$\phi_1^{(j)} = \phi_2^{(j)} \qquad \text{on } x=a, \ 0<y<h_1 \quad j=1,2 \tag{3.4.4}$$

$$\frac{\partial \phi_1^{(2)}}{\partial y} = U^{(2)} \qquad \text{on } y=h_1, \ 0<x<a \tag{3.4.5}$$

$$\frac{\partial \phi_1^{(1)}}{\partial y} = 0 \qquad \text{on } y=h_1, \ 0<x<a \tag{3.4.6}$$

$$\frac{\partial \phi_1^{(2)}}{\partial x} = 0 \qquad \text{on } x=0, \ 0<y<h_1 \tag{3.4.7}$$

$$\phi_1^{(1)} = 0 \qquad \text{on } x=0, \ 0<y<h_1 \tag{3.4.8}$$

$$\left.\frac{\partial \phi_2^{(j)}}{\partial x}\right|_{x=a} = \begin{cases} \left.\dfrac{\partial \phi_1^{(j)}}{\partial x}\right|_{x=a} & 0<y<h_1 \\ U^{(1)}\delta_{j1} & h_1<y<h \end{cases} . \tag{3.4.9}$$

In order to solve this problem two complete orthogonal sets of functions will be required, one for the region $\Re_1$ and one for $\Re_2$. These will be denoted by $f_n(y)$ and $g_n(y)$ $n=0,1,2,\ldots$ respectively. Thus

$$f_n(y) = N_n^{-1/2} \cos \alpha_n(y - h_1) \qquad n=0,1,2,\ldots$$

$$N_n = \frac{1}{2}\left[1 + \frac{\sin 2\alpha_n h_1}{2\alpha_n h_1}\right]$$

$$\alpha_n \tan \alpha_n h_1 + K = 0$$

$$g_n(y) = M_n^{-1/2} \cos \beta_n(y - h) \qquad n=0,1,2,\ldots$$

$$M_n = \frac{1}{2}\left[1 + \frac{\sin 2\beta_n h}{2\beta_n h}\right]$$

$$\beta_n \tan \beta_n h + K = 0 \ .$$

The constants α_n and β_n $n > 0$ are real and positive but α_0 and β_0 are pure imaginary and correspond to the wavenumbers κ_1 and κ for the two different fluid regions:

$$\alpha_0 = i\kappa_1$$

$$\beta_0 = i\kappa \ .$$

For further detail see §3.3.

Due to the nature of the boundary conditions we write

$$\phi_1^{(2)} = U^{(2)}\left[y - \frac{1}{K} + \sum_{n=0}^{\infty} A_n^{(2)} \frac{\cosh \alpha_n x}{\alpha_n \sinh \alpha_n a} f_n(y)\right], \qquad (3.4.10)$$

where the first two terms are included so as to satisfy the inhomogeneous condition on $y = h_1$, $0 < x < a$ and the free surface condition,

$$\phi_1^{(1)} = U^{(1)} \sum_{n=0}^{\infty} A_n^{(1)} \frac{\sinh \alpha_n x}{\alpha_n \cosh \alpha_n a} f_n(y) \qquad (3.4.11)$$

$$\phi_2^{(j)} = U^{(j)} \sum_{n=0}^{\infty} B_n^{(j)} \frac{\exp(-\beta_n(x-a))}{-\beta_n} g_n(y) \qquad (3.4.12)$$

$j=1,2.$

With this choice all the boundary conditions of the problem are satisfied except those on the boundary between the two regions, namely equations (3.4.4) and (3.4.9). Equation (3.4.4) gives

$$y - \frac{1}{K} + \sum_{n=0}^{\infty} A_n^{(2)} \frac{\coth \alpha_n a}{\alpha_n} f_n(y) = - \sum_{n=0}^{\infty} B_n^{(2)} \frac{g_n(y)}{\beta_n} \qquad (3.4.13)$$

and

$$\sum_{n=0}^{\infty} A_n^{(1)} \frac{\tanh \alpha_n a}{\alpha_n} f_n(y) = - \sum_{n=0}^{\infty} B_n^{(1)} \frac{g_n(y)}{\beta_n} \; . \qquad (3.4.14)$$

Both of these equations must be valid in the region $0 < y < h_1$. In order to simplify the algebra we define

$$C_{mn} = \frac{1}{h_1} \int_0^{h_1} f_m(y) \; g_n(y) \; dy \; . \qquad (3.4.15)$$

Multiplying by $f_m(y)$ and integrating equations (3.4.13) and (3.4.14) over the range 0 to h_1 then leads to

$$A_m^{(2)} + \frac{h}{h_1} \alpha_m h_1 \tanh \alpha_m a \sum_{n=0}^{\infty} B_n^{(2)} \frac{C_{mn}}{\beta_n h} = - \frac{\tanh \alpha_m a}{\alpha_m h_1 \; N_m^{1/2}} \qquad (3.4.16)$$

$$A_m^{(1)} + \frac{h}{h_1} \alpha_m h_1 \coth \alpha_m a \sum_{n=0}^{\infty} B_n^{(1)} \frac{C_{mn}}{\beta_n h} = 0 \qquad (3.4.17)$$

$$m=0,1,2,\ldots$$

where the inhomogeneity in the first equation is due to the term $y - 1/K$ in the expression for the potential.

The boundary condition concerning the horizontal fluid velocity on the line $x = a$ is now applied. This results in another equation

connecting the A's and the B's:

$$B_k^{(j)} = \frac{h_1}{h} \sum_{n=0}^{\infty} A_n^{(j)} C_{nk} + \delta_{j1} \frac{M_k^{-1/2}}{\beta_k h} \sin \beta_k (h-h_1). \qquad (3.4.18)$$

Combining equation (3.4.18) with equations (3.4.16) and (3.4.17) leads to the following system of equations:

$$A_m^{(2)} + \alpha_m h_1 \tanh \alpha_m a \sum_{n=0}^{\infty} D_{mn} A_n^{(2)} = - \frac{\tanh \alpha_m a}{\alpha_m h_1 N_m^{1/2}} \qquad (3.4.19)$$

$$A_m^{(1)} + \frac{\alpha_m h_1}{\tanh \alpha_m a} \sum_{n=0}^{\infty} D_{mn} A_n^{(1)} = - \frac{h}{h_1} \frac{\alpha_m h_1}{\tanh \alpha_m a} \sum_{k=0}^{\infty} C_{mk} \frac{\sin \beta_k (h-h_1)}{(\beta_k h)^2 M_k^{1/2}}$$

$$m=0,1,2,... \qquad (3.4.20)$$

where

$$D_{mn} = \sum_{k=0}^{\infty} \frac{C_{nk} C_{mk}}{\beta_k h} .$$

This infinite system of equations for $A_m^{(j)}$ is solved using the same truncation procedure as described in §3.3. It was found that truncating all the series to ten terms gave accuracy to within at least 1%.

The force in the direction of motion is given by

$$X_R^{(2)} = 2\rho\omega i U^{(2)} \int_0^a \phi_1^{(2)}(x,h_1)\, dx \qquad (3.4.21)$$

$$X_R^{(1)} = 2\rho\omega i U^{(1)} \int_{h_1}^{h} \phi_2^{(1)}(a,y)\, dy \qquad (3.4.22)$$

and this leads to the following expressions for the added-mass and damping coefficients (non-dimensionalised with respect to the mass of

fluid displaced by the block):

$$\mu^{(2)} - i\nu^{(2)} = \frac{h_1}{h-h_1}\left[1 - \frac{1}{Kh_1} - \frac{A_0^{(2)}}{\kappa_1 a\ \kappa_1 h_1\ N_0^{1/2}} + \sum_{n=1}^{\infty} \frac{A_n^{(2)}}{\alpha_n a\ \alpha_n h_1\ N_n^{1/2}}\right] \quad (3.4.23)$$

$$\mu^{(1)} - i\nu^{(1)} = \frac{h}{h-h_1} \sum_{n=0}^{\infty} \frac{B_n^{(1)}}{\beta_n a\ \beta_n h\ M_n^{1/2}} \sin \beta_n(h_1-h) \ . \quad (3.4.24)$$

In order to use equation (3.4.24) it is necessary to evaluate the B's in terms of the A's. This is done using equation (3.4.18).

It is important to note what problem is actually being solved in the heave case. No account has been taken of the fact that as the block moves upwards a gap will be created at the bottom which would result in another region of fluid. In fact the problem that has been solved is that of a block that is continually changing shape so that it remains in contact with the bottom while the top oscillates.

Some curves of μ and ν, plotted against Kh are shown in figures (3.4.2)-(3.4.5). The heaving block exhibits the phenomenon of negative added mass when the block is close to the free surface. This phenomenon has been discussed in detail by McIver and Evans (1984). In an appendix they prove the following result due to Falnes (unpublished note):

$$T - V = \tfrac{1}{4}MU^2 \quad (3.4.25)$$

where T and V are respectively the kinetic and potential energies of the total fluid motion averaged over a period, M is the added mass and U is the velocity amplitude of a body oscillating in a single mode of motion. At large depths of submergence the effect of the free surface, and hence V, is negligible and so M is positive. Clearly however if the effect of the free surface is such that $V > T$ then negative added mass will result. It should also be noted that the long wave limits of

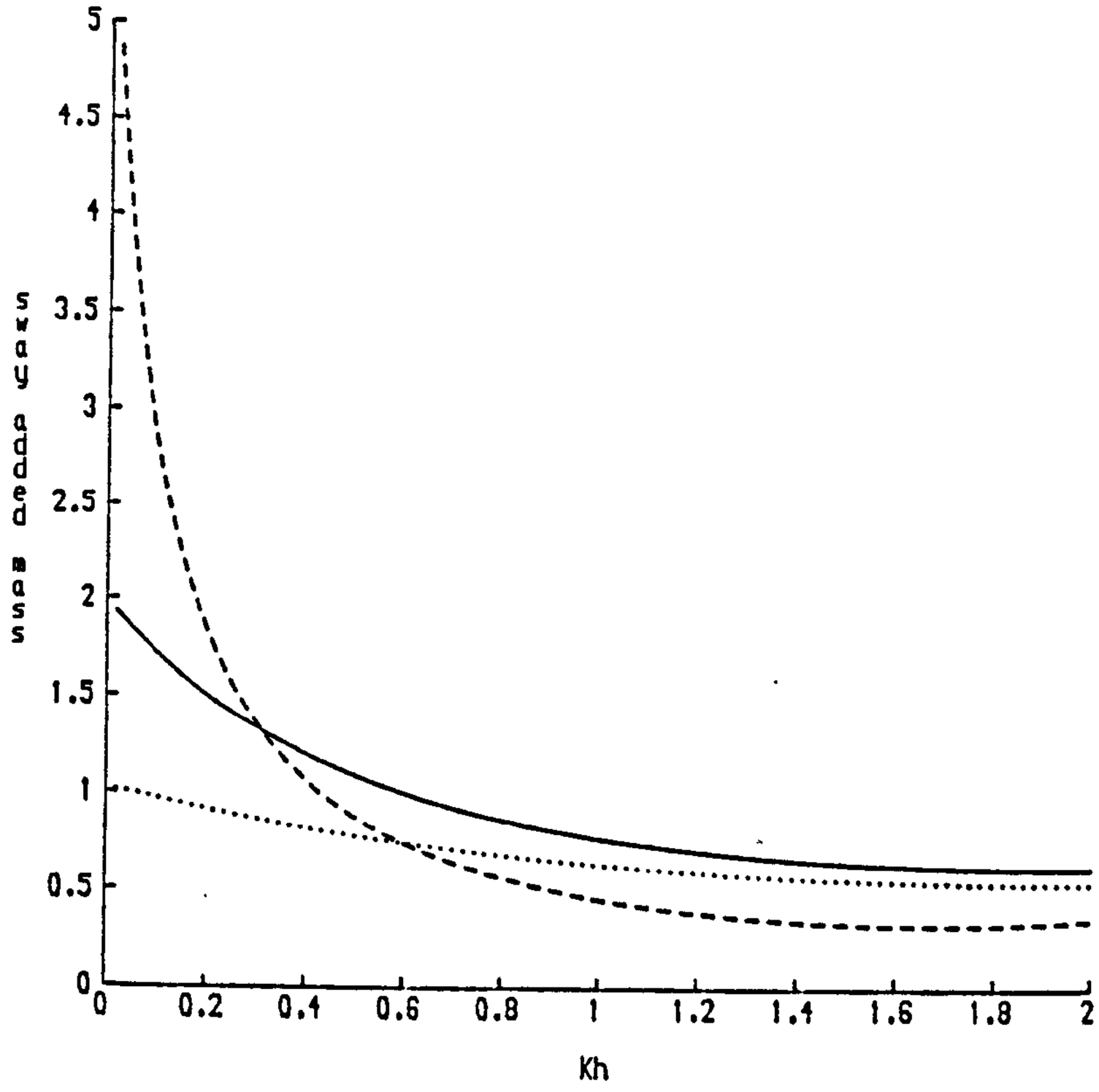

Figure 3.4.2. μ (sway) plotted against Kh for three blocks. In all cases a/h=0.5. – – – h_1/h=0.2; ——— h_1/h=0.5; ····· h_1/h=0.7.

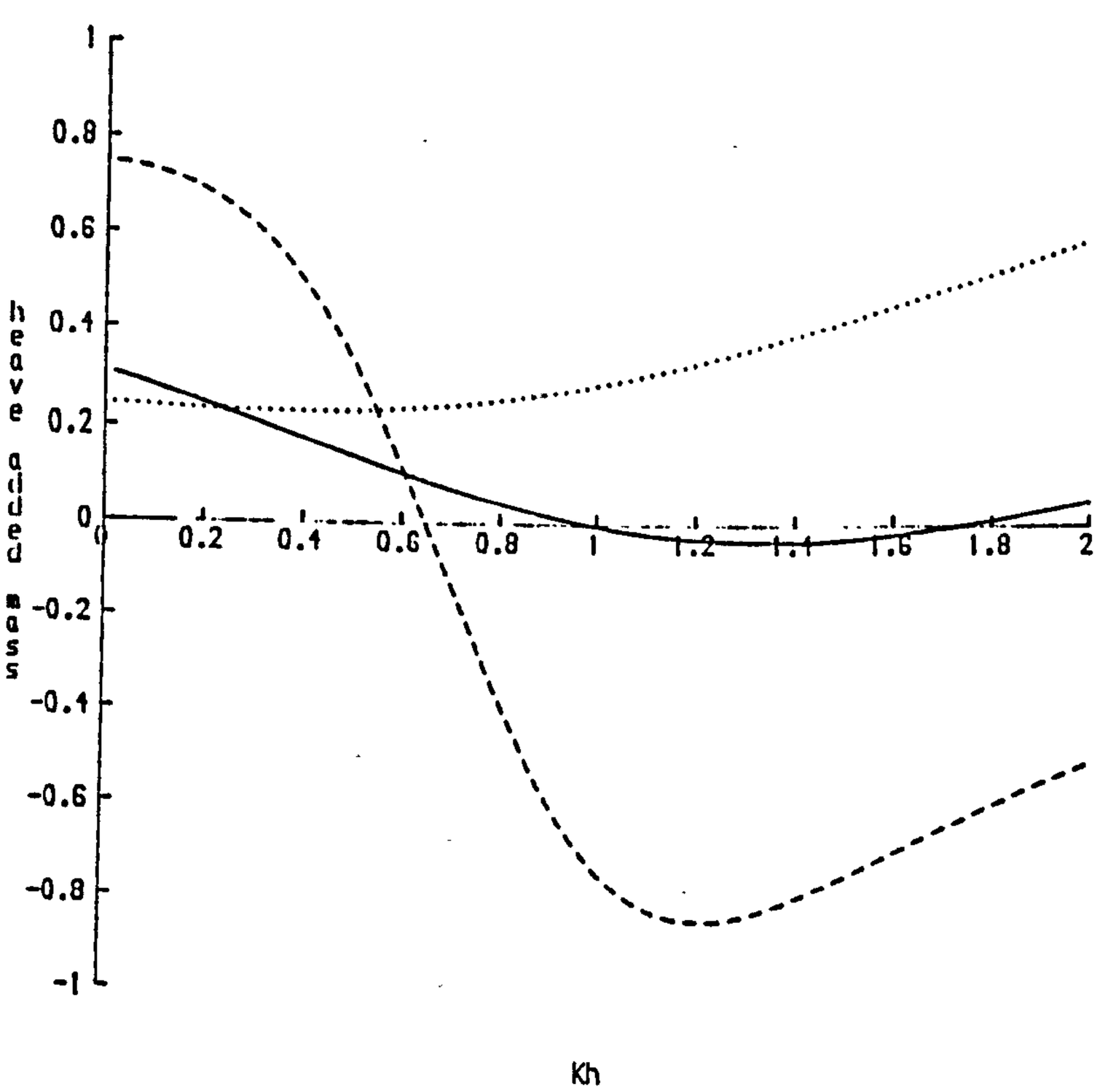

Figure 3.4.3. μ (heave) plotted against Kh for three blocks. In all cases a/h=0.5. – – – h_1/h=0.2; ——— h_1/h=0.5; ····· h_1/h=0.7.

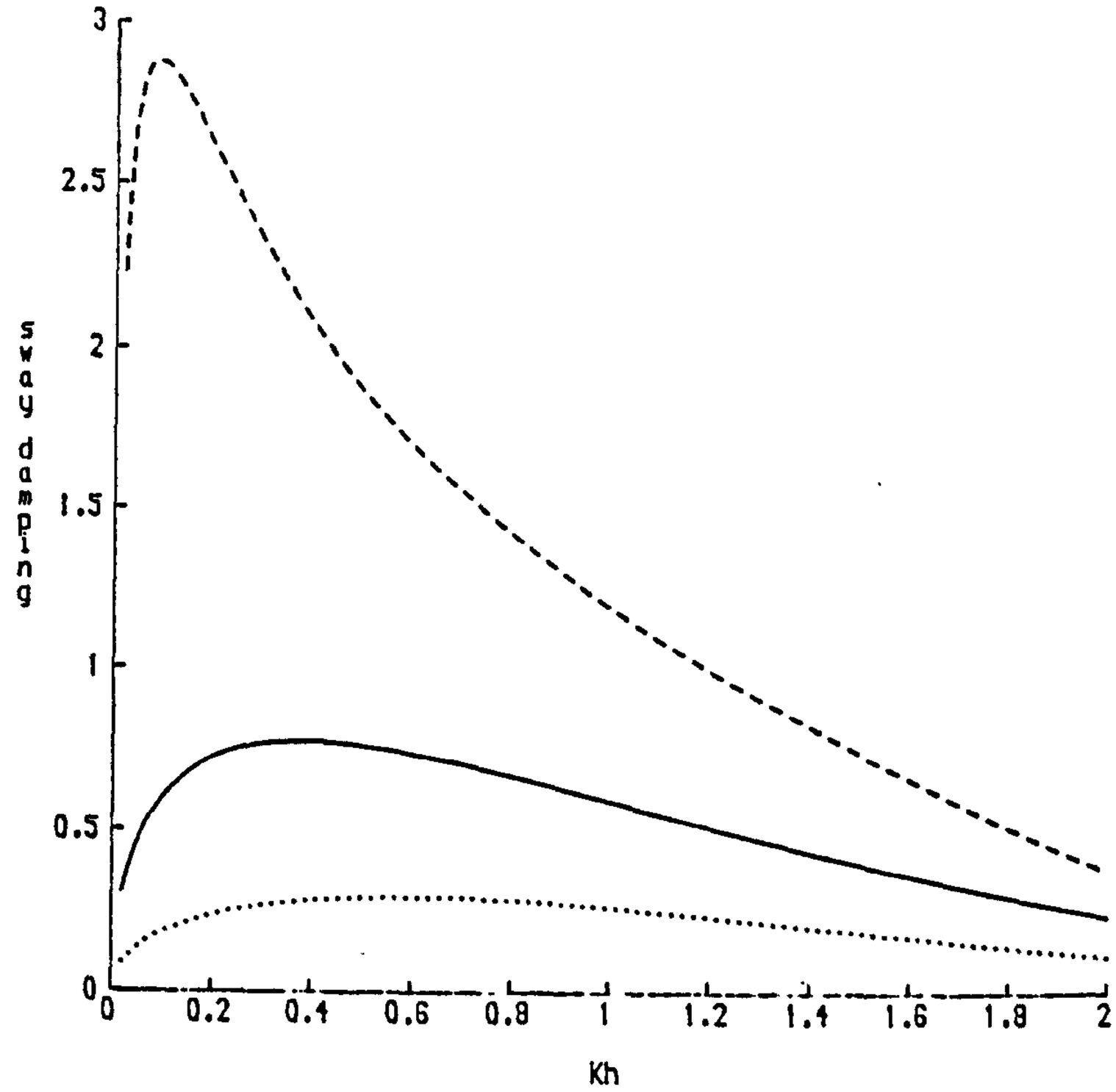

Figure 3.4.4. ν (sway) plotted against Kh for three blocks. In all cases a/h=0.5. – – – h_1/h=0.2; ——— h_1/h=0.5; ····· h_1/h=0.7.

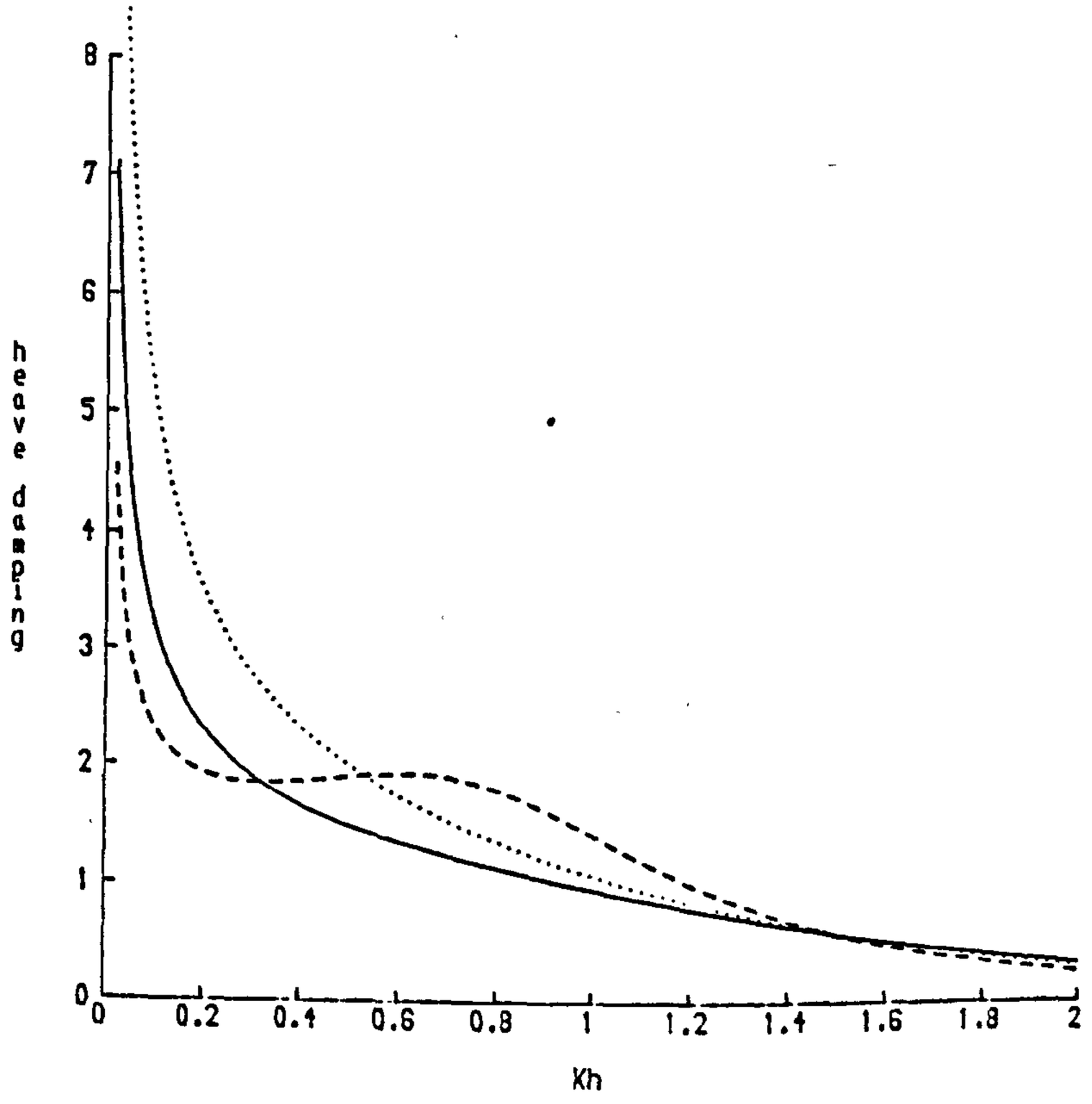

Figure 3.4.5. ν (heave) plotted against Kh for three blocks. In all cases a/h=0.5. – – – h_1/h=0.2; ——— h_1/h=0.5; ····· h_1/h=0.7.

the heave added mass differ from results obtained by Bai (1977) for the case of a block immersed through the free surface. A careful analysis of the zero frequency limit shows that the two problems are not in fact equivalent.

Equation (3.4.12) implies that as $x \longrightarrow \infty$

$$\phi^{(j)} \sim i\kappa^{-1} U^{(j)} B_0^{(j)} e^{-i\kappa(x-a)} g_0(y) \qquad (3.4.26)$$

and so if it is assumed that as $x \longrightarrow \infty$

$$\phi^{(j)} \sim U^{(j)} A_+^{(j)} e^{-i\kappa x} \frac{\cosh \kappa(y-h)}{\cosh \kappa h}$$

the following expression is obtained for the complex amplitude:

$$A_+^{(j)} = iB_0^{(j)} e^{i\kappa a} \frac{\cosh \kappa h}{\kappa M_0^{1/2}} . \qquad (3.4.27)$$

The Newman relations, equations (1.2.41)-(1.2.44), therefore give

$$R + (-1)^j T = - A_+^{(j)}/\bar{A}_+^{(j)} = e^{2i\kappa a} B_0^{(j)}/\bar{B}_0^{(j)} . \qquad (3.4.28)$$

As in the previous section, the relation between the damping coefficient and the far field amplitudes, equation (1.2.32), can and was used to provide a check on the calculations. In this case the identity obtained is

$$\nu^{(j)} = \frac{h}{h-h_1} \frac{|B_0^{(j)}|^2}{\kappa a} . \qquad (3.4.29)$$

The results obtained for R and T were also checked against curves shown in McIver (1985) who solved the scattering problem for the block by the same method.

3.5 Comparison with Shallow Water Theory

Lamb (1932) p. 262 used the shallow water approximation to solve the two-dimensional problem of wave reflection by a step. The following statement is added in a footnote: "It will be understood that the problem admits only an approximate treatment, on account of the rapid change in the character of the motion near the point of discontinuity."

The shallow water equations, by assuming that horizontal velocity does not vary with depth, are obviously inadequate in problems with sudden depth changes. Tuck (1976) looked at this problem and showed how progress can be made by considering a small region encompassing the depth change and using matching techniques to match the solution obtained in this region to the standard solution obtained from the 'outer' region.

In chapter 2 the shallow water equations are used, without any such refinement, to solve problems with rectangular blocks on the sea bed. The results for the reflection and transmission coefficients for a single block can now be compared with those from the full linear theory given by equation (3.4.28). Figure (3.5.1) shows such a comparison for three blocks of different heights. The results show that, as expected, the shallow water approximation is not that good for this problem, but in the region $0 < Kh < 0.3$ where the shallow water equations should be most applicable the results are accurate to within a few percent.

3.6 Results

The condition for zero transmission is given by equation (3.2.30) which is

$$\lambda = (M + I)\omega^2 \mp B\omega\chi$$

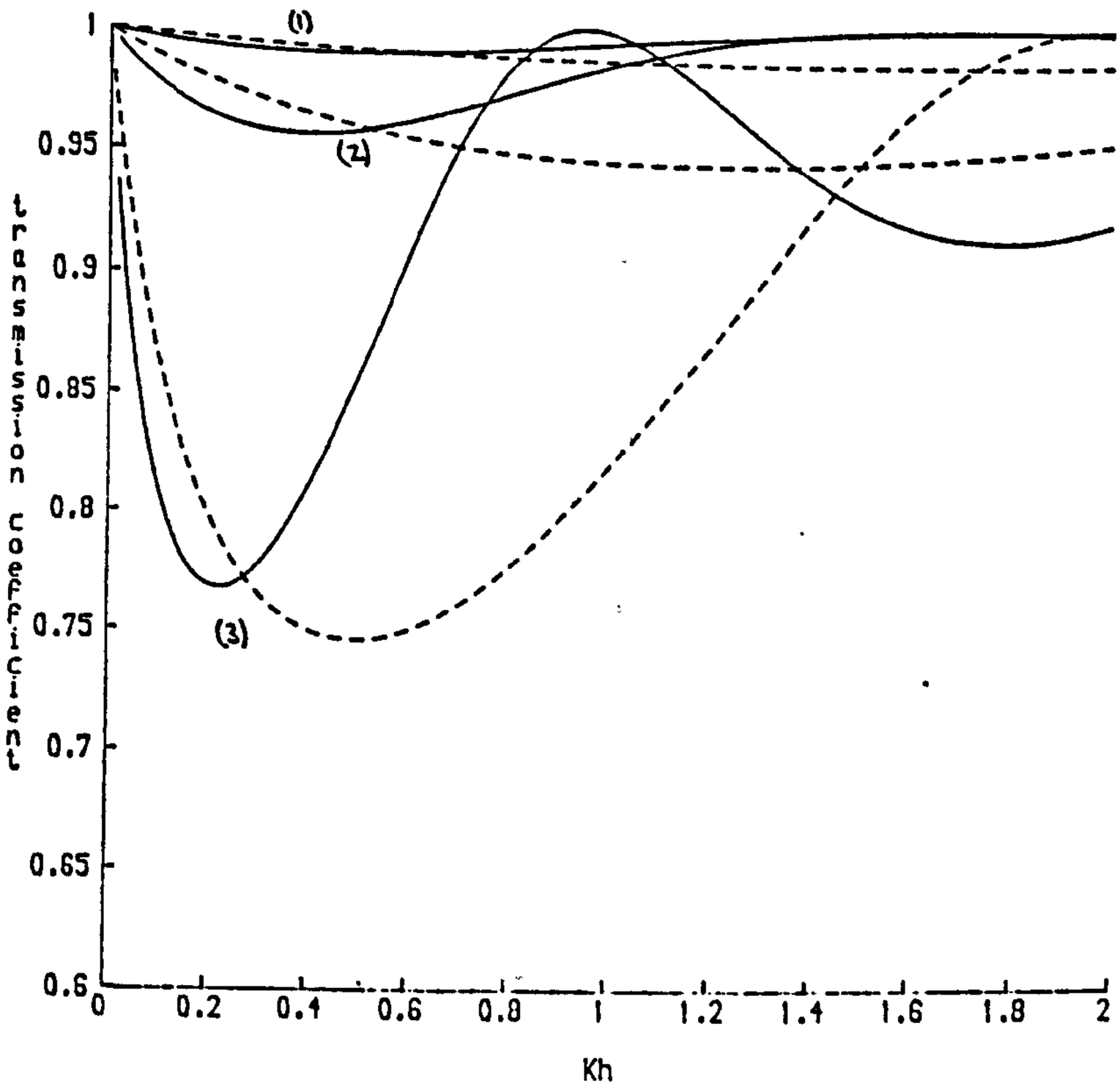

Figure 3.5.1. Comparison between shallow water and full linear theory. $|T|$ plotted against Kh for three blocks. In all cases $a/h=0.5$. ——— full linear theory; - - - shallow water theory. (1) $h_1/h=0.7$; (2) $h_1/h=0.5$; (3) $h_1/h=0.2$.

with the upper sign for heave and the lower for sway and roll. Thus if a body is tuned to a frequency ω_o, the force constant, λ, must be given by

$$\lambda = (M_o + I)\omega_o^2 \mp B_o\omega_o\chi_o \qquad (3.6.1)$$

in an obvious notation. The transmission coefficient, $|T_1|$, is given by equation (3.2.28) and this can now be written

$$T_1 = T\,\frac{(M + I)\omega^2 - (M_o + I)\omega_o^2 \mp B_o\omega_o\chi_o \mp B\omega\chi}{(M + I)\omega^2 - (M_o + I)\omega_o^2 \mp B_o\omega_o\chi_o - iB\omega}\,. \qquad (3.6.2)$$

It is convenient to non-dimensionalise the quantities that appear in this equation. If M' is used to represent a typical fluid mass or inertia then a suitable non-dimensionalisation is given by

$$I = M's \quad ; \quad M = M'\mu \quad ; \quad B = M'\omega\nu.$$

The resulting expression for T_1 is then

$$T_1 = T\,\frac{(\mu + s) \pm \nu\chi - \{(\mu_o + s) \mp \nu_o\chi_o\}(\omega_o/\omega)^2}{(\mu + s) - i\nu - \{(\mu_o + s) \mp \nu_o\chi_o\}(\omega_o/\omega)^2}\,. \qquad (3.6.3)$$

In §§3.3 and 3.4 methods for the calculation of μ, ν, χ and T were discussed for two simple cases and these results can now be used in equation (3.6.3) to see what sort of results can be obtained from such devices. In the case of the vertical hinged plate of length a the inertia used for M' was ρa^4 (see equation (3.3.27)), whilst for the block of length $2a$ and height $h - h_1$ the mass of displaced water was used, i.e. $M' = 2\rho a(h - h_1)$, (see equations (3.4.23) and (3.4.24)). For the block therefore s represents the specific gravity and in the results shown we will assume that the block is neutrally buoyant so that $s = 1$. For the vertical hinged plate s is the ratio of the mass of

the plate to the mass of a large block of fluid and is clearly going to be small. In the calculations $s = 0$ is used. Note that the method for generating the appropriate force constant, λ, is not discussed. It is assumed that such a restoring force can be created by some means. In chapter 4, when we will examine a device in much more detail, this problem will be addressed.

Let us start with a vertical plate hinged at the sea bed which is allowed to perform rolling motions in response to an incident wave. Let us further assume that some sort of restoring force is in operation that results in the body being 'tuned', in the sense that equation (3.2.30) is satisfied, with, say $Kh \equiv \omega^2 h/g = 1$. Figure (3.6.1) shows curves of $|T_1|$ against non-dimensional frequency, Kh, for three different plate lengths: $a/h = 0.3$, 0.5 and 0.8. All the curves satisfy $|T_1| = 0$ at $Kh = 1$ but the bandwidth of frequencies over which $|T_1|$ is small is narrow when $a/h \leq 0.5$. Nevertheless the increased reflection being achieved here is a great improvement on the amount of reflection that was obtained from fixed devices in chapter 2. The results also compare very favourably with those presented by Leach et al. (1985) for the rolling plate that extends through the free surface and is subject to a restoring force provided by cables connecting the top of the plate to the sea bed on either side of the hinge. In their paper curves are shown which indicate a large degree of reflection but predominantly in the short wave régime ($Kh > 4$). (Clearly if the mooring forces are stiff enough the whole device will be rigid and since the plate extends through the free surface total reflection will result). In the case considered here however, large amounts of reflection can be achieved with waves of more typical frequencies ($Kh < 2$) even when the plate is well clear of the free surface.

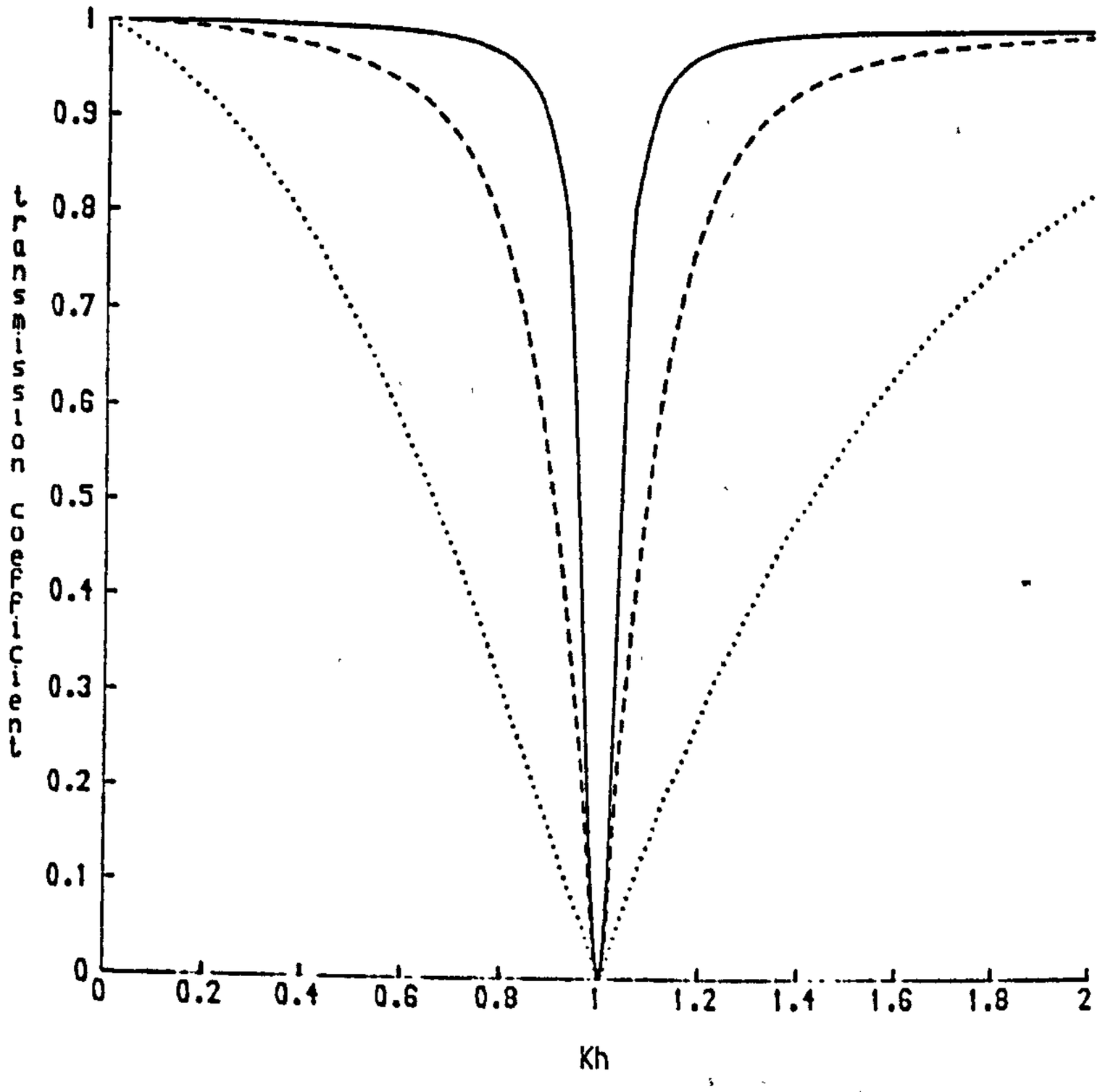

Figure 3.6.1. $|T_1|$ plotted against Kh for three vertical hinged plates all tuned to Kh=1. ——— a/h=0.3; – – – a/h=0.5; ····· a/h=0.8

The results for the block are better. Figure (3.6.2) shows the case of a block in sway while the case of a heaving block is shown in figure (3.6.3), both for three different clearances: $h_1/h = 0.2$, 0.5, and 0.7. In all cases the parameter a/h was taken to be 0.5 and thus the block length is equal to the water depth. Again the curves are shown against Kh and here also it is assumed that all the blocks are tuned to $Kh = 1$.

The results for the large swaying block are remarkably good with near perfect reflection being achieved at two points other than the tuning frequency. Other examples of this phenomenon are given in §4.7. Even in the other cases the bandwidth of the curves is greater than those achieved by the rolling plate especially in the case of heave.

Clearly the reflection capabilities of a device that is allowed to move in response to the incoming waves are much greater than those of fixed obstacles. In chapter 4 we will take a particular object, a submerged cylinder, and examine the reflection properties in more detail.

3.7 Real Seas

So far the waves incident on a body have been assumed to be monochromatic, i.e. consisting of just one frequency. This is clearly not the case in the open ocean or in harbours, where a whole spectrum of waves of different heights, frequencies and directions will exist. The problem of modelling a real sea is not an easy one and much has been written on the subject. In this section some of the most important aspects of the problem will be discussed and then a description of how to adapt the theory from §3.2 will be given. For a detailed discussion together with a comprehensive bibliography see Carter et al. (1986).

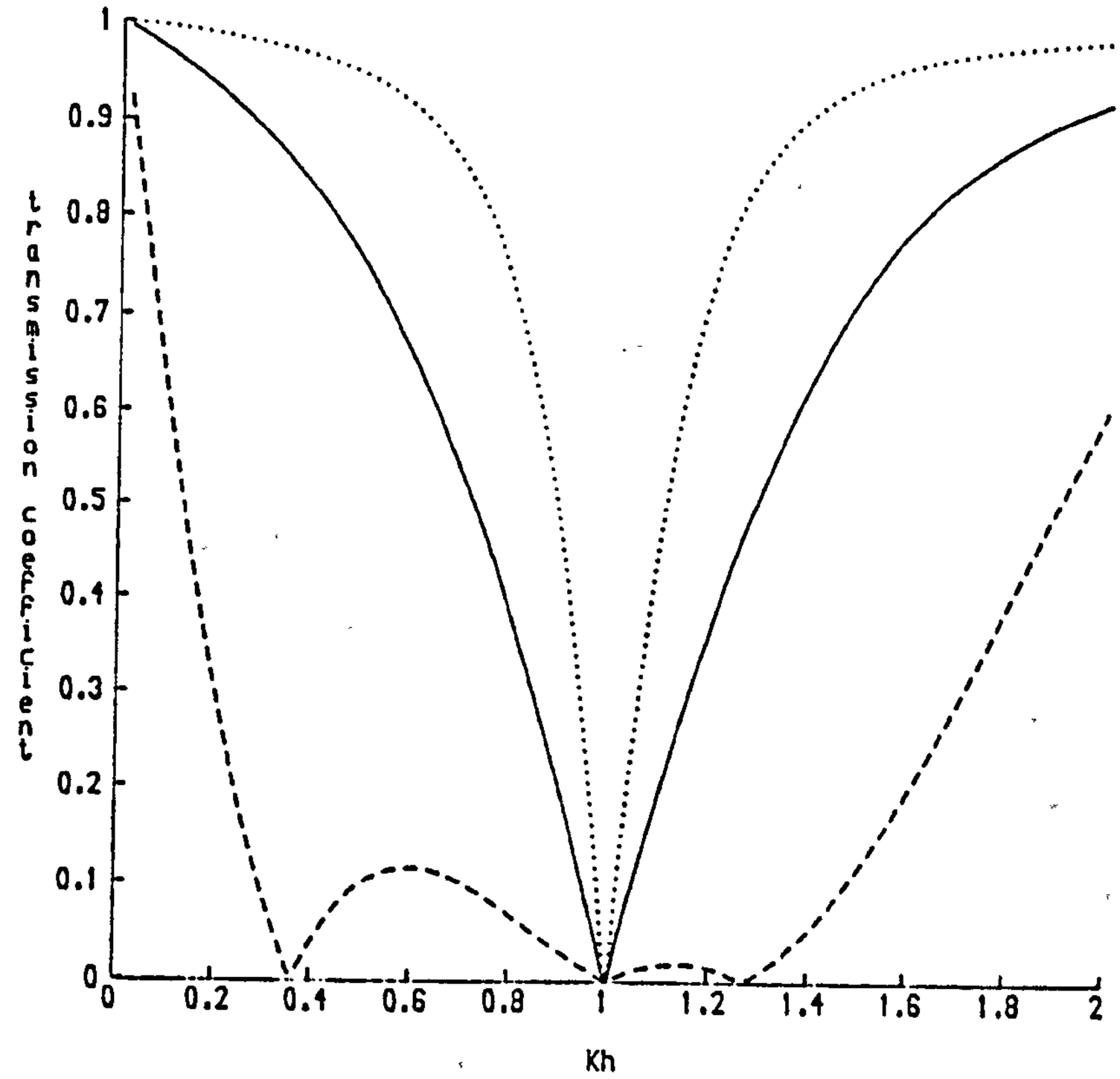

Figure 3.6.2. $|T_1|$ plotted against Kh for three swaying blocks all tuned to Kh=1. In all cases a/h=0.5. ····· h_1/h=0.7; ——— h_1/h=0.5; – – – h_1/h=0.2.

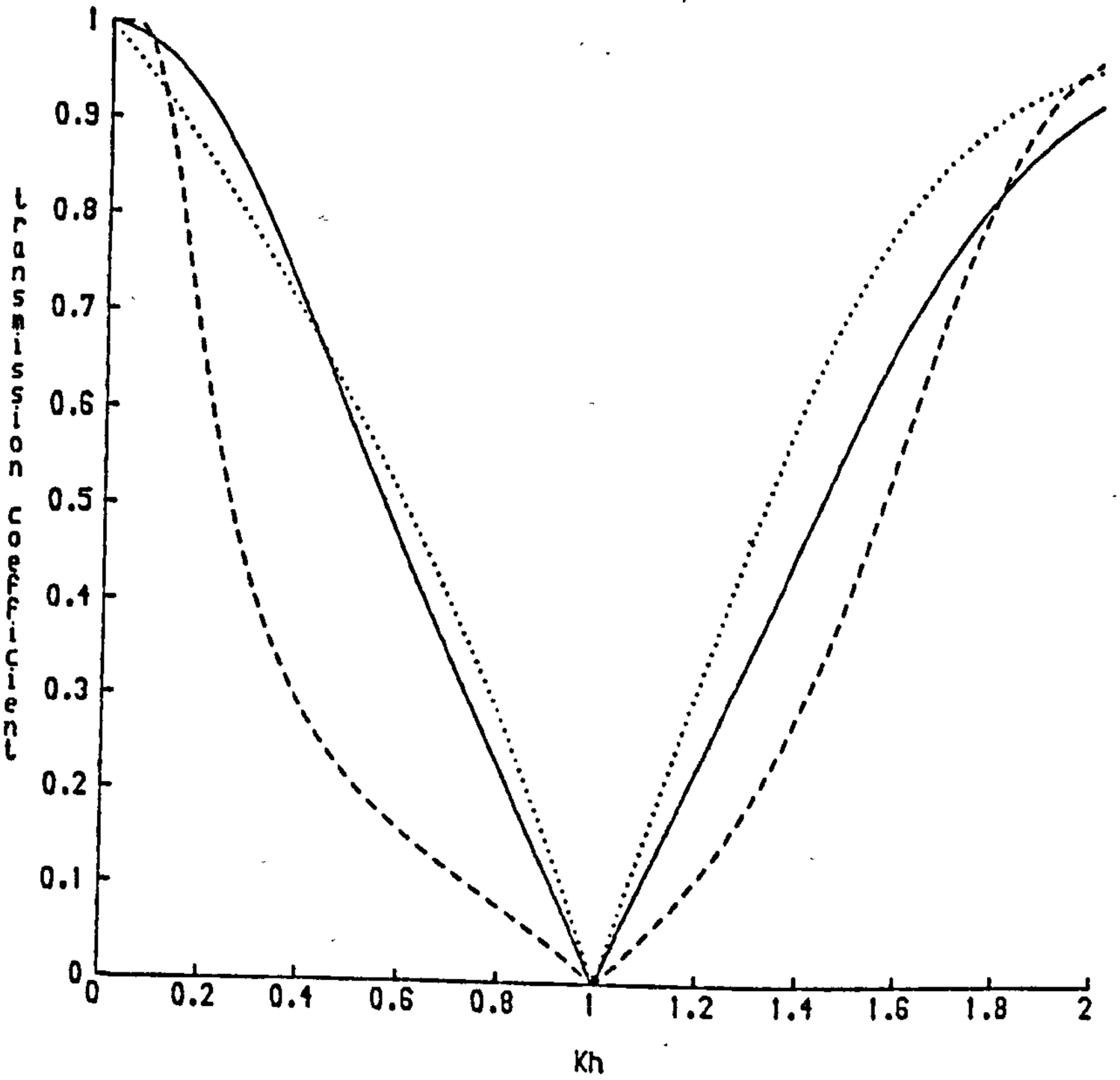

Figure 3.6.3. $|T_1|$ plotted against Kh for three heaving blocks all tuned to Kh=1. In all cases a/h=0.5. ····· h_1/h=0.7; ——— h_1/h=0.5; – – – h_1/h=0.2.

The reason that a whole spectrum of waves is found in one area of the sea at the same time is due to the fact that once created (usually by the action of the wind on the sea surface) waves dissipate very little energy and thus travel considerable distances. Waves at any particular location may therefore have been created at places with widely different wind conditions.

There are two different types of wave that are encountered; swell, which refers to waves generated by distant storms (hundreds of kilometres away) and sea, which refers to waves generated by local winds. Locally generated waves have relatively short wavelengths compared to swell since waves with short wavelengths dissipate over a much shorter distance. Usually a different mathematical description of the sea surface is required to model each of these two régimes.

There are many different ways of describing the surface of a real sea. If, as is the case here, the sea is two-dimensional then the most useful way of describing it is to represent it by a power spectral density function, $S(\omega)$. This function represents the proportion of energy in the waves that is due to waves of a particular angular frequency ω, i.e. if ω_1 and ω_2 are two angular frequencies then the ratio $S(\omega_1)/S(\omega_2)$ gives the ratio of the energy in the waves due to waves of frequency ω_1 and ω_2 respectively. The function S is defined up to an arbitrary multiplicative constant.

Pierson and Moskowitz (1964) used dimensional analysis to suggest a possible form of $S(\omega)$ for fully developed wind seas, i.e seas for which $S(\omega)$ has reached a steady-state independent of the duration in time and the distance over which the wind is acting on the free surface (see Newman (1977)). Their solution has its drawbacks, notably that it fails to model swell, and it has been refined and improved on over the years. However it is very simple and we will use it here to illustrate the way the theory of §3.2 can be used for incident wave spectra. It is

more common, when discussing real seas, to use f $(= \omega/2\pi)$, i.e. Hertz, as the frequency variable. This has the advantage that it is readily convertible into wave periods since the period is equal to $1/f$. Pierson and Moskowitz's form for S is then given by

$$S(f) = \alpha g^2 (2\pi)^{-4} f^{-5} \exp[-\beta(2\pi)^{-4}(g/U)^4 f^{-4}] \qquad (3.7.1)$$

where $\alpha = 0.0081$ and $\beta = 0.74$. Two points require explanation. Firstly the leading factor is included so as to give S the units m^2/Hz and secondly the parameter U is the mean wind speed measured at a level of 19.6m above the sea surface and is the sole parameter describing the spectrum under fully developed conditions. Typical values of U are in the range $8\text{-}16\ ms^{-1}$.

The theory of §3.2 can be considered as a 'black box' which converts a given parameter, ω, into another, $|T_1|$. This means that a wave of height one at frequency ω becomes a wave of height $|T_1|$ at the same frequency. However the energy in a wave is proportional to the square of the amplitude so that if the incoming wave has energy one then the outgoing or transmitted wave will have energy $|T_1|^2$. The consequence of this is that if the power spectral density function of the waves incident on a body is $S(f)$ then the power spectral density function of the waves transmitted downstream will be, since the problem is completely linear, $S_T(f)$ where

$$S_T(f) = |T_1(f)|^2 \, S(f). \qquad (3.7.2)$$

The function $|T_1(f)|^2$ is called the power transfer function.

As an example figure (3.7.1) shows the effect of a 4m long vertical plate hinged at the bottom in water of depth 5m on a sea described by equation (3.7.1) with $U = 8\ ms^{-1}$. The reduction in wave amplitude is

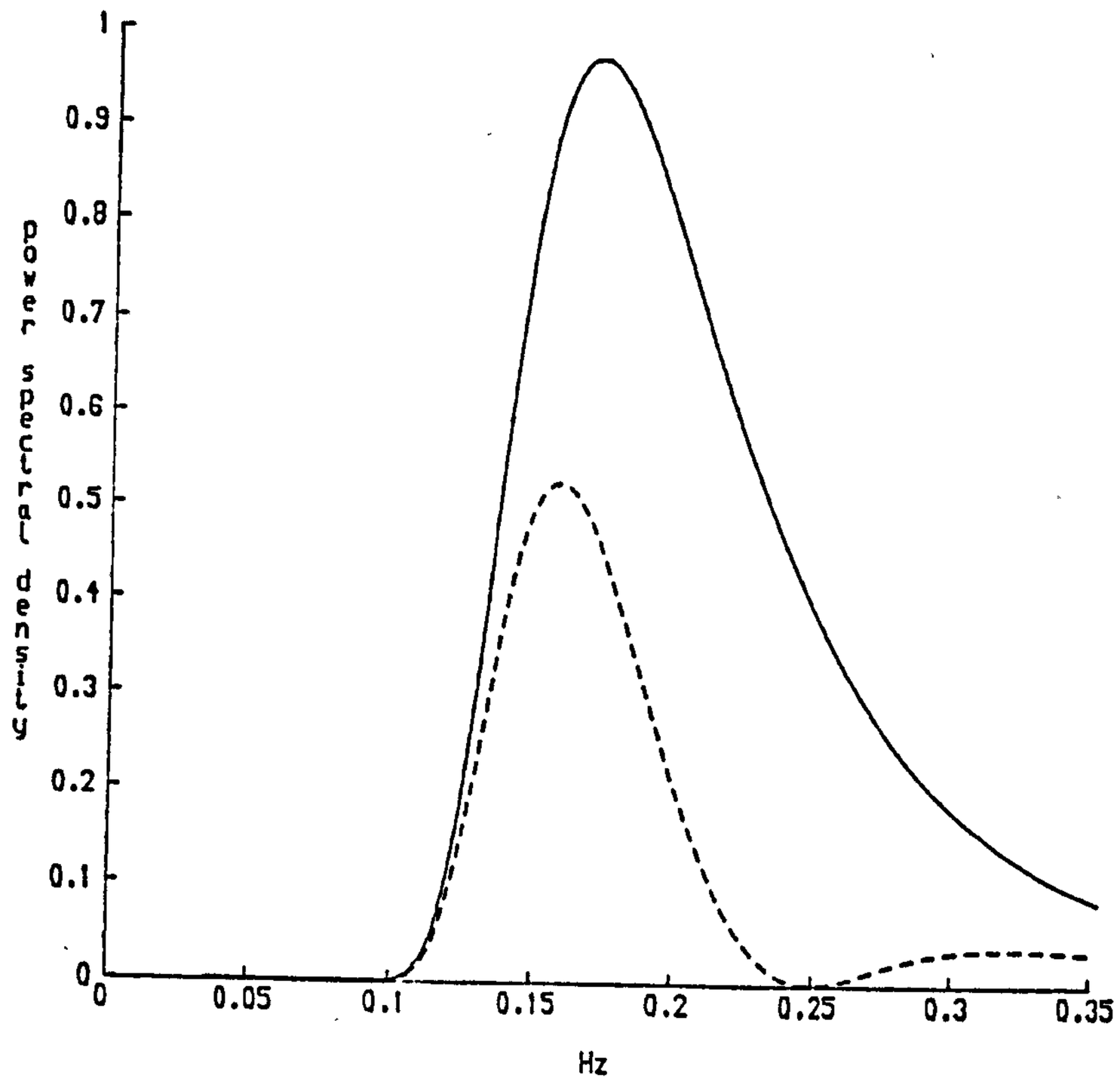

Figure 3.7.1. The effect of a vertical hinged plate with a/h=0.8 tuned to Ka=1 on a real sea. ——— S(f) for a Pierson and Moskowitz sea with U=8; - - - $S_T(f)$ downstream of the vertical hinged plate.

quite impressive even though the frequency to which the plate is tuned does not correspond to the peak in the power spectrum of the incoming wave. Clearly in any practical application of this theory the local wave climate would play a large part in determining the design of the body that was used.

3.8 Conclusion

In this chapter we have looked at the general two-dimensional problem of waves incident on a body which is allowed to move in response. In order to simplify the theory it was assumed that the body was symmetric about the vertical axis $x = 0$. It was shown that with a suitable choice of restoring force the body could be tuned to reflect all the waves of a particular frequency without any work needing to be put in or taken out of the system.

To demonstrate the theory it is necessary to know the hydrodynamic characteristics of the body in question. To this end two simple problems were solved: the radiation of waves by a vertical plate, hinged at the bottom, and performing rolling motions and the radiation of waves by a block on the bottom, in both sway and heave. The general theory was applied to these bodies to see how good they would be as wave reflectors and the results show that the performance of these moving bodies as wave reflectors is much better than any of the fixed devices considered in chapter 2.

Clearly in any practical situation the incident wave on such a body would not be monochromatic and so a description of how to extend the results of the general theory to the case of incident wave spectra has also been given.

CHAPTER 4

Submerged cylinders

4.1 Introduction

In §3.1 it was pointed out that Evans (1976) showed that a submerged horizontal circular cylinder could be an efficient absorber of wave power. The problem of wave absorption and wave reflection are closely linked and it will be shown in this chapter that such a body can also be a good reflector of wave energy. This is a remarkable result since it can be shown using linear water wave theory that in infinitely deep water a *fixed* submerged circular cylinder reflects no waves (Dean (1948)), and further, that a freely floating neutrally buoyant cylinder reflects no waves either (Ogilvie (1963)).

In this chapter the hydrodynamic characteristics of a submerged cylinder in finite depth are calculated using the method of expansion in multipoles pioneered by Ursell (1950) for the case of infinite depth. Multipoles are discussed in §4.2 and are used throughout this and the next chapter.

The use of multipole expansions, like the method of matched eigenfunction expansions used in §§3.3 and 3.4, reduces certain problems to the solution of an infinite system of linear equations for the unknown strengths of the multipoles. These can then be solved on a computer by truncating to N equations and checking the convergence of the solutions for increasing N. In this case we also require the numerical evaluation of principal value integrals, a problem which is discussed in §4.3.

Sections 4.4 and 4.5 are concerned with the full solution of the single cylinder problem. In §4.6 the case of a tethered buoyant cylinder is examined and the results of chapter 3 are applied to this device to give the results shown in §4.7.

In the context of harbour breakwaters it may be necessary to know the hydrodynamic characteristics of a submerged cylinder next to a wall. Problems concerning cylinders next to walls can be reformulated as problems with two parallel spaced cylinders (and no wall) oscillating in such a manner as to make the fluid on a vertical line midway between them behave as if it were a wall. Two cylinder problems are examined in §§4.8-4.10. The work is an extension of Wang (1981) who considered this problem in infinitely deep water, though here the method of solution used is much simpler. The case of small vertical oscillations (heave) for two parallel spaced identical cylinders is equivalent to the problem of heave for a single cylinder in the presence of a vertical wall. By considering two cylinders making small horizontal oscillations (sway), exactly out of phase with each other, the problem of sway next to a wall can be solved. This is the problem that is of interest in the context of using tethered cylinders as harbour breakwaters. For completeness a third case, that of two cylinders in sway and in phase with each other (e.g. the sway of a catamaran hull) is also considered. As well as these radiation problems, the problem of the scattering of waves by a cylinder next to a wall will also be solved.

4.2 Multipole Expansions

The method used here to calculate the hydrodynamic characteristics of submerged cylinders is to express the time-dependent velocity

potential $\Phi(x,y,t)$ in the form

$$\Phi(x,y,t) = \mathrm{Re}[\phi(x,y)\ e^{i\omega t}] \qquad (4.2.1)$$

and then to represent the time-independent potential ϕ as an infinite linear combination of multipole potentials, each of which is a harmonic function in the fluid region, except at a point, satisfies the free surface and bottom boundary conditions and which describes a wave travelling outwards as $|x| \longrightarrow \infty$.

Depending on the problem under consideration either symmetric or antisymmetric multipoles will be appropriate. The following convention is used: $q = 1\ (2)$ refers to antisymmetric (symmetric) multipoles; where a bracketed pair appears, the top (bottom) element is applicable if $q = 1\ (2)$.

With this convention the multipole potentials, given by Thorne (1953), can be written

$$\phi_{n,q} = \frac{a^{n+1}}{nr^n} \begin{Bmatrix}\sin n\theta \\ \cos n\theta\end{Bmatrix} + \frac{1}{n!}\int_0^\infty \frac{g(k,q)}{Kh\cosh kh - kh\sinh kh} \begin{Bmatrix}\sin kx \\ \cos kx\end{Bmatrix} dk$$

$$- \frac{i}{n!}\,\ell(\kappa,q) \begin{Bmatrix}\sin \kappa x \\ \cos \kappa x\end{Bmatrix} \qquad n = 1,2,.... \qquad (4.2.2)$$

where κ is given by the dispersion relation (3.2.8),

$$g(k,q) = a^2h\ (ka)^{n-1}\ [e^{-k(h-f)}\{K\sinh ky - k\cosh ky\}$$

$$- (-1)^{n+q}\ (K+k)\ e^{-kf}\cosh k(h-y)] \qquad (4.2.3)$$

and

$$\ell(\kappa,q) = 2\pi a\ \frac{(\kappa a)^n\cosh \kappa(y-h)}{2\kappa h + \sinh 2\kappa h}\ [e^{-\kappa(h-f)} + (-1)^{n+q}\ e^{\kappa(h-f)}]. \qquad (4.2.4)$$

Note that a factor of a^{n+1}/n has been included for convenience. These multipoles are harmonic everywhere in $0 < y < h$, $-\infty < x < \infty$, except for the point (0,f), and they satisfy the boundary conditions on $y = 0$ and $y = h$, equations (1.2.8) and (1.2.7) respectively.

Note also that the multipole with a $\ln r$ singularity has been omitted. This is because as the multipoles are to be centred at points inside the cylinder, a $\ln r$ singularity in ϕ would result in an instantaneous flux of fluid across the surface of the cylinder which is physically unacceptable.

To simplify the writing of these expressions four functions are defined:

$$c_1(u) = -(Kh + u)\,[e^{-u} + (-1)^{n+q}\, e^{u(1-2f/h)}] \qquad (4.2.5)$$

$$c_2(u) = (Kh - u)\, e^{u(2f/h-1)} - (Kh + u)\,(-1)^{n+q}\, e^{-u} \qquad (4.2.6)$$

$$c_3(u) = 1 + (-1)^{n+q}\, e^{2u(1-f/h)} \qquad (4.2.7)$$

$$c_4(u) = e^{2u(f/h-1)} + (-1)^{n+q}\ . \qquad (4.2.8)$$

Then

$$\phi_{n,q} = \frac{a^{n+1}}{nr^n} \begin{Bmatrix}\sin n\theta \\ \cos n\theta\end{Bmatrix}$$

$$+ \frac{a^2}{2n!} \int_0^\infty (ka)^{n-1}\, \frac{[c_1(kh)\, e^{k(f-y)} + c_2(kh)\, e^{k(y-f)}]}{Kh \cosh kh - kh \sinh kh} \begin{Bmatrix}\sin kx \\ \cos kx\end{Bmatrix} dk$$

$$- \frac{i\pi a\, (\kappa a)^n}{(2\kappa h + \sinh 2\kappa h)\, n!}\, [c_3(\kappa h)\, e^{\kappa(f-y)} + c_4(\kappa h)\, e^{\kappa(y-f)}] \begin{Bmatrix}\sin \kappa x \\ \cos \kappa x\end{Bmatrix}. \qquad (4.2.9)$$

These multipoles can be expanded in polar coordinates centred on (0,f) using the following two identities:

$$e^{k(f-y)}\begin{Bmatrix}\sin kx\\ \cos kx\end{Bmatrix} = (-1)^q \sum_{m=0}^{\infty} \frac{(-kr)^m}{m!}\begin{Bmatrix}\sin m\theta\\ \cos m\theta\end{Bmatrix}$$

$$e^{k(y-f)}\begin{Bmatrix}\sin kx\\ \cos kx\end{Bmatrix} = \sum_{m=0}^{\infty} \frac{(kr)^m}{m!}\begin{Bmatrix}\sin m\theta\\ \cos m\theta\end{Bmatrix}. \qquad (4.2.10)$$

This gives

$$\phi_{n,q} = \frac{a^{n+1}}{nr^n}\begin{Bmatrix}\sin n\theta\\ \cos n\theta\end{Bmatrix} + \sum_{m=1}^{\infty} \frac{a}{m}\left[\frac{r}{a}\right]^m A_{mn,q}\begin{Bmatrix}\sin m\theta\\ \cos m\theta\end{Bmatrix} + A_{on,q} \qquad (4.2.11)$$

where

$$A_{on,q} = \left[\frac{a}{h}\right]^n \frac{a}{2n!}\Bigg[\int_0^{\infty} \frac{(-1)^q c_1(u) + c_2(u)}{Kh\cosh u - u\sinh u}\, u^{n-1}\, du$$

$$- 2\pi i\, (\kappa h)^n \frac{(-1)^q c_3(\kappa h) + c_4(\kappa h)}{2\kappa h + \sinh 2\kappa h}\Bigg] \begin{Bmatrix}0\\ 1\end{Bmatrix} \qquad (4.2.12)$$

$$A_{mn,q} = \frac{(a/h)^{n+m}}{2n!(m-1)!}\Bigg[\int_0^{\infty} \frac{(-1)^{m+q} c_1(u) + c_2(u)}{Kh\cosh u - u\sinh u}\, u^{n-1}\, du$$

$$- 2\pi i\, (\kappa h)^{n+m} \frac{(-1)^{m+q} c_3(\kappa h) + c_4(\kappa h)}{2\kappa h + \sinh 2\kappa h}\Bigg] \qquad (4.2.13)$$

$$m = 1,2,\ldots \quad .$$

This expansion for $\phi_{n,q}$ is valid in the region $r < 2f$. (See Thorne 1953).

The behaviour of $\phi_{n,q}$ as $|x| \to \infty$ is also of interest and will be needed later. We only need to consider the case $x \to +\infty$ since

$$\phi_{n,q}(x,y) = (-1)^q\, \phi_{n,q}(-x,y). \qquad (4.2.14)$$

The first term in the expression for $\phi_{n,q}$, equation (4.2.2), clearly makes no contribution as $x \to \infty$. To examine the behaviour of the second term we look at

$$I_1 \equiv \frac{1}{n!} \int_\Gamma \frac{g_1(k,q)}{Kh \cosh kh - kh \sinh kh} \, dk \qquad (4.2.15)$$

where

$$g_1(k,q) = g(k,q)\, e^{ikx} \qquad (4.2.16)$$

and Γ is the contour:

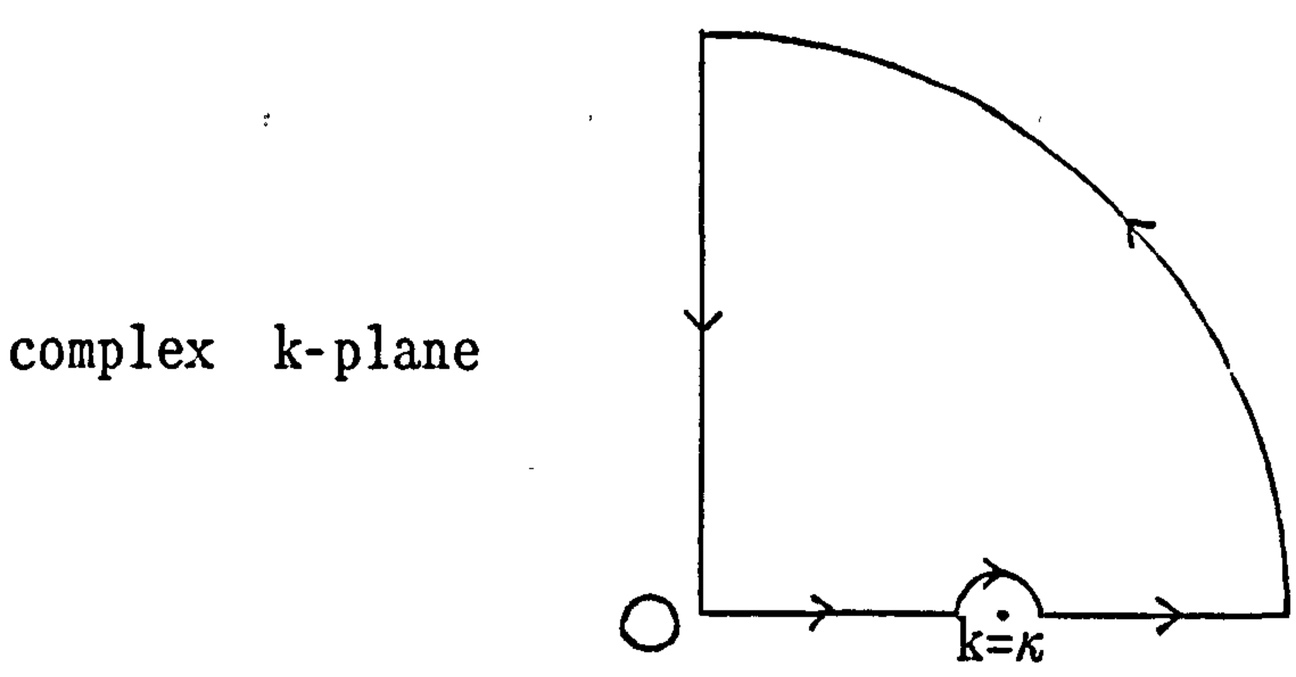

It is easily shown, using the Riemann-Lebesgue lemma, that the only contribution to I_1 as $x \to \infty$ is from the integral along the real axis and around the pole at $k = \kappa$. Thus since there are no singularities inside this contour Cauchy's theorem implies that, as $x \to \infty$

$$\frac{1}{n!} \int_0^\infty \frac{g_1(k,q)}{Kh \cosh kh - kh \sinh kh} \, dk - \frac{\pi i}{hn!} \frac{g_1(\kappa,q)}{(Kh-1) \sinh \kappa h - \kappa h \cosh \kappa h} \to 0. \qquad (4.2.17)$$

The second term, which is the contribution from the pole, can be simplified by using the dispersion relation, equation (3.2.8), giving

$$\frac{1}{n!} \int_0^\infty \frac{g_1(k,q)}{Kh \cosh kh - kh \sinh kh} \, dk \to - \frac{2\pi i}{hn!} \frac{\cosh \kappa h \; g_1(\kappa,q)}{2\kappa h + \sinh 2\kappa h}. \qquad (4.2.18)$$

Therefore

$$\frac{1}{n!}\int_0^{\infty}\frac{g(k,q)}{Kh\cosh kh - kh\sinh kh}\begin{Bmatrix}\sin kx\\ \cos kx\end{Bmatrix}dk \longrightarrow -\begin{Bmatrix}\mathrm{Im}\\ \mathrm{Re}\end{Bmatrix}\frac{2\pi i}{hn!}\frac{\cosh \kappa h\, g_1(\kappa,q)}{2\kappa h + \sinh 2\kappa h}$$

$$\text{as} \quad x \longrightarrow \infty. \tag{4.2.19}$$

After some algebra this gives the result that as $x \longrightarrow \infty$

$$\phi_{n,q} \longrightarrow 2\pi a\,\frac{(\kappa a)^n \cosh \kappa(y-h)}{n!\,(2\kappa h + \sinh 2\kappa h)}\left[e^{\kappa(f-h)} + (-1)^{n+q}\, e^{\kappa(h-f)}\right]e^{-i\kappa x}\begin{Bmatrix}1\\ -i\end{Bmatrix}. \tag{4.2.20}$$

4.3 Calculation of Principal Value Integrals

In order to evaluate the coefficients $A_{mn,q}$ in equation (4.2.11) principal value integrals need to be computed numerically. The following technique is employed.

Let $I = \int_0^{\infty}\frac{g(k)}{h(k)}\,dk$ where $h(\kappa) = 0$, $h'(\kappa) \neq 0$. This implies, by definition, that

$$I = \lim_{\epsilon\to 0}\left\{\int_0^{\kappa-\epsilon} + \int_{\kappa+\epsilon}^{\infty}\right\}\frac{g(k)}{h(k)}\,dk\ . \tag{4.3.1}$$

The problem arises from the fact that both integrals in (4.3.1) are divergent and so cannot be evaluated independently. However we note that

$$\int_0^{2\kappa}\frac{dk}{k-\kappa} \equiv \lim_{\epsilon\to 0}\left\{\int_0^{\kappa-\epsilon} + \int_{\kappa+\epsilon}^{2\kappa}\right\}\frac{dk}{k-\kappa}$$

$$= \lim_{\epsilon\to 0}\left\{\left[\ln(\kappa-k)\right]_0^{\kappa-\epsilon} + \left[\ln(k-\kappa)\right]_{\kappa+\epsilon}^{2\kappa}\right\}$$

$$= 0\ . \tag{4.3.2}$$

Therefore we can write

$$I = \int_0^{2\kappa} \left\{ \frac{g(k)}{h(k)} - \frac{g(\kappa)}{(k-\kappa)\, h'(\kappa)} \right\} dk + \int_{2\kappa}^{\infty} \frac{g(k)}{h(k)}\, dk \ . \qquad (4.3.3)$$

Since $h(k) \sim (k-\kappa)\, h'(\kappa)$ as $k \to \kappa$, the integrand in the first integral is well behaved near $k = \kappa$. To calculate the integrand near $k = \kappa$ now requires the subtraction of two large numbers. Computationally this is straightforward if we use double precision arithmetic, provided κ is known with sufficient accuracy.

4.4 The Radiation Problem for a Single Cylinder

The problems of sway and heave will be treated simultaneously using the notation that was introduced in the previous section. The time independent velocity potential, ϕ_q, satisfies the following boundary-value problem:

$$\nabla^2 \phi_q = 0 \qquad \text{in the fluid} \qquad (4.4.1)$$

$$K\phi_q + \frac{\partial \phi_q}{\partial y} = 0 \qquad \text{on} \quad y = 0 \qquad (4.4.2)$$

$$\frac{\partial \phi_q}{\partial y} = 0 \qquad \text{on} \quad y = h \qquad (4.4.3)$$

$$\frac{\partial \phi_q}{\partial r} = U \begin{Bmatrix} \sin\theta \\ \cos\theta \end{Bmatrix} \qquad \text{on} \quad r = a \qquad (4.4.4)$$

where U is the time-independent velocity of the body.

The multipole potentials $\phi_{n,q}$ discussed in §4.2 satisfy $\nabla^2 \phi_{n,q} = 0$ in $y > 0$ except at $(0,f)$ which is not in the fluid. They also satisfy the appropriate free surface and bottom boundary conditions.

Therefore to solve the radiation problem put

$$\phi_q = U \sum_{n=1}^{\infty} c_{n,q}\, \phi_{n,q} \qquad (4.4.5)$$

where $c_{n,q}$ $n = 1,2,....$ are constants to be determined.

Substituting from equation (4.2.11) into equation (4.4.5) and then using equation (4.4.4) gives

$$\sum_{n=1}^{\infty} c_{n,q}\left[- \begin{Bmatrix}\sin n\theta \\ \cos n\theta\end{Bmatrix} + \sum_{m=1}^{\infty} A_{mn,q} \begin{Bmatrix}\sin m\theta \\ \cos m\theta\end{Bmatrix} \right] = \begin{Bmatrix}\sin \theta \\ \cos \theta\end{Bmatrix}$$

or

$$- c_{m,q} + \sum_{n=1}^{\infty} A_{mn,q}\, c_{n,q} = \delta_{1m} \qquad m = 1,2,\ldots . \qquad (4.4.6)$$

This infinite system of equations is now solved numerically by truncation (see §3.3) and the convergence of the system is good. It was found that in all cases of interest choosing $N = 4$ gave at least three figure accuracy and all the results that will be shown were calculated using this value for the truncation size.

The time-independent hydrodynamic force on the cylinder in the direction of motion, f_q, is given by integrating the pressure times the appropriate component of the normal around the cylinder, i.e

$$f_q = -\rho\omega i \int_{-\pi}^{\pi} \phi_q(a,\theta) \begin{Bmatrix}\sin \theta \\ \cos \theta\end{Bmatrix} a\, d\theta \ . \qquad (4.4.7)$$

Substituting from equation (4.2.11) into equations (4.4.5) and (4.4.7) gives

$$f_q = -\rho\omega i U a^2 \pi \left[c_{1,q} + \sum_{n=1}^{\infty} c_{n,q}\, A_{1n,q} \right] . \qquad (4.4.8)$$

This expression can be simplified by noting that equation (4.4.6) with m = 1 is

$$\sum_{n=1}^{\infty} A_{1\,n,q}\, c_{n,q} = 1 + c_{1,q}$$

so that

$$f_q = -\rho\omega i U a^2 \pi\ (1 + 2c_{1,q}). \qquad (4.4.9)$$

Thus the added mass and damping coefficients, non-dimensionalised with respect to the maximum acceleration of the cylinder and the mass of fluid displaced by the cylinder, are given by

$$\mu_q - i\nu_q = -\ (1 + 2c_{1,q}) \qquad (4.4.10)$$

and depend only upon the first unknown coefficient in the multipole expansion.

In order to examine the far field behaviour equation (4.2.19) is used together with equation (4.4.5) giving

$$\phi_q \sim 2\pi a U \sum_{n=1}^{\infty} c_{n,q}\, \frac{(\kappa a)^n \cosh \kappa(y-h)}{n!\ (2\kappa h + \sinh 2\kappa h)} [e^{\kappa(f-h)} + (-1)^{n+q}\, e^{\kappa(h-f)}] e^{-i\kappa x} \begin{Bmatrix} 1 \\ -i \end{Bmatrix} \qquad (4.4.11)$$

as $x \to \infty$. If A_q is defined by

$$A_q = \frac{2\pi a \cosh \kappa h}{2\kappa h + \sinh 2\kappa h} \sum_{n=1}^{\infty} r_{n,q} \qquad (4.4.12)$$

where

$$r_{n,q} = \frac{(\kappa a)^n}{n!}\ [e^{\kappa(f-h)} + (-1)^{n+q}\, e^{\kappa(h-f)}] \begin{Bmatrix} 1 \\ -i \end{Bmatrix} c_{n,q} \qquad (4.4.13)$$

then

$$\phi_q \sim U A_q \frac{\cosh \kappa(y-h)}{\cosh \kappa h}\, e^{-i\kappa x} \qquad \text{as} \quad x \to \infty\ . \qquad (4.4.14)$$

The reflection and transmission coefficients for the scattering problem, R and T, can be obtained via the Newman relations, equations (1.2.41)-(1.2.44), whence the results can be written

$$R + T = \left[\sum_{n=1}^{\infty} r_{n,2}\right] \Big/ \overline{\left[\sum_{n=1}^{\infty} r_{n,2}\right]} \quad . \tag{4.4.15}$$

$$R - T = \left[\sum_{n=1}^{\infty} r_{n,1}\right] \Big/ \overline{\left[\sum_{n=1}^{\infty} r_{n,1}\right]} \quad . \tag{4.4.16}$$

The damping coefficient ν_q is related to the far field amplitude A_q by equation (1.2.32),

$$\pi a^2 \rho \omega \nu_q = 2\rho c_g \frac{\omega^2}{g^2} |A_q|^2,$$

where c_g is the group velocity. This simplifies to

$$\nu_q = \frac{2\pi}{2\kappa h + \sinh 2\kappa h} \left| \sum_{n=1}^{\infty} r_{n,q} \right|^2 \quad . \tag{4.4.17}$$

An identity has thus been derived which can be used as a check on the numerical results obtained by solving equation (4.4.6):

$$\frac{\pi}{2\kappa h + \sinh 2\kappa h} \left| \sum_{n=1}^{\infty} r_{n,q} \right|^2 = \mathrm{Im}(c_{1,q}) \quad . \tag{4.4.18}$$

There are two parameters in this problem: a/h and f/h. The effect of varying these parameters on the hydrodynamic characteristics of a cylinder are shown in figures (4.4.1)-(4.4.12). These figures are grouped into two sections: figures (4.4.1)-(4.4.5) are for cylinders

with a constant value of f/a, namely $f/a = 1.5$, whereas figures (4.4.6)-(4.4.12) are for cylinders with a constant value of a/h, namely $a/h = 0.2$.

To start with we will look at the case $f/a = 1.5$. The case of infinite depth corresponds to $a/h = 0$. Increasing the parameter a/h from zero corresponds to bringing the bottom up towards the cylinder. The value of a/h for a cylinder which is just touching the bottom is 0.4, (since $f/h + a/h = 1$ in this case). Thus a/h must lie in the range $0 \leq a/h < 0.4$. The case $a/h = 0.4$ will be discussed later.

Figures (4.4.1)-(4.4.4) show curves of added mass and damping coefficients against non-dimensional frequency, Ka, in both sway and heave for five different values of a/h : 0 (infinite depth), 0.1, 0.2, 0.3 and 0.39. It is difficult to obtain results using the multipole method described above if Kh is too large, ($Kh < 8$ was the criterion used in the calculations described here), and so the curves for $a/h = 0.1$ stop at $Ka = 0.8$. This is not much of a handicap however as beyond $Ka = 0.8$ the infinite depth results provide a very good approximation. Figures (4.4.1) and (4.4.2) show a marked difference in the behaviour of the added mass coefficient between the sway and heave cases. As the bottom approaches the cylinder the heave added mass changes very rapidly whereas in sway this is only true in long waves.

In infinite depth the added mass and damping coefficients for the sway case are the same as those for heave, a result first shown by Ogilvie (1963). Figures (4.4.3) and (4.4.4) show that the effect of finite depth is to increase the damping coefficient in sway but to decrease it in heave. In chapter 5 it will be shown that the same phenomenon occurs in the case of the submerged sphere.

Dean (1948) showed that in infinite depth a fixed submerged cylinder reflects no waves, i.e. $R = 0$. Figure (4.4.5) shows how this result is affected by the presence of a bottom. Curves are shown for the same

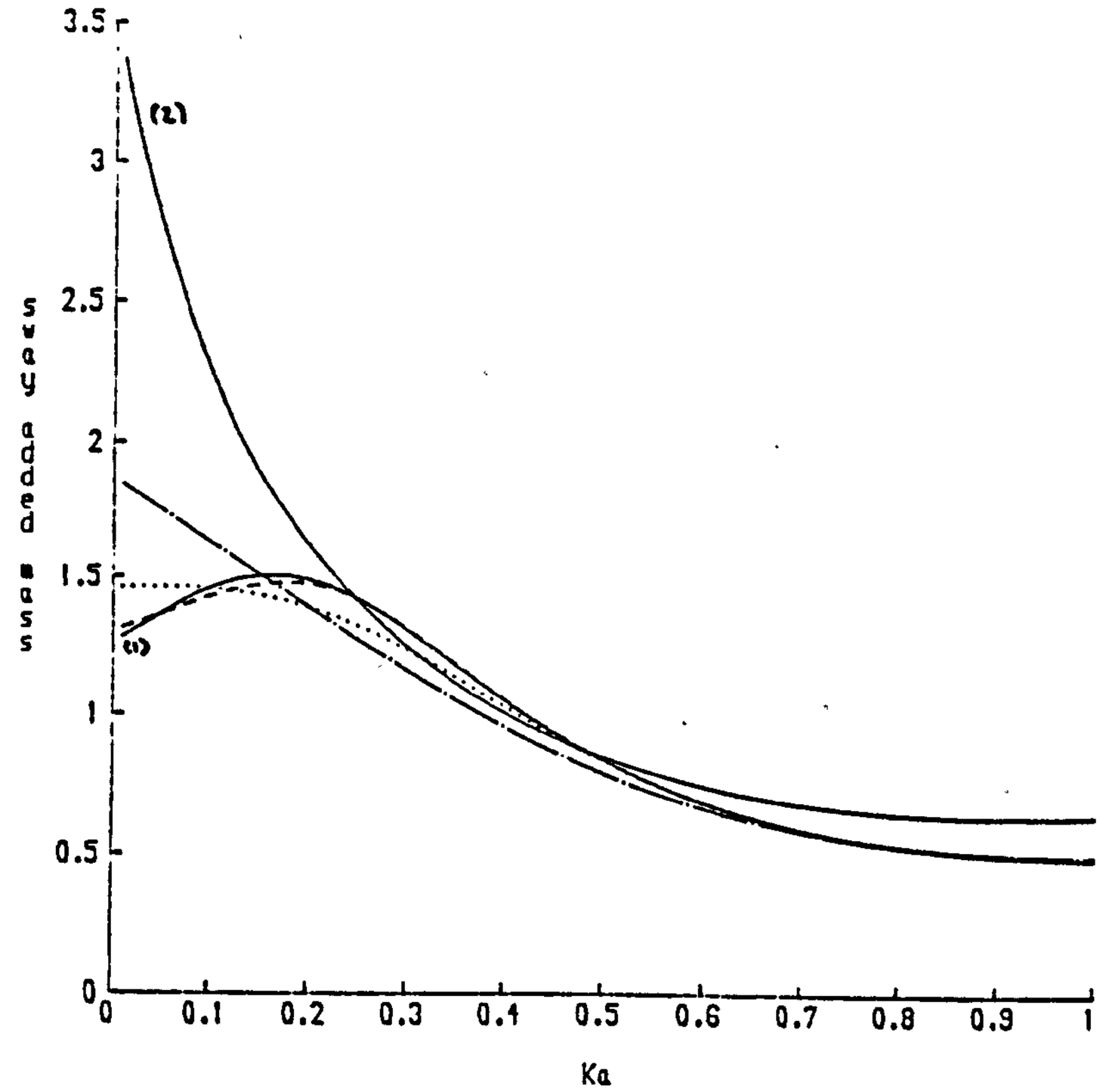

Figure 4.4.1. μ (sway) plotted against Ka for a submerged cylinder (f/a=1.5) in different depths of water. ——— (1) infinite depth; – – – a/h=0.1; ····· a/h=0.2; –·–·– a/h=0.3; ——— (2) a/h=0.39.

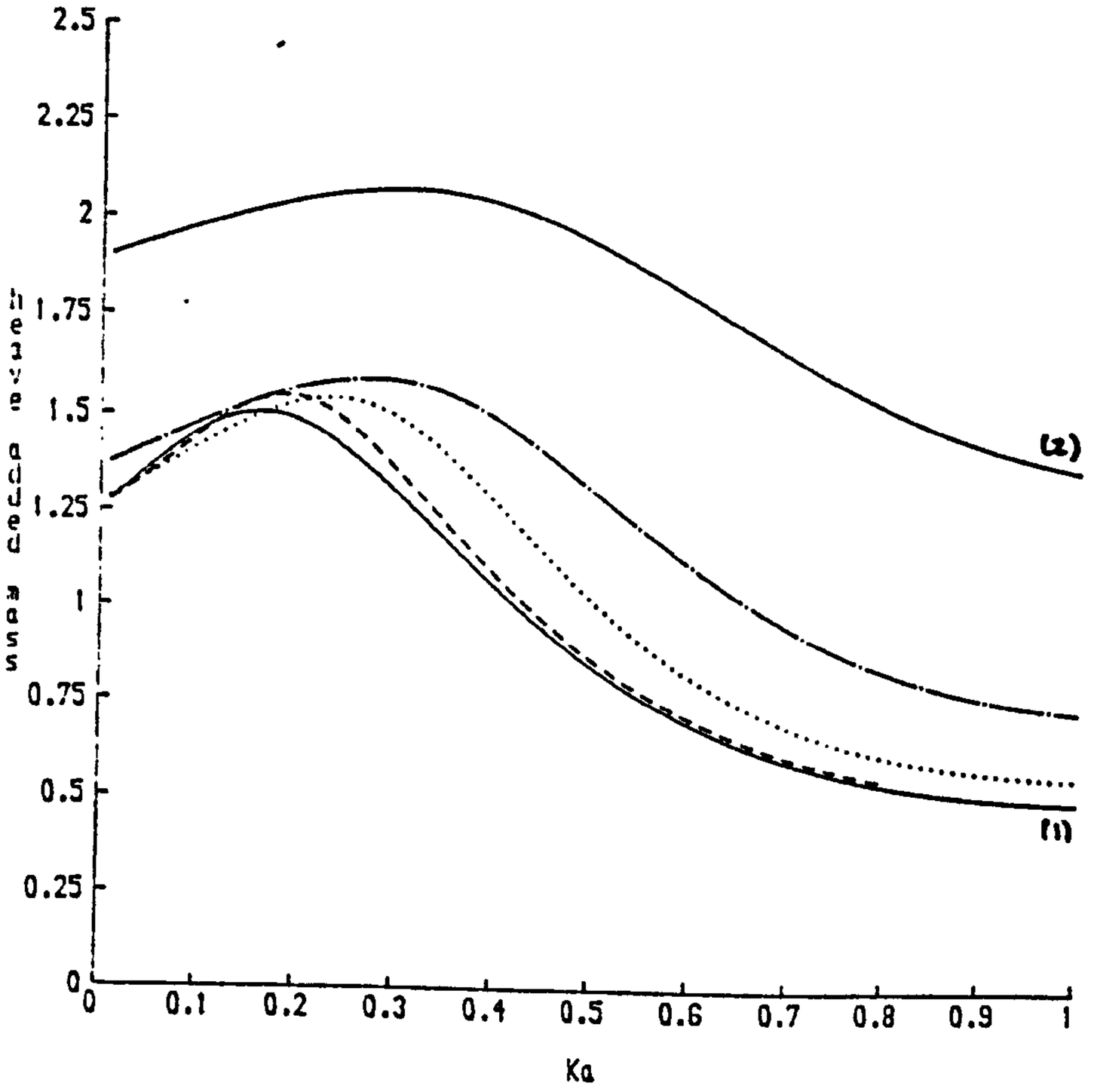

Figure 4.4.2. μ (heave) plotted against Ka for a submerged cylinder (f/a=1.5) in different depths of water. ——— (1) infinite depth; – – – a/h=0.1; ····· a/h=0.2; –·–·– a/h=0.3; ——— (2) a/h=0.39.

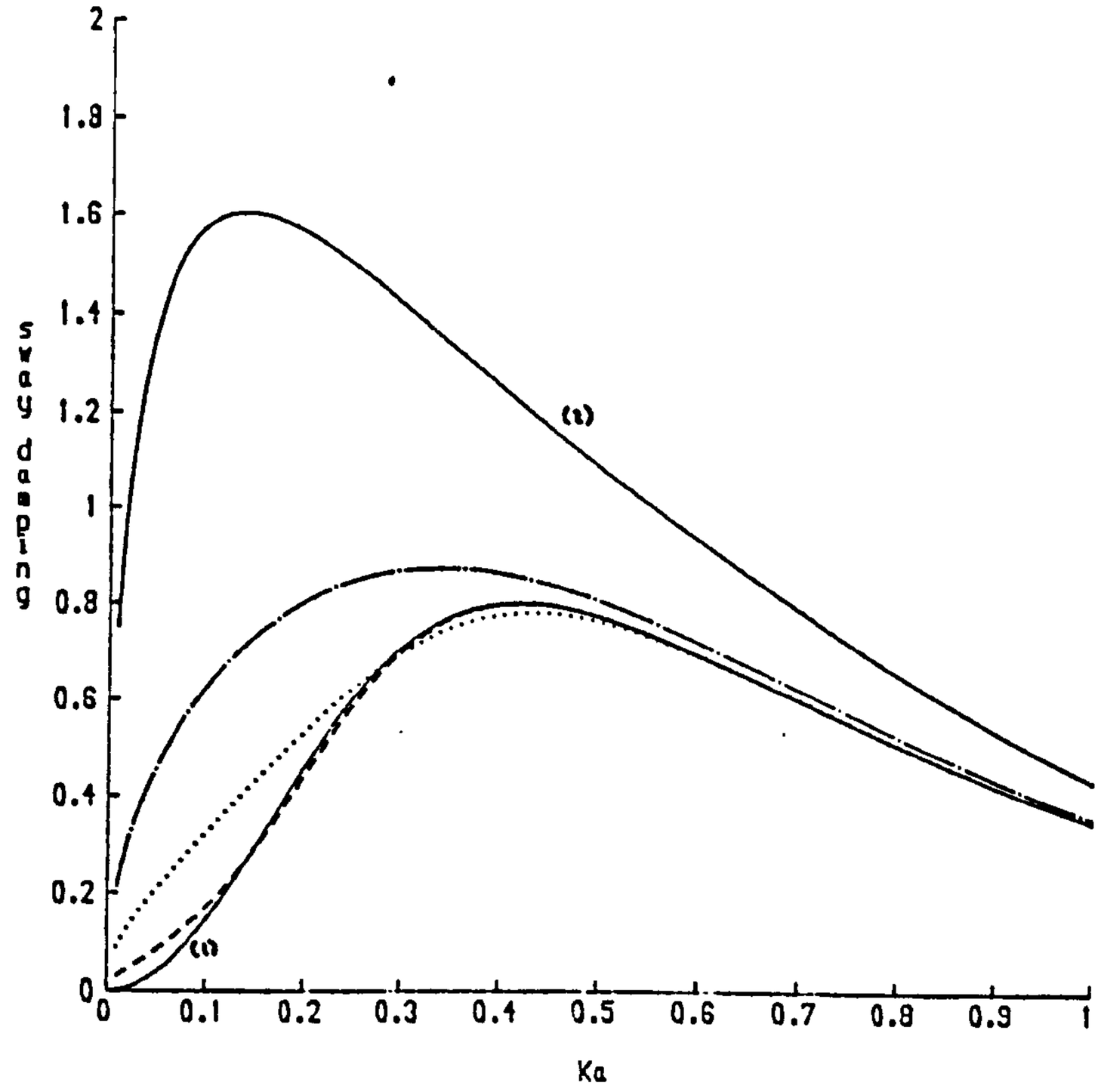

Figure 4.4.3. ν (sway) plotted against Ka for a submerged cylinder (f/a=1.5) in different depths of water. ——— (1) infinite depth; – – – a/h=0.1; ····· a/h=0.2; –·–·– a/h=0.3; ——— (2) a/h=0.39.

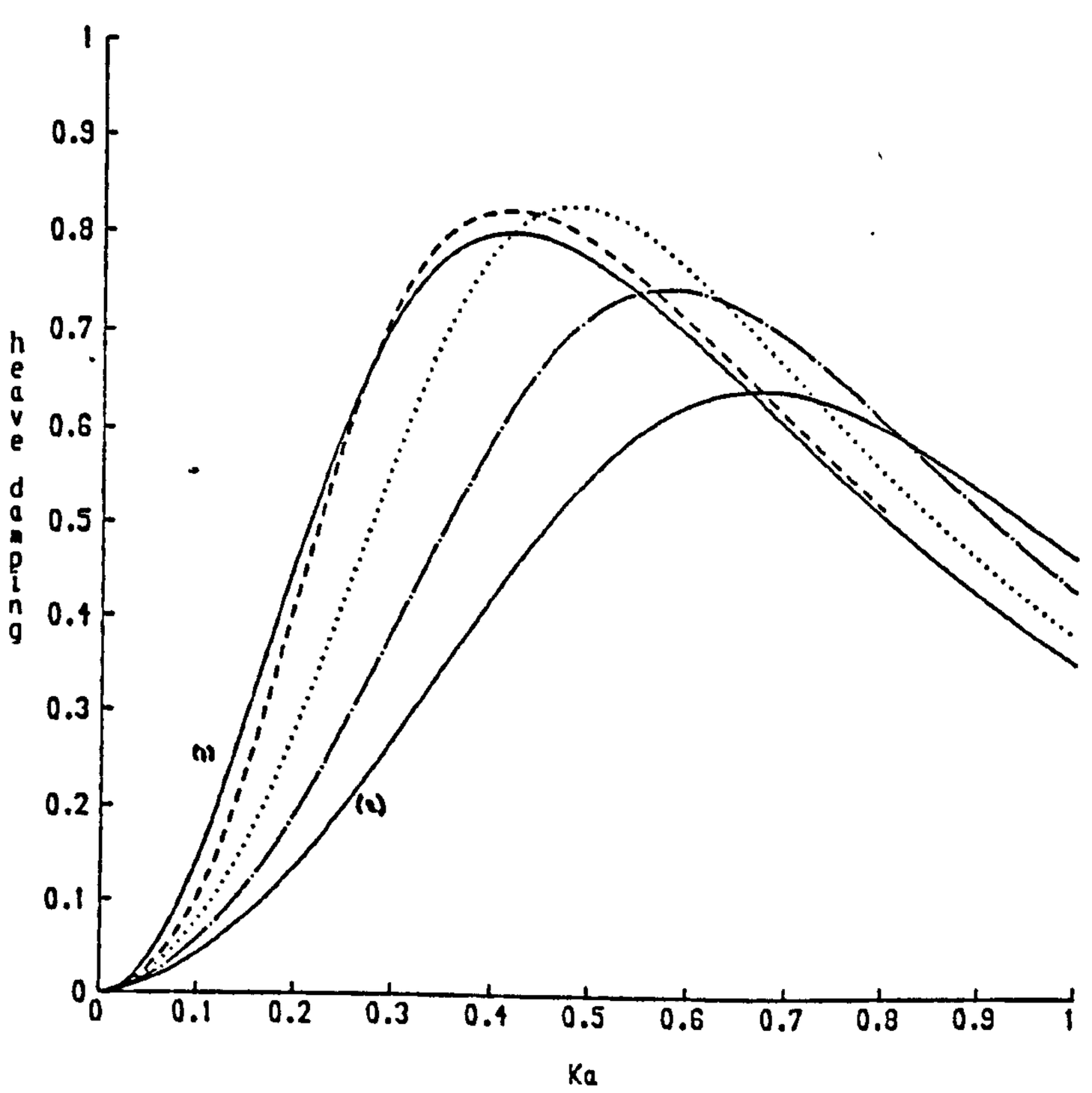

Figure 4.4.4. ν (heave) plotted against Ka for a submerged cylinder (f/a=1.5) in different depths of water. ——— (1) infinite depth; – – – a/h=0.1; ····· a/h=0.2; –·–·– a/h=0.3; ——— (2) a/h=0.39.

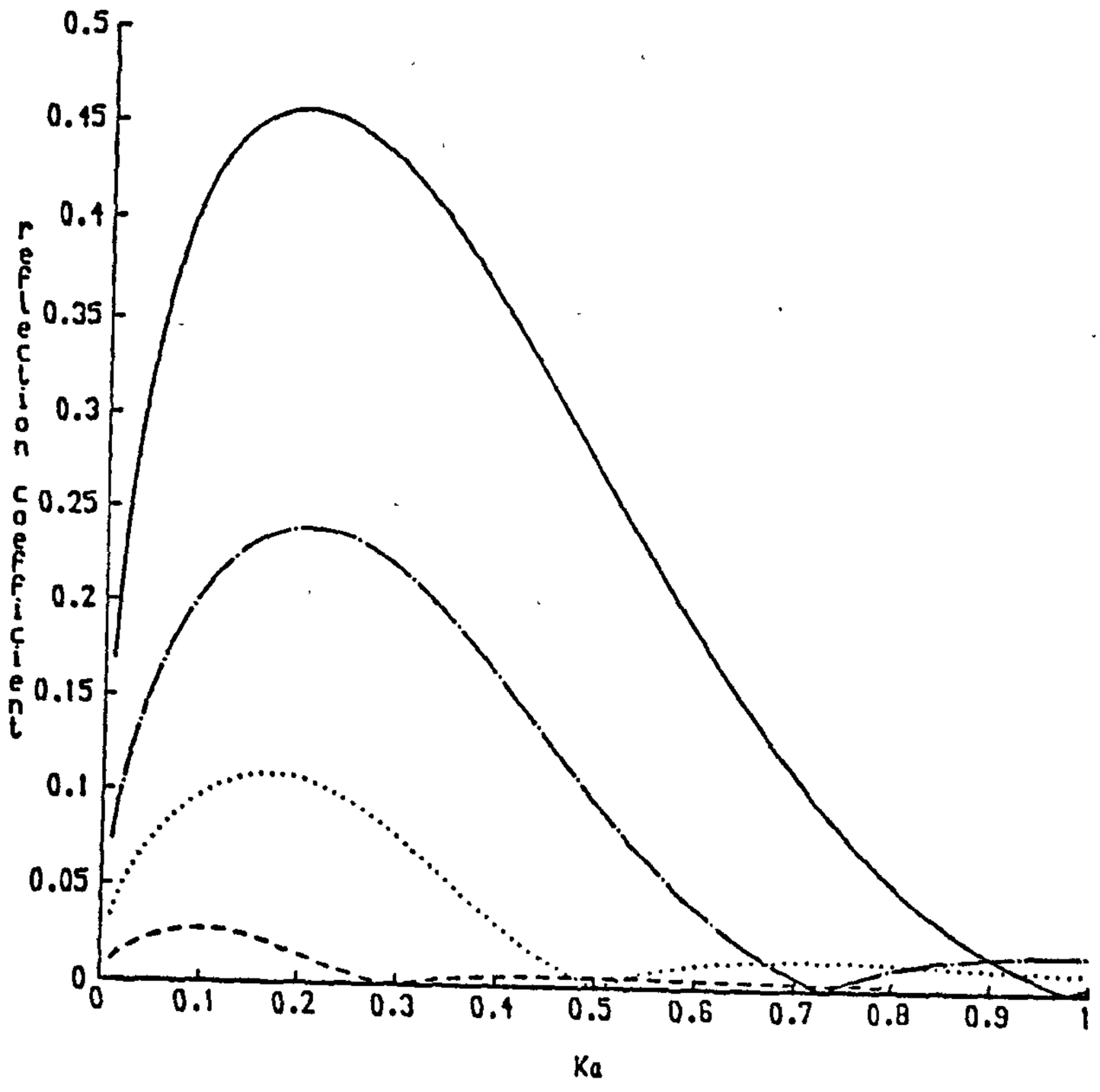

Figure 4.4.5. |R| plotted against Ka for a submerged cylinder (f/a=1.5) in different depths of water. – – – a/h=0.1; ····· a/h=0.2; –·–·– a/h=0.3; ——— a/h=0.39.

four non-zero values of a/h as were used in figures (4.4.1)-(4.4.4) and it is evident that the effects of finite depth are quite small since when $a/h = 0.3$ (in which case the cylinder is blocking over half the depth) the reflection coefficient is still always less than 0.25, which corresponds to a value of $|T|$ of about 0.97 since $|T|^2 = 1 - |R|^2$. There is however a big increase as the bottom gets very close to the cylinder with $|R|$ approaching 0.5 at some frequencies. The curves show that, whatever the depth, if $f/a = 1.5$ the cylinder is most effective in reflecting waves in the region $0.1 < Ka < 0.3$.

In all the remaining figures the ratio of the cylinder radius to the depth will be kept constant at 0.2 and the immersion depth will be varied. In this case the possible values of f/a lie in the range $1 < f/a < 4$. The limiting values of 1 and 4 correspond to the situations when the cylinder is just touching the free surface and just touching the bottom respectively. The case $f/a = 4$ will be discussed later.

Figures (4.4.6)-(4.4.9) show curves of added mass and damping coefficients against non-dimensional frequency, Ka, in both sway and heave for five values of the parameter f/a : 1.1, 1.5, 2, 3 and 3.9. Figures (4.4.6) and (4.4.7) show that the cylinder close to the free surface exhibits the phenomenon of negative added mass in both sway and heave. This phenomenon has been discussed in §3.4. Another noteworthy feature of the curves is that as the cylinder approaches the bottom in the heave case the added mass becomes almost completely independent of frequency.

The curves of damping coefficient, figures (4.4.8) and (4.4.9), simply show that the deeper the cylinder is immersed the less good it is at making waves, with a big increase in this ability as the cylinder approaches the free surface. This is exactly the same as for the case of infinite depth.

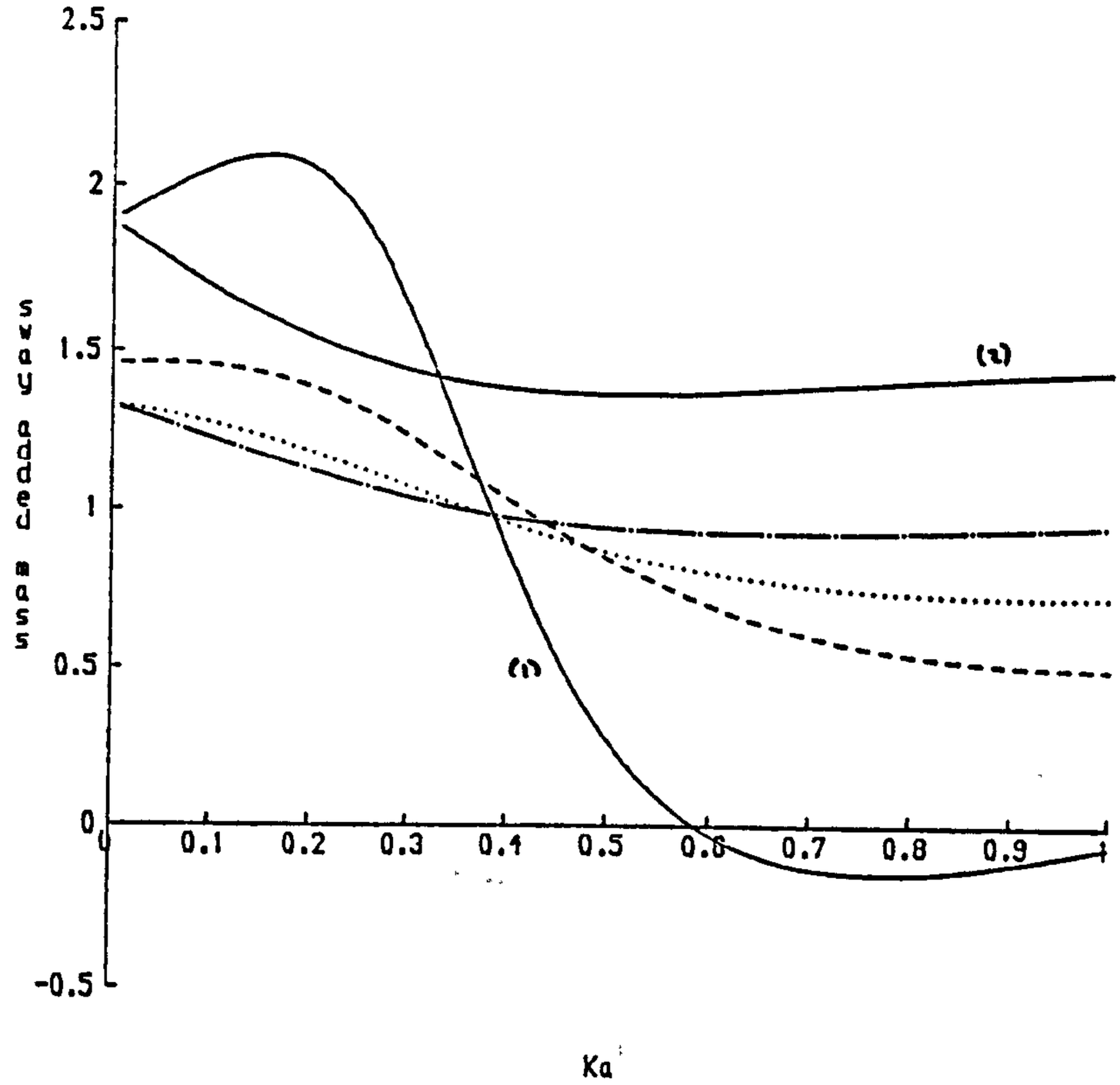

Figure 4.4.6. μ (sway) plotted against Ka for a submerged cylinder (a/h=0.2) with different clearances. ——— (1) f/a=1.1; – – – f/a=1.5; ····· f/a=2; –·–·– f/a=3; ——— (2) f/a=3.9.

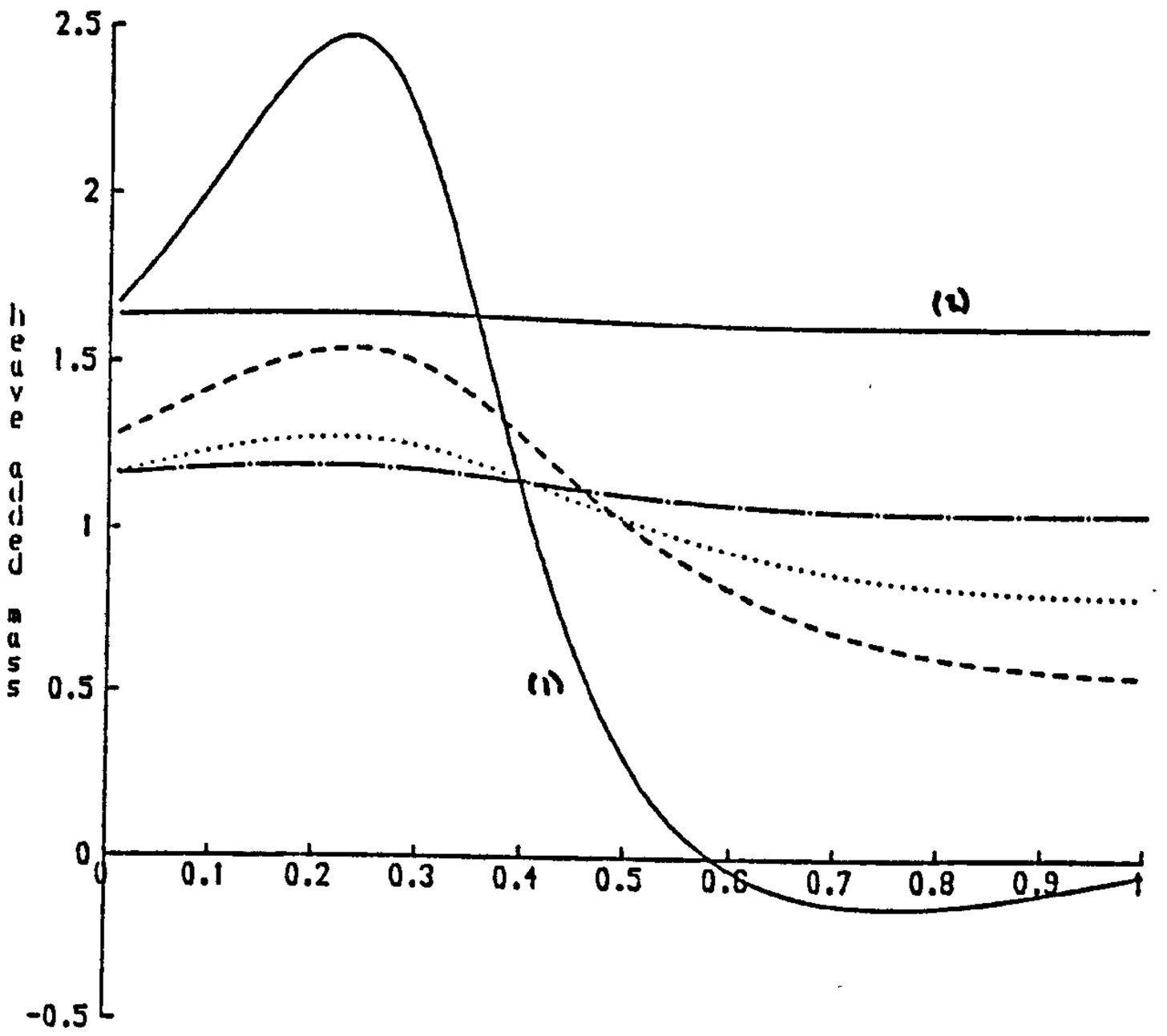

Figure 4.4.7. μ (heave) plotted against Ka for a submerged cylinder (a/h=0.2) with different clearances. ——— (1) f/a=1.1; – – – f/a=1.5; ····· f/a=2; –·–·– f/a=3; ——— (2) f/a=3.9.

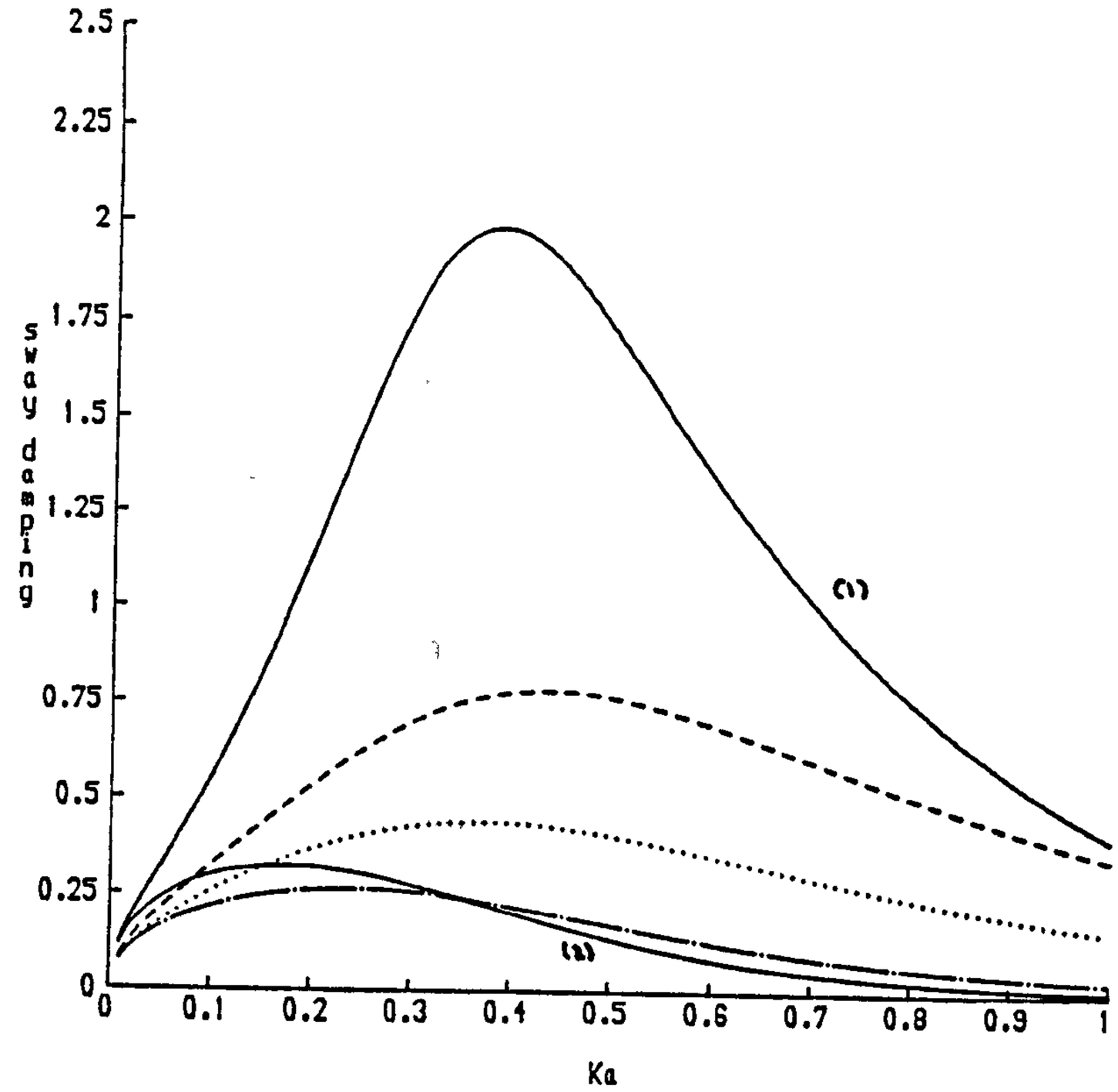

Figure 4.4.8. ν (sway) plotted against Ka for a submerged cylinder (a/h=0.2) with different clearances. ——— (1) f/a=1.1; - - - f/a=1.5; ····· f/a=2; -·-·- f/a=3; ——— (2) f/a=3.9.

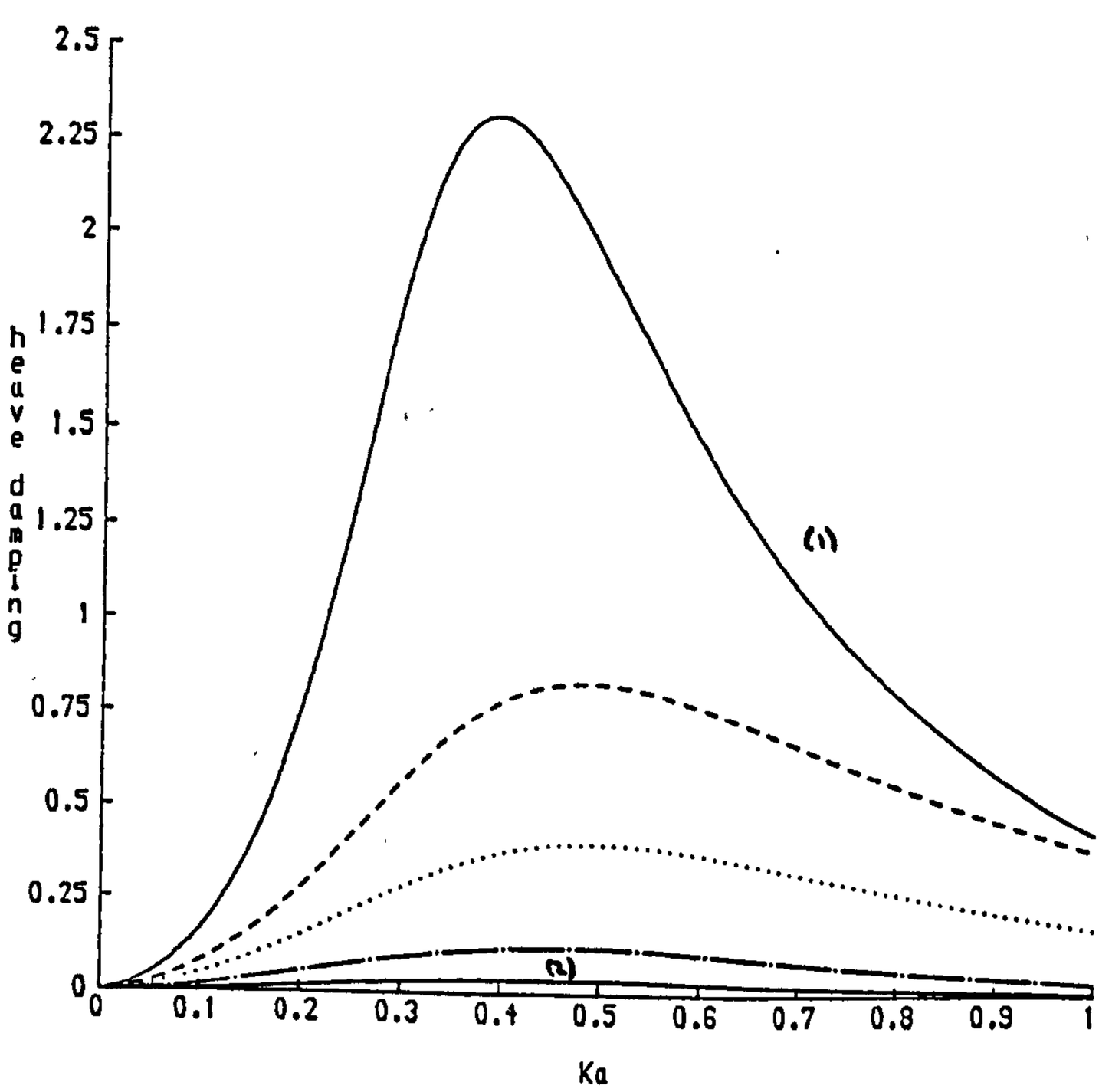

Figure 4.4.9. ν (heave) plotted against Ka for a submerged cylinder (a/h=0.2) with different clearances. ——— (1) f/a=1.1; - - - f/a=1.5; ····· f/a=2; -·-·- f/a=3; ——— (2) f/a=3.9.

The reflection coefficients for these five cases are shown in figure (4.4.10) and it can be seen that the effect of altering the immersion depth on $|R|$ is small.

It is interesting to examine the behaviour of the hydrodynamic characteristics of a cylinder as the gap between the cylinder and the bottom approaches zero. This can be done in two ways: fix f/a and let a/h tend to its limiting value or fix a/h and let f/a tend to its limiting value. The behaviour turns out to be essentially the same and so here we will just consider the latter with $a/h = 0.2$. There are possible problems in both the heave and sway cases. In heave, when $f/a = 4$, there will be a discontinuity in the derivative of the velocity potential at the point of contact between the cylinder and the bottom since the motion of the cylinder will imply a non-zero value of $\frac{\partial \phi}{\partial y}$ whereas the presence of the bottom will imply $\frac{\partial \phi}{\partial y} = 0$. In sway this problem does not arise but another one is present. Due to the antisymmetry of the problem there is likely to be an oscillating flow beneath the cylinder which for small gaps might have a large velocity. When $f/a = 4$ however this flow is no longer possible and the transition from one state to the other may be very delicate.

Let x be the non-dimensional gap width, i.e. $x = 1 - a/h - f/h$, and let $\xi(x)$ represent some hydrodynamic characteristic of the cylinder. Then $\xi(x) - \xi(0)$ must tend to zero as $x \longrightarrow 0$. However due to the problems described above the convergence is likely to be slow. A sensible guess for the behaviour of $\xi(x)$ as $x \longrightarrow 0$ would therefore be

$$\xi(x) - \xi(0) \sim A\, x \ln x \qquad \text{as} \quad x \longrightarrow 0 \qquad (4.4.19)$$

where A is some constant. Figures (4.4.11) and (4.4.12) show two curves of $|\xi(x) - \xi(0)|$ against $-x \ln x$ for the cases $\xi \equiv$ heave

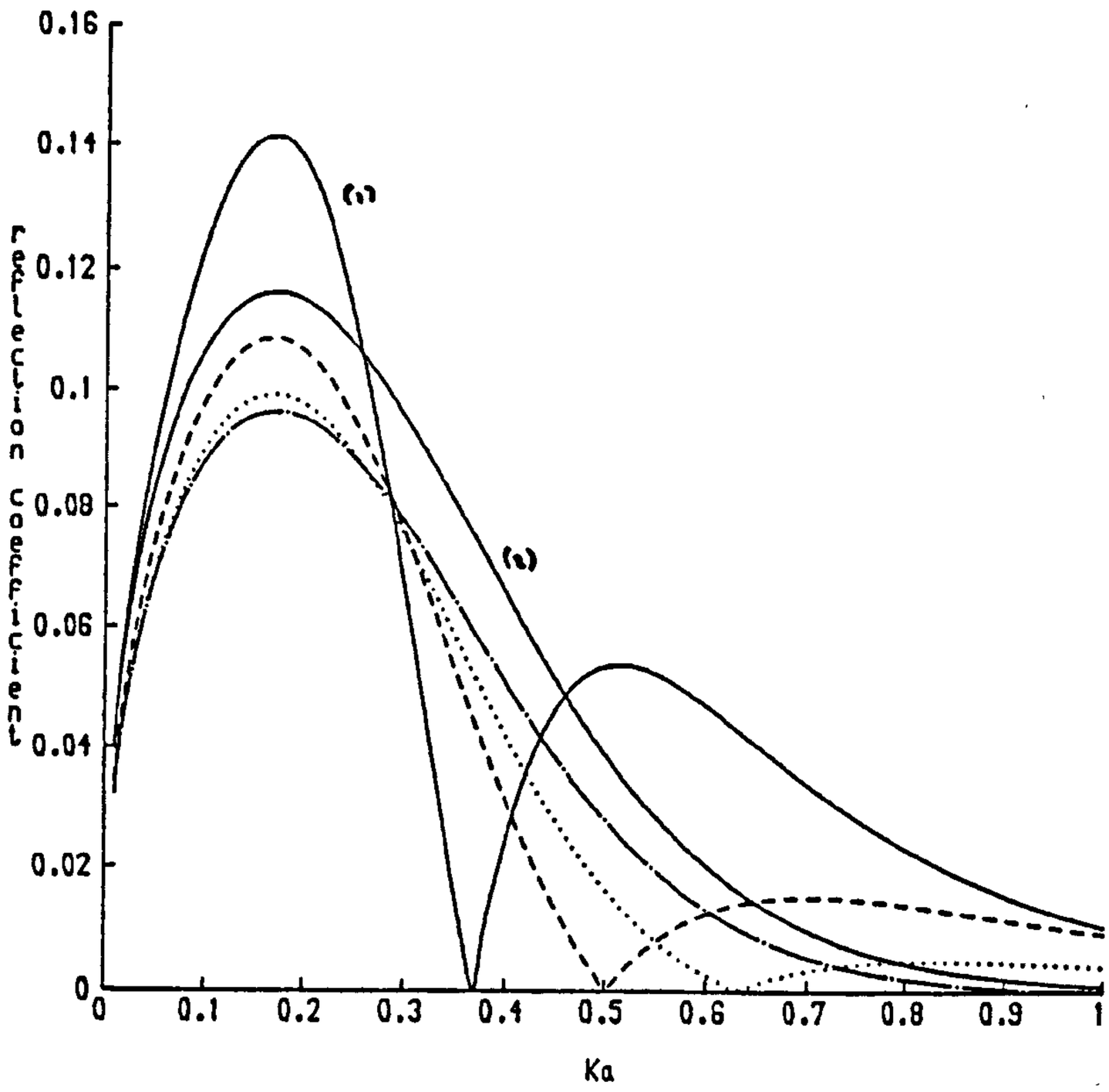

Figure 4.4.10. |R| plotted against Ka for a submerged cylinder (a/h=0.2) with different clearances. ——— (1) f/a=1.1; - - - f/a=1.5; ····· f/a=2; -·-·- f/a=3; ——— (2) f/a=3.9.

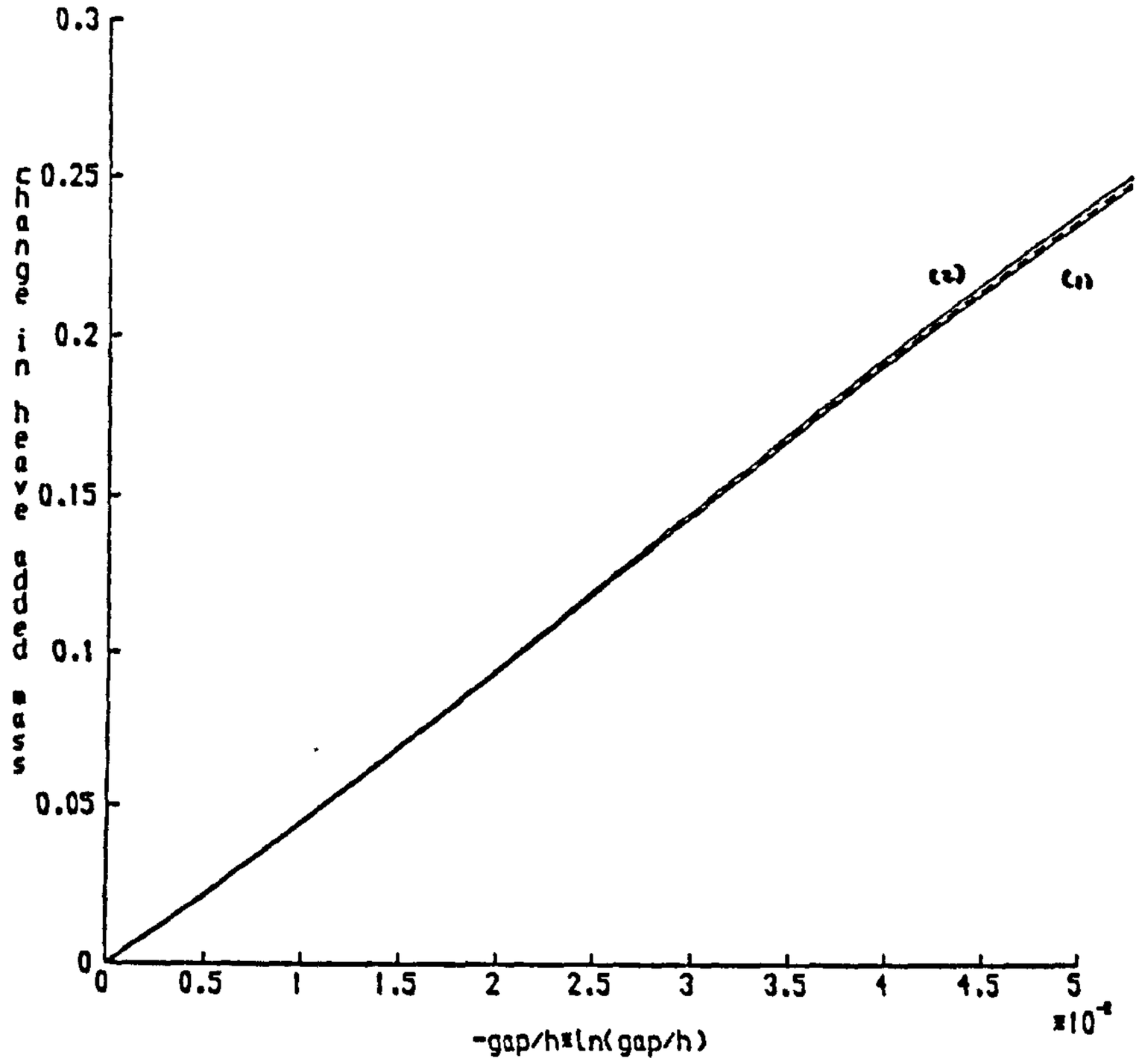

Figure 4.4.11. $|\xi(x)-\xi(0)|$ plotted against $-x \ln x$ when $\xi \equiv \mu$ (heave) for a submerged cylinder (a/h=0.2) at different frequencies. ——— (1) Ka=0.2; – – – Ka=0.4; ····· Ka=0.6; –·–·– Ka=0.8; ——— (2) Ka=1.

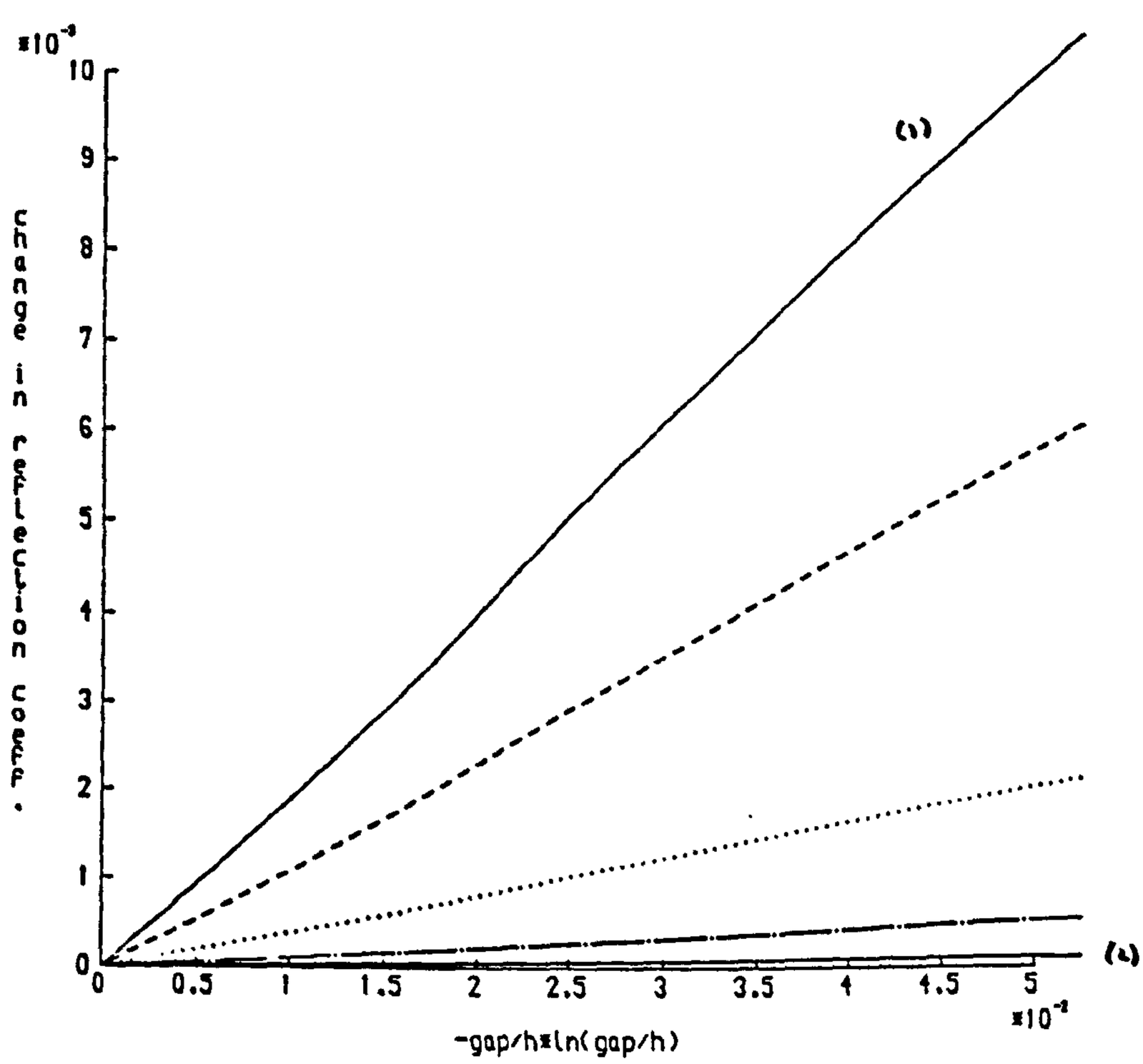

Figure 4.4.12. $|\xi(x)-\xi(0)|$ plotted against $-x \ln x$ when $\xi \equiv |R|$ for a submerged cylinder (a/h=0.2) at different frequencies. ——— (1) Ka=0.2; – – – Ka=0.4; ····· Ka=0.6; –·–·– Ka=0.8; ——— (2) Ka=1.

added mass and $\xi \equiv |R|$. In both cases curves are shown for five different frequencies, Ka = 0.2, 0.4, 0.6, 0.8 and 1.0. The figures show that equation (4.4.19) is indeed a good approximation near $x = 0$. In the case $\xi \equiv |R|$ it is clear that the constant is dependent on Ka but in the case $\xi \equiv$ heave added mass A is clearly independent of Ka. Other choices of ξ result in similar curves. In these two figures the range $0 < -x \ln x < 0.05$ is equivalent to the range $0 <$ gap/h < 0.011 for the non-dimensional gap.

4.5 The Scattering Problem for a Single Cylinder

The method used in §4.4 is not directly applicable to the scattering problem but the problem can be reformulated in such a way as to make the problem solvable by the multipole method. The time-independent velocity potential, ϕ_s, satisfies equations (4.4.1), (4.4.2), (4.4.3),

$$\frac{\partial \phi_s}{\partial r} = 0 \qquad \text{on} \quad r = a, \tag{4.5.1}$$

and

$$\phi_s \sim \frac{gA}{\omega} \frac{\cosh \kappa(y-h)}{\cosh \kappa h} \begin{cases} e^{i\kappa x} + Re^{-i\kappa x} & x \to +\infty \\ Te^{i\kappa x} & x \to -\infty \end{cases}. \tag{4.5.2}$$

If the potential ψ is defined by

$$\phi_s = \frac{gA}{\omega} \frac{\cosh \kappa(y-h)}{\cosh \kappa h} e^{i\kappa x} + \psi \tag{4.5.3}$$

then ψ also satisfies equations (4.4.1), (4.4.2), and (4.4.3) together with

$$\frac{\partial \psi}{\partial r} = - \frac{\partial}{\partial r}\left[\frac{gA}{\omega} \frac{\cosh \kappa(y-h)}{\cosh \kappa h} e^{i\kappa x}\right] \qquad \text{on} \quad r = a \tag{4.5.4}$$

and

$$\psi \sim \frac{gA}{\omega} \frac{\cosh \kappa(y-h)}{\cosh \kappa h} \begin{cases} Re^{-i\kappa x} & x \to +\infty \\ (T-1)e^{i\kappa x} & x \to -\infty \end{cases} . \qquad (4.5.5)$$

The function ψ is therefore an asymmetric radiation potential and so it can be represented by a combination of symmetric and antisymmetric multipoles:

$$\psi = \frac{gA}{a\omega} \sum_{n=1}^{\infty} (\alpha_n \phi_{n,1} + \beta_n \phi_{n,2}). \qquad (4.5.6)$$

Using equation (4.2.11) we have

$$\left.\frac{\partial \psi}{\partial r}\right|_{r=a} = \frac{gA}{a\omega} \sum_{n=1}^{\infty} \Big[- \alpha_n \sin n\theta - \beta_n \cos n\theta + \sum_{m=1}^{\infty} (\alpha_n \dot{A}_{mn,1} \sin m\theta + \beta_n \dot{A}_{mn,2} \cos m\theta) \Big]. \qquad (4.5.7)$$

Expanding the right hand side of equation (4.5.4) about $r = 0$ and then using equation (4.5.7) leads to uncoupled sets of equations for α_m and β_m:

$$\alpha_m - \sum_{n=1}^{\infty} A_{mn,1} \alpha_n = \frac{i}{2 \cosh \kappa h} \frac{(\kappa a)^m}{(m-1)!} [e^{\kappa(f-h)} - (-1)^m e^{\kappa(h-f)}] \qquad (4.5.8)$$

$$\beta_m - \sum_{n=1}^{\infty} A_{mn,2} \beta_n = \frac{1}{2 \cosh \kappa h} \frac{(\kappa a)^m}{(m-1)!} [e^{\kappa(f-h)} + (-1)^m e^{\kappa(h-f)}].$$

These equations can again be solved using a truncation procedure.

The results were used to calculate R and T directly and this provided a check, since these values have already been calculated when solving the radiation problem. (See equations (4.4.15) and (4.4.16)).

Naftzger and Chakrabarti (1979) used a numerical technique based on Green's theorem to solve this problem. The particular quantities that are calculated and plotted in their paper are the vertical and horizontal forces on the cylinder due to the wave motion. The formulation of the problem used here gives these quantities very simply. For example, the horizontal force is given by

$$f_H = -\rho\omega i \int_{-\pi}^{\pi} \phi_s(a,\theta)\ a \sin\theta\ d\theta \qquad (4.5.9)$$

which, using equations (4:5.3) and (4.5.6) gives

$$f_H = -\ i\rho g A \pi a \left[i\kappa a \frac{\cosh \kappa(f-h)}{\cosh \kappa h} + \alpha_1 + \sum_{n=1}^{\infty} \alpha_n A_{1n,1} \right]. \qquad (4.5.10)$$

Finally, using equation (4.5.8) with $m = 1$ gives

$$f_H = -\ 2i\rho g A \pi a\ \alpha_1 \qquad (4.5.11)$$

If this expression for f_H is normalised in the same way as in Naftzger and Chakrabarti (1979) then

$$\bar{f}_H \equiv \left| \frac{f_H}{\rho g a A} \right| = 2\pi\ |\alpha_1| \ . \qquad (4.5.12)$$

Similarly, the result for the vertical force is

$$\bar{f}_V = 2\pi\ |\beta_1| \ . \qquad (4.5.13)$$

Figures (4.5.1) and (4.5.2) show graphs of $\bar{f}_H$ and $\bar{f}_V$ against Ka for two cylinders at the same immersion depth but in different depths of water. The values obtained agree, as accurately as can be assessed from

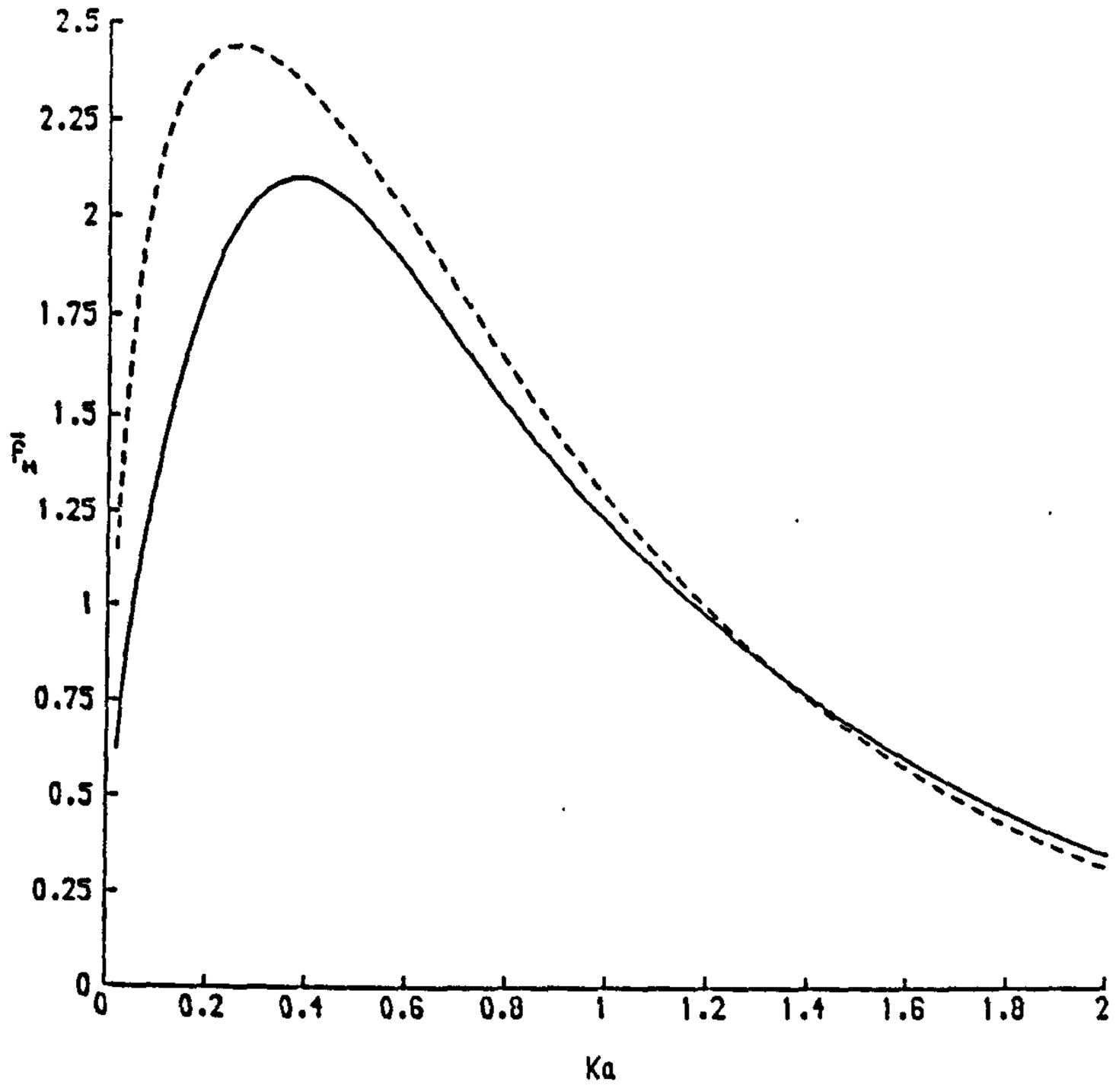

Figure 4.5.1. $\bar{f}_H$ plotted against Ka for a fixed cylinder (f/a=1.25) in two different water depths. ——— a/h=0.25; - - - a/h=0.4.

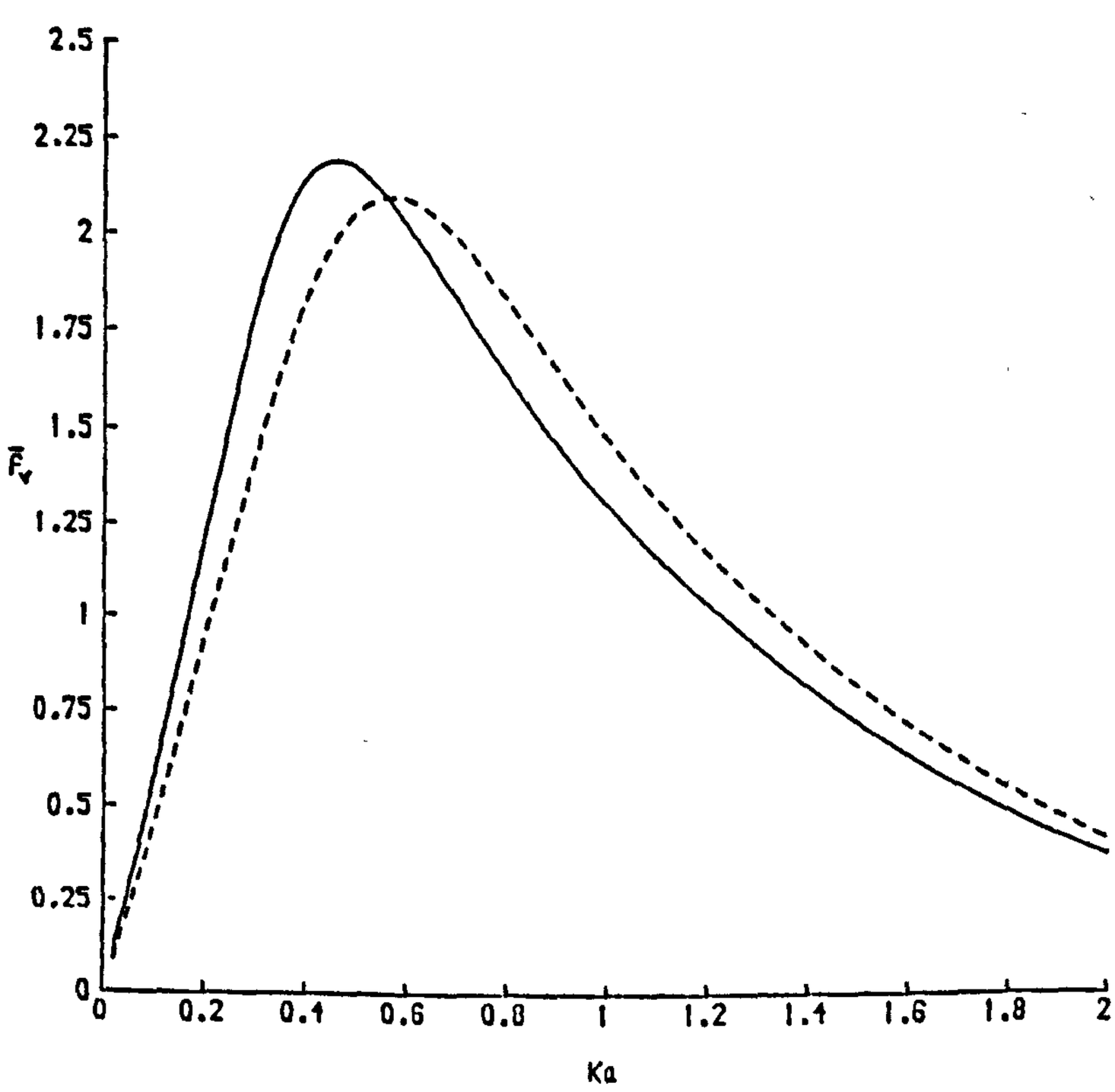

Figure 4.5.2. $\bar{f}_V$ plotted against Ka for a fixed cylinder (f/a=1.25) in two different water depths. ——— a/h=0.25; - - - a/h=0.4.

the graphs in their paper, with those of Naftzger and Chakrabarti (1979). The effects of finite depth are small, but it is noteworthy that in shallower water the maximum horizontal force is increased whereas the maximum vertical force decreases (in infinite depth these forces are equal, see Ogilvie (1963)).

4.6 Tethered Cylinders

We are now in a position to apply the theory of §3.2 to the case of a submerged horizontal cylinder. Since a body will have to be moored in any event, to prevent it drifting away, the tension in the mooring line of the buoyant cylinder can be used to provide the spring constant λ. The cylinder is held down by two inextensible cables, one at each end. During the passage of the waves the cylinder makes small horizontal oscillations about the vertical. (Any slight offset which may develop due to second order mean drift forces will be neglected).

Let the cylinder have specific gravity s, so that the mass of the cylinder, I, is given by $I = M's$ where M' is the mass of water displaced by the cylinder, and let the cables have length ℓ. Then for small horizontal oscillations the acceleration of the cylinder is opposed by the the horizontal component of the tension in the cables. This in turn is just the difference between the upthrust and the weight of the cylinder. For small motions we may neglect the small additional oscillatory vertical force due to the waves. Thus

$$\lambda = M'(1 - s)g/\ell \tag{4.6.1}$$

and for $T_1 = 0$ equation (3.2.30) implies that, for frequency ω,

$$(1 - s)g/\ell = \{(\mu + s) + \nu\chi\}\omega^2 \tag{4.6.2}$$

where $\mu = M/M'$, $\nu = B/M'\omega$ are the non-dimensional added-mass and radiation-damping coefficients respectively, each varying with wave frequency.

Equation (4.6.2) provides a relation between incident wave frequency ω, specific gravity s, and cable length ℓ to ensure tuning. For example it may be re-written

$$s = \frac{1 - (\mu + \nu\chi)K\ell}{1 + K\ell} \qquad (K = \omega^2/g) \ . \tag{4.6.3}$$

Suppose ℓ, s and hence λ are chosen so as to tune the cylinder to cancel a wave of frequency ω_o. Then

$$\lambda \equiv \lambda_o = (M_o + I)\omega_o^2 + B_o\omega_o\chi_o \tag{4.6.4}$$

where the suffix denotes values of those quantities at frequency ω_o.

Substitution of equation (4.6.4) into equation (3.2.28) gives

$$T_1 = T\,\frac{(\mu + s) + \nu\chi - \{(\mu_o + s) + \nu_o\chi_o\}(\omega_o/\omega)^2}{(\mu + s) - i\nu - \{(\mu_o + s) + \nu_o\chi_o\}(\omega_o/\omega)^2} \tag{4.6.5}$$

for the variation of the transmitted wave amplitude with wave frequency. It can be seen clearly from equation (4.6.5) that $T_1 = 0$ when $\omega = \omega_o$. A similar expression can be derived for R_1.

The velocity amplitude is given, from equations (3.2.23) and (3.2.17) by

$$|U| = \frac{gA}{\omega}\,\frac{1}{|A_s|(1 + C^2)^{1/2}} \tag{4.6.6}$$

and this can be re-written in terms of the wavemaking coefficient, W_c, defined as the ratio of the amplitude of the waves radiated to infinity to the amplitude of the forced motion of the cylinder in sway. Thus

from equations (3.2.9), (3.2.11) and (3.2.12) it follows that

$$W_c = K|A_s| \tag{4.6.7}$$

whence the non-dimensional cylinder velocity $\bar{U}$ is

$$|\bar{U}| \equiv \frac{|U|}{A\omega} = \frac{1}{W_c(1 + C^2)^{1/2}} \ . \tag{4.6.8}$$

The maximum amplitude of the free surface over a period is given by

$$|\eta| = \frac{\omega}{g} \ |\phi_s(x,0) + U\phi_R(x,0)| \ .$$

Thus, using equation (3.2.13),

$$\left|\frac{\eta}{A}\right| = \left|\frac{\omega}{gA}\phi_s(x,0) + \frac{(T - T_1)}{A_s}\phi_R(x,0)\right| . \tag{4.6.9}$$

Equations (4.4.5), (4.5.3) and (4.5.6) imply that

$$\left|\frac{\eta}{A}\right| = \left| \ e^{i\kappa x} + \sum_{n=1}^{\infty} \left[\left[\frac{\alpha_n}{a} + \frac{(T - T_1)}{A_1}c_{n,1}\right]\phi_{n,1}(x,0) + \frac{\beta_n}{a}\phi_{n,2}(x,0)\right] \ \right| . \tag{4.6.10}$$

In order to calculate $|\eta/A|$ the original representation for $\phi_{n,q}$, equation (4.2.2), was used since the expansion in polar coordinates, equation (4.2.11), is only valid for $r < 2f$. Evaluation of equation (4.2.2) requires the evaluation of oscillatory integrals which is time consuming but not a major problem.

4.7 Results and Discussion

If the cylinder is fastened to cables which are fixed to the sea bed the length of the cables, ℓ, is just $h - f$ and so the condition for

perfect reflection, equation (4.6.2), can be written

$$1 - s = K\,(h - f)\,(\mu + s + \nu\chi)\ . \qquad (4.7.1)$$

For a given cylinder this can be solved to find a frequency at which this relation is satisfied. If such a frequency exists it will be represented by ω_o and as in the previous section a subscript zero will refer to the value of a frequency-dependent quantity at ω_o.

There are basically three parameters in the problem; a/h, f/h, and s. How the value of s affects the reflection characteristics of a tethered cylinder will be examined first by considering a cylinder for which a/h = 0.25 and f/h = 0.5. Table (4.7.1) shows how the tuning frequency varies as s is increased from a very small value, 0.01, to almost water density. It is clear that the smaller s is the shorter the wavelength of the waves which will be totally reflected by the cylinder. The sort of waves that might be encountered, for example, in a harbour entrance are likely to be in the range $\lambda/2a < 10$ and so for the device to be a practical possibility the specific gravity must be small. This is an attractive feature since a small value of s would ensure that the mooring lines were always taut, even in severe weather, and it would also allow the device to be built out of some cheap, light, rubber material.

s	$K_o a$	$\lambda_o/2a$
0.01	0.61	5.1
0.06	0.49	6.2
0.1	0.41	7.1
0.2	0.29	9.5
0.3	0.22	11.2
0.4	0.17	13.7
0.5	0.13	15.7
0.6	0.10	18.5
0.7	0.07	22.4
0.8	0.04	31.4
0.9	0.02	44.9

Table 4.7.1

Figure (4.7.1) shows how $|T_1|$, calculated from equation (4.6.5) varies with non-dimensional frequency, Ka, for five values of the specific gravity, s, with the same cylinder dimensions as described above. The figure illustrates the crucial problem which a good wave reflector must overcome. While all the curves are zero at their respective tuned frequencies the range of values, or bandwidth, of frequencies over which $|T_1|$ is small varies dramatically from curve to curve. The fact that the bandwidth is greater for small values of s is encouraging for the reasons described in the previous paragraph.

Figure (4.7.2) shows exactly the same curves plotted against non-dimensional wavelength, $\lambda/2a$. It is noticeable that in this figure the bandwidths of the five different curves are very similar, though a close inspection reveals that the bandwidth still increases as s decreases. This is due to the fact that the relation between Ka and $\lambda/2a$ is not linear ($Ka = 2\pi a\lambda^{-1} \tanh 2\pi h\lambda^{-1}$). Using $\lambda/2a$ as the

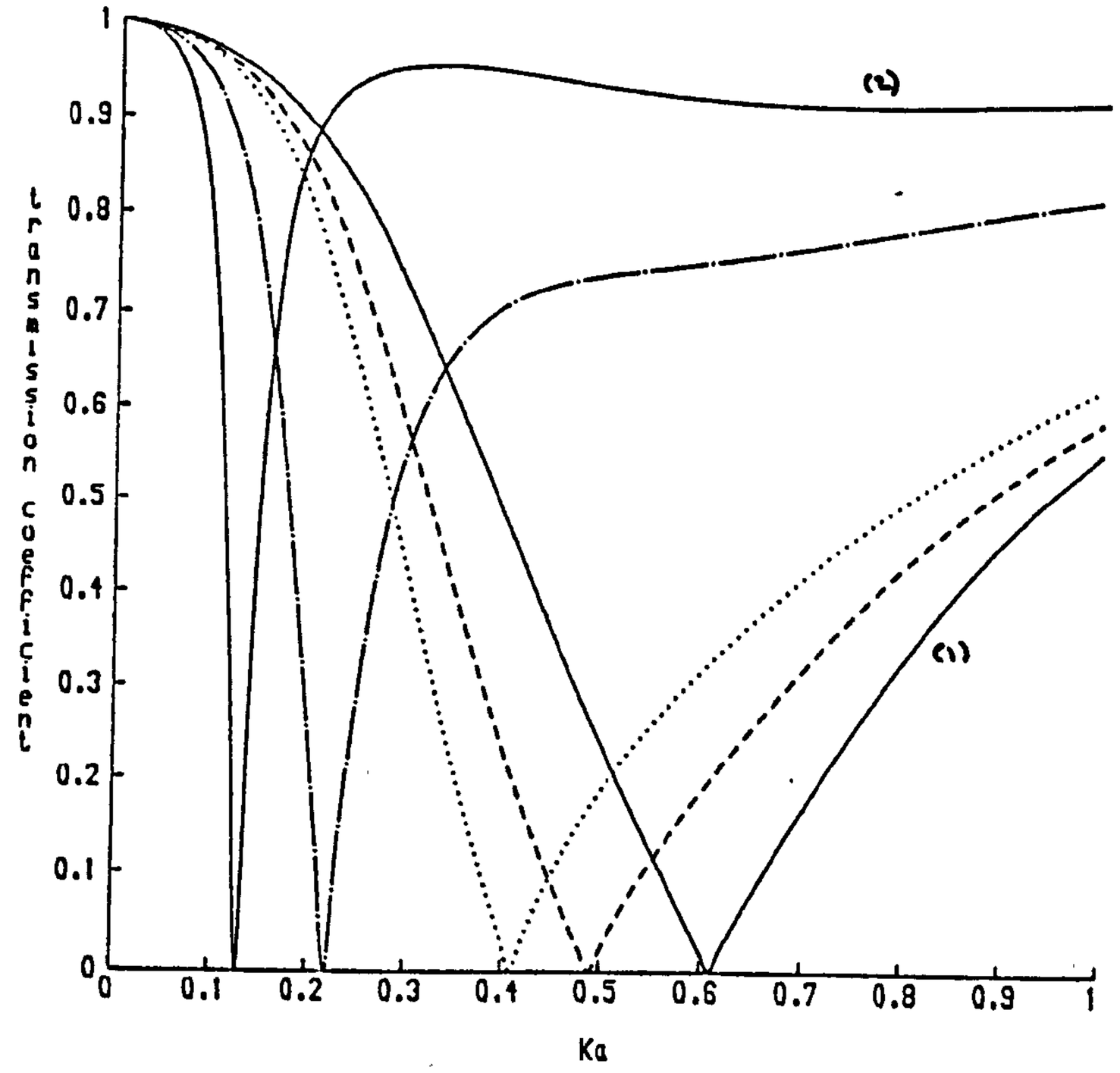

Figure 4.7.1. $|T_1|$ plotted against Ka for tethered cylinders (a/h=0.25, f/h=0.5) with different specific gravities. ——— (1) s=0.01; – – – s=0.06; ····· s=0.1; –·–·– s=0.3; ——— (2) s=0.5.

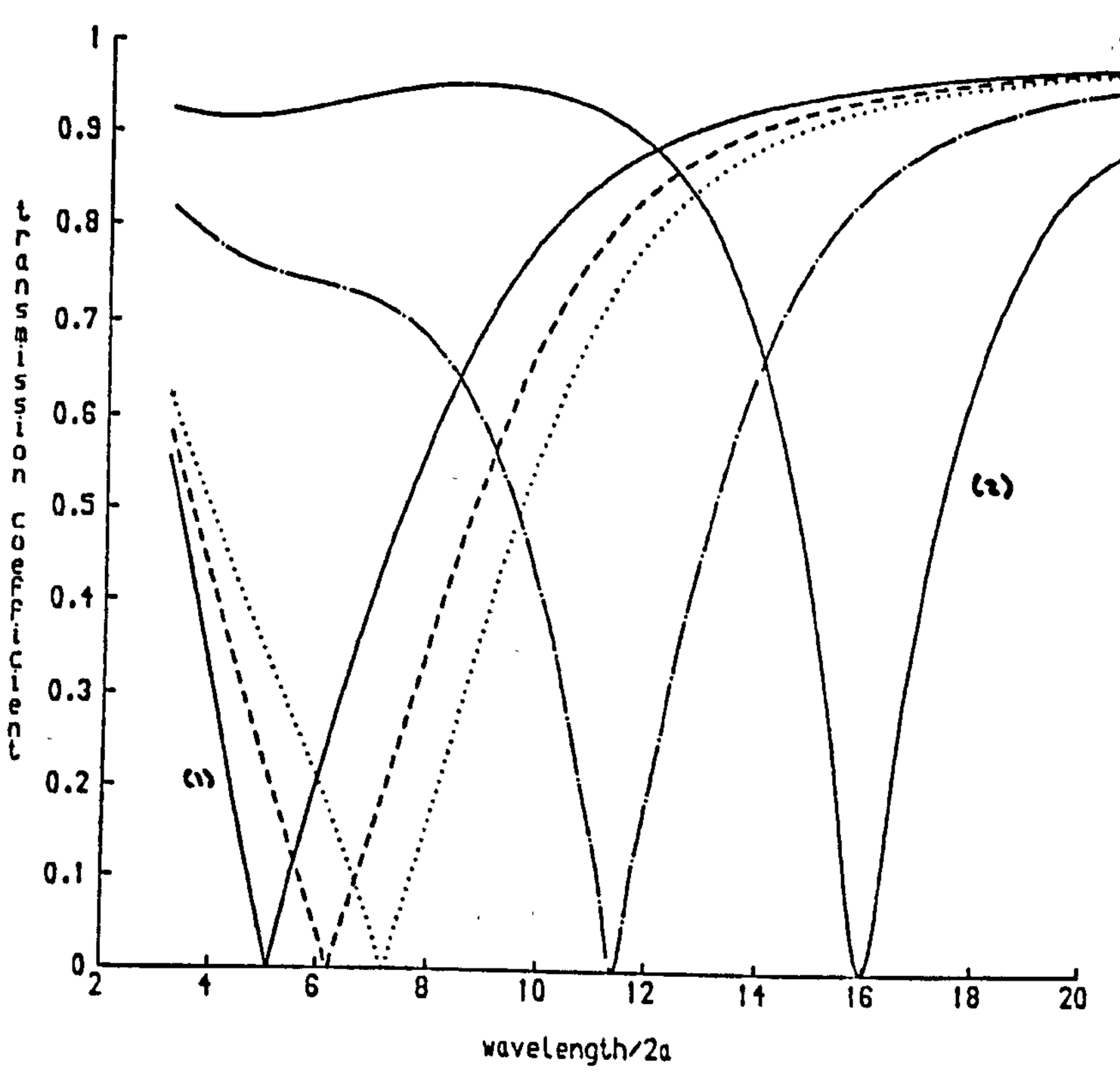

Figure 4.7.2. $|T_1|$ plotted against $\lambda/2a$ for tethered cylinders (a/h=0.25, f/h=0.5) with different specific gravities. ——— (1) s=0.01; – – – s=0.06; ····· s=0.1; –·–·– s=0.3; ——— (2) s=0.5.

x-coordinate makes it easier to interpret the results. Thus we see that when $s = 0.06$ the transmission coefficient is less than 0.3 for wavelengths of between 4 and 6 diameters which provides a clearer impression of the capacity of the cylinder to reflect waves of different wavelengths. It is also more important from an engineering point of view to have a large bandwidth in terms of the more familiar wavelength than in terms of the slightly artificial parameter Ka. For this reason all the results in this section, except those from experiments, will be plotted with $\lambda/2a$ as the x-coordinate.

To simplify the rest of this results section we shall fix a particular value of the specific gravity and use it in all the remaining calculations. In the experiments which will be discussed later a cylinder with $s = 0.06$ was used and so it will be convenient to use this value throughout.

One of the attractive features of using a tethered cylinder as a wave reflector is that large reductions in wave intensity can be achieved while still having a considerable gap between the top of the cylinder and the free surface, large enough to allow the passage of a small vessel for example. Figure (4.7.3) shows curves of $|T_1|$ against $\lambda/2a$ for three cylinders all with a constant immersion depth to radius ratio, $f/a = 2$. The different curves correspond to different water depths: $a/h = 0.1$, 0.2, and 0.25. Shallower water results in shorter cables and as a result the cylinder is tuned to shorter waves together with an increase in the bandwidth. This makes this sort of device suitable for installation in areas of shallow water like harbour entrances or for the protection of other coastal installations.

The bandwidth of the curves can be examined in more detail. For example when $a/h = 0.25$, $|T_1|$ is less than 0.5 for wavelengths of between 4 and 8 diameters. This corresponds to a reflection coefficient of greater than 0.87 or equivalently one can say that the cylinder

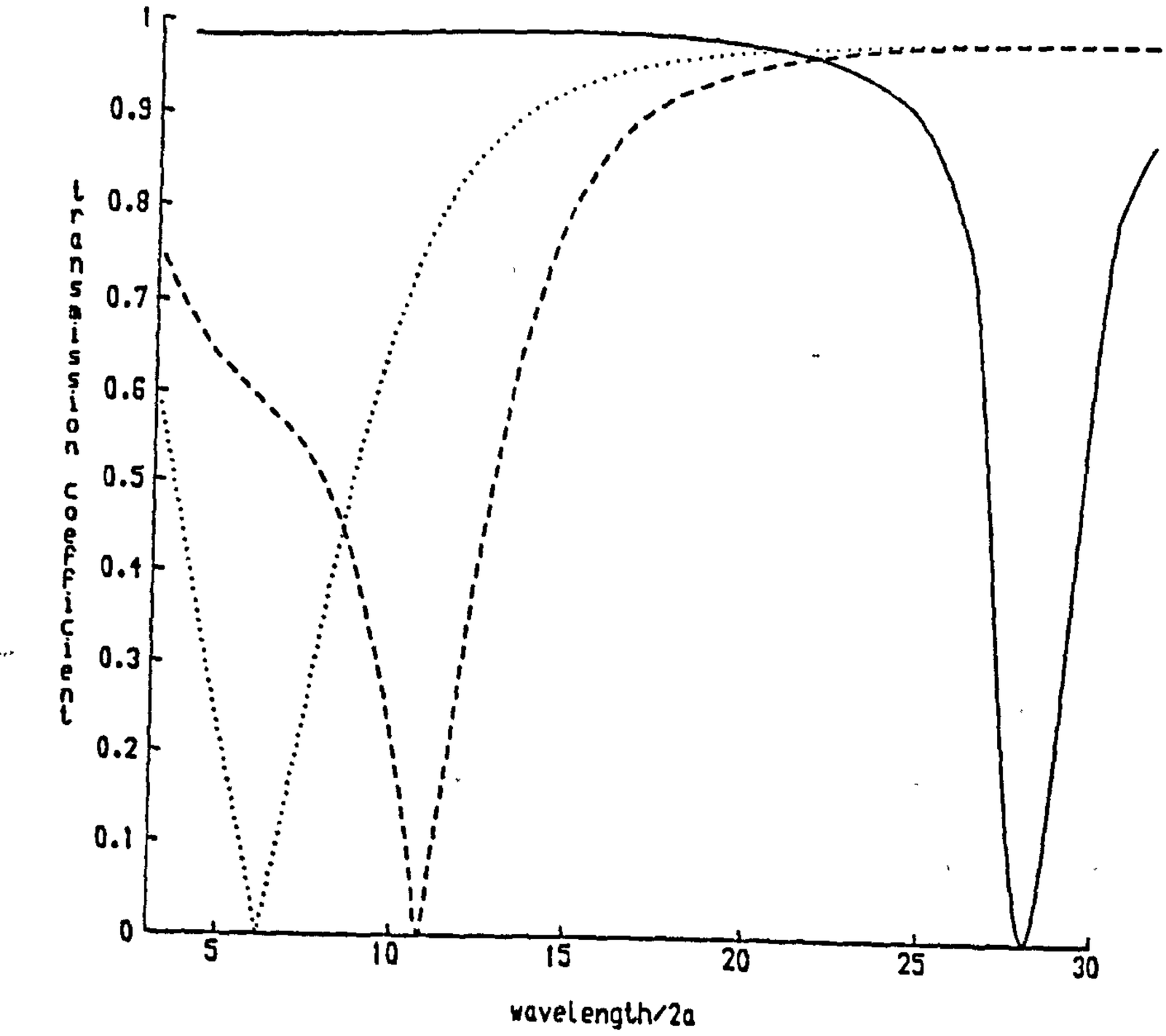

Figure 4.7.3. $|T_1|$ plotted against $\lambda/2a$ for tethered cylinders (f/a=2) in different water depths. ——— a/h=0.1; – – – a/h=0.2; ····· a/h=0.25.

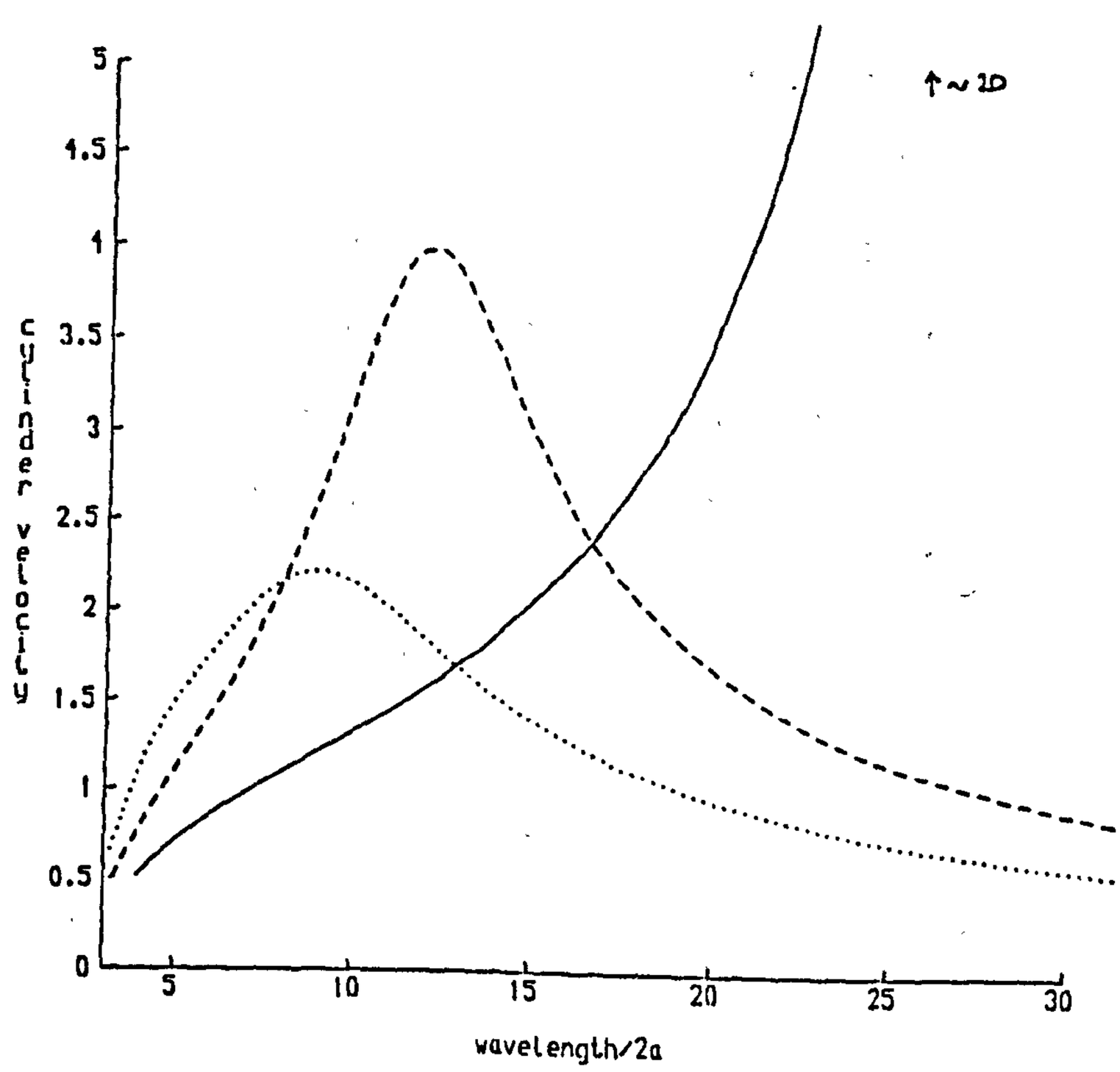

Figure 4.7.4. $|\bar{U}|$ plotted against $\lambda/2a$ for tethered cylinders (f/a=2) in different water depths. ——— a/h=0.1; – – – a/h=0.2; ····· a/h=0.25.

reflects over 75% of the incoming wave energy over this range.

It is of interest to know the sort of cylinder velocities required to achieve this degree of reflection. This is illustrated in figure (4.7.4) for the same three cases that were shown in the previous figure. The graph shows $|\bar{U}|$, defined by equation (4.6.8), plotted against $\lambda/2a$ and shows that although the bandwidths in figure (4.7.3) look quite similar the smaller a/h is the less likely it is that these results will be achieved in practice. Even when $a/h = 0.25$, $|\bar{U}|$ is greater than 2 for some wavelengths, indicating that the cylinder has a maximum speed over twice as great as that of a typical water particle in the free surface. This turns out to be possible, as the experiments discussed later confirm, whereas $|\bar{U}| \simeq 20$ corresponding to $a/h = 0.1$ is clearly not realisable in practice.

A comparison of the curves for $a/h = 0.25$ in figures (4.7.3) and (4.7.4) shows that the maximum value of $|\bar{U}|$ does not occur at the point of zero transmission as one might intuitively expect. The equation for $|\bar{U}|$, equation (4.6.8), shows that amongst other things $|\bar{U}|$ is inversely proportional to the wavemaking coefficient, W_c, and curves of W_c are shown in figure (4.7.5). It can be seen from these curves that in the situations under consideration W_c has a maximum near $\lambda/2a = 3$ and then gradually decreases as λ increases. Clearly, since $|\bar{U}|$ is bounded as $\lambda/2a \rightarrow 0$ and as $\lambda/2a \rightarrow \infty$, a complicated balance exists between this ability to make waves and the forces on the cylinder which appear in equation (4.6.8) through the term $(1 + C^2)^{-1/2}$.

Figures (4.7.6)-(4.7.8) show curves of $|T_1|$, $|\bar{U}|$ and W_c for three cylinders slightly closer to the free surface (with $f/a = 1.5$). Comparing the curve for $a/h = 0.2$ with that shown in figure (4.7.3) shows that by moving the cylinder closer to the free surface the length of the cables has increased and the cylinder is tuned to slightly longer waves. There is a slight reduction in the bandwidth of the main peak

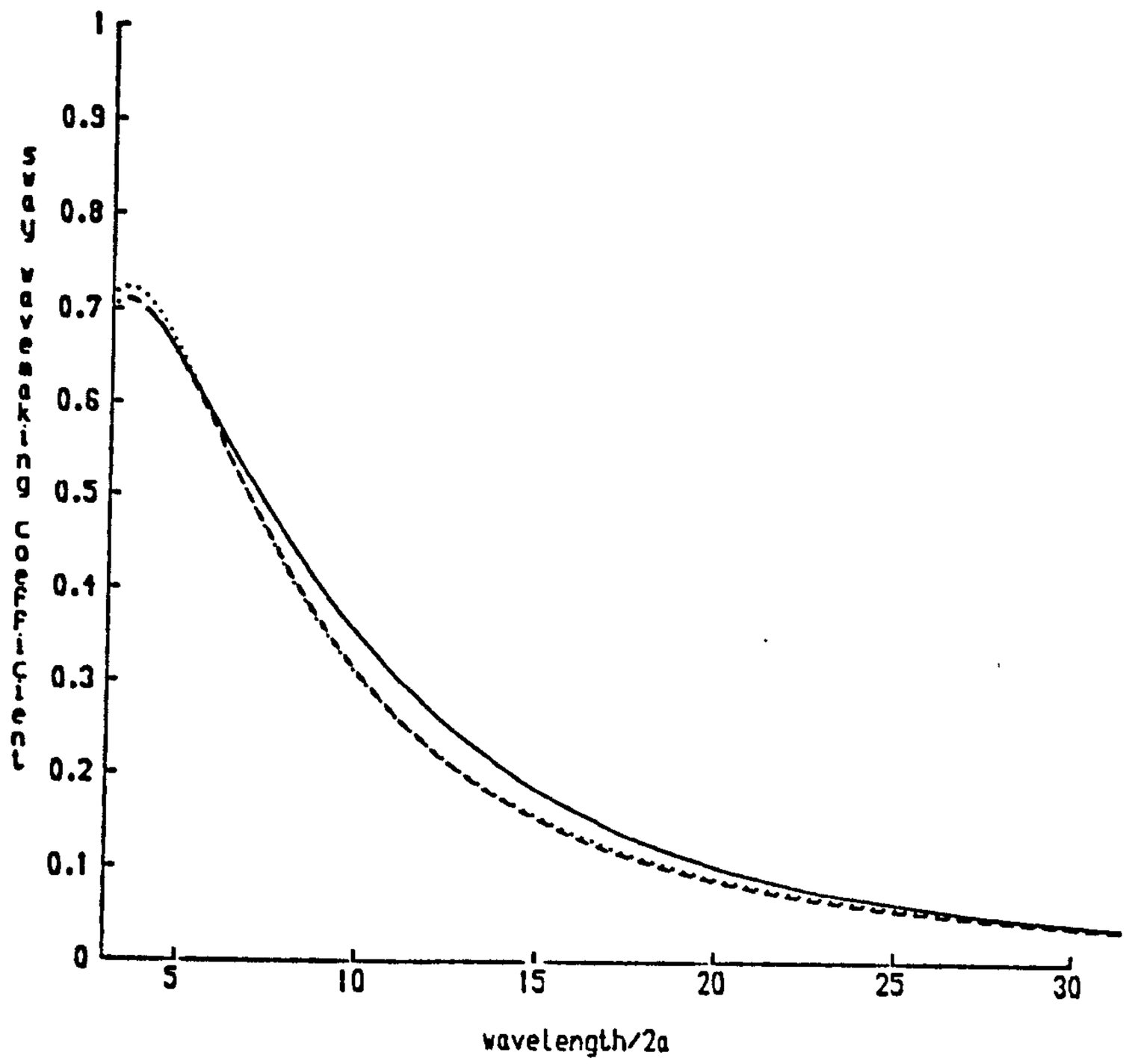

Figure 4.7.5. W_c (sway) plotted against $\lambda/2a$ for submerged cylinders (f/a=2) in different water depths. ——— a/h=0.1; – – – a/h=0.2; ····· a/h=0.25.

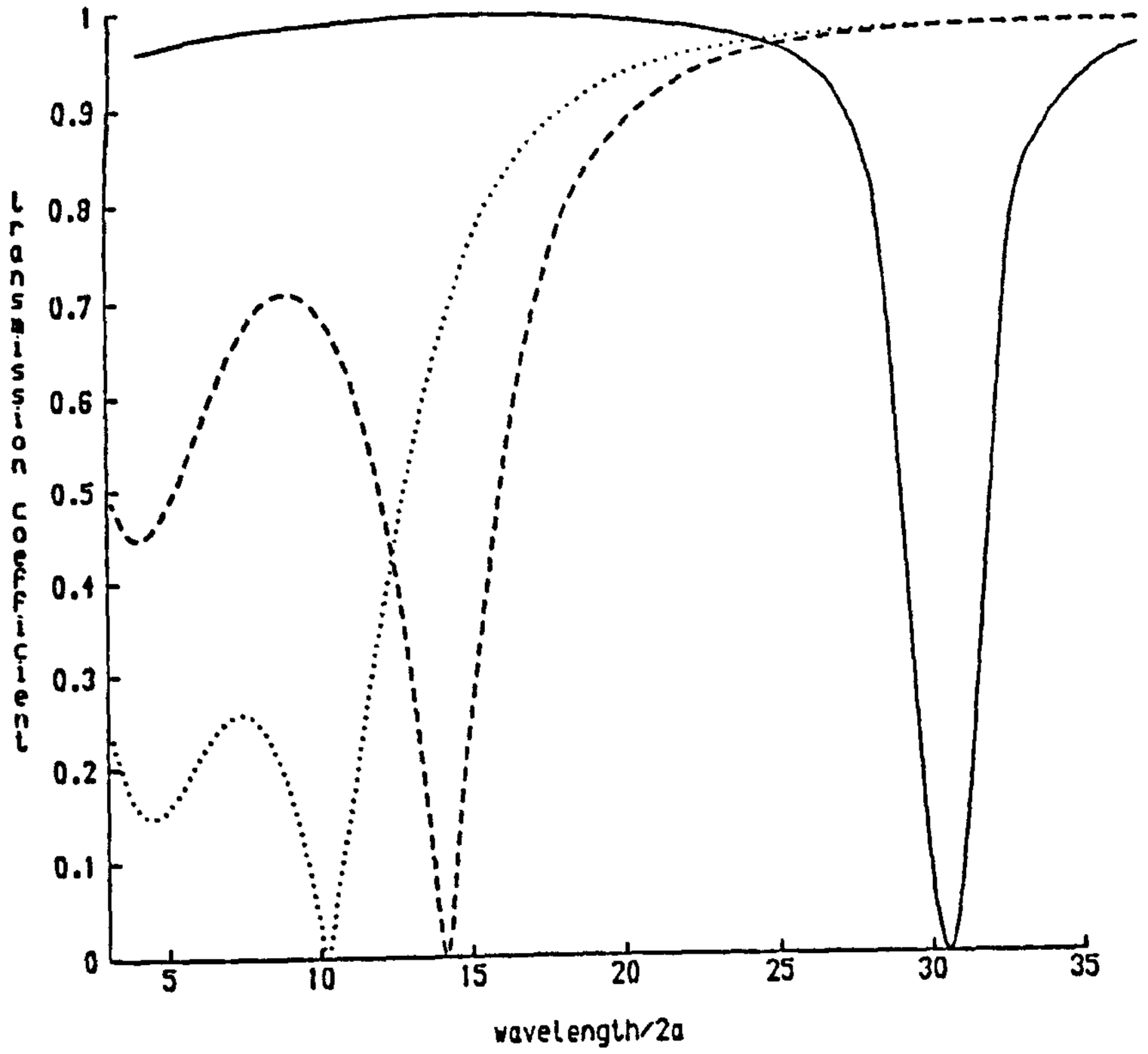

Figure 4.7.6. $|T_1|$ plotted against $\lambda/2a$ for tethered cylinders (f/a=1.5) in different water depths. ——— a/h=0.1; – – – a/h=0.2; ····· a/h=0.25.

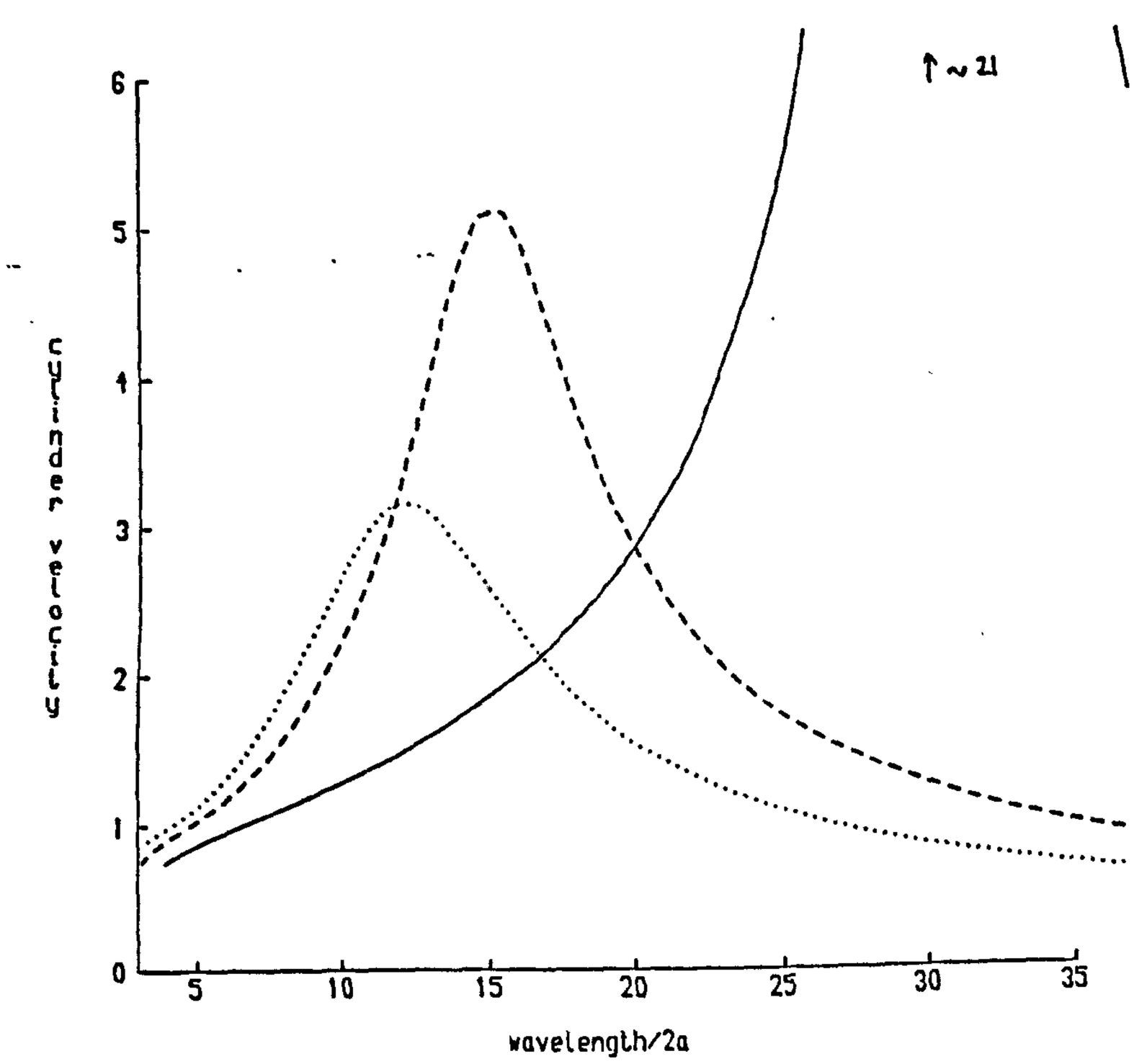

Figure 4.7.7. $|\bar{U}|$ plotted against $\lambda/2a$ for tethered cylinders (f/a=1.5) in different water depths. ——— a/h=0.1; – – – a/h=0.2; ····· a/h=0.25.

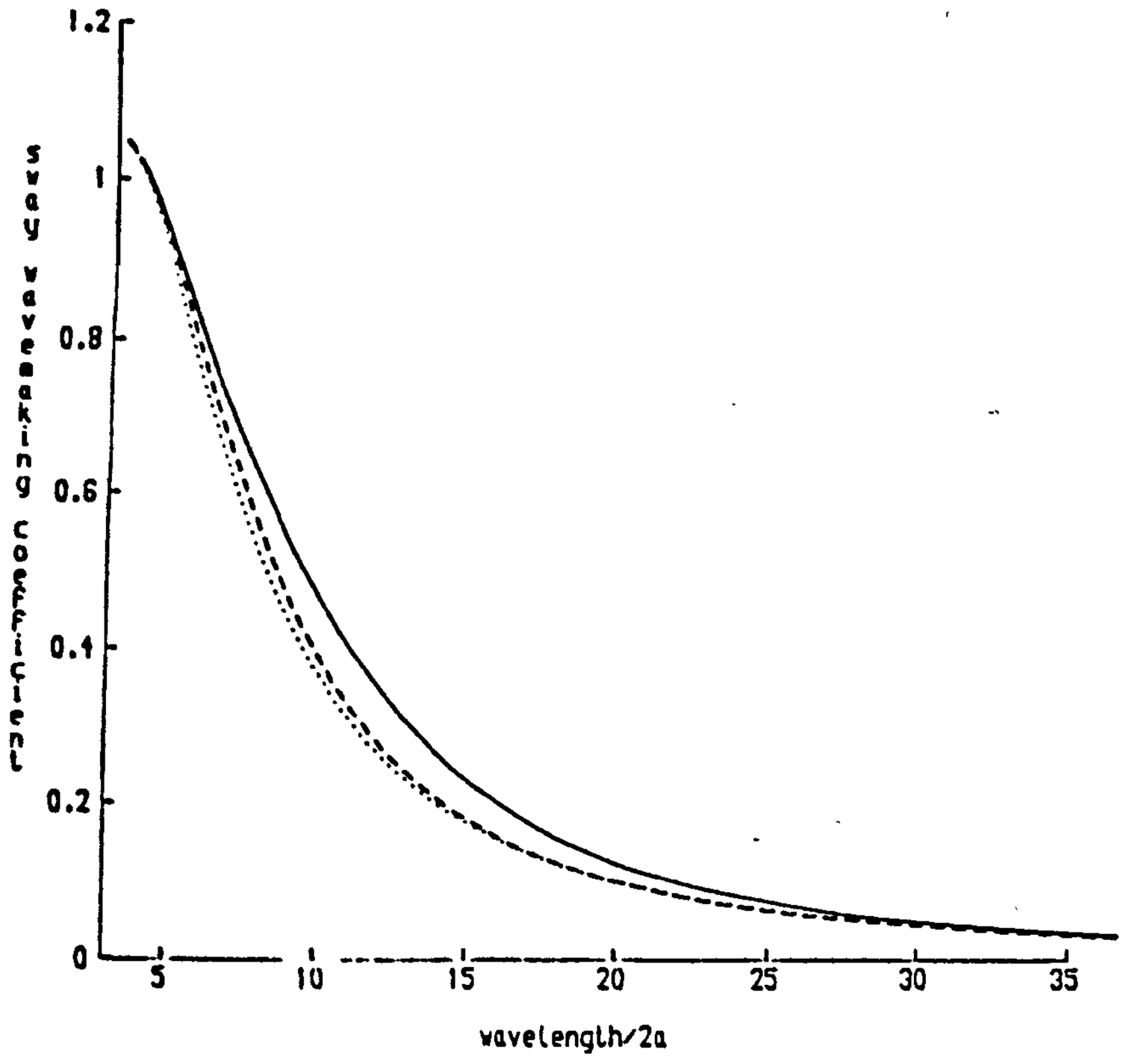

Figure 4.7.8. W_c (sway) plotted against $\lambda/2a$ for submerged cylinders (f/a=1.5) in different water depths. ——— a/h=0.1; – – – a/h=0.2; ····· a/h=0.25.

but the wavemaking capabilities of the cylinder are greatly enhanced when it is close to the free surface and this results in a small secondary peak. The cylinder velocities required to achieve these transmission coefficients is seen, by comparing figures (4.7.4) and (4.7.7) to be slightly greater than in the case when $f/a = 2$.

Figure (4.7.9) shows how $|T_1|$ varies, as a cylinder with $a/h = 0.2$ moves closer to the free surface, in more detail. When $f/a = 1.1$ the cylinder is tuned to $\lambda/2a \simeq 19$ but $|T_1|$ is almost zero near $\lambda/2a = 7$ and is zero again near $\lambda/2a = 2.5$. The associated cylinder velocity, shown in figure (4.7.10), for this curve is very large near the tuned wavelength but is small near the secondary peak where the sway wavemaking coefficient, shown in figure (4.7.11), is much greater. The sway wavemaking coefficient decreases as $\lambda/2a$ decreases from 5 and the cylinder velocity at the zero of transmission near $\lambda/2a = 2.5$ is larger again. This suggests that such a cylinder would be a much better reflector if it were tuned to a wavelength of about 7 diameters which could be done by using some form of semi-elastic rod to moor the device or by attaching the cables to some fixed point above the bottom. Figure (4.7.12) shows that this is indeed the case with more than 70% of the incident wave energy reflected over the whole range from, $3 < \lambda/2a < 16$. Figure (4.7.13) emphasises the practicality of this result with the non-dimensional cylinder velocity about 1 for wavelengths in the range $3 < \lambda/2a < 10$.

Figure (4.7.14) shows another particularly good configuration: $a/h = 0.3$, $f/h = 0.4$. In this case however the tuning is not artificial. The curve for $a/h = 0.2$, $f/h = 0.4$ is shown for comparison (see figures (4.7.3)-(4.7.5)). Again a very wide bandwidth with small transmission coefficient is achieved with relatively small cylinder velocities, as can be seen from figure (4.7.15).

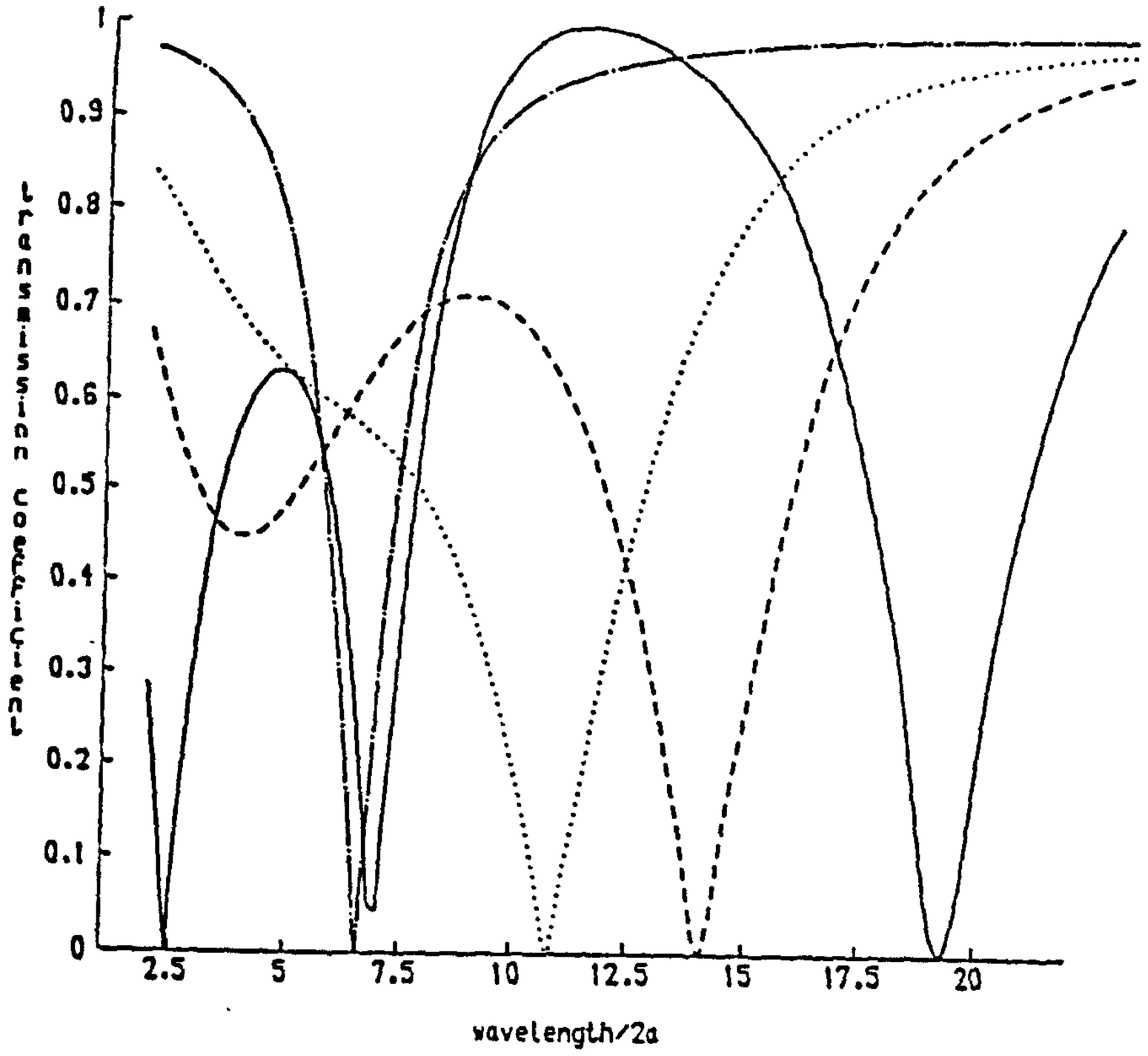

Figure 4.7.9. $|T_1|$ plotted against $\lambda/2a$ for tethered cylinders (a/h=0.2) with different clearances. ——— f/a=1.1; - - - f/a=1.5; ····· f/a=2; -·-·- f/a=3.

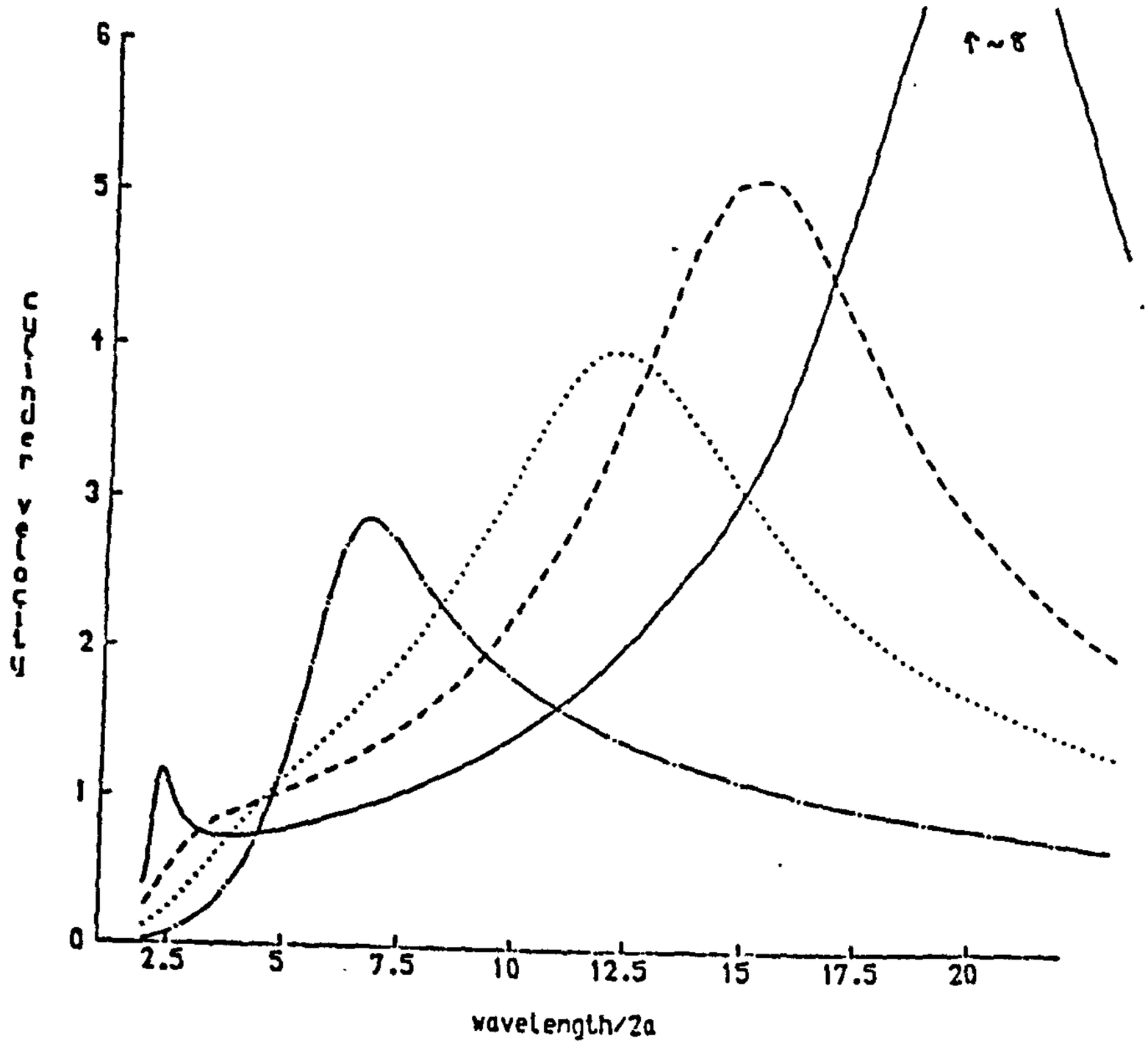

Figure 4.7.10. $|\bar{U}|$ plotted against $\lambda/2a$ for tethered cylinders (a/h=0.2) with different clearances. ——— f/a=1.1; - - - f/a=1.5; ····· f/a=2; -·-·- f/a=3.

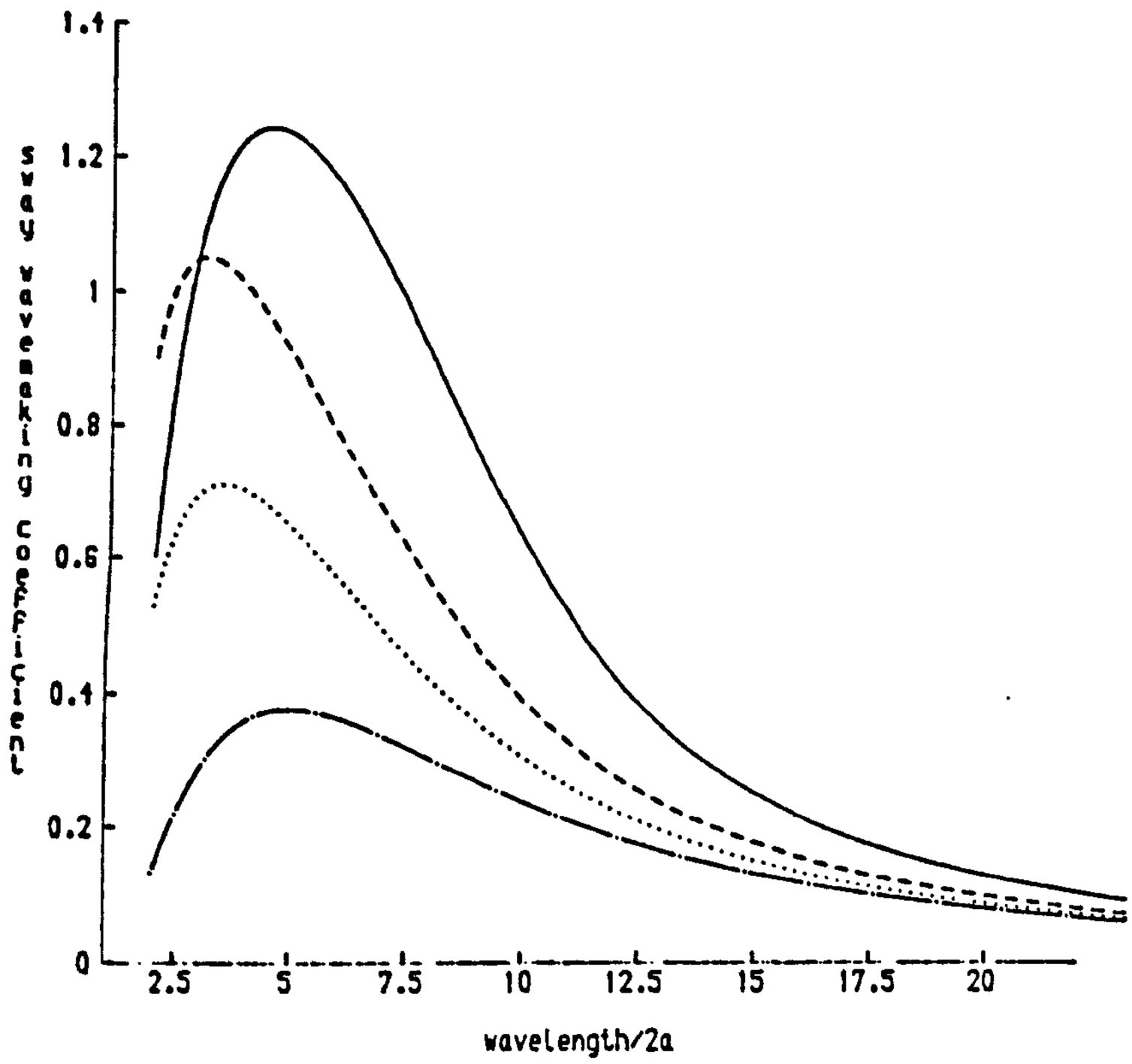

Figure 4.7.11. W_c (sway) plotted against $\lambda/2a$ for submerged cylinders (a/h=0.2) with different clearances. ——— f/a=1.1; – – – f/a=1.5; ····· f/a=2; –·–·– f/a=3.

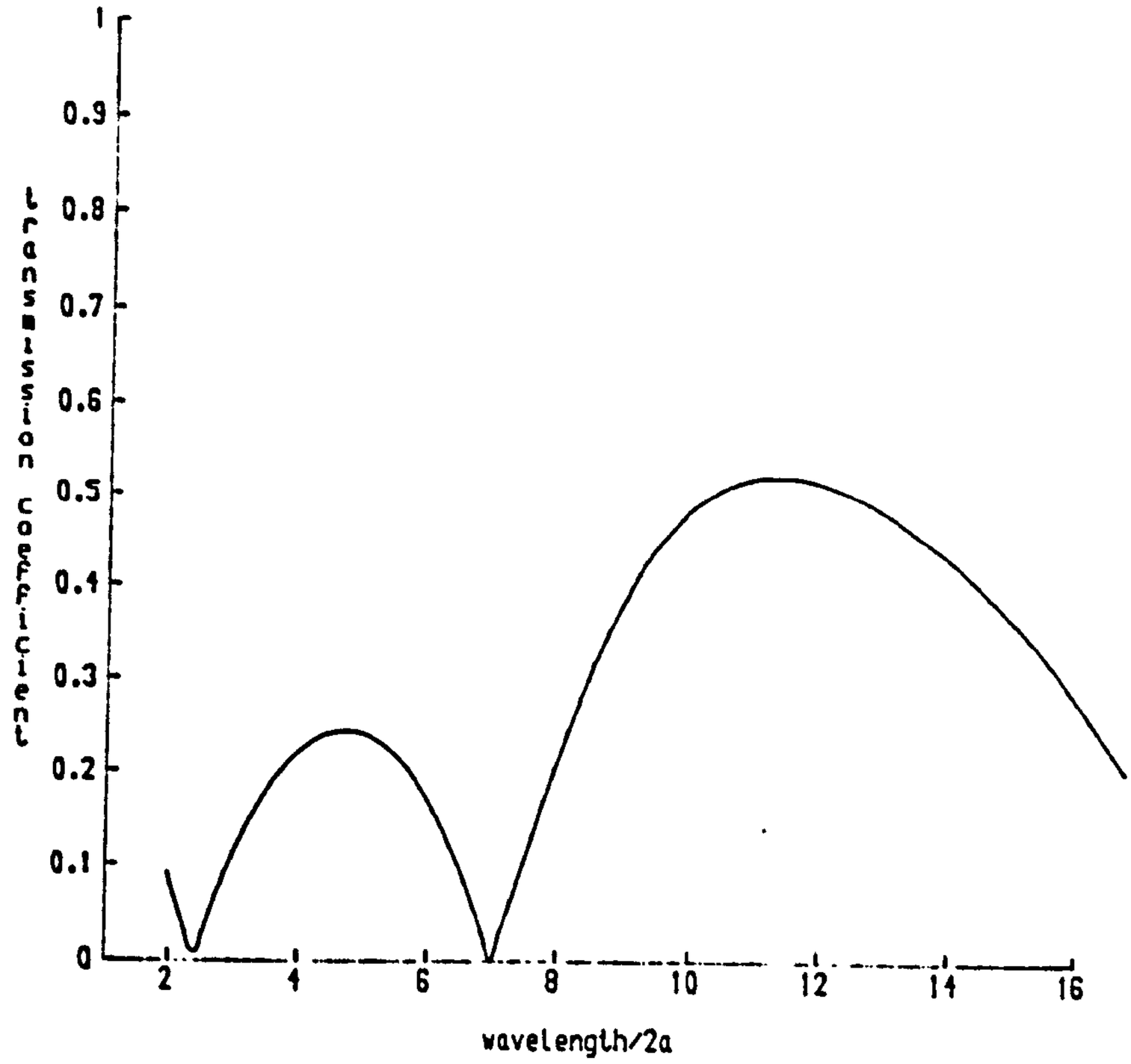

Figure 4.7.12. $|T_1|$ plotted against $\lambda/2a$ for a tethered cylinder (a/h=0.2, f/a=1.1) which is artificially tuned to Ka=0.44.

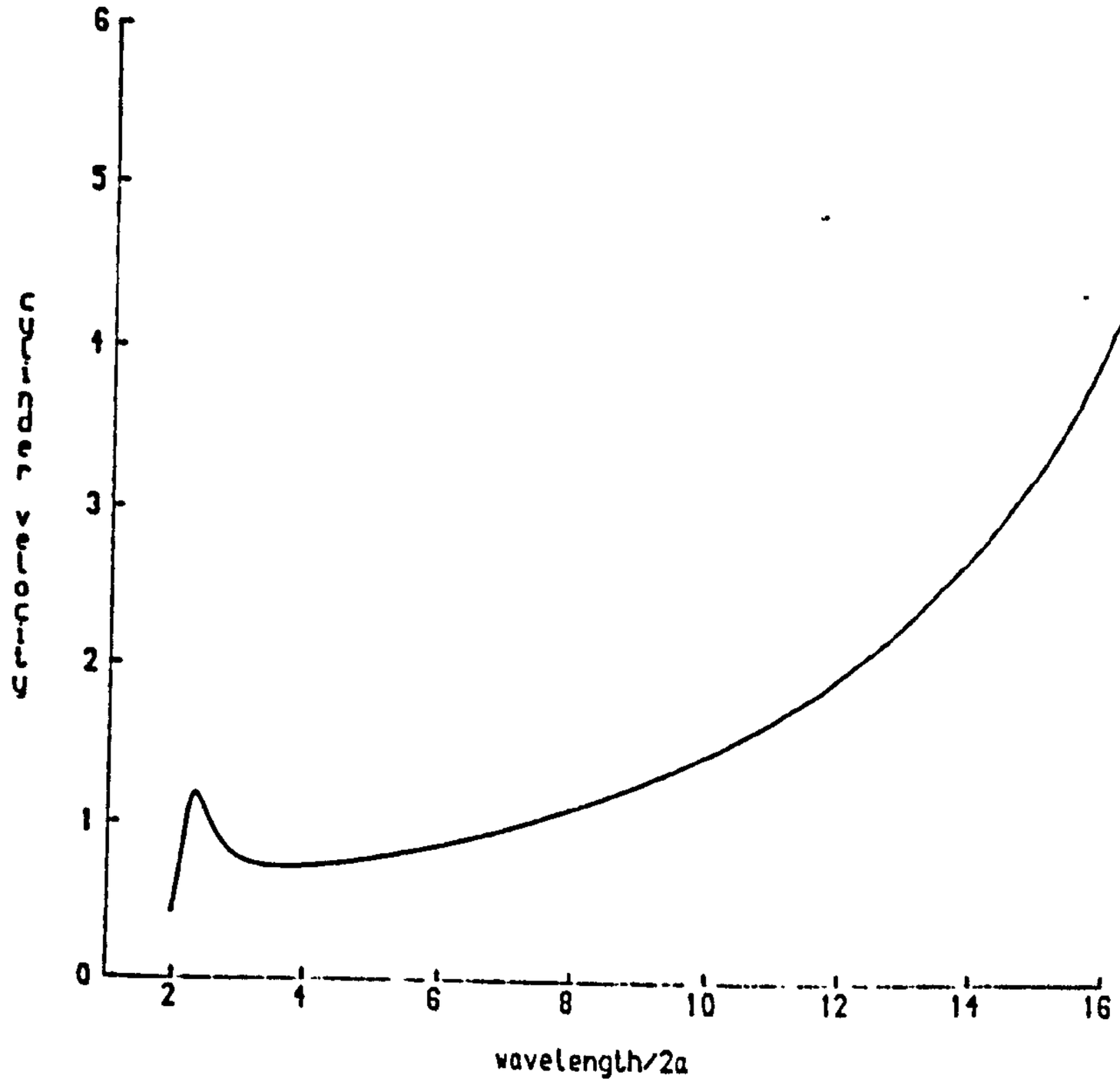

Figure 4.7.13. $|\bar{U}|$ plotted against $\lambda/2a$ for a tethered cylinder (a/h=0.2, f/a=1.1) which is artificially tuned to Ka=0.44.

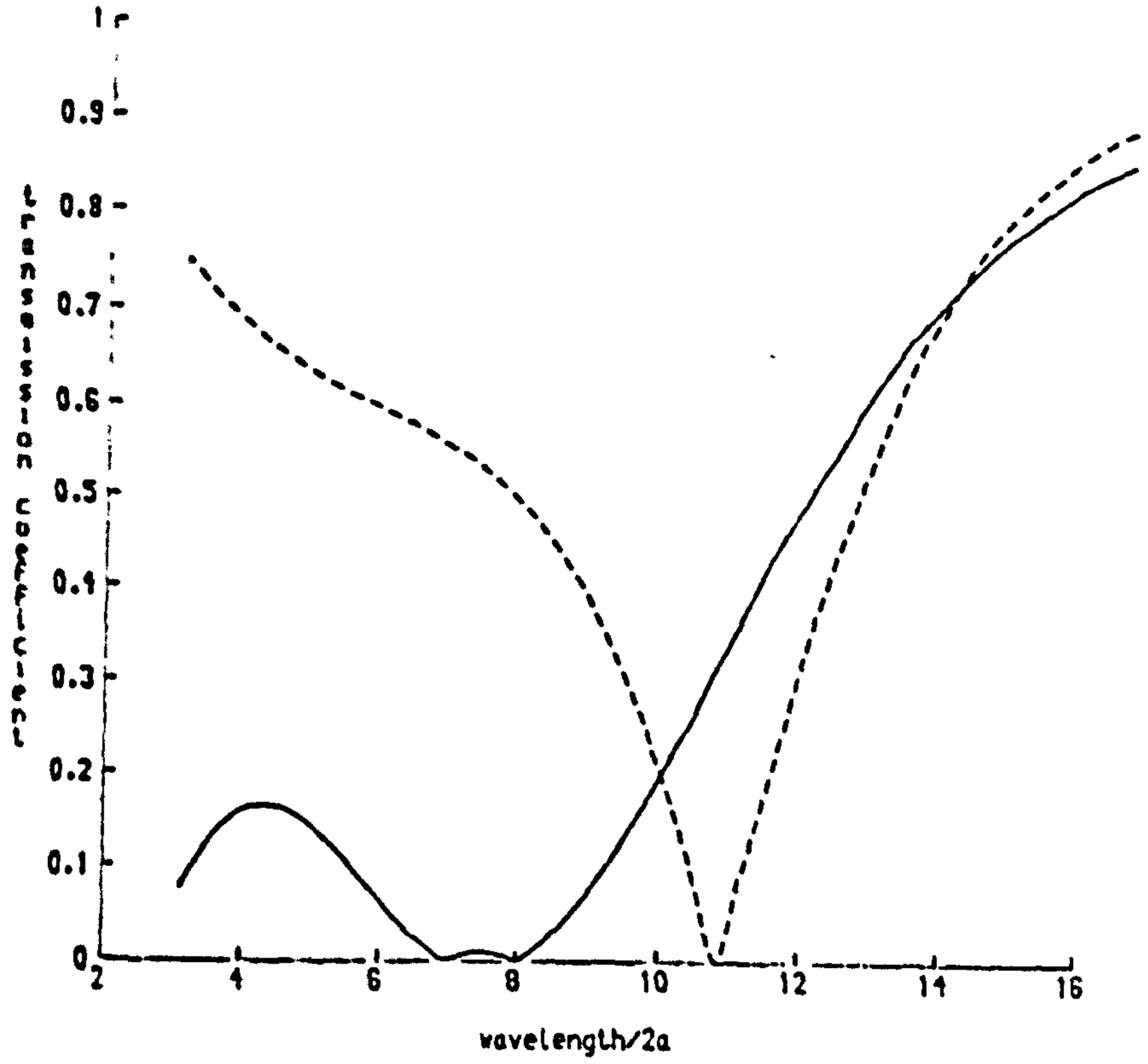

Figure 4.7.14. $|T_1|$ plotted against $\lambda/2a$ for tethered cylinders (f/h=0.4) with different values of a/h. ——— a/h=0.2; - - - a/h=0.3.

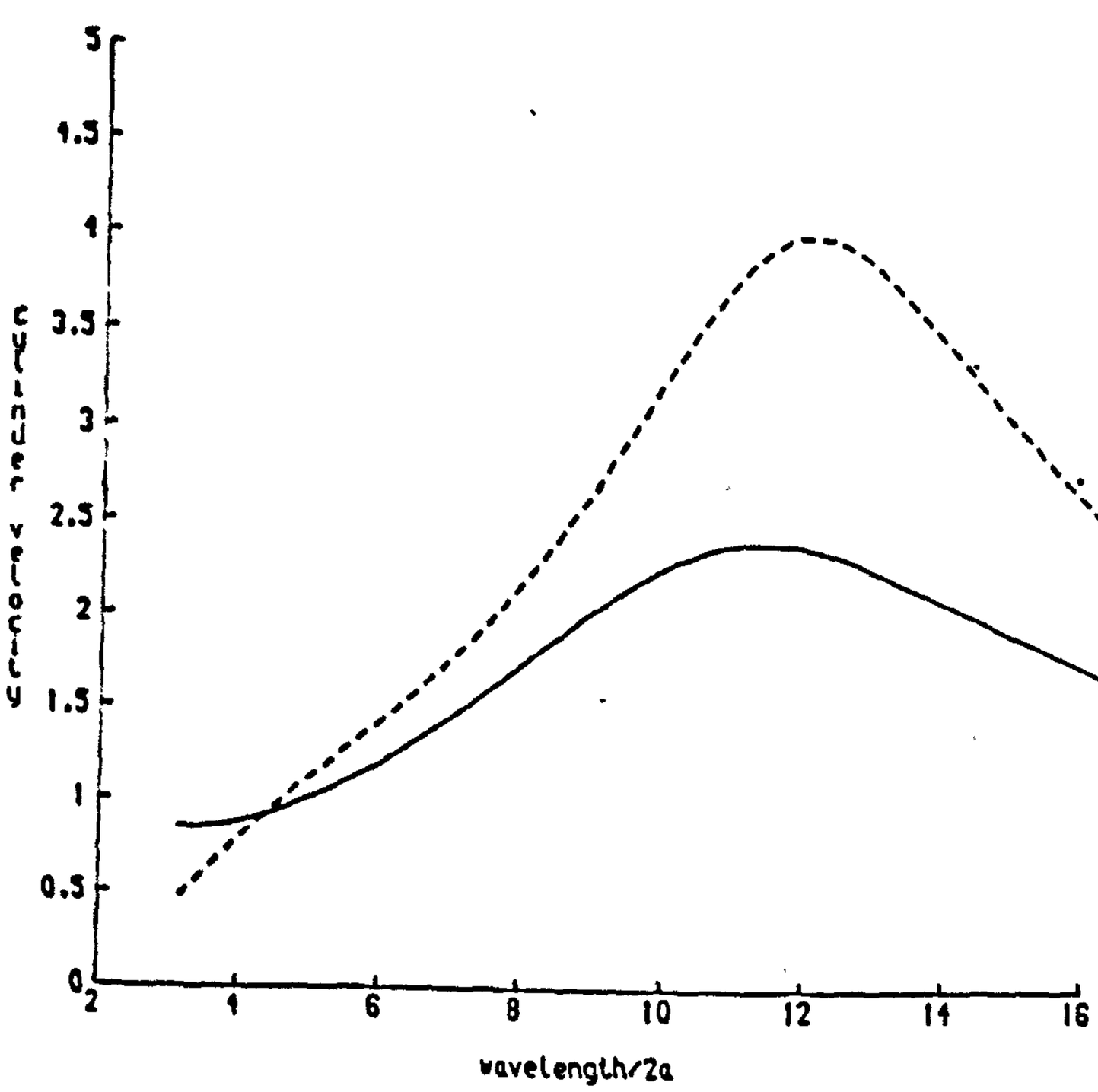

Figure 4.7.15. $|\bar{U}|$ plotted against $\lambda/2a$ for tethered cylinders (f/h=0.4) with different values of a/h. ——— a/h=0.2; - - - a/h=0.3.

The behaviour of the free surface near the cylinder can be examined by solving the scattering problem and using equation (4.6.10). Figures (4.7.16)-(4.7.19) show curves of $|\eta/A|$ against $x/2a$ for a cylinder with $a/h = 0.25$, $f/a = 2$ at four different frequencies. The quantity $|\eta/A|$ represents the maximum height of the water at a particular point in space over one wave period. Figure (4.7.17) shows what happens at the tuning frequency, $Ka = K_o a = 0.49$. The curve shows that the incoming wave is cancelled within four cylinder diameters of the cylinder and also that there are no abnormally large waves above the cylinder. Upstream of the cylinder the curve represents the superposition of the incoming and reflected waves. The other three curves show the behaviour of the free surface at other values of Ka (0.4, 0.6, and 1.0). In all cases the transition over the cylinder is smooth and no large waves are created. Such waves would be undesirable in the context of a coastal protection device since they would make it difficult for small vessels to pass over the cylinder.

Comparison between theory and experiment is shown in figure (4.7.20), again using a cylinder for which $a/h = 0.25$ and $f/h = 0.5$. The experiments were performed in a narrow wave tank in the Civil Engineering Department at the University of Bristol. The radius of the cylinder that was used for the experiments was 51mm. The voltage applied to the wavemaker at each frequency was the same and this resulted in the amplitude of the incident wave varying between 2mm and 3.5mm. No account was taken of wave attenuation along the tank, which may account for the fact that the experimental readings are mostly slightly lower than the theoretical predictions. The agreement, both qualitative and quantitative, between theory and experiment is very good. Experimental runs were made with larger incoming waves though no measurements were taken. It was clear from these runs that the

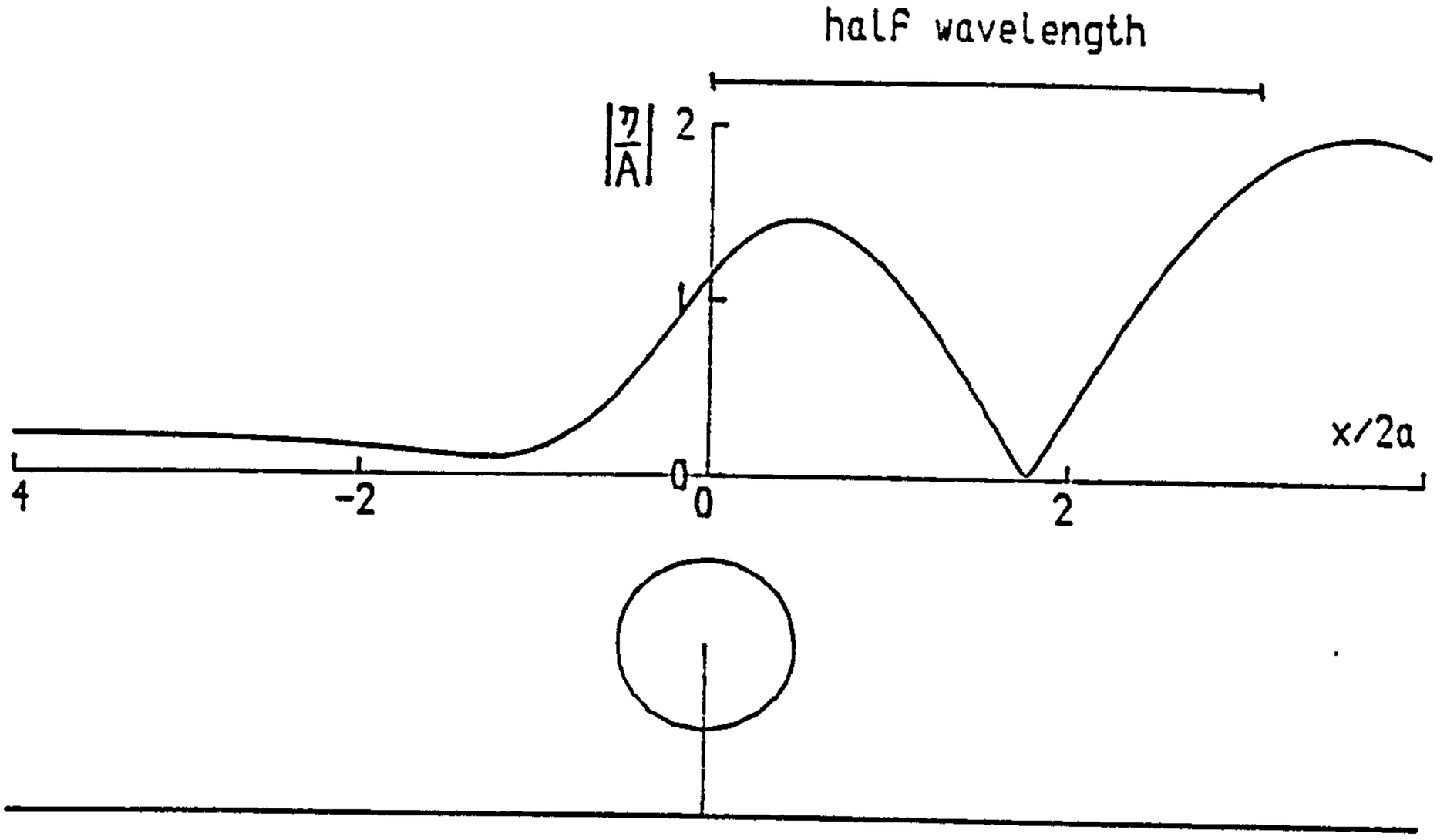

Ka = 0.40

Figure 4.7.16. $|\eta/A|$ plotted against $x/2a$ for a wave of frequency $Ka=0.4$ incident from $x = +\infty$ on a tethered cylinder ($a/h=0.25$, $f/a=2$, $K_o a=0.49$).

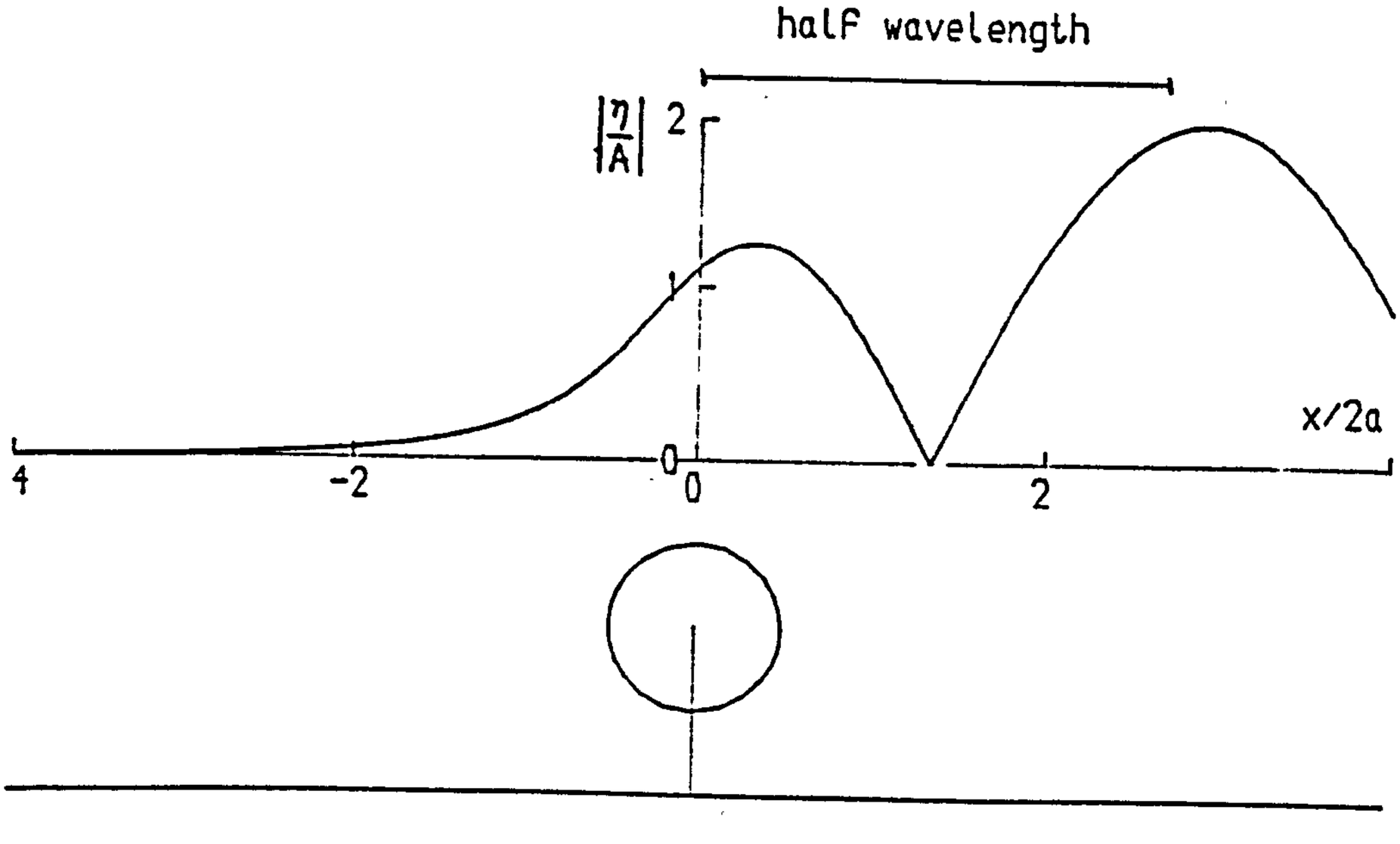

Ka = 0.49

Figure 4.7.17. $|\eta/A|$ plotted against $x/2a$ for a wave of frequency $Ka=0.49$ incident from $x = +\infty$ on a tethered cylinder ($a/h=0.25$, $f/a=2$, $K_o a=0.49$).

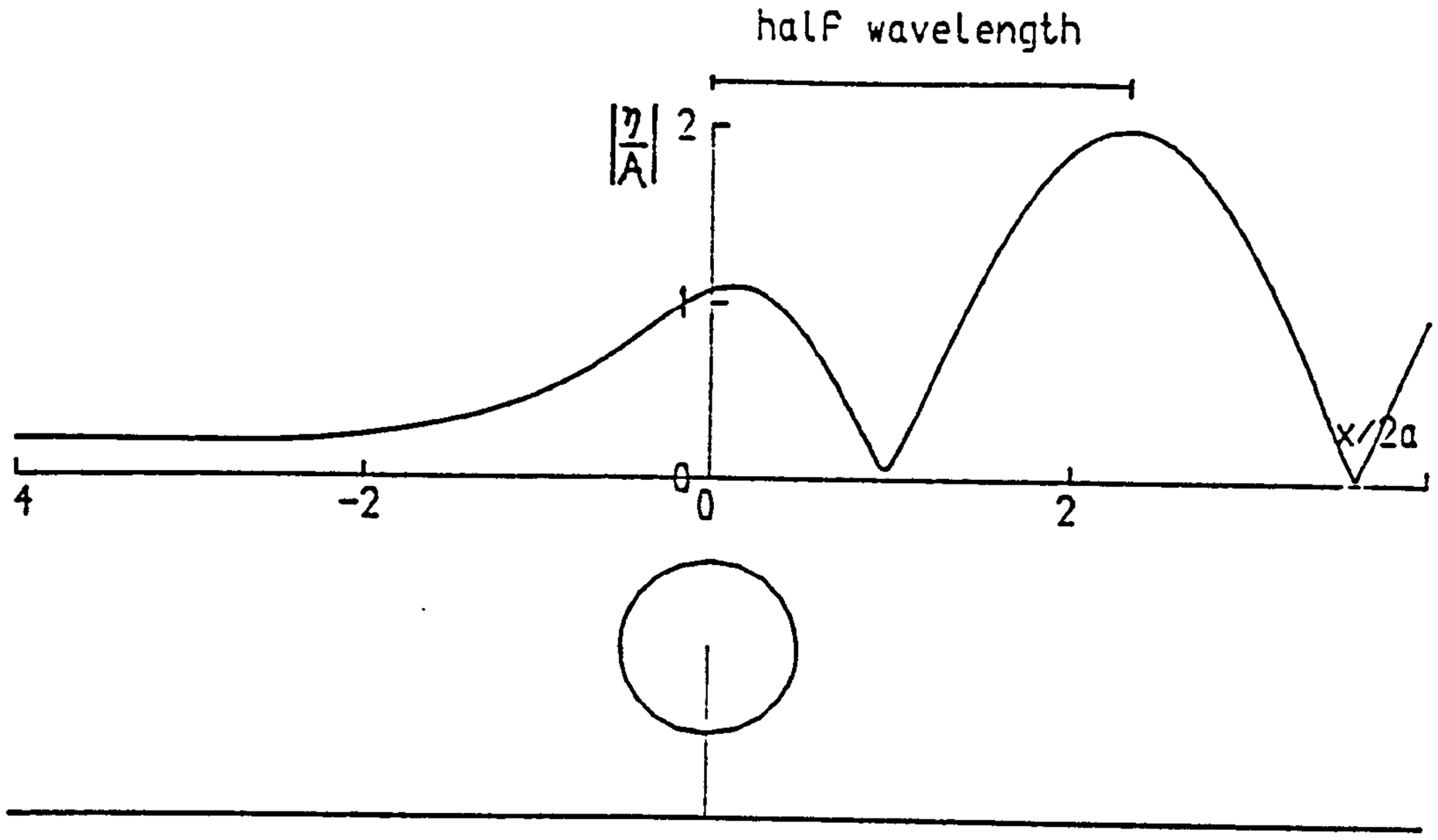

Figure 4.7.18. $|\eta/A|$ plotted against x/2a for a wave of frequency Ka=0.6 incident from $x = +\infty$ on a tethered cylinder (a/h=0.25, f/a=2, $K_o a$=0.49).

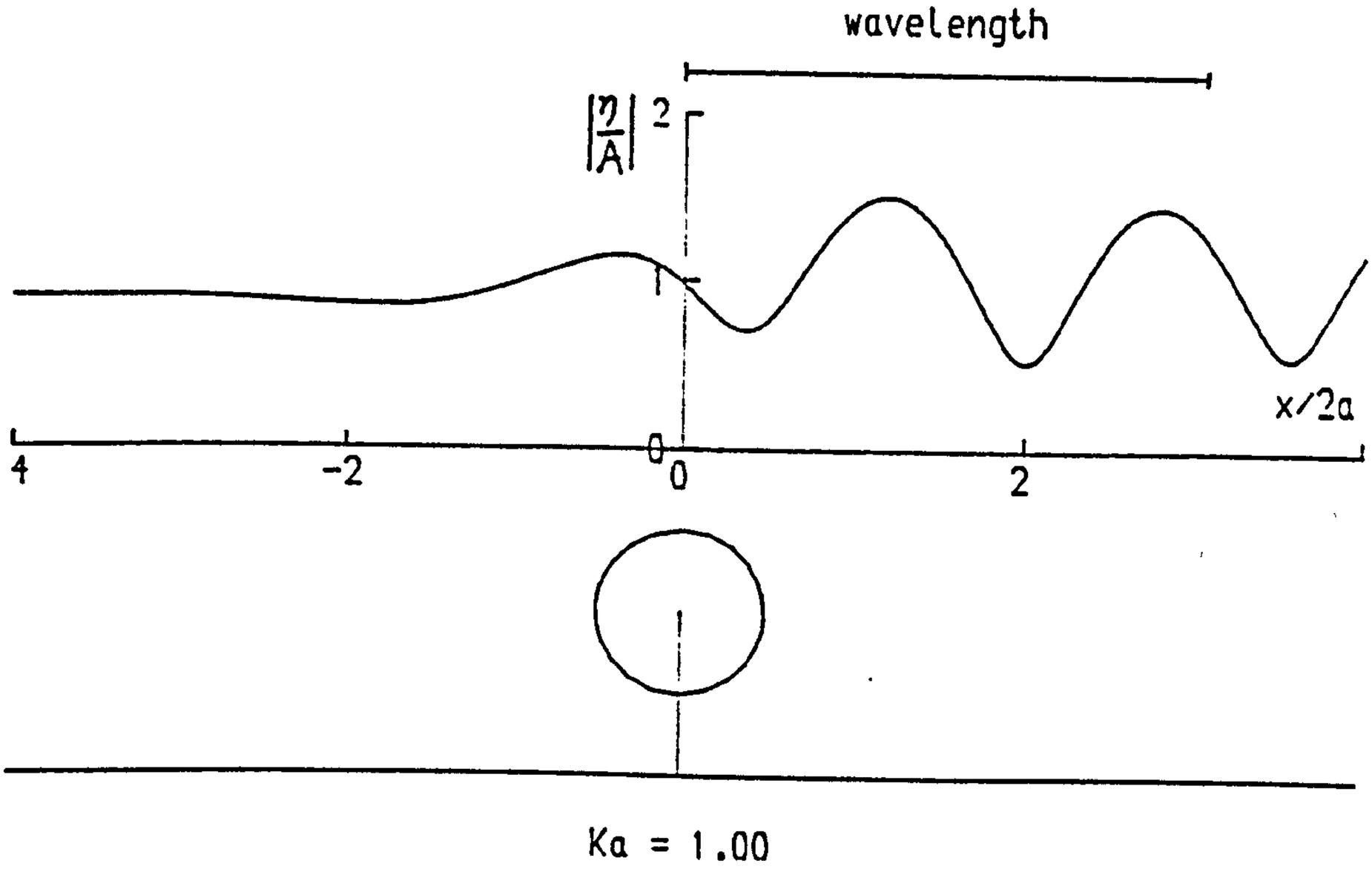

Figure 4.7.19. $|\eta/A|$ plotted against x/2a for a wave of frequency Ka=1.0 incident from $x = +\infty$ on a tethered cylinder (a/h=0.25, f/a=2, $K_o a$=0.49).

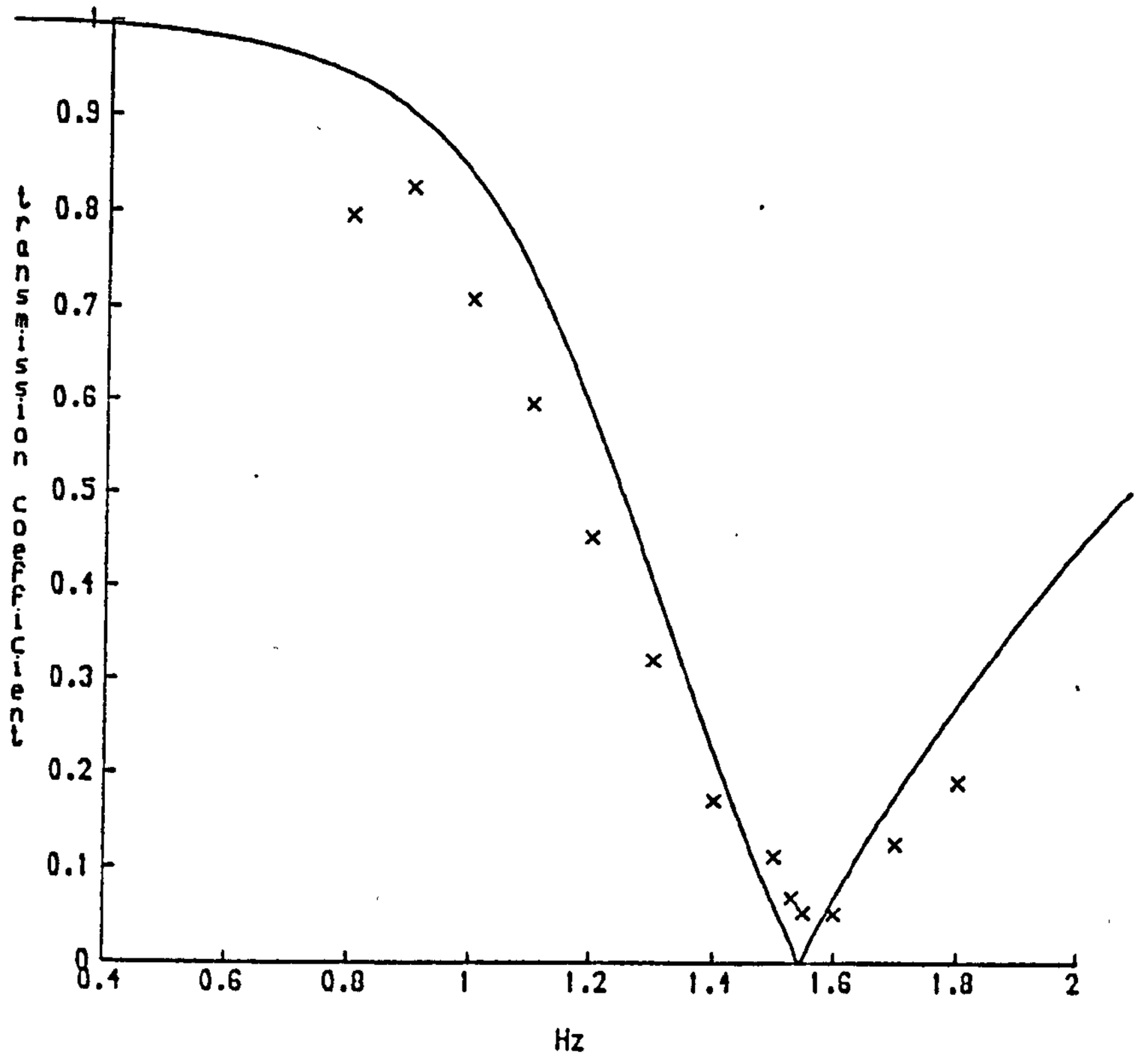

Figure 4.7.20. Comparison between theory and experiment. $|T_1|$ plotted against f (Hz) for a tethered cylinder with a/h=0.25, f/a=2. ——— theoretical prediction; × × × experimental points.

qualitative behaviour of the device as a wave reflector was still the same for these large waves.

4.8 Single Cylinder next to a Wall

If a breakwater is installed in a harbour it may be more suitable to treat the region behind the obstacle as closed rather than infinite in extent as has been done up to now. It may thus be necessary to calculate the hydrodynamic characteristics of a cylinder next to a wall. Such a problem is most easily solved by reformulating it in terms of two identical submerged cylinders oscillating in a coordinated manner. There are three situations that will be covered in this and the following two sections. First the case where the cylinders oscillate together in heave. This is a symmetric problem and is equivalent to just one cylinder oscillating in heave next to a wall. In the same section the problem of a cylinder in sway next to a wall will also be solved. This is equivalent to two cylinders oscillating in sway exactly out of phase with one another and is also the case that is relevant to the use of tethered cylinders as harbour breakwaters. Secondly in §4.9 the problem of wave scattering by a cylinder next to a wall is examined and finally the problem of two cylinders oscillating in sway and in phase with each other is solved in §4.10. All the problems will be formulated as if two cylinders were present.

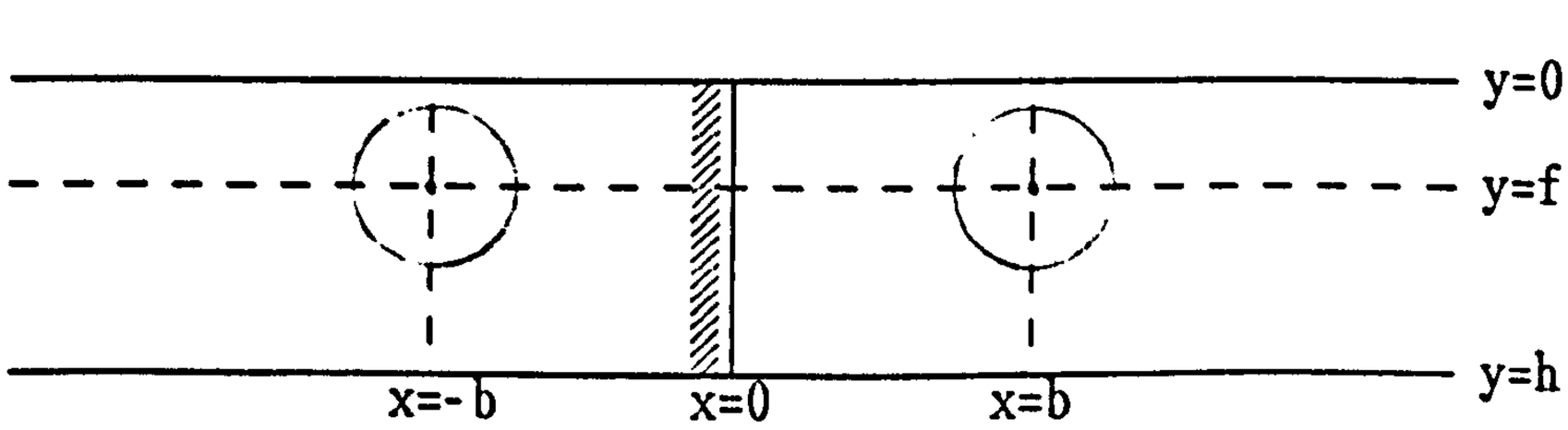

Figure 4.8.1

The cylinders are centred on (-b,f) and (b,f), see figure (4.8.1), and in this section the problems considered will be equivalent to that of a wall on x = 0. In other words the solutions will satisfy

$$\frac{\partial \phi}{\partial x} = 0 \qquad \text{on } x=0. \tag{4.8.1}$$

The problem is simplified by the introduction of a second complex number j, ($j^2 = -1$), and then a point in the x,y plane can be represented by $z = x + jy$. There will therefore be two complex numbers present in the analysis which follows, j as mentioned above, and i which appears through the time dependence condition, equation (4.2.1). Which complex number is referred to by the functions real and imaginary part will be indicated by suffices, e.g. Im_j.

Let the point (-b,f) be z_1 and (b,f) be z_2. Then, using polar coordinates centred on these points

$$\begin{aligned} z = z_1 + r_1 \exp[j(\tfrac{\pi}{2} - \theta_1)] &= z_1 + j\, r_1 \exp(-j\theta_1) \\ &= z_2 + j\, r_2 \exp(-j\theta_2) \end{aligned} \tag{4.8.2}$$

and

$$z_2 - z_1 = 2b. \tag{4.8.3}$$

The method that will be used here is to write the solution in terms of multipoles centred at the centres of the two cylinders. Using the same conventions concerning symmetric and antisymmetric multipoles as were used for the single cylinder case these multipoles can be written

$$\phi_{n,q}^{(1)} = \frac{a^{n+1}}{n\, r_1^n} \begin{Bmatrix} \sin n\theta_1 \\ \cos n\theta_1 \end{Bmatrix} + \sum_{m=1}^{\infty} \frac{a}{m} A_{mn,q} \left[\frac{r_1}{a}\right]^m \begin{Bmatrix} \sin m\theta_1 \\ \cos m\theta_1 \end{Bmatrix} \tag{4.8.4}$$

$$\phi^{(2)}_{n,q} = \frac{a^{n+1}}{n\ r_2^n} \begin{Bmatrix} \sin\ n\theta_2 \\ \cos\ n\theta_2 \end{Bmatrix} + \sum_{m=1}^{\infty} \frac{a}{m} A_{mn,q} \left[\frac{r_2}{a}\right]^m \begin{Bmatrix} \sin\ m\theta_2 \\ \cos\ m\theta_2 \end{Bmatrix}. \qquad (4.8.5)$$

These expansions are valid in the region $r_i < 2f$, $i = 1,2$.

The boundary condition on the wall is satisfied by the following time independent potential:

$$\phi = U \sum_{n=1}^{\infty} [c_n(\phi^{(1)}_{n,1} - \phi^{(2)}_{n,1}) + d_n(\phi^{(1)}_{n,2} + \phi^{(2)}_{n,2})] \ . \qquad (4.8.6)$$

This ensures that ϕ is symmetric and thus if the boundary condition on one of the cylinders is satisfied the other one must also be. Applying the boundary condition on $r_2 = a$ gives

$$\sum_{n=1}^{\infty} \left[c_n \left[\frac{\partial \phi^{(1)}_{n,1}}{\partial r_2} - \frac{\partial \phi^{(2)}_{n,1}}{\partial r_2}\right] + d_n \left[\frac{\partial \phi^{(1)}_{n,2}}{\partial r_2} + \frac{\partial \phi^{(2)}_{n,2}}{\partial r_2}\right]\right] = \begin{Bmatrix} \sin\ \theta_2 & (\text{surge}) \\ \cos\ \theta_2 & (\text{heave}) \end{Bmatrix} \quad \text{on } r_2 = a. \qquad (4.8.7)$$

Equation (4.8.5) gives

$$\left.\frac{\partial \phi^{(2)}_{n,q}}{\partial r_2}\right|_{r_2=a} = - \begin{Bmatrix} \sin\ n\theta_2 \\ \cos\ n\theta_2 \end{Bmatrix} + \sum_{m=1}^{\infty} A_{mn,q} \begin{Bmatrix} \sin\ m\theta_2 \\ \cos\ m\theta_2 \end{Bmatrix} \ . \qquad (4.8.8)$$

In order to evaluate the other terms needed in equation (4.8.7) it is necessary to go back to the original representation of the multipole potentials, equation (4.2.2), and express it in terms of polar coordinates r_2, θ centred on (b,f). Equation (4.2.2) can be written

$$\phi^{(1)}_{n,q} = \frac{a^{n+1}}{n\ r_1^n} \begin{Bmatrix} \sin\ n\theta_1 \\ \cos\ n\theta_1 \end{Bmatrix} + \begin{Bmatrix} \text{Im}_j \\ \text{Re}_j \end{Bmatrix} \psi_{n,q} \qquad (4.8.9)$$

where

$$\psi_{n,q} = \frac{a^2}{2n!} \int_0^\infty \frac{(ka)^{n-1}}{Kh \cosh kh - kh \sinh kh} \sum_{m=0}^{\infty} [(-1)^m e^{2jkb} c_1(kh)$$

$$+ (-1)^q e^{-2jkb} c_2(kh)] \frac{(kr_2)^m}{m!} \exp(-jm\theta_2)\ dk$$

$$- i \frac{\pi a}{n!} \frac{(\kappa a)^n}{2\kappa h + \sinh 2\kappa h} \sum_{m=0}^{\infty} [(-1)^m e^{2j\kappa b} c_3(\kappa h)$$

$$+ (-1)^q e^{-2j\kappa b} c_4(\kappa h)] \frac{(\kappa r_2)^m}{m!} \exp(-jm\theta_2)\ . \qquad (4.8.10)$$

The functions $c_i(u)$, $i = 1,4$ are defined by equations (4.2.5)-(4.2.8). After some manipulation the second term in equation (4.8.9) can be written

$$\begin{Bmatrix} Im_j \\ Re_j \end{Bmatrix} \psi_{n,q} = \sum_{m=0}^{\infty} \left[\frac{a}{2n!m!} \left[\frac{a}{h}\right]^{n+m} \left[\frac{r_2}{a}\right]^m \int_0^\infty \frac{u^{n+m-1}}{Kh \cosh u - u \sinh u} \right.$$

$$[(-1)^m c_1(u) + c_2(u)] \begin{Bmatrix} \sin 2ub/h \\ \cos 2ub/h \end{Bmatrix} du$$

$$\left. - i \frac{\pi a}{n!m!} \frac{(\kappa a)^n (\kappa r_2)^m}{2\kappa h + \sinh 2\kappa h} [(-1)^m c_3(\kappa h) + c_4(\kappa h)] \begin{Bmatrix} \sin 2\kappa b \\ \cos 2\kappa b \end{Bmatrix} \right] \cos m\theta_2$$

$$+ \sum_{m=0}^{\infty} \left[\frac{a}{2n!m!} \left[\frac{a}{h}\right]^{n+m} \left[\frac{r_2}{a}\right]^m \int_0^\infty \frac{u^{n+m-1}}{Kh \cosh u - u \sinh u} \right.$$

$$[(-1)^m c_1(u) - c_2(u)](-1)^q \begin{Bmatrix} \cos 2ub/h \\ \sin 2ub/h \end{Bmatrix} du$$

$$\left. - i \frac{\pi a}{n!m!} \frac{(\kappa a)^n (\kappa r_2)^m}{2\kappa h + \sinh 2\kappa h} [(-1)^m c_3(\kappa h) - c_4(\kappa h)](-1)^q \begin{Bmatrix} \cos 2\kappa b \\ \sin 2\kappa b \end{Bmatrix} \right] \sin m\theta_2 .$$

(4.8.11)

It is convenient to define some new functions:

$$c_5(u) = (a/h)^{n+m}\, u^{n+m-1}/[2n!\ (m-1)!\ (Kh\cosh u - u\sinh u)]$$

$$c_6(u) = -\ \pi\ (ua/h)^{n+m}/[n!\ (m-1)!\ (2u - \sinh 2u)]$$

$$Q_{mn,q} = \int_0^\infty c_5(u)\ [(-1)^m c_1(u) - c_2(u)](-1)^q \begin{Bmatrix}\cos\ 2ub/h\\ \sin\ 2ub/h\end{Bmatrix} du$$

$$+\ i\ c_6(\kappa h)\ [(-1)^m c_3(\kappa h) - c_4(\kappa h)](-1)^q \begin{Bmatrix}\cos\ 2\kappa b\\ \sin\ 2\kappa b\end{Bmatrix}$$

$$S_{mn,q} = \int_0^\infty c_5(u)\ [(-1)^m c_1(u) + c_2(u)] \begin{Bmatrix}\sin\ 2ub/h\\ \cos\ 2ub/h\end{Bmatrix} du$$

$$+\ i\ c_6(\kappa h)\ [(-1)^m c_3(\kappa h) + c_4(\kappa h)] \begin{Bmatrix}\sin\ 2\kappa b\\ \cos\ 2\kappa b\end{Bmatrix}$$

$$B_{n,q} = \left[\frac{a}{h}\right]^n \frac{1}{2n!} \int_0^\infty \frac{u^{n-1}\ [c_1(u) + c_2(u)]}{Kh\cosh u - u\sinh u} \begin{Bmatrix}\sin\ 2ub/h\\ \cos\ 2ub/h\end{Bmatrix} du$$

$$-\ \frac{i\pi}{n!}\ (\kappa a)^n\ \frac{c_3(\kappa h) + c_4(\kappa h)}{2\kappa h + \sinh 2\kappa h} \begin{Bmatrix}\sin\ 2\kappa b\\ \cos\ 2\kappa b\end{Bmatrix}.$$

Then $\phi_{n,q}$ satisfies

$$\begin{Bmatrix}\mathrm{Im}_j\\ \mathrm{Re}_j\end{Bmatrix} \phi_{n,q} = aB_{n,q} + \sum_{m=1}^{\infty} \frac{a}{m} \left[\frac{r_2}{a}\right]^m [Q_{mn,q}\sin m\theta_2 + S_{mn,q}\cos m\theta_2]\ . \tag{4.8.12}$$

Referring back to equation (4.8.9) it can be seen that the second term in the expression for $\phi_{n,q}^{(1)}$ has been expanded about $r_2 = 0$. The next step is to do the same for the first term. Following McIver (1985) let

$$F_n = \frac{j^n}{(z - z_1)^n} = \frac{\exp(jn\theta_1)}{r_1^n}, \tag{4.8.13}$$

i.e a function whose real and imaginary parts are those functions that appear in equation (4.8.9). The function F_n is analytic everywhere in the complex j plane except at $z = z_1$ where there is a pole of order n. The function F_n can therefore be expanded in a Taylor series about $z = z_2$ and the expansion will be valid on $r_2 = a$.

$$F_n = \sum_{m=0}^{\infty} \left.\frac{d^m F_n}{dz^m}\right|_{z=z_2} \frac{(z - z_2)^m}{m!}$$

$$= \sum_{m=0}^{\infty} \frac{(-1)^m\, j^n\, (n+m-1)!}{(n-1)!\, (z_2 - z_1)^{n+m}} \frac{(z - z_2)^m}{m!}$$

$$= \sum_{m=0}^{\infty} \frac{(-1)^m\, j^n\, (n+m-1)!}{(n-1)!\, (2b)^{n+m}}\, j^m\, r_2^m \frac{\exp(-jm\theta_2)}{m!}$$

$$= \frac{e^{jn\pi/2}}{(2b)^n} + \sum_{m=1}^{\infty} \frac{n}{m} \left[\frac{r_2}{a}\right]^m \frac{C_{mn}}{a^n} \exp\left[j\left(\frac{\pi}{2}(n+m) - m\theta_2\right)\right]$$

where

$$C_{mn} = \frac{(-1)^m\, (n+m-1)!}{(m-1)!\, n!}\, (a/2b)^{n+m} \ .$$

The time independent potential, defined by equation (4.8.6), can now be written as an expansion about $r_2 = a$.

$$\phi = Ua \sum_{n=1}^{\infty} \Bigg[c_n \left[(a/2b)^n \frac{\sin n\pi/2}{n} + B_{n,1} - (a/r_2)^n \frac{\sin n\theta_2}{n}\right.$$

$$+ \sum_{m=1}^{\infty} \left[\frac{r_2}{a}\right]^m \Bigg[\frac{C_{mn}}{m} \left[\sin (n+m)\frac{\pi}{2} \cos m\theta_2 - \cos (n+m)\frac{\pi}{2} \sin m\theta_2\right]$$

$$\left. + \frac{1}{m} \left[\left(Q_{mn,1} - \frac{A_{mn,1}}{m}\right) \sin m\theta_2 + S_{mn,1} \cos m\theta_2\right]\Bigg]\Bigg]$$

$$+ d_n \left[(a/2b)^n \frac{\cos n\pi/2}{n} + B_{n,2} + (a/r_2)^n \frac{\cos n\theta_2}{n} \right.$$

$$+ \sum_{m=1}^{\infty} \left[\frac{r_2}{a}\right]^m \left[\frac{C_{mn}}{m} \left[\cos (n+m)\frac{\pi}{2} \cos m\theta_2 + \sin (n+m)\frac{\pi}{2} \sin m\theta_2\right] \right.$$

$$\left. \left. + \frac{1}{m} \left[Q_{mn,2} \sin m\theta_2 + (S_{mn,2} + \frac{A_{mn,2}}{m}) \cos m\theta_2\right] \right] \right] . \qquad (4.8.14)$$

Equation (4.8.7), the boundary condition on the cylinder, can now be applied to give the following infinite system of equations.

$$e_{2n-1} = c_n \; ; \; e_{2n} = d_n \qquad n = 1,2,...$$

$$\sum_{n=1}^{\infty} M_{mn} e_n = \begin{cases} \delta_{1m} & \text{(surge)} \\ \delta_{2m} & \text{(heave)} \end{cases} \qquad m = 1,2,... \qquad (4.8.15)$$

where

$$M_{2m-1,2n-1} = \delta_{mn} + Q_{mn,1} - A_{mn,1} - C_{mn} \cos (n+m)\frac{\pi}{2}$$

$$M_{2m-1,2n} = Q_{mn,2} + C_{mn} \sin (n+m)\frac{\pi}{2}$$

$$M_{2m,2n-1} = S_{mn,1} + C_{mn} \sin (n+m)\frac{\pi}{2} \qquad (4.8.16)$$

$$M_{2m,2n} = - \delta_{mn} + A_{mn,2} + S_{mn,2} + C_{mn} \cos (n+m)\frac{\pi}{2} .$$

This infinite system of equations is solved by truncation and values for e_n (and therefore c_n and d_n) $n = 1,2,...$ obtained. The added mass and damping coefficients can then be calculated from

$$U\omega\pi a^2 \rho i(\mu - i\nu) = - a\rho\omega i \int_{-\pi}^{\pi} \phi(a,\theta_2) \begin{cases} \sin \theta_2 \\ \cos \theta_2 \end{cases} d\theta_2 \quad \begin{matrix} \text{(surge)} \\ \text{(heave)} \end{matrix} . \qquad (4.8.17)$$

For sway this gives

$$\mu - i\nu = c_1 + \sum_{n=1}^{\infty} \left[c_n \left(C_{1n} \cos (n+1)\frac{\pi}{2} - Q_{1n,1} + A_{1n,1} \right) + d_n \left(Q_{1n,2} + C_{1n} \sin (n+1)\frac{\pi}{2} \right) \right].$$

This can be simplified by using equation (4.8.14) with $m = 1$. The resulting equation is

$$\mu - i\nu = -1 + 2c_1 \ . \qquad (4.8.18)$$

The same procedure can be carried out for the heave case, this time using equation (4.8.14) with $m = 2$, to get

$$\mu - i\nu = -1 - 2d_1 \ . \qquad (4.8.19)$$

The far field behaviour of ϕ can be examined in much the same way as was done for the single cylinder case. After some algebra the following result is obtained.

$$\phi \sim UA_w \frac{\cosh \kappa(h-y)}{\cosh \kappa h} e^{-i\kappa x} \qquad \text{as} \quad x \longrightarrow \infty \qquad (4.8.20)$$

where

$$A_w = - \frac{4\pi i a \cosh \kappa h}{2\kappa h + \sinh 2\kappa h} \sum_{n=1}^{\infty} \left[p_{n,1} \sin \kappa b + p_{n,2} \cos \kappa b \right] \qquad (4.8.21)$$

and

$$p_{n,q} = \frac{(\kappa a)^n}{n!} \left[e^{-\kappa(h-f)} + (-1)^{n+q} e^{\kappa(h-f)} \right] \begin{Bmatrix} c_n \\ d_n \end{Bmatrix} \ . \qquad (4.8.22)$$

Equation (1.2.32) connecting the damping coefficient with the energy radiated to infinity does not hold when a wall is present but it is a

simple exercise to work out that the appropriate relation is

$$B = \frac{\rho\omega^2 c_g}{g} |A_w|^2 \ . \qquad (4.8.23)$$

(Alternatively the problem can be considered as that of the radiation of waves by an obstacle consisting of two parallel spaced identical cylinders; the damping coefficient would then be twice as big and equation (1.2.32) would then apply, giving the same answer since the waves radiated to $\pm\infty$ have the same amplitudes.)

The resulting formula, which can be used as a check on the solutions obtained from equation (4.8.15), is

$$\nu = \frac{4\pi}{2\kappa h + \sinh 2\kappa h} \left| \sum_{n=1}^{\infty} p_{n,1} \sin \kappa b + p_{n,2} \cos \kappa b \right|^2 \qquad (4.8.24)$$

and is analogous to equation (4.4.17) for the single cylinder case.

The presence of the wall implies that the reflection coefficient for the fixed cylinder must satisfy $|R|^2 = 1$ whence $T = 0$. The Newman relations in this case can then easily be shown to reduce to

$$R = - A_w/\bar{A}_w. \qquad (4.8.25)$$

The problem of the scattering of waves by a tethered cylinder next to a wall can be solved with a simple change to the work presented in §3.2. Rather than going through all the theory again we will simply note those aspects of the problem that are different in this case.

In the same way that $|R| = 1$, the presence of a wall implies that $|R_1| = 1$ and thus that the transmission coefficient, T_1, is zero. With A_w defined by equation (4.8.21), equation (3.2.13) becomes

$$R_1 = R + \frac{\omega U A_w}{gA} \ . \qquad (4.8.26)$$

The Haskind relation, equation (3.2.18), is still valid here but the relation connecting the damping coefficient to the far field amplitude is given by equation (4.8.23) and not by equation (3.2.19). Combining equations (3.2.18), (4.8.23) and (4.8.26) together with equations (3.2.16), (3.2.17), (3.2.22) and (4.8.25) gives

$$R_1 = R - \frac{2R}{1+iC}$$

where $C = \{(M+I)\omega^2 - \lambda\}/B\omega$. This can be written

$$R_1 = R\,\frac{C + i}{C - i} \qquad (4.8.27)$$

which is just equation (3.2.27) with $T_1 = T = 0$. This ensures that $|R_1| = 1$ since $|R| = 1$ and C is real.

We will now return to the radiation problem and examine the behaviour of the added mass and damping coefficients as given by equations (4.8.18) and (4.8.19). There are three geometrical parameters in this problem, a/h, f/h, and b/h, and by varying them individually their various effects can be examined. In fact we will consider three different physical ideas. The first is the effect of the proximity of the wall. In this case it is a/h and f/h that are held fixed, at a/h = 0.2 and f/h = 0.3 (f/a = 1.5). The parameter b/h (or b/a) then measures the distance from the wall to the centre of the cylinder and clearly must satisfy b/a > 1. The behaviour of hydrodynamic characteristics as the gap between the cylinder and rigid boundaries approaches zero was discussed in §4.4 and here the limiting cases will be avoided. Thus figures (4.8.2)-(4.8.5) show curves for four values of b/a, namely b/a = 1.05, 1.5, 2.5 and 5.0. One feature that appears in all four figures is the increase in the number of oscillations of the

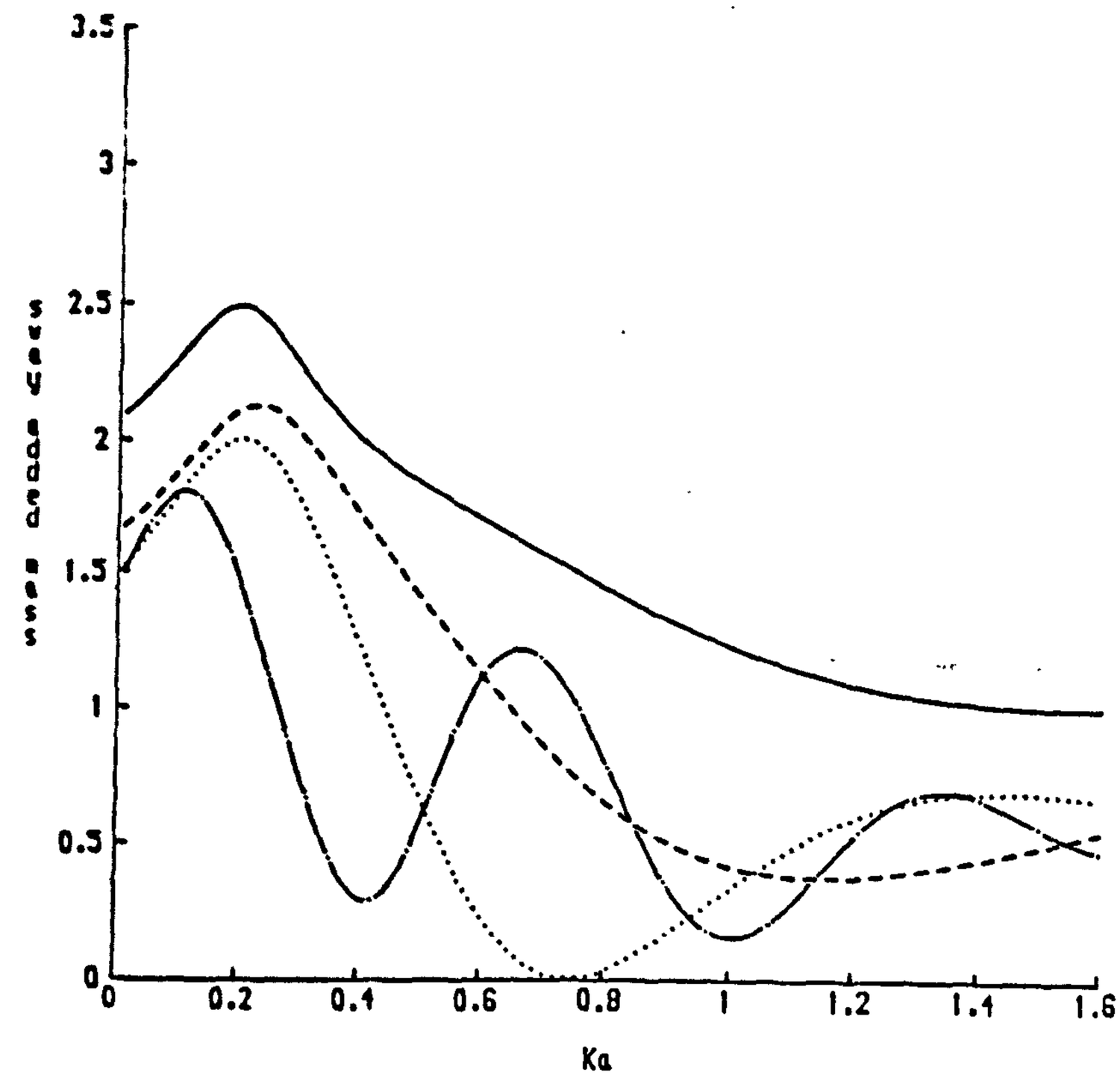

Figure 4.8.2. μ (sway) plotted against Ka for a cylinder next to a wall (a/h=0.2, f/a=1.5) at different distances from the wall.
——— b/h=0.21; - - - b/h=0.3; ····· b/h=0.5; -·-·- b/h=1.

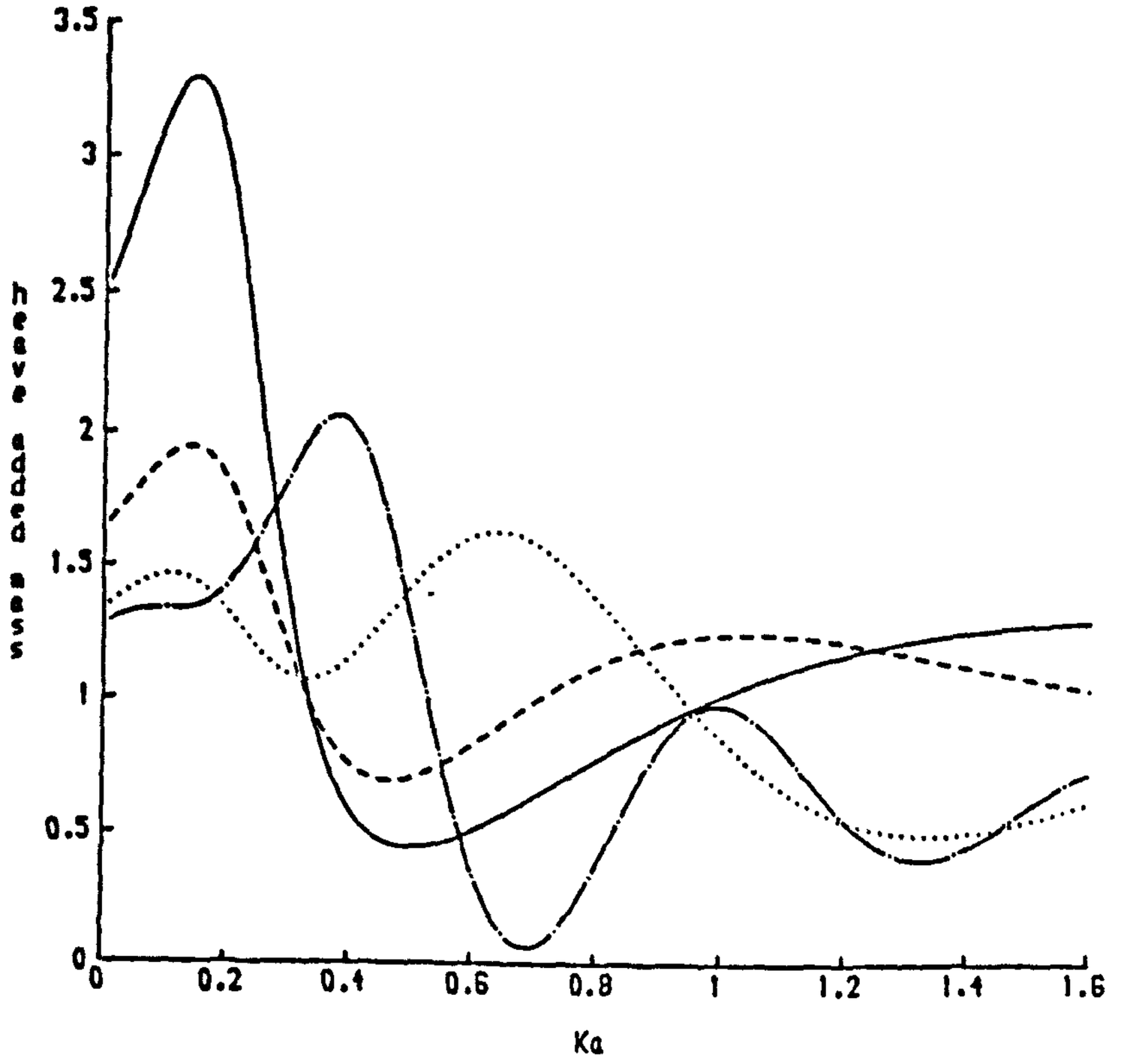

Figure 4.8.3. μ (heave) plotted against Ka for a cylinder next to a wall (a/h=0.2, f/a=1.5) at different distances from the wall.
——— b/h=0.21; - - - b/h=0.3; ····· b/h=0.5; -·-·- b/h=1.

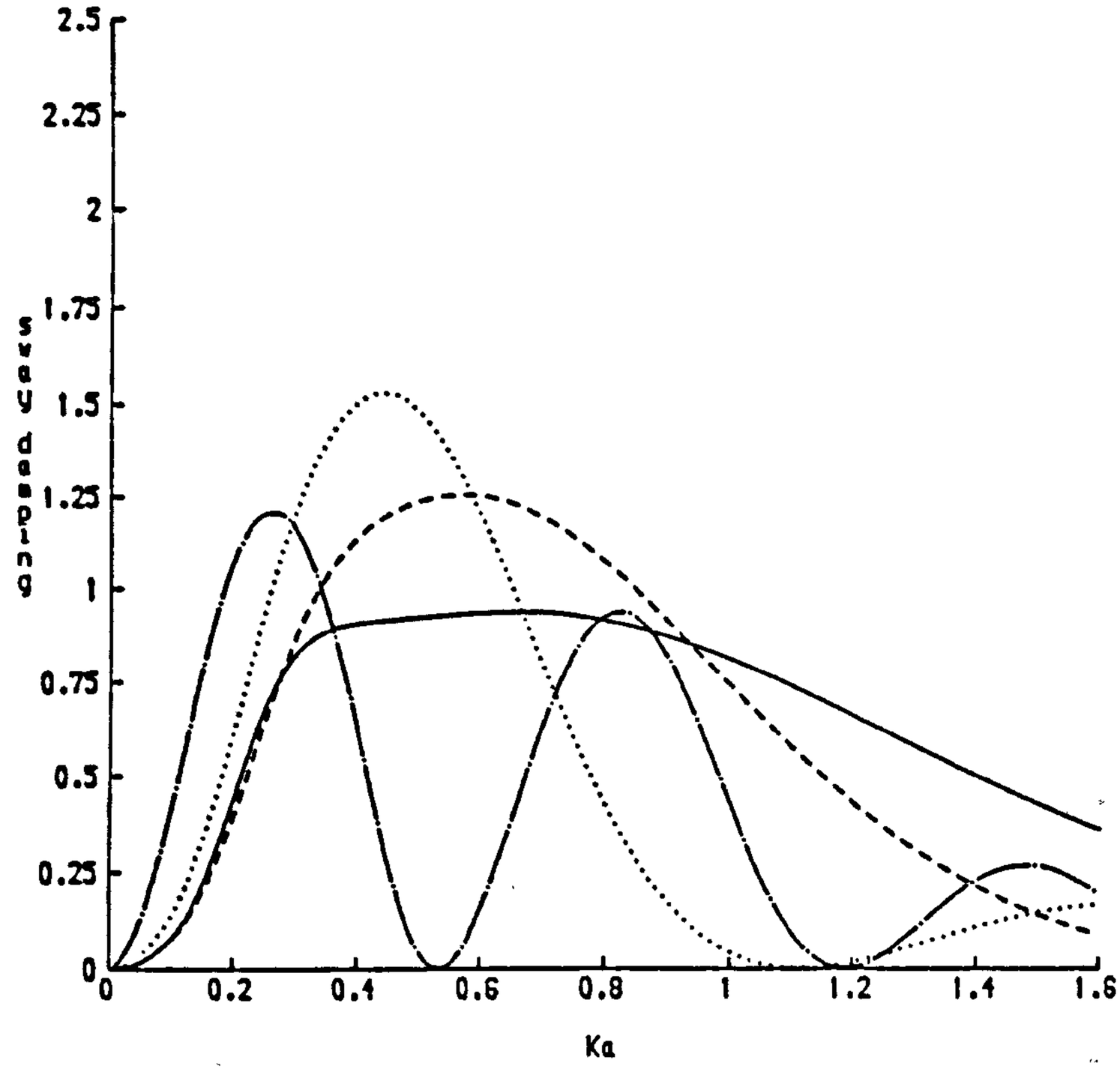

Figure 4.8.4. ν (sway) plotted against Ka for a cylinder next to a wall (a/h=0.2, f/a=1.5) at different distances from the wall.
——— b/h=0.21; – – – b/h=0.3; ····· b/h=0.5; –·–·– b/h=1.

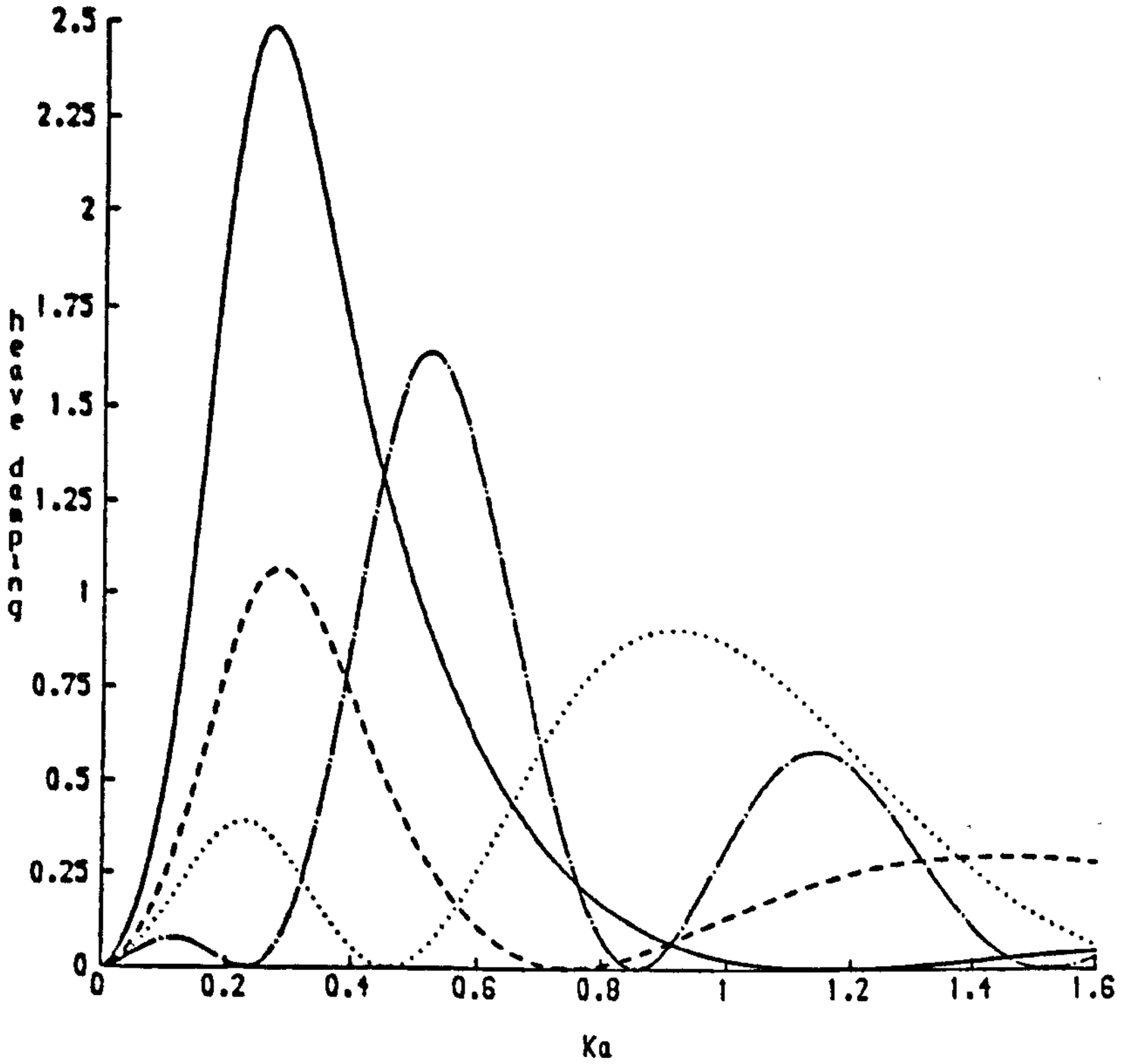

Figure 4.8.5. ν (heave) plotted against Ka for a cylinder next to a wall (a/h=0.2, f/a=1.5) at different distances from the wall.
——— b/h=0.21; – – – b/h=0.3; ····· b/h=0.5; –·–·– b/h=1.

curves as b/a increases. This is not particularly surprising since as the wall gets further away from the cylinder more wavelengths can fit between the cylinder and the wall. If the number of wavelengths that lie between $x = 0$ and $x = b$ is denoted by Λ then

$$\Lambda = \frac{b}{\lambda} = \frac{b}{h}\,\frac{\kappa h}{2\pi} \ . \qquad (4.8.28)$$

Taking $b/h = 1$ and $a/h = 0.2$ it is easily shown that as Ka varies between 0 and 1.26 Λ varies between 0 and 1. This compares very well with the curves which complete one cycle in approximately this range.

The curves for $b/h = 1.05$ show that the maximum value of the damping coefficient in sway is lowered as the gap between the cylinder and the wall decreases whereas the maximum value of the sway added mass together with those of both the added mass and damping coefficient in heave are increased. It is interesting to note that for the larger values of b/a the damping coefficients for sway and heave are almost exactly out of phase with each other.

It can be seen from figures (4.8.4) and (4.8.5) that, unlike the single isolated cylinder, the cylinder next to a wall has zero damping coefficient at some values of Ka. Thus equation (4.8.23) implies that no waves are radiated out to infinity. One consequence of this is that no net work is required to keep the cylinder oscillating at these frequencies.

Figures (4.8.6)-(4.8.9) show the effect of immersion depth on the hydrodynamic characteristics of the cylinder. The parameters a/h and b/h are fixed at 0.2 and 0.5 respectively and f/a is allowed to vary between 1 and 4. The damping coefficients in sway and heave are again almost exactly out of phase with each other, particularly for small immersion depths. Like an isolated cylinder, a cylinder next to a

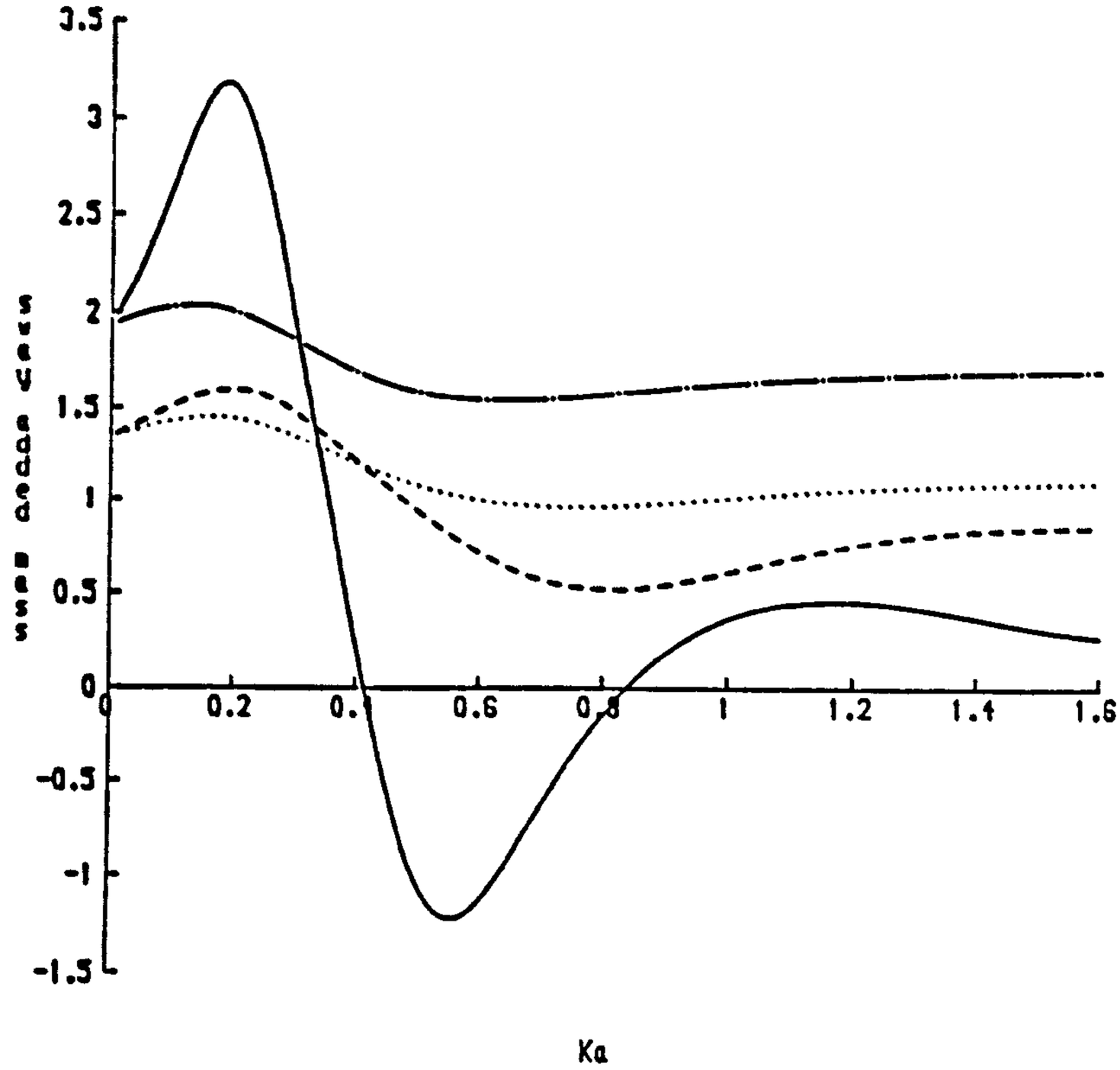

Figure 4.8.6. μ (sway) plotted against Ka for a cylinder next to a wall (a/h=0.2, b/h=0.5) with diiferent clearances. ——— f/a=1.1; – – – f/a=2; ····· f/a=3; –·–·– f/a=3.9.

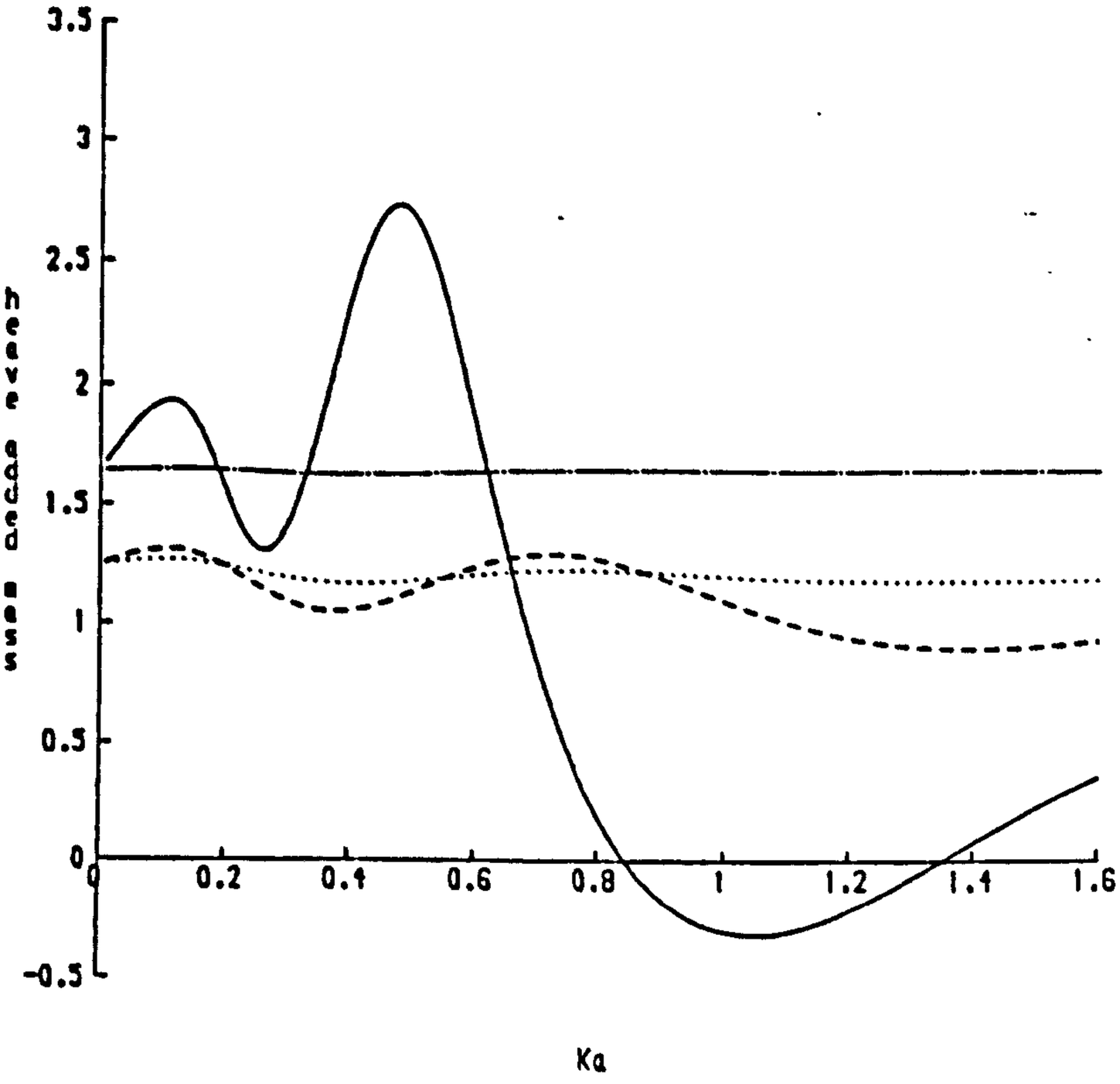

Figure 4.8.7. μ (heave) plotted against Ka for a cylinder next to a wall (a/h=0.2, b/h=0.5) with diiferent clearances. ——— f/a=1.1; – – – f/a=2; ····· f/a=3; –·–·– f/a=3.9.

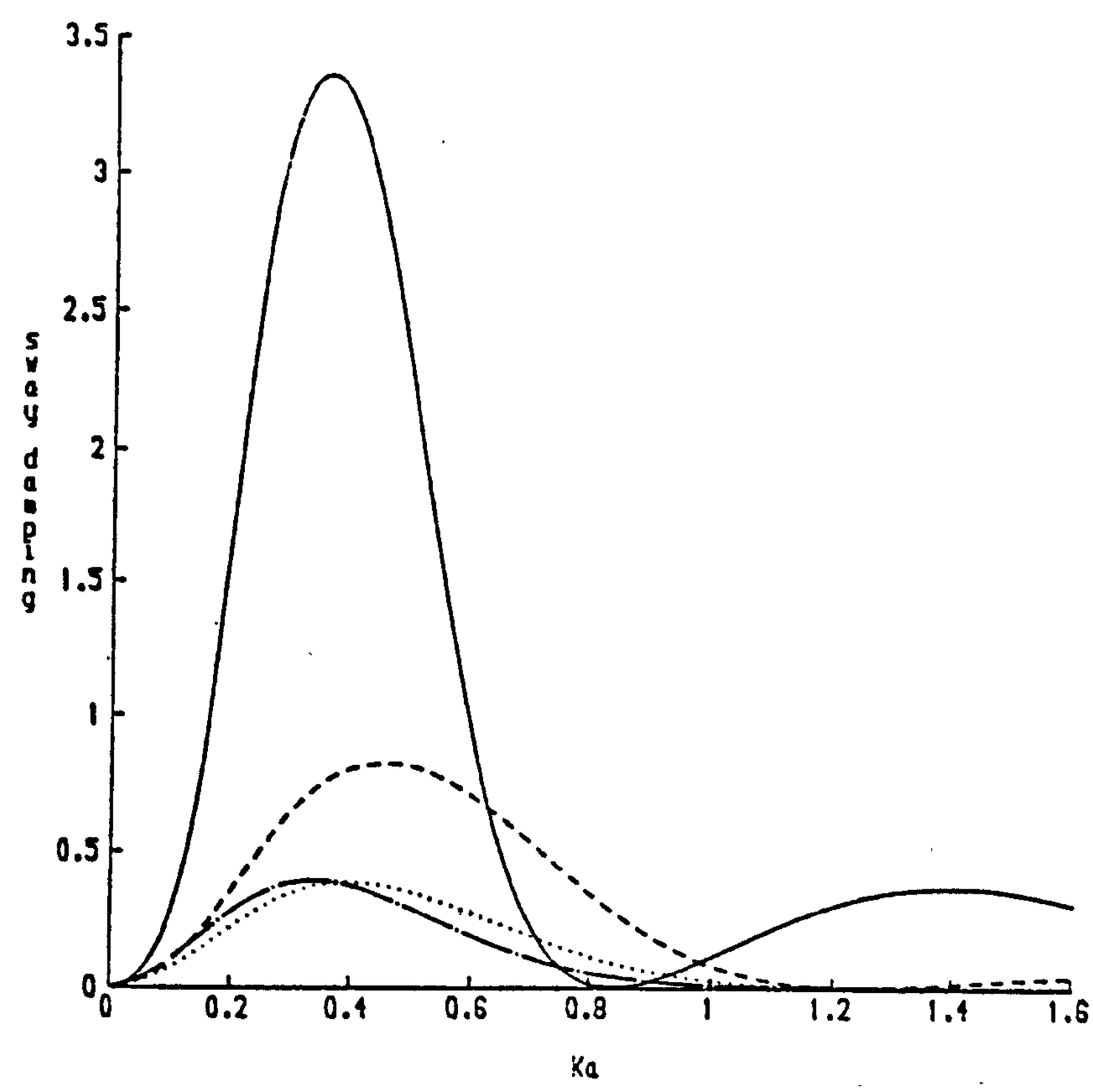

Figure 4.8.8. ν (sway) plotted against Ka for a cylinder next to a wall (a/h=0.2, b/h=0.5) with different clearances. ——— f/a=1.1; – – – f/a=2; ····· f/a=3; –·–·– f/a=3.9.

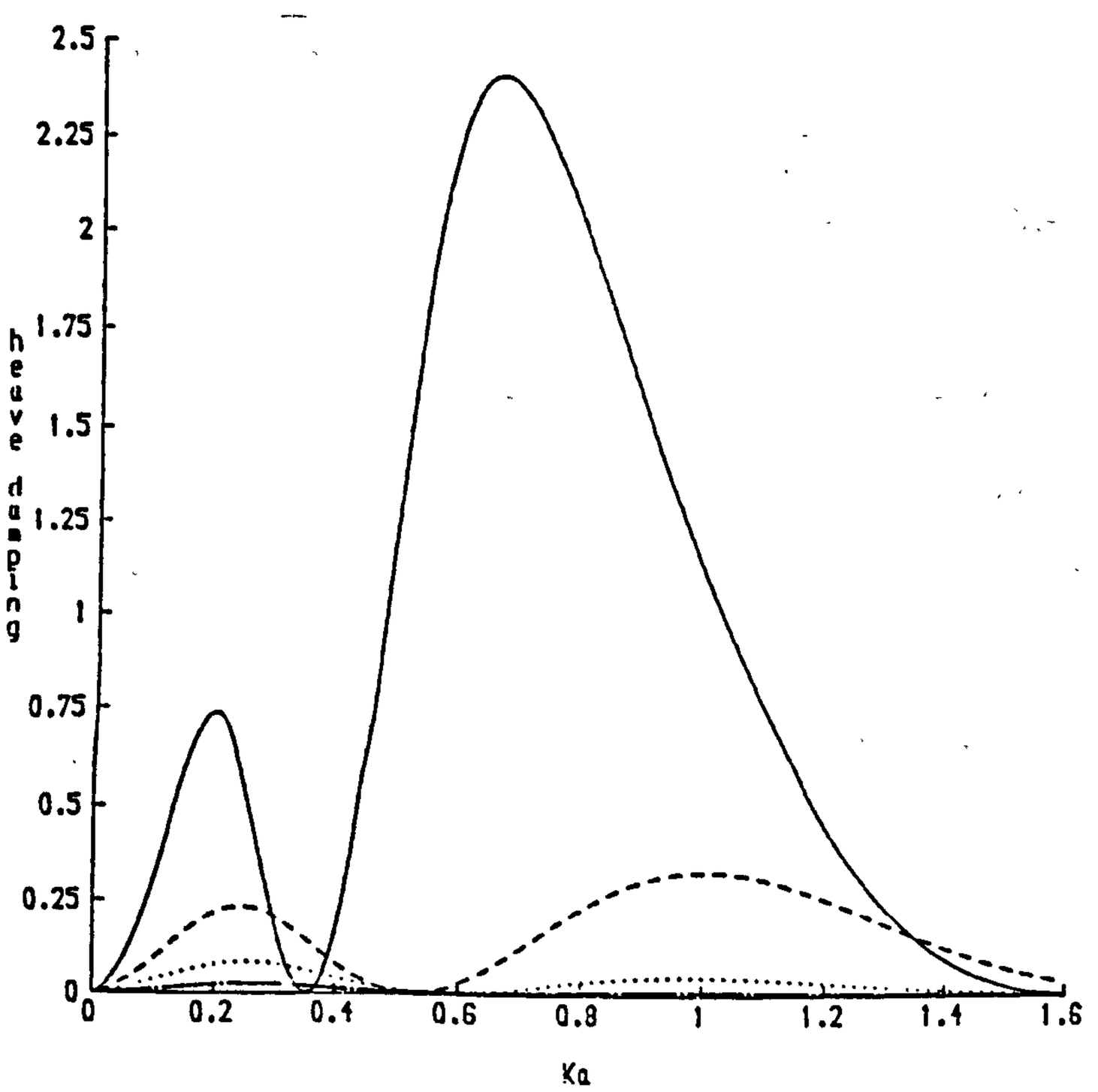

Figure 4.8.9. ν (heave) plotted against Ka for a cylinder next to a wall (a/h=0.2, b/h=0.5) with different clearances. ——— f/a=1.1; – – – f/a=2; ····· f/a=3; –·–·– f/a=3.9.

wall which is very close to the free surface has negative added mass at some frequencies. See §3.4 for a discussion of this phenomenon.

The third situation that will be considered is that of bringing the bottom up to meet the cylinder. In this case the parameters f/a and b/a are held fixed, at 1.5 and 2.5 respectively, and a/h is allowed to vary between 0 and 0.4. Curves for a/h = 0.1, 0.2, 0.3 and 0.39 are shown in figures (4.8.10)-(4.8.13). For the heave case curves for a/h = 0 are given in Wang (1981) and it is found that the difference between the a/h = 0.1 curves and those for infinite depth is very small (less than about 2%) as one would expect. The effect of decreasing the water depth until the cylinder is almost touching the bottom is seen to have a large effect on the sway characteristics in long waves but not otherwise. Again the damping coefficients are almost exactly out of phase, particularly for small values of a/h.

4.9 The Scattering Problem

The method used to solve the scattering problem for a cylinder next to a wall is the same as that used in §4.5 for the isolated cylinder. Again the problem is a boundary value problem for the time-independent velocity potential, ϕ_s, which can be reformulated in terms of a radiation potential, ψ, so that the results of §4.8 can be used. Let

$$\phi_s = \frac{gA}{\omega} \frac{\cosh \kappa(y-h)}{\cosh \kappa h} (e^{i\kappa x} + e^{-i\kappa x}) + \psi. \qquad (4.9.1)$$

Then since

$$\phi_s \sim \frac{gA}{\omega} \frac{\cosh \kappa(y-h)}{\cosh \kappa h} (e^{i\kappa x} + R\, e^{-i\kappa x}) \quad \text{as} \quad x \longrightarrow \infty \qquad (4.9.2)$$

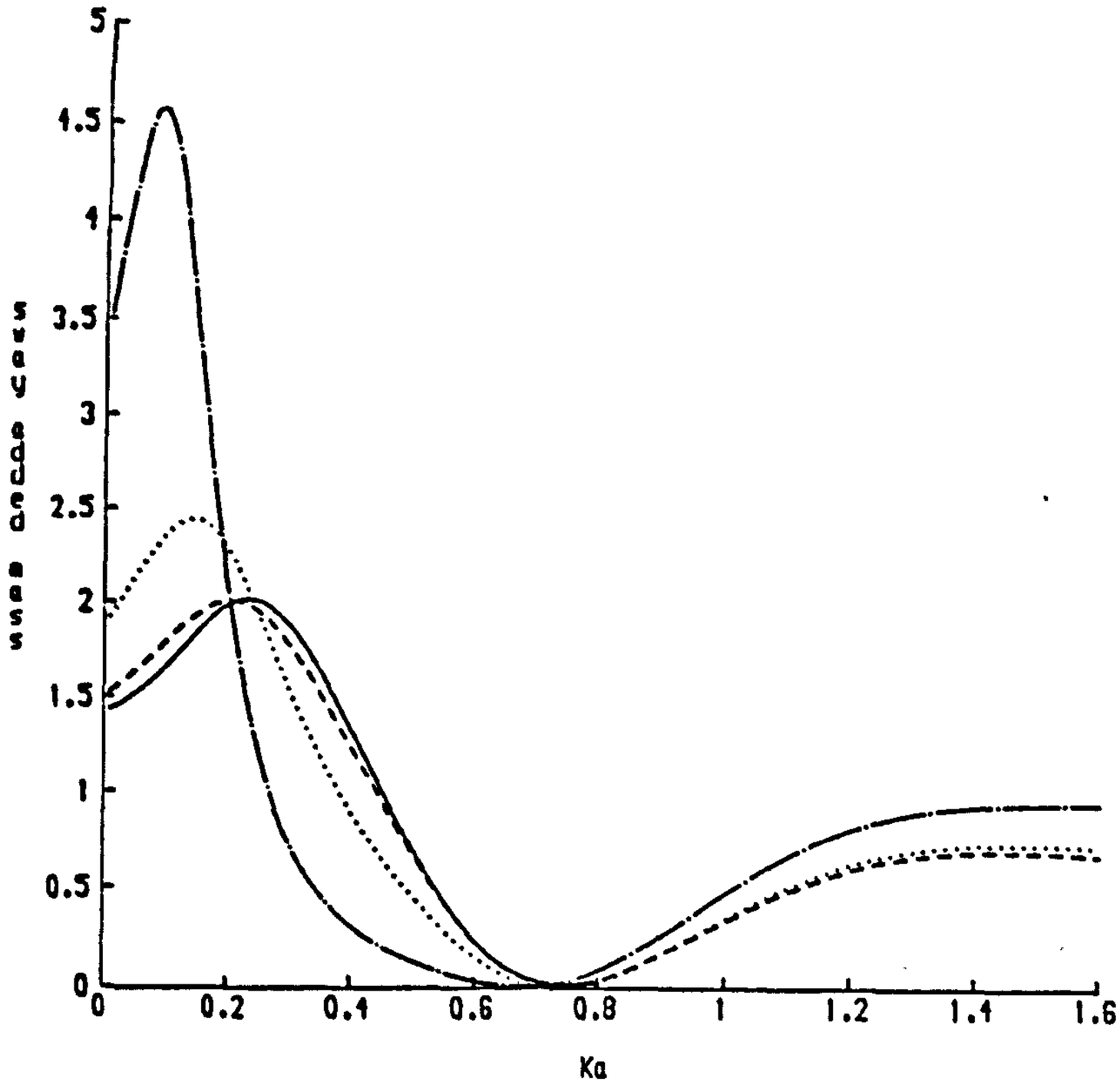

Figure 4.8.10. μ (sway) plotted against Ka for a cylinder next to a wall (f/a=1.5, b/a=2.5) in different depths of water. ——— a/h=0.1; – – – a/h=0.2; ····· a/h=0.3; –·–·– a/h=0.39.

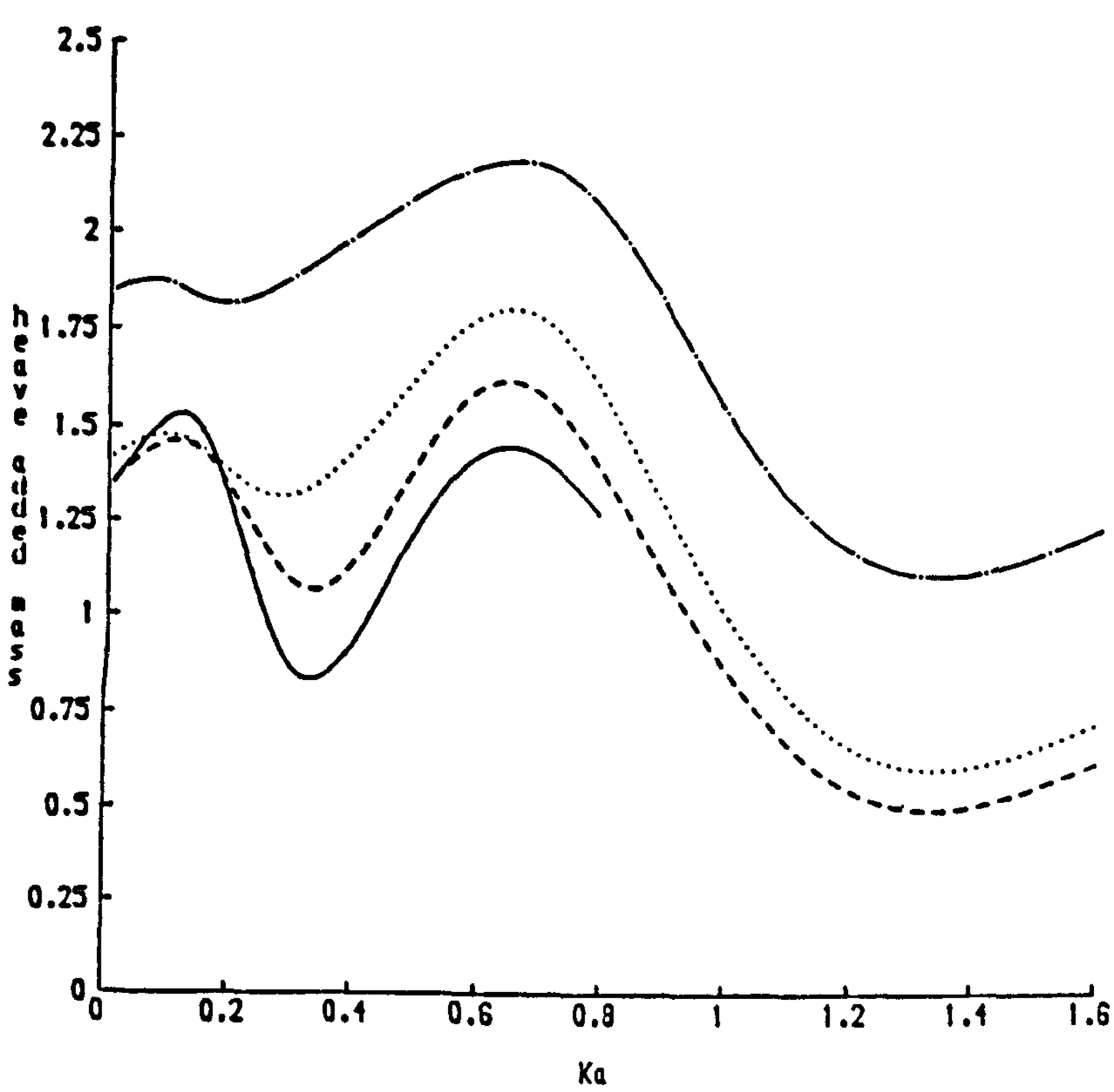

Figure 4.8.11. μ (heave) plotted against Ka for a cylinder next to a wall (f/a=1.5, b/a=2.5) in different depths of water. ——— a/h=0.1; – – – a/h=0.2; ····· a/h=0.3; –·–·– a/h=0.39.

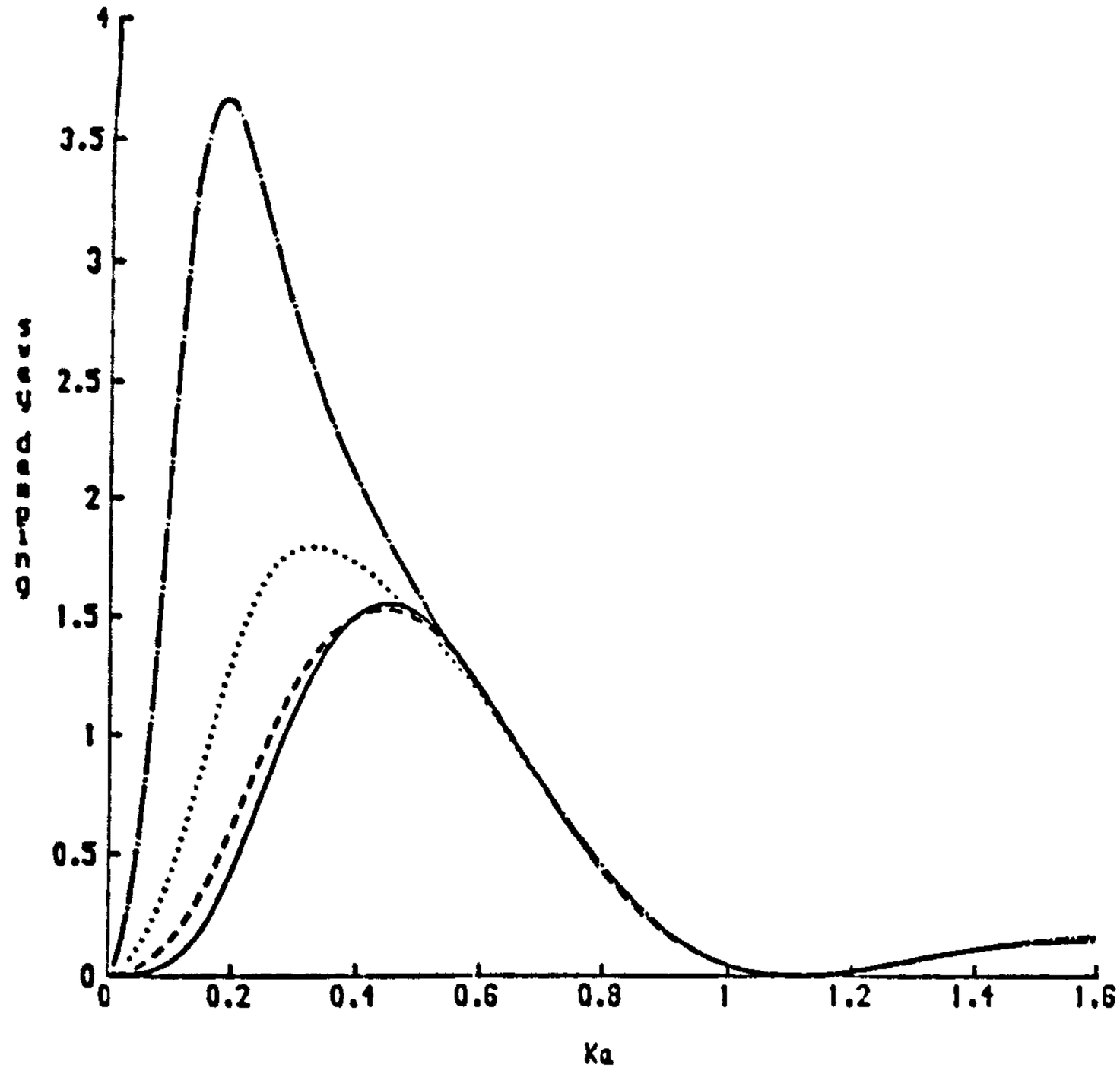

Figure 4.8.12. ν (sway) plotted against Ka for a cylinder next to a wall (f/a=1.5, b/a=2.5) in different depths of water. ——— a/h=0.1; – – – a/h=0.2; ····· a/h=0.3; –·–·– a/h=0.39.

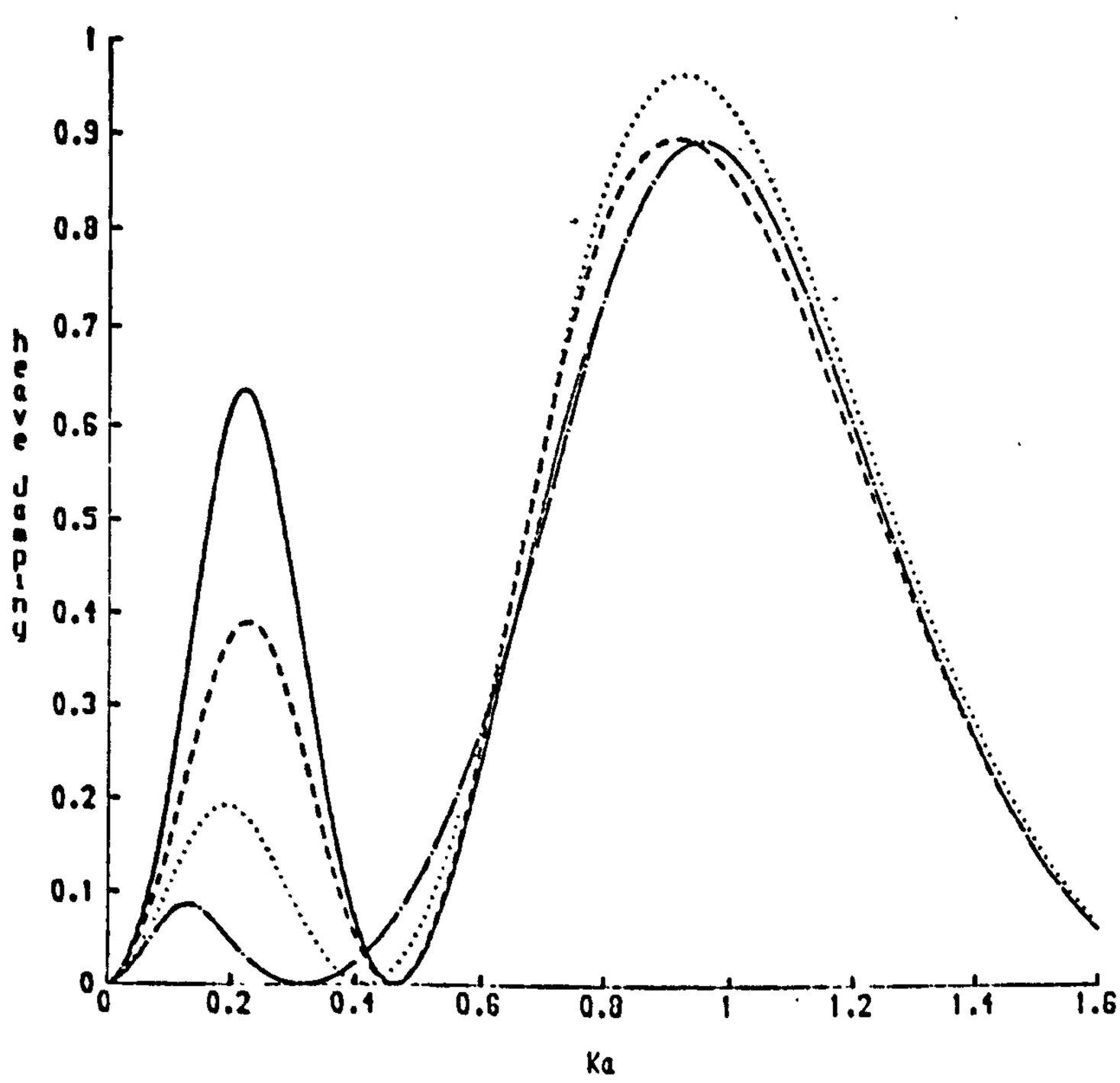

Figure 4.8.13. ν (heave) plotted against Ka for a cylinder next to a wall (f/a=1.5, b/a=2.5) in different depths of water. ——— a/h=0.1; – – – a/h=0.2; ····· a/h=0.3; –·–·– a/h=0.39.

ψ must satisfy

$$\psi \sim \frac{gA}{\omega} \frac{\cosh \kappa(y-h)}{\cosh \kappa h} (R-1)\ e^{-i\kappa x} \qquad \text{as} \quad x \longrightarrow \infty. \tag{4.9.3}$$

Thus ψ is a radiation potential which satisfies

$$\omega \frac{\partial \psi}{\partial r_2} = -gA \frac{\partial}{\partial r_2} \left[\frac{gA}{\omega} \frac{\cosh \kappa(y-h)}{\cosh \kappa h} (e^{i\kappa x} + e^{-i\kappa x})\right] \qquad \text{on } r_2=a. \tag{4.9.4}$$

The term in square brackets can be expanded about the point $r_2 = 0$, valid in the region $r_2 < f$, to give

$$\sum_{m=0}^{\infty} \frac{(\kappa r_2)^m}{m!} [(e^{\kappa(f-h)} + (-1)^m e^{\kappa(h-f)}) \cos m\theta_2 \cos \kappa b$$

$$- (e^{\kappa(f-h)} - (-1)^m e^{\kappa(h-f)}) \sin m\theta_2 \sin \kappa b].$$

The function ψ is asymmetric so we need to consider a combination of symmetric and antisymmetric multipoles. Thus let

$$\psi = \frac{gA}{a\omega} \sum_{n=1}^{\infty} [\alpha_n (\phi_{n,1}^{(1)} - \phi_{n,1}^{(2)}) + \beta_n (\phi_{n,2}^{(1)} + \phi_{n,2}^{(2)})]. \tag{4.9.5}$$

This ensures that ϕ_s satisfies the condition of no normal velocity at the wall. The results of the previous section then imply that the coefficients α_n and β_n can be obtained by solving the following matrix equation:

$$\sum_{n=1}^{\infty} M_{mn}\ \gamma_n = R_m \qquad m = 1,2,\ldots \tag{4.9.6}$$

where

$$\gamma_{2n-1} = \alpha_n \; ; \; \gamma_{2n} = \beta_n \qquad n = 1,2,\ldots$$

$$R_{2m-1} = \frac{-1}{\cosh \kappa h} \frac{(\kappa a)^m}{(m-1)!} \left[(-1)^m e^{\kappa(h-f)} - e^{\kappa(f-h)}\right] \sin \kappa b$$

$$R_{2m} = \frac{-1}{\cosh \kappa h} \frac{(\kappa a)^m}{(m-1)!} \left[(-1)^m e^{\kappa(h-f)} + e^{\kappa(f-h)}\right] \cos \kappa b$$

and M_{mn} is given by equation (4.8.16).

4.10 Two Cylinders in Sway and in Phase

In 1981 Wang solved the radiation problem for two parallel spaced cylinders in infinite depth, for both heave and sway motions. The motivation for this work came from the study of catamaran type vessels. This is not particularly relevant to the problem of wave reflection but for completeness the sway problem for such a configuration will be solved here. Note that the heave case is the same as for a cylinder next to a wall and has been solved in §4.8.

The problem of sway next to a wall was also solved in §4.8 and in this case the boundary condition on $x = 0$ is $\frac{\partial \phi}{\partial x} = 0$. When two parallel spaced cylinders are in sway and in phase with each other the the problem is antisymmetric about $x = 0$ and the appropriate boundary condition on this line is $\phi = 0$.

Very little work is required to change the formulation of §4.8 in order to satisfy this new boundary condition. The representation for ϕ given by equation (4.8.6) was chosen so that $\frac{\partial \phi}{\partial x} = 0$ would be automatically satisfied. It is easy to show that the representation required for this new case is

$$\phi = U \sum_{n=1}^{\infty} \left[c_n \left(\phi_{n,1}^{(1)} + \phi_{n,1}^{(2)}\right) + d_n \left(\phi_{n,2}^{(1)} - \phi_{n,2}^{(2)}\right)\right]. \qquad (4.10.1)$$

The analysis is identical to that which was done for the case of sway next to a wall with terms coming from $\phi_{n,q}^{(2)}$ $q = 1,2$ being multiplied by -1. The resulting infinite system of equations is

$$\sum_{n=1}^{\infty} M_{mn}\, e_n = \delta_{1m} \qquad m = 1,2,... \tag{4.10.2}$$

where

$$e_{2n-1} = c_n \quad ; \quad e_{2n} = d_n \qquad n = 1,2,...$$

and the matrix M_{mn} is given by

$$M_{2m-1,2n-1} = -\delta_{mn} + Q_{mn,1} + A_{mn,1} - C_{mn} \cos (n+m)\frac{\pi}{2}$$

$$M_{2m-1,2n} = Q_{mn,2} + C_{mn} \sin (n+m)\frac{\pi}{2}$$

$$M_{2m,2n-1} = S_{mn,1} + C_{mn} \sin (n+m)\frac{\pi}{2} \tag{4.10.3}$$

$$M_{2m,2n} = \delta_{mn} - A_{mn,2} + S_{mn,2} + C_{mn} \cos (n+m)\frac{\pi}{2} .$$

The added mass and damping coefficients are again given by equation (4.8.18).

Figures (4.10.1) and (4.10.2) show some curves of added mass and damping coefficients against non-dimensional wavenumber, Ka, for fixed values of f/a (=1.5) and b/a (=2.5) with varying a/h. Curves for a/h = 0 can be found in Wang (1981) and they are within a few percent of the a/h = 0.1 curves shown. Figure (4.10.2) shows that, like a cylinder next to a wall, two parallel cylinders in sway have zero damping coefficient at some frequencies (see §4.8). A comparison with figures (4.8.13) and (4.8.14) shows that the damping coefficient in this

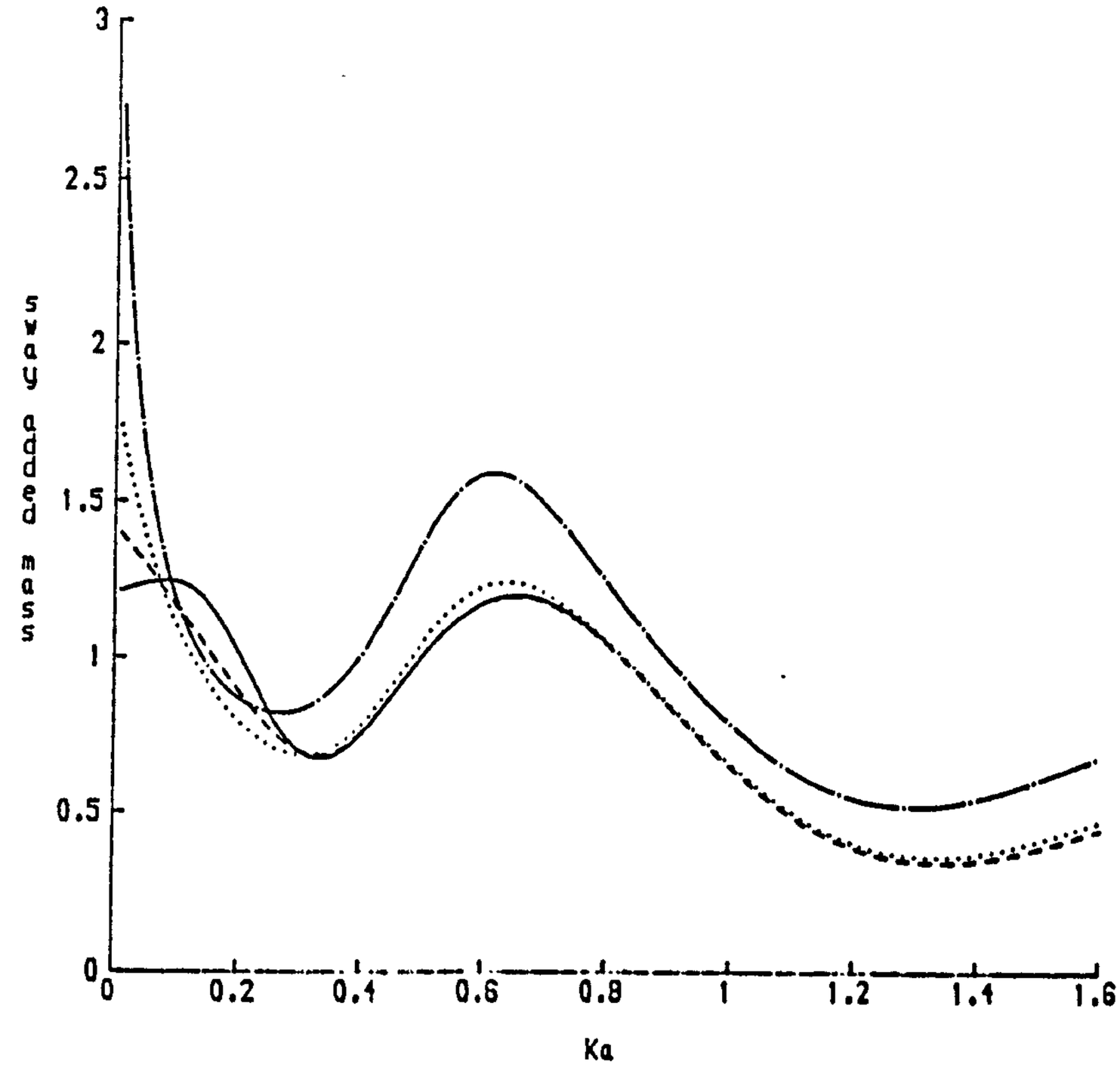

Figure 4.10.1. μ plotted against Ka for two parallel cylinders in sway (f/a=1.5, b/a=2.5) in different depths of water.
——— a/h=0.1; - - - a/h=0.2; ····· a/h=0.3; -·-·- a/h=0.39.

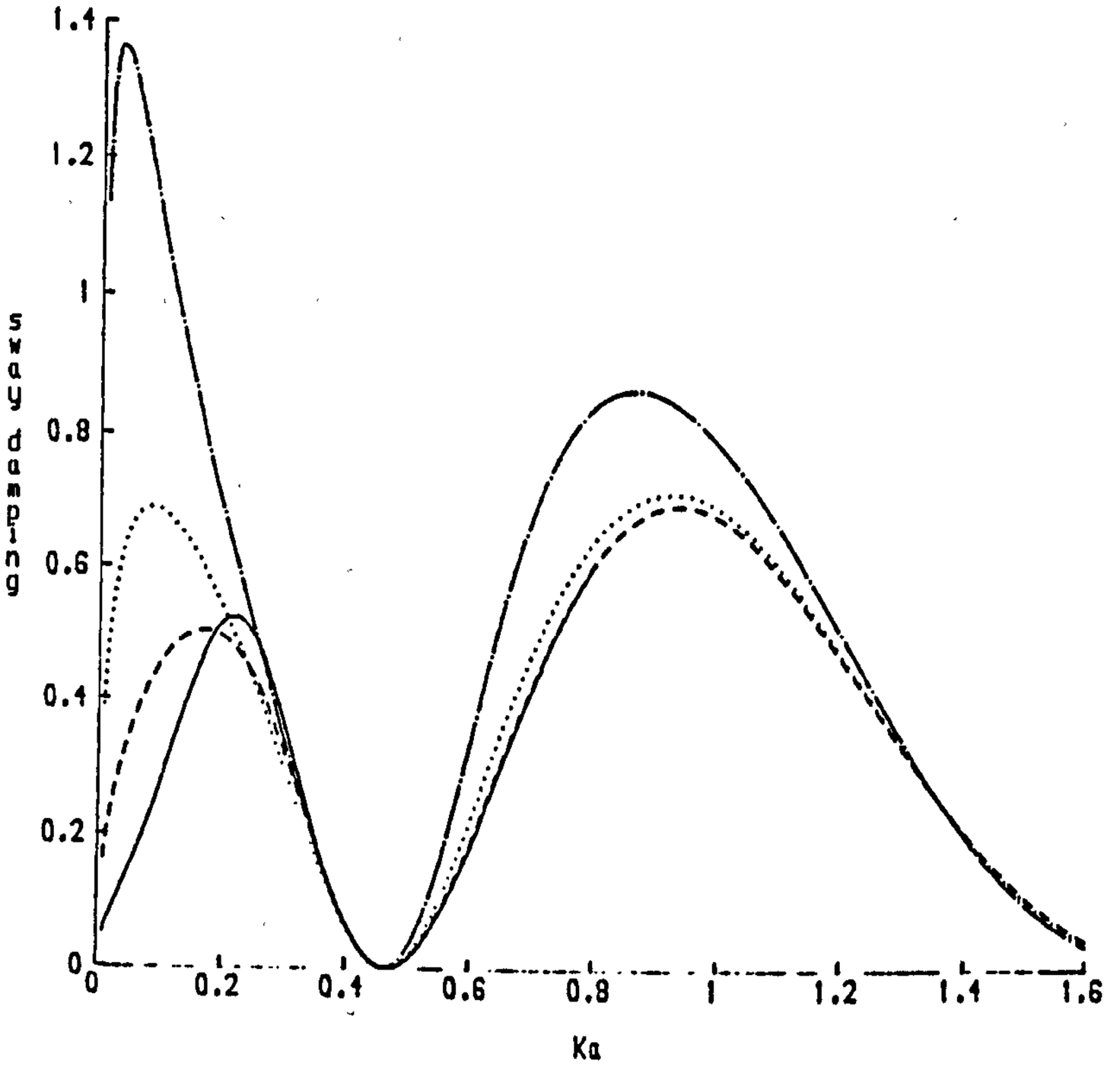

Figure 4.10.2. ν plotted against Ka for two parallel cylinders in sway (f/a=1.5, b/a=2.5) in different depths of water.
——— a/h=0.1; - - - a/h=0.2; ····· a/h=0.3; -·-·- a/h=0.39.

case is almost exactly in phase with that for the heave case. Why this is the case whereas for sway next to a wall it is almost exactly out of phase (see §4.8) is unclear.

4.11 Conclusion

Eight problems concerning submerged cylinders in water of finite depth have been solved in this chapter using multipole expansions. They are

1) The radiation of waves by a single cylinder in heave.
2) The radiation of waves by a single cylinder in sway.
3) The scattering of waves by a single cylinder.
4) The scattering of waves by a tethered buoyant cylinder.
5) The radiation of waves by a cylinder in heave next to a wall.
6) The radiation of waves by a cylinder in sway next to a wall.
7) The scattering of waves by a cylinder next to a wall.
8) The radiation of waves by two parallel cylinders in sway.

The multipole expansion method has been shown to be an efficient way to solve such problems provided a sensible approach is taken to the evaluation of the principal value integrals that appear. A lot of the work in this chapter is the extension to the finite depth case of work of other authors. The major exception is the problem of the scattering of waves by a tethered buoyant cylinder.

This problem was studied with a view to proposing a wave reflection device suitable for the protection of coastal installations while allowing the passage of small vessels over it. The need for wave reflection devices has been highlighted recently by the realisation that the platforms in the Norwegian Ekofisk oil field in the North Sea are gradually sinking as oil is extracted and as they do so they become more susceptible to damage by large waves.

The results shown in §4.7 show that a tethered buoyant submerged cylinder, if sensibly 'tuned', can be an excellent wave reflector. The results show that the best performance can be achieved by very light cylinders in fairly shallow water and this makes the device highly suitable for coastal sites.

CHAPTER 5

The added mass and damping coefficients of a submerged sphere in finite depth

5.1 Introduction

The general theory presented in §3.2 is only applicable in two dimensions. It is hoped that in the future this theory will be extended to cover three-dimensional problems. One of the simplest three-dimensional problems that could be looked at would be reflection by a tethered submerged sphere. The hydrodynamic characteristics of such a body would need to be evaluated and this is done in this chapter using the multipole method.

Srokosz (1979) used the multipole method to solve the problem of the radiation of waves (in sway and heave) by a submerged sphere in infinitely deep water. In this chapter the techniques described in chapter 4 will be used to solve the same problem in finite depth.

The numerical evaluation of three-dimensional multipole potentials again involves calculating principal value integrals and the method described in §4.3 will again be used.

The quantities R and T, i.e. the reflection and transmission coefficients, do not appear in this chapter since these concepts are meaningless in three dimensions, since the amplitude of any diverging wave tends to zero as the distance from the wave source tends to infinity.

5.2 Spherical Multipole Expansions

Spherical polar coordinates (r,θ,α), with their origin at $x = z = 0$, $y = f$ will be used with θ measured from the downward vertical (the positive y-axis). The cylindrical polar coordinate $R \equiv (x^2 + z^2)^{1/2}$ will also be used.

Time independent spherical multipole potentials centred on (0,f) can then be written (see Thorne (1953))

$$\phi_n^m = \cos m\alpha \left[a \left[\frac{a}{r}\right]^{n+1} P_n^m(\cos\theta) + \frac{a^{n+2}}{(n-m)!} \int_0^\infty \frac{k^n J_m(kR)}{Kh \cosh kh - kh \sinh kh} \right.$$

$$\left[e^{k(f-h)} (K \sinh ky - k \cosh ky) - (-1)^{n+m} (K+k) e^{-kf} \cosh k(h-y) \right] dk$$

$$\left. - \frac{2\pi i a(\kappa a)^{n+1} \cosh \kappa(y-h)}{(n-m)!\ (2\kappa h + \sinh 2\kappa h)} \left[e^{\kappa(f-h)} + (-1)^{n+m} e^{\kappa(h-f)} \right] J_m(\kappa R) \right]$$

$$n = 0,1,\ldots \quad m \leq n \qquad (5.2.1)$$

where κ is given by the dispersion relation (3.2.8), J_m $m = 0,1,\ldots$ are Bessel functions and P_n^m are Legendre functions. The superscript m represents the azimuthal mode.

With the functions c_i $i = 1,2,3,4$ defined by equations (4.2.5)-(4.2.8) with q replaced by m this can be written

$$\phi_n^m = \cos m\alpha \left[a \left[\frac{a}{n}\right]^{n+1} P_n^m(\cos\theta) \right.$$

$$+ \frac{a^2}{2(n-m)!} \int_0^\infty (ka)^n \frac{[c_1(kh)\ e^{k(f-y)} + c_2(kh)\ e^{k(y-f)}]}{Kh \cosh kh - kh \sinh kh} J_m(kR)\ dk$$

$$\left. - \frac{1}{2(n-m)!} \frac{2\pi i a\ (\kappa a)^{n+1}}{2\kappa h + \sinh 2\kappa h} [c_3(\kappa h)\ e^{\kappa(f-y)} + c_4(\kappa h)\ e^{\kappa(y-f)}]\ J_m(\kappa R) \right].$$

(5.2.2)

These multipoles can be expanded in spherical polar coordinates centred on (0,f) using the following two identities (See Thorne (1953) and Abramowitz and Stegun equation (9.1.35)):

$$e^{k(f-y)}\ J_m(kR) = (-1)^m \sum_{s=m}^{\infty} \frac{(-kr)^s}{(s+m)!}\ P_s^m(\cos\theta)$$

$$e^{k(y-f)}\ J_m(kR) = \sum_{s=m}^{\infty} \frac{(kr)^s}{(s+m)!}\ P_s^m(\cos\theta). \qquad (5.2.3)$$

This gives

$$\phi_n^m = a\cos m\alpha \left[\left[\frac{a}{r}\right]^{n+1} P_n^m(\cos\theta) + \sum_{s=m}^{\infty} \left[\frac{r}{a}\right]^s A_{ns}^m\ P_s^m(\cos\theta) \right] \qquad (5.2.5)$$

where

$$A_{ns}^m = \frac{(a/h)^{n+s+1}}{2(n-m)!(s+m)!} \left[\int_0^{\infty} \frac{(-1)^{m+s}c_1(u) + c_2(u)}{Kh\cosh u - u\sinh u}\ u^{n+s}\ du \right.$$

$$\left. - 2\pi i\ (\kappa h)^{n+s+1}\ \frac{(-1)^{m+s}c_3(\kappa h) + c_4(\kappa h)}{2\kappa h + \sinh 2\kappa h} \right].$$

$$n = 0,1,\ldots \quad m \le n \qquad (5.2.6)$$

This expansion for ϕ_n^m is valid in the region $r < 2f$. (See Thorne (1953)).

5.3 Formulation and Solution

In order to calculate the added mass and damping coefficients we must solve the following boundary value problem for the time-independent

potential ϕ:

$$\nabla^2\phi = 0 \qquad \text{in the fluid} \qquad (5.3.1)$$

$$K\phi + \frac{\partial\phi}{\partial y} = 0 \qquad \text{on } y = 0 \qquad (5.3.2)$$

$$\frac{\partial\phi}{\partial y} = 0 \qquad \text{on } y = h \qquad (5.3.3)$$

$$\frac{\partial\phi}{\partial r} = U \begin{cases} \sin\theta \cos\alpha \\ \cos\theta \end{cases} \quad \text{on } r = a \quad \begin{cases} \text{(surge)} \\ \text{(heave)} \end{cases} \qquad (5.3.4)$$

where U is the time-independent velocity of the sphere.

Note that $P_1^0(\cos\theta) = \cos\theta$ and $P_1^1(\cos\theta) = \sin\theta$ and so from the boundary condition on the sphere, equation (5.3.4), it is clear that the potentials for sway and heave can be written solely in terms of ϕ_n^1 and ϕ_n^0 respectively. In order to be able to solve both problems simultaneously let ϕ^m, $m = 0,1$, represent the solution to the heave and sway problems respectively. The boundary condition on the sphere can now be written

$$\frac{\partial\phi^m}{\partial r} = U P_1^m(\cos\theta) \cos m\alpha \qquad \text{on } r = a,\ 0<\theta<\pi. \qquad (5.3.5)$$

Let

$$\phi^m = \sum_{n=1}^{\infty} c_n^m \phi_n^m \ . \qquad (5.3.6)$$

Note that the $n = 0$ term which could appear in the expansion for ϕ^0 has been omitted. This term corresponds to a r^{-1} singularity at the centre of the sphere which is physically unacceptable as it would imply an instantaneous flux of fluid across the surface of the sphere in exactly the same way that the $\ln r$ singularity was unacceptable in the case of the submerged cylinder (see §4.2). However if this term were

left in we would simply find that its coefficient was zero.

Application of the boundary condition, equation *(5.3.6)*, *gives*

$$\sum_{n=1}^{\infty} c_n^m \left[- (n+1) P_n^m(\cos\theta) + \sum_{s=m}^{\infty} s A_{ns}^m P_s^m(\cos\theta) \right] = P_1^m(\cos\theta). \tag{5.3.7}$$

This can be converted into an infinite system of linear equations by applying the operator

$$\int_0^{\pi} \ldots P_r^m(\cos\theta) \sin\theta \, d\theta \qquad r \geq m$$

and using the orthogonality relations

$$\int_0^{\pi} P_s^m(\cos\theta) P_r^m(\cos\theta) \sin\theta \, d\theta = \delta_{rs} \begin{cases} 2/(2r+1) & m = 0 \\ 2r(r+1)/(2r+1) & m = 1 \end{cases}. \tag{5.3.8}$$

The resulting system is

$$c_r^m - \sum_{n=1}^{\infty} \left[\frac{r}{r+1}\right] A_{nr}^m c_n^m = - \delta_{1r}/2 \tag{5.3.9}$$

which can be solved numerically by truncation (*see* §3.3).

The time-independent hydrodynamic force on the sphere in the direction of motion, f^m, is given by integrating the appropriate component of the pressure around the cylinder, i.e.

$$f^m = - \rho\omega i \int_0^{2\pi} \int_0^{\pi} \phi^m(a,\theta,\alpha) P_1^m(\cos\theta) \cos m\alpha \, a^2 \sin\theta \, d\theta \, d\alpha \tag{5.3.10}$$

$$= - \tfrac{4}{3} \pi a^3 U \rho\omega i \left[c_1^m + \sum_{n=1}^{\infty} A_{n1}^m c_n^m \right].$$

Using equation (5.3.7) with $r = 1$ and non-dimensionalising with respect to the fluid displaced by the sphere gives the final result

$$\mu^m - i\nu^m = - (1 + 3c_1^m) \ . \qquad (5.3.11)$$

The three-dimensional equivalent of equation (1.2.32), which relates the damping coefficient to the energy radiated to infinity, is given by Mei (1983) p. 321 as

$$B = 2 \frac{\rho g}{\pi\kappa} c_g \int_0^{2\pi} |A(\alpha)|^2 \, d\alpha$$

where it is assumed that

$$|\phi| \sim \frac{g}{\omega} |A(\alpha)| \frac{\cosh \kappa(y-h)}{\cosh \kappa h} \left[\frac{2}{\pi\kappa R}\right]^{1/2} \qquad \text{as} \quad R \longrightarrow \infty.$$

This can be used to provide a check on the results obtained from the system of equations (5.3.9). The method used is identical to that described described in §4.2 and the resulting identity that is obtained is

$$Im(c_1^m) = [2\kappa a \ (2\kappa h + \sinh 2\kappa h)]^{-1} \left| \sum_{n=1}^{\infty} r_n^m \right|^2 \begin{cases} 2\pi & m = 0 \\ \pi & m = 1 \end{cases} \qquad (5.3.12)$$

where

$$r_n^m = \frac{(\kappa a)^{n+1}}{(n-m)!} [e^{\kappa(f-h)} + (-1)^{n+m} e^{\kappa(h-f)}] \ c_n^m \ .$$

5.4 Results and Discussion

Curves of added mass and damping coefficients for four spheres are shown in figures (5.4.1)-(5.4.4). In all the curves the immersion depth

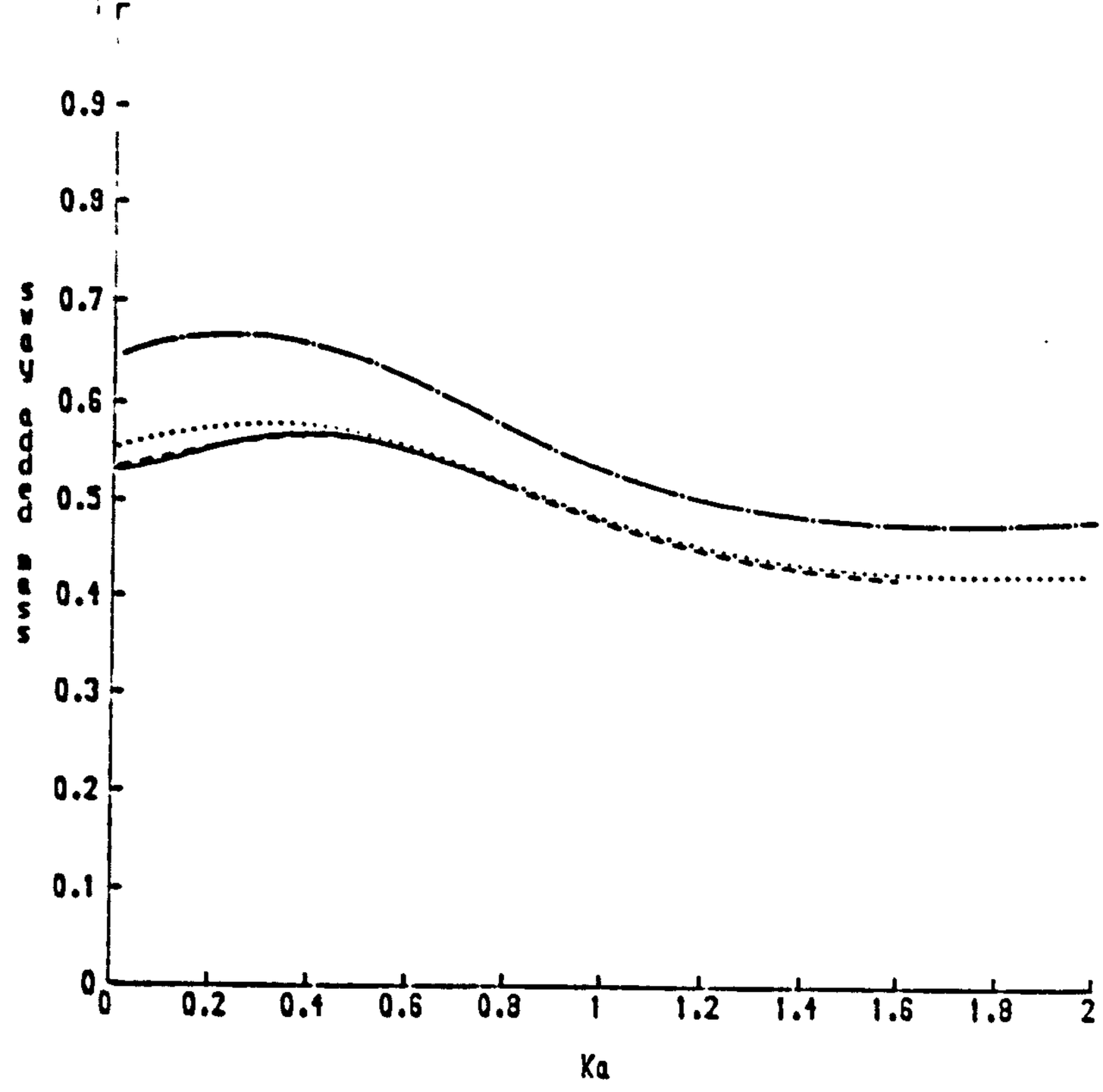

Figure 5.4.1. μ (sway) plotted against Ka for a submerged sphere (f/a=1.5) in different depths of water. ——— a/h=0.1; – – – a/h=0.2; ····· a/h=0.3; –·–·– a/h=0.39.

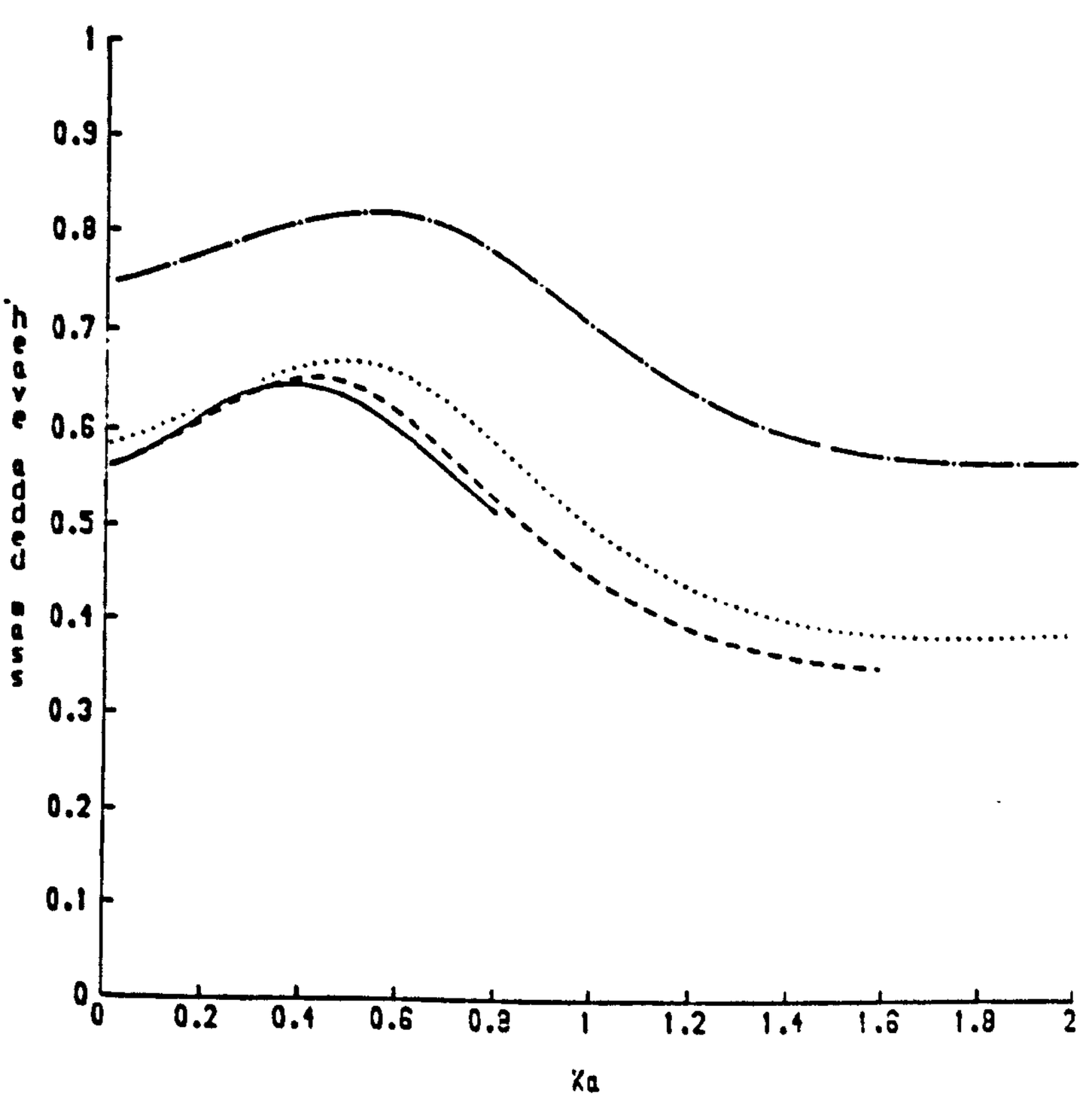

Figure 5.4.2. μ (heave) plotted against Ka for a submerged sphere (f/a=1.5) in different depths of water. ——— a/h=0.1; – – – a/h=0.2; ····· a/h=0.3; –·–·– a/h=0.39.

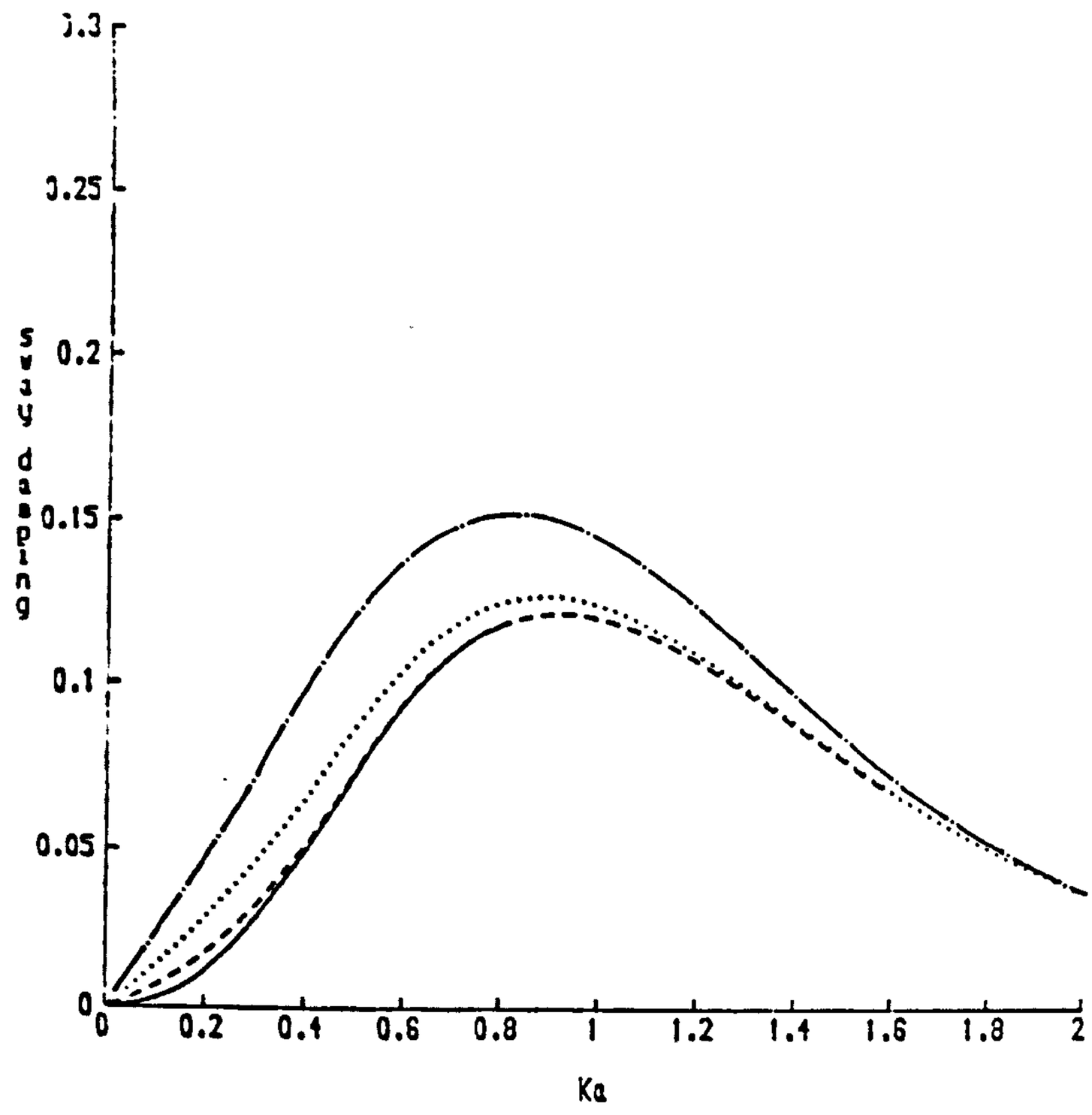

Figure 5.4.3. ν (sway) plotted against Ka for a submerged sphere (f/a=1.5) in different depths of water. ——— a/h=0.1; – – – a/h=0.2; ····· a/h=0.3; –·–·– a/h=0.39.

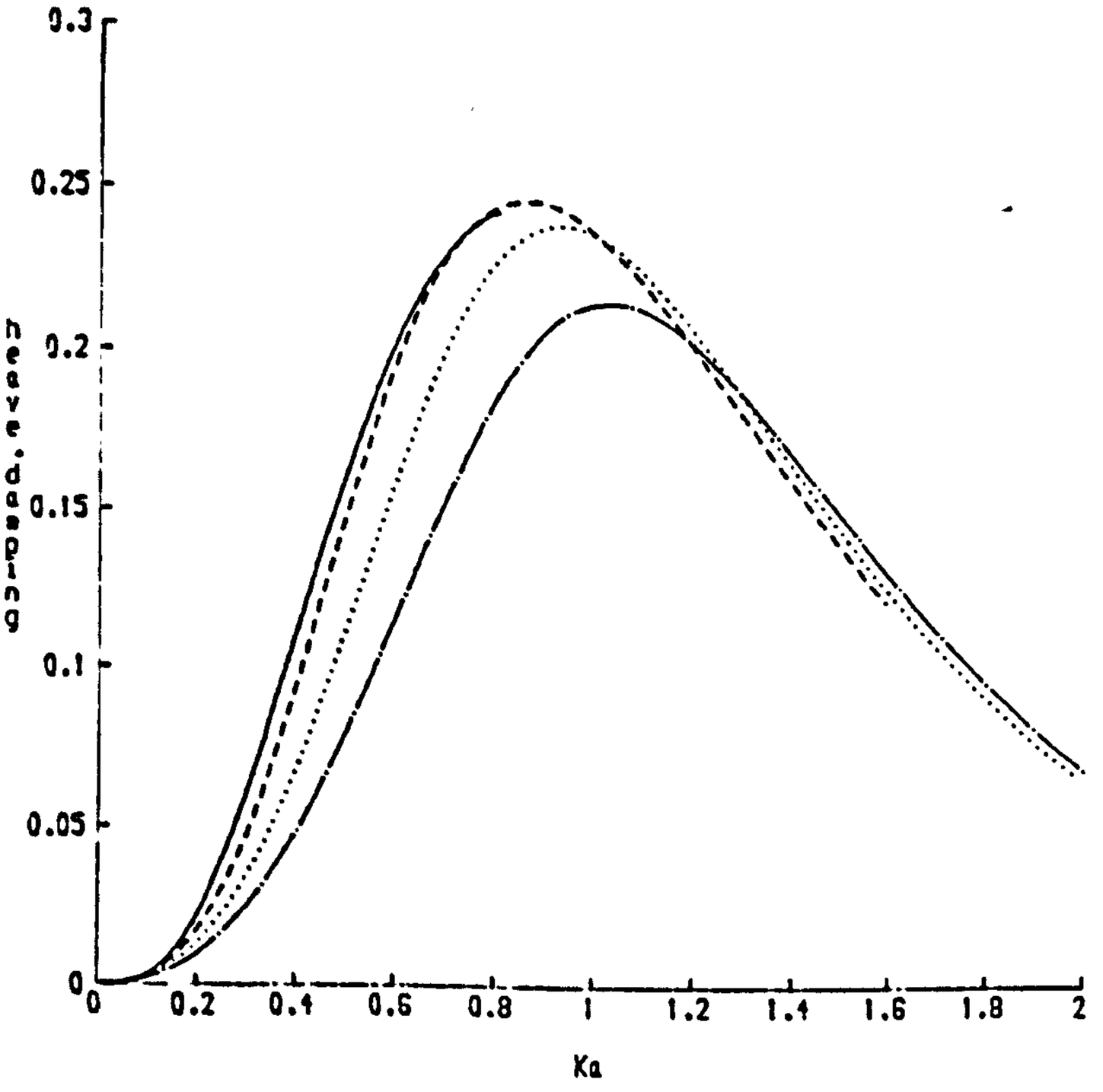

Figure 5.4.4. ν (heave) plotted against Ka for a submerged sphere (f/a=1.5) in different depths of water. ——— a/h=0.1; – – – a/h=0.2; ····· a/h=0.3; –·–·– a/h=0.39.

to radius ratio is the same, namely 3/2. The different curves thus correspond to radius to depth ratios in the range $0 \leq a/h < 0.4$. The case $a/h = 0.4$ is the extreme case of a sphere just touching the sea bed and the problems associated with this value are discussed with reference to submerged cylinders in §4.4.

The multipole method is a particularly efficient method for solving the radiation problem for a sphere in finite depth provided that Kh is small enough. (Results are difficult to obtain if Kh is greater than about 8.) However in the region $Kh < 8$ the convergence of the method is excellent and using a truncation size of 1 gives accuracy within 2%. All the results shown in this section were calculated using a truncation size of 4.

The results for a sphere with a radius to depth ratio of 0.1 are very close to those shown in Srokosz (1979) for the infinite depth case and in fact unless the sphere is very close to the bottom the effects of finite depth are quite small.

Figures (5.4.1) and (5.4.2) show the added mass coefficients for sway and heave respectively. It can be seen that the nearer the sphere is to the bottom the greater its added mass. The curves shown in these two figures can all be considered as deviations from $\frac{1}{2}$, the added mass of a sphere which is infinitely submerged in infinitely deep water.

Figures (5.4.3) and (5.4.4) show that the effect of finite depth is to increase the damping coefficient for sway motion and lower that for heave motion, which is precisely the same as in the case of the submerged cylinder, though the heave damping coefficient still remains the larger of the two. Note that, unlike the two-dimensional problem of the submerged cylinder, the sphere in deep water does not exhibit the property that the added mass and damping coefficients in sway are the same as those in heave.

CHAPTER 6

The sloshing of fluid in a half-full sphere

6.1 Introduction

In chapters 4 and 5 the method of multipoles has been used to solve problems in which one or more submerged bodies have been present together with a free surface. Problems in which bodies lie in the free surface can sometimes be solved more easily by representing the potential ϕ as a sum of a wave source and a linear combination of wave-free potentials. This method was pioneered by Ursell (1949) who solved the problem of the heaving motion of a half-immersed circular cylinder. The problem of the floating hemisphere making periodic heaving oscillations was solved first by Havelock (1955) using this method and then a greatly improved solution was given by Hulme (1982) who also solved the problem of surge.

Here we consider the problem of fluid motion *inside* a hemisphere for which a very similar method can be used. As the fluid domain is finite we do not require a wave source and instead of wave-free potentials, potentials which are valid outside the sphere and radiate no waves to infinity, we require harmonic potentials which are bounded inside the sphere, and which satisfy the free surface boundary condition.

All motion is assumed to be time harmonic with angular frequency ω. This leads to a condition which ω must satisfy in order for there to be a solution. We call these allowable values of ω, suitably non-dimensionalised, the normal modes of oscillation, or sloshing frequencies, of the body.

The problem is formulated and solved in §6.2 and then the limiting case of small waves is considered in §6.3. Results are then given in §6.4.

A solution to the *exterior* problem of the forced motion of a surface-piercing body can be obtained by solving a Fredholm integral equation of the second kind for the unknown velocity potential on the body. Unfortunately this method breaks down for values of the forcing frequency at which the *interior* problem, with the velocity potential vanishing on the body boundary, has a non-trivial solution (see Mei (1983) §7.8.2). The same method as was used to calculate the sloshing frequencies can be used to calculate these irregular frequencies. This is done and results are shown in §6.5.

6.2 Formulation and Solution

Spherical polar coordinates (r,θ,ψ) will be used with θ measured from the downward vertical, together with cylindrical polar coordinates (x,ψ,y), with y increasing with depth and ψ as before. We will adopt the convention that n,m,M refer to integers, whilst μ,ν are used to represent real numbers.

The motion can be represented by a velocity potential $\Phi(x,\psi,y,t)$ which is harmonic in the fluid region, R ($y > 0$ $r < a$). As we have done in previous chapters we remove the time dependence by writing

$$\Phi(x,\psi,y,t) = \mathrm{Re}[\phi(x,\psi,y)e^{i\omega t}]. \qquad (6.2.1)$$

Then ϕ is harmonic in R and satisfies the free surface boundary condition

$$K\phi + \frac{\partial\phi}{\partial y} = 0 \qquad \text{on} \quad y = 0, \qquad (6.2.2)$$

together with

$$\frac{\partial \phi}{\partial r} = 0 \qquad \text{on} \quad r = a. \tag{6.2.3}$$

The first step in the method of solution is to construct a function which is equal to ϕ in the fluid region but which is harmonic in the whole sphere $r < a$. To do this we will use an argument similar to that given in Ursell (1968) p825 where he does the same for wave functions (functions which satisfy the Helmholtz equation) in a semicircle.

The function Ψ, defined in R by

$$\Psi = K\phi + \frac{\partial \phi}{\partial y}, \tag{6.2.4}$$

is harmonic in the fluid region and is zero on $y = 0$. If Green's theorem is applied to this function together with $G(x,y;\xi,\eta) \equiv [(x-\xi)^2 + (y-\eta)^2]^{-1/2} - [(x-\xi)^2 + (y+\eta)^2]^{-1/2}$ we obtain

$$4\pi \Psi(\xi,\psi,\eta) = \int_S [\Psi(x,\psi,y) \frac{\partial}{\partial n} G(x,y;\xi,\eta) - G(x,y;\xi,\eta) \frac{\partial}{\partial n} \Psi(x,\psi,y)] \, ds(x,y) \tag{6.2.5}$$

where S is the curved surface of the hemisphere. Here the facts that $\nabla^2 G = 4\pi\delta(x-\xi)\delta(y-\eta)$ in R and that $G = 0$ on $y = 0$ have both been used.

It is clear from equation (6.2.5) that if the point (ξ,η) lies inside the sphere $r = a$ then $\Psi(\xi,\psi,\eta)$ is not singular and harmonic in the whole sphere $r < a$. It also coincides with the function Ψ defined in R by equation (6.2.4) and so equation (6.2.5) provides the continuation of Ψ into the whole sphere. Since $G(x,y;\xi,\eta) = - G(x,y;\xi,-\eta)$ it can be seen that the function Ψ defined in R by equation (6.2.4) can be continued into the whole sphere by means of the construction

$$\Psi(x,\psi,-y) = -\Psi(x,\psi,y). \tag{6.2.6}$$

Solving equation (6.2.4) shows that in R

$$\phi(x,\psi,y) = e^{K(Y-y)}\ \phi(x,\psi,Y) + e^{-Ky}\int_Y^y e^{Ku}\ \Psi(x,\psi,u)\ du \tag{6.2.7}$$

where $Y > 0$ is some fixed value of y in R. But the right hand side of equation (6.2.7) defines a harmonic function in $r \leq a$ which coincides with $\phi(x,\psi,y)$ on $y = 0$, $|r| < a$, so that equation (6.2.7) provides the continuation of $\phi(x,\psi,y)$ into the sphere $r \leq a$.

It follows that ϕ has an expansion in spherical polar coordinates of the form

$$\phi(r,\theta,\psi) = \sum_{n=0}^{\infty} a_n\ P_n^M(\cos\ \theta)\ r^n\ \cos M\psi\ . \tag{6.2.8}$$

Here without loss of generality we have restricted the ψ dependence to be just $\cos M\psi$. Equation (6.2.8) can be rewritten

$$\phi = \sum_{n=0}^{\infty} [a_{2n}\ P_{2n}^M(\cos\ \theta)\ r^{2n} + a_{2n+1}\ P_{2n+1}^M(\cos\ \theta)\ r^{2n+1}]\ \cos M\psi. \tag{6.2.9}$$

Now ϕ must satisfy (6.2.2), which in polar coordinates can be written

$$K\phi \mp \frac{1}{r}\frac{\partial\phi}{\partial\theta} = 0 \qquad \text{on} \quad \theta = \pm\frac{\pi}{2}\ .$$

Therefore

$$\sum_{n=0}^{\infty} [\, K\, a_{2n}\, P_{2n}^{M}(\cos\theta)\, r^{2n} + K\, a_{2n+1}\, P_{2n+1}^{M}(\cos\theta)\, r^{2n+1}$$

$$+ \sin\theta\, (a_{2n}\, P_{2n}^{M\prime}(\cos\theta)\, r^{2n-1} + a_{2n+1}\, P_{2n+1}^{M\prime}(\cos\theta)\, r^{2n})]$$

$$= 0 \qquad \text{on} \quad \theta = \frac{\pi}{2}. \qquad (6.2.10)$$

We now use the following identity (Abramowitz and Stegun (8.5.4)):

$$P_{\nu}^{\mu\prime}(0) = (\nu + \mu)\, P_{\nu-1}^{\mu}(0) \qquad \forall\ \nu,\ \mu.$$

This gives

$$\sum_{n=0}^{\infty} [K\, a_{2n}\, P_{2n}^{M}(0)\, r^{2n} + K\, a_{2n+1}\, P_{2n+1}^{M}(0)\, r^{2n+1}$$

$$+ (2n+M)\, a_{2n}\, P_{2n-1}^{M}(0)\, r^{2n-1} + (2n+2M+1)\, a_{2n+1}\, P_{2n}^{M}(0)\, r^{2n}] = 0. \qquad (6.2.11)$$

If the order M is assumed to be even, we can write $M = 2m$, $(m \geq 0)$. We use the fact that

$$P_{2n+1}^{2m}(0) = 0 \qquad \forall\ n \geq 0$$

and

$$P_{n}^{M}(x) \equiv 0 \qquad \text{if } M > n \geq 0.$$

Equation (6.2.11) can then be rewritten as

$$\sum_{n=m}^{\infty} [K\, a_{2n}\, P_{2n}^{2m}(0)\, r^{2n} + (2n+2m+1)\, a_{2n+1} P_{2n}^{2m}(0)\, r^{2n}]$$

$$+ 2m\, a_{o}\, P_{-1}^{2m}(0)\, r^{-1} = 0. \qquad (6.2.12)$$

Since $P_{-1}^{2m}(0) = P_0^{2m}(0)$ (Abramowitz and Stegun (8.2.1)), the last term is zero and we have

$$\sum_{n=m}^{\infty} [K\, a_{2n}\, P_{2n}^{2m}(0)\, r^{2n} + (2n+2m+1)\, a_{2n+1} P_{2n}^{2m}(0)\, r^{2n}] = 0.$$

This implies that

$$K\, a_{2n} = -(2n+2m+1)\, a_{2n+1}. \qquad (6.2.13)$$

If we define $d_n = a_{2n+1}/K$, *then*

$$\phi = \sum_{n=m}^{\infty} d_n\, [K\, P_{2n+1}^{2m}(\cos\theta)\, r^{2n+1} - (2n+2m+1)\, P_{2n}^{2m}(\cos\theta)\, r^{2n}] \cos 2m\psi. \qquad (6.2.14)$$

The term in square brackets is the internal equivalent of a wave-free potential (see Hulme (1982)).

Using equation (6.2.3), the boundary condition on the hemisphere, gives

$$\sum_{n=m}^{\infty} [Ka\, (2n+1)\, P_{2n+1}^{2m}(x) - 2n\, (2n+2m+1)\, P_{2n}^{2m}(x)]\, d_n = 0 \quad 0 \le x \le 1. \qquad (6.2.15)$$

There are two cases which must be considered separately :

(i) $m = 0$.

Define $p_n = (2n+1)\, d_n$ so that (6.2.15) becomes

$$\sum_{n=0}^{\infty} [Ka\, P_{2n+1}(x) - 2n\, P_{2n}(x)]\, p_n = 0. \qquad (6.2.16)$$

For convenience the parameter λ $(= 1/Ka)$ is introduced and then the

operator $\int_0^1 \ldots P_{2s}(x)\, dx$ $(s = 0,1,2,\ldots)$ is applied to equation (6.2.16). We will employ the notation (see Hulme (1982))

$$I(\nu,\sigma;M) = \int_0^1 P_\nu^M(x)\, P_\sigma^M(x)\, dx \qquad (6.2.17)$$

for which Hulme gives an explicit formula. This leads to the following eigenvalue problem:

$$\lambda\, p_s\, \frac{2s}{4s+1} = \sum_{n=0}^{\infty} p_n\, I(2n+1,2s;0) \qquad s\geq 1$$

and (6.2.18)

$$0 = \sum_{n=0}^{\infty} p_n\, I(2n+1,0;0).$$

The $s = 0$ equation can be solved for d_0, and this value then substituted back into the other equations. Using the fact that $I(1,0;0) = \frac{1}{2}$ we get

$$d_0 = -2 \sum_{n=1}^{\infty} d_n\, I(2n+1,0;0) \qquad (6.2.19)$$

and

$$\lambda\, d_s\, \frac{2s}{4s+1} = \sum_{n=1}^{\infty} d_n\, [I(2n+1,2s;0) - 2\, I(2n+1,0;0)\, I(1,2s;0)]. \qquad (6.2.20)$$

Thus the normal modes of oscillation can be found from the eigenvalues, λ, of the matrix

$$A_{ij} = \frac{4i+1}{2s}[I(2j+1,2i;0) - 2\, I(2j+1,0;0)\, I(1,2i;0)] \qquad (6.2.21)$$

where I is given by equation (6.2.17). A description of how to

calculate the eigenvalues of such a matrix is given in §6.4.

(ii) $m \geq 1$.

For this case we simply apply the operator $\int_0^1 \ldots P_{2s}^{2m}(x)\, dx$ to equation (6.2.16) and use the result

$$I(2n,2s;2m) = \delta_{n,s} \frac{1}{4s+1} \frac{(2s+2m)!}{(2s-2m)!} .$$

This gives

$$\sum_{n=m}^{\infty} d_n \left[Ka\ (2n+1)\ I(2n+1,2s,2m)\right] = \frac{2s\ (2s+2m+1)!}{(4s+1)\ (2s-2m)!}\, d_s \quad \forall\ s \geq m. \tag{6.2.22}$$

In order to make the summation run from 1 rather than m we put

$$n = m+j-1 \ ;\ s = m+i-1 \ .$$

Now

$$\sum_{j=1}^{\infty} d_{m+j-1}\ (2m+2j-1)\ I(2m+2j-1,2m+2i-2;2m)$$

$$= \frac{(2m+2i-2)\ (2i+4m-1)!}{Ka\ (4m+4i-3)\ (2i-2)!}\, d_{m+i-1} \qquad \forall\ i \geq 1. \tag{6.2.23}$$

If we substitute back for M, and again write $\lambda = 1/Ka$ we can calculate the normal modes of the system from the eigenvalues, λ, of the matrix

$$A_{i,j} = \frac{(4i+2M-3)\ (2i-2)!\ (2j+M-1)}{(2i+M-2)\ (2i+2M-1)!}\, I(2j+M-1,2i+M-2,M) \ . \tag{6.2.24}$$

Next we must consider the case when M is odd. To this end we write $M = 2m+1$, $(m \geq 0)$. Now we have (Abramowitz and Stegun (8.6.1))

$$P_{2n}^{2m+1}(0) = 0 \qquad \forall\ n \geq 0$$

and so, from equation (6.2.11),

$$\sum_{n=0}^{\infty} [K\, a_{2n+1}\, P_{2n+1}^{2m+1}(0)\, r^{2n+1} + (2n+2m+1)\, a_{2n}\, P_{2n-1}^{2m+1}(0)\, r^{2n-1}] = 0. \tag{6.2.25}$$

In order to make the summation run from 1 rather than 0 we use the fact that (Abramowitz and Stegun (8.2.1))

$$P_{-1}^{2m+1}(0) = P_{0}^{2m-1}(0) = 0.$$

Therefore

$$\sum_{n=1}^{\infty} [K\, a_{2n-1}\, P_{2n-1}^{2m+1}(0)\, r^{2n-1} + (2n+2m+1)\, a_{2n}\, P_{2n-1}^{2m+1}(0)\, r^{2n-1}] = 0 \tag{6.2.26}$$

which implies that

$$K\, a_{2n-1} = -(2n+2m+1)\, a_{2n} \qquad \forall\ n \geq 1. \tag{6.2.27}$$

The velocity potential ϕ can now be written as

$$\phi = \sum_{n=m+1}^{\infty} d_n\, [K\, r^{2n}\, P_{2n}^{2m+1}(\cos\theta) - (2n+2m+1)\, r^{2n-1}\, P_{2n-1}^{2m+1}(\cos\theta)] \cos(2m+1)\psi \tag{6.2.28}$$

and the boundary condition (6.2.3) then gives

$$\sum_{n=m+1}^{\infty} d_n\, [Ka\ 2n\, P_{2n}^{2m+1}(x) - (2n-1)\,(2n+2m+1)\, P_{2n-1}^{2m+1}(x)] = 0 \qquad 0 \leq x \leq 1. \tag{6.2.29}$$

Applying the operator $\int_0^1 \ldots P_{2s-1}^{2m+1}(x)\,dx$ gives

$$\sum_{n=m+1}^{\infty} d_n \; Ka\; 2n\; I(2n,2s-1;2m+1) = \frac{(2s-1)\;(2s+2m+1)!}{(4s-1)\;(2s-2m-2)!}\, d_s \qquad \forall\ s \geq m+1. \tag{6.2.30}$$

In the same way as for the case of even order the summation variables will be changed so as to make the summation run from 1. This is done by putting

$$n = m+j \;;\; s = m+i.$$

Then

$$\sum_{j=1}^{\infty} d_{m+j}\; 2(m+j)\; I(2m+2j,2m+2i-1;2m+1) = \frac{(2m+2i-1)\;(2i+4m+1)!}{(4m+4i-1)\;(2i-2)!}\, d_{m+1}. \qquad \forall\ i \geq 1 \tag{6.2.31}$$

Substituting back for M and again *writing* $\lambda = 1/Ka$ we see that the normal modes are related to the eigenvalues, λ, of the matrix

$$A_{ij} = \frac{(4i+2M-3)\;(2i-2)!\;(2j+M-1)}{(2i+M-2)\;(2i+2M-1)!}\; I(2j+M-1,2i+M-2,M) \tag{6.2.32}$$

which is exactly the same as for the case of the even modes.

6.3 Short Wave Asymptotics

In this section we simply note the results of Davis (1975).

If, instead of a hemisphere, we considered a vertical circular cylinder, then simple separation of variables would give the normal modes, $K_n a$, as the zeros of the function $J_m'(Ka)$, where J_m $m = 1,2,\ldots$ are Bessel functions and m represents the azimuthal mode of oscillation.

When Ka is very large the disturbance is concentrated very near the free surface and the effect of the spherical nature of the bottom is small. We would therefore expect the first term in an asymptotic expansion for $K_n a$ to be j'_{mn}, where j'_{mn} is the nth zero of J'_m.

By constructing a generalised Green's function Davis obtains an integral equation which yields an iterative solution for ϕ as $n \longrightarrow \infty$. Using this solution the normal modes can be expressed in terms of an integral over the surface of the hemisphere and a detailed asymptotic analysis leads to the result

$$K_n a \sim j'_{mn} - \frac{1}{4j'_{mn}} - \frac{1}{3\pi j'^{2}_{mn}} - \frac{1}{2j'^{3}_{mn}}\left[m^2 + \frac{661}{768} + \frac{4}{3\pi^2}\right] \quad \text{as} \quad n \to \infty \ . \tag{6.3.1}$$

This result can be used as a check on the numerical results obtained from eigenvalues of the matrices given in equations (6.2.21) and (6.2.24).

6.4 Results

The sloshing frequencies, $K_n a$, of the hemisphere are related to the eigenvalues, λ_n, of an *infinite matrix by* $K_n a = 1/\lambda_n$. If the motion is axisymmetric, i.e. $m = 0$, then this matrix, A, is given by equation (6.2.21) otherwise it is given by equation (6.2.24).

In order to evaluate the eigenvalues of an infinite matrix a truncation procedure similar to that described in §3.3 is used. The infinite matrix A is truncated to an $N \times N$ matrix and the eigenvalues of this finite matrix are calculated. If by increasing N the eigenvalues converge then the values to which they converge will be assumed to be the eigenvalues of the infinite system. As there is no dissipation or energy input into the physical system under consideration the values obtained for ω must be real. This in turn implies that the

eigenvalues of A must be real. However no such statement can be made about any finite truncation of A. In fact all truncations except a 1×1 system do produce some complex conjugate eigenvalues which in the context of this problem are meaningless and thus will be ignored.

An $N \times N$ approximation to A will thus produce an approximation to the first M sloshing frequencies where $M \leq N$. In practice M is much less than N, e.g. if $N = 20$, $M = 4$.

As will be seen, the asymptotic formula for large n given in §6.3 is very accurate for $n > 3$ and not too bad for $n = 2$ and 3. The most important result that is required however, in terms of practical application, is the dominant mode which is given by $K_1 a$. The formulation described above is particularly well suited to this task with a truncation size of 20 requiring very little computer time to solve and giving $K_1 a$ to four significant figures.

Table (6.4.1) shows how the results vary with truncation size for one particular value of the azimuthal mode, in this case $m = 3$. The table shows values of $1/\lambda_n$ for all the real eigenvalues of the $N \times N$ matrix with $N = 1,5,10,20,40$ and 60 together with the value for $K_n a$ given by the asymptotic formula, equation (6.3.1). The convergence of the eigenvalues is clear and a 40×40 truncation gives the first seven sloshing frequencies to five significant figures.

	Asymp.	N = 1	N = 5	N = 10	N = 20	N = 40	N = 60
n=1	4.06827	2.74286	3.98407	3.99302	3.99398	3.99414	3.99415
2	7.97269			7.96382	7.97245	7.97275	7.97279
3	11.31964				11.31934	11.31986	11.31993
4	14.56660				14.56526	14.56663	14.56673
5	17.77347					17.77336	17.77351
6	20.95977					20.95956	20.95974
7	24.13401					24.13370	24.13393
8	27.30052					27.30013	27.30041
9	30.46177					30.47849	30.46134
10	33.61929					31.97674	33.62171
11	36.77404						36.95168
12	38.17995						38.17995

Table 6.4.1

In table (6.4.2) the truncation size N is fixed at 40 and results are shown for the first three azimuthal modes: $m = 0,1$ and 2. The accuracy of the results is indicated by the number of non-italicised figures. Figures in italics are probably not correct. The asymptotic values associated with the $m = 0$ column are calculated using equation (6.3.1) but with n replaced with $n+1$. This is because the first zero of $J_0'(x)$ is at $x = 0$. This solution corresponds to the vertical rigid body motion of fluid in a vertical cylinder without a bottom which clearly is not applicable to the problem being considered here since it contradicts the law of mass conservation.

	m = 0	Asymp.	m = 1	Asymp.	m = 2	Asymp.
n=1	3.74516	3.75038	1.56015	1.51422	2.81968	2.87334
2	6.97632	6.97635	5.27552	5.27423	6.65937	6.65821
3	10.14740	10.14740	8.50438	8.50397	9.94121	9.94080
4	13.30404	13.30412	11.68334	11.68325	13.14977	13.14968
5	16.45479	16.45495	14.84592	14.84598	16.33118	16.33126
6	19.60254	19.60277	18.00098	18.00115	19.49930	19.44949
7	22.74854	22.74885	21.15195	21.15222	22.65985	22.66013
8	25.89345	25.89383	24.30044	24.30079	25.81568	25.81605
9	29.03850	29.03808	27.44735	27.44776	28.96911	28.96882
10	31.44005	32.18180	30.46419	30.59361	31.42665	32.11937

Table 6.4.2

6.5 Irregular Frequencies

A solution to the (exterior) problem of a hemisphere lying in the free surface making periodic forced oscillations can be obtained by solving a Fredholm integral equation of the second kind for the unknown velocity potential on the body. This method has the drawback that it fails at certain values of the forcing frequency corresponding to the eigenvalues of the interior problem with the condition $\phi = 0$ on the boundary of the hemisphere. When solving the exterior problem using this integral equation method it is useful to know these 'irregular frequencies' so that they can be avoided in the numerical computation.

Equation (6.2.14) and the boundary condition $\phi = 0$ on $r = a$ give

$$\sum_{n=m}^{\infty} \left[Ka\, P^{2m}_{2n+1}(x) - (2n+2m+1)\, P^{2m}_{2n}(x) \right] d_n = 0 \qquad 0 \le x \le 1 \qquad (6.5.1)$$

for the even modes and for the odd modes equation (6.2.28) gives

$$\sum_{n=m+1}^{\infty} \left[Ka\, P_{2n}^{2m+1}(x) - (2n+2m+1)\, P_{2n-1}^{2m+1}(x) \right] d_n = 0 \qquad 0 \le x \le 1. \qquad (6.5.2)$$

If we proceed exactly as in §6.2 we find we no longer have to treat the $m = 0$ case separately and it is straightforward to show that the irregular frequencies are given by $1/\lambda_n$ where λ_n are the eigenvalues of

$$A_{ij} = \frac{4i+2M-3}{(2i+2M-1)!}\,(2i-2)!\; I(2j+M-1,2i+M-2;M) \qquad M=0,1,2,\ldots \quad . \qquad (6.5.3)$$

The argument presented in §6.3 for the first term in the asymptotic formula for $K_n a$ as $n \longrightarrow \infty$ can again be used here and it is clear that

$$K_n a \sim j_{m,n} \qquad \text{as} \quad n \longrightarrow \infty \qquad (6.5.4)$$

where $j_{m,n}$ is the nth zero of J_m.

Table (6.5.1) shows results based on a 40×40 truncation of A as given by equation (6.5.3) for the first three azimuthal modes $m = 0,1$ and 2. Again the accuracy of the results is indicated by the number of non-italicised figures. The convergence of the eigenvalues in this case is slightly faster than in the case of the sloshing frequencies.

	m = 0	Asymp.	m = 1	Asymp.	m = 2	Asymp.
n=1	2.55732	2.40483	3.91881	3.83171	5.19700	5.13562
2	5.57370	5.52008	7.05632	7.01559	8.45059	8.41724
3	8.68576	8.65373	10.20031	10.17347	11.64313	11.61984
4	11.81438	11.79153	13.34375	13.32369	14.81391	14.79595
5	14.94868	14.93092	16.48665	16.47063	17.97446	17.95982
6	18.08559	18.07106	19.62920	19.61586	21.12936	21.11700
7	21.22394	21.21164	22.77153	22.76008	24.28083	24.27011
8	24.36315	24.35247	25.91370	25.90367	27.43004	27.42057
9	27.50296	27.49348	29.05671	29.04683	30.60294	30.56920
10	30.49699	30.63461	31.44567	32.18968	31.95896	33.71652

Table 6.5.1

6.6 Conclusion

In this chapter two problems were considered. The evaluation of the normal modes of oscillation of fluid in a half-full sphere and the evaluation of the irregular frequencies which arise when the problem of the forced motion of a half-immersed sphere is solved using a Fredholm integral equation of the second kind for the unknown velocity potential on the body. These problems are closely connected, see §6.1.

By expanding the velocity potential in spherical harmonics we were able to construct functions that are harmonic inside the hemisphere and satisfy the free surface boundary condition. The application of the body boundary condition, $\frac{\partial \phi}{\partial r} = 0$ on $r = a$ in the case of the interior problem and $\phi = 0$ on $r = a$ in the case of the irregular frequencies, then resulted in the need to calculate the eigenvalues of a doubly

infinite matrix which was done by truncation. This method is particularly efficient when calculating the largest eigenvalues (i.e. the lowest frequencies) which correspond to the dominant modes of oscillation. The main drawback of the method is that it is only applicable to simple geometries although, as the work in this chapter shows, there is no need for these geometries to be two-dimensional.

REFERENCES

ABRAMOWITZ, M. & STEGUN, I.A. 1965 Handbook of mathematical functions. *Dover Publications inc. New York.*

ALKER, G. 1974 High frequency waves trapped in a two-dimensional canal. *Quart. J. Mech. Appl. Math.* 27, 347-363.

BAI, K.J. 1977 The added mass of two-dimensional cylinders heaving in water of finte depth. *J. Fluid Mech.* 81, 85-105.

BLACK, J.L., MEI, C.C. & BRAY, M.C.G. 1971 Radiation and scattering of water waves by rigid bodies. *J. Fluid Mech.* 46, 151-164.

BUDIANSKY, B. 1960 Sloshing of liquids in circular canals and spherical tanks. *J. Aerospace Sci.* 27, 161-173.

CARTER, D.J.T., CHALLONER, P.G., EWING, J.A., PITT, E.G., SROKOSZ, M.A. & TUCKER, M.J. 1986 Estimating wave climate parameters for engineering applications. *Offshore Technology Report OTH 86 228, Dept. of Energy.*

CRAGGS, J.W. & DUCK, P.W. 1978 A power series method for treating mixed boundary value problems. *J. Inst. Math. Applic.* 21, 1-12.

DAVIES, A.G. 1982 The reflection of wave energy by undulations on the sea bed. *Dynamics of Atmospheres and Oceans* 6, 207-232.

DAVIS, A.M.J. 1974 Short surface waves in a canal; dependence of frequency on the curvatures and their derivatives. *Quart. J. Mech. Appl. Math.* 27, 523-535.

DAVIS, A.M.J. 1975 Small oscillations in a hemispherical lake. *Quart. J. Mech. Appl. Math.* 28, 157-179.

DEAN, R.G. & URSELL, F. 1959 Interaction of a fixed semiimmersed circular cylinder with a train of surface waves. *Technical Report No. 37, Hydrodynamics Lab. MIT*, 91 pages.

DEAN, W.R. 1945 On the reflexion of surface waves by a flat plate floating vertically. *Proc. Camb. Phil. Soc.* 41, 231-238.

DEAN, W.R. 1948 On the reflexion of surface waves by a submerged circular cylinder. *Proc. Camb. Phil. Soc.* 44, 483-491

EVANS, D.V. 1976 A theory for wave-power absorption by oscillating bodies. *J. Fluid Mech.* 77, 1-25.

EVANS, D.V., JEFFREY, D.C., SALTER, S.H. & TAYLOR, J.R.M. 1979 Submerged cylinder wave energy device : theory and experiment. *Applied Ocean Research* 1 (1), 3-12.

EVANS, D.V. & LINTON, C.M. Active devices for the reduction of wave intensity. *Applied Ocean Research* (to appear).

FOX, D.W. & KUTTLER, J.R. 1983 Sloshing frequencies. *J. Appl. Math. Phys. (ZAMP)* 34, 668-696.

GUEVEL, P. ,LANDEL, E. ,BOUCHET, R. & MANZONE, J.M. 1985 Le phénomène d'un mur d'eau oscillant et son application pour protéger un site côtier soumis à l'action de la houle. *Bulletin de l'Association Technique Maritime et Aéronautique.* 85, 229-245.

HASKIND, M.D. 1959 The exciting forces and wetting of ships in waves. (In Russian). *Izv. Akad. Nauk SSSR, Otd. Tekh. Nauk* 7, 65-79. English translation available as *David Taylor Model Basin Translation No. 307.*

HAVELOCK, T.H. 1929 Forced surface waves on water. *Phil. Mag.* 8, 1929, 569-577.

HAVELOCK, T.H. 1955 Waves due to a floating sphere making periodic heaving oscillations. *Proc. Roy. Soc. Lond.* A 231, 1-7.

HULME, A. 1982 The wave forces on a floating hemisphere undergoing forced periodic oscillations. *J. Fluid Mech.* 121, 443-463.

HULME, A. 1985 The heave added-mass and damping coefficients of a submerged torus. *J. Fluid Mech.* 155, 511-530.

JOHN, F. 1950 On the motion of floating bodies II. *Comm. Pure Appl. Math.* 3, 45-101.

KIRBY, J.T. & DALRYMPLE, R.A. 1983 Propagation of obliquely incident water waves over a trench. *J. Fluid Mech.* 133, 47-63.

KREISEL, G. 1949 Surface waves. *Quart. Appl. Math.* 7, 21-44.

LAMB, H. 1932 Hydrodynamics (6th ed.). *Cambridge University Press.*

LEACH, P.A. ,McDOUGAL, W.G. & SOLLITT, C.K. 1985 Hinged floating breakwater. *J. Waterway, Port, Coastal and Ocean Eng.* 111, No. 5, 895-909.

LEVINE, H. 1965 Scattering of surface waves by a submerged circular cylinder. *J. Math. Physics* 6, No. 8, 1231-1243.

McIVER, M. 1985 The interaction of water waves with submerged bodies. *Ph.D. Thesis*, University of Bristol.

McIVER, P. & EVANS, D.V. 1984 The occurrence of negative added mass in free surface problems involving submerged bodies. *J. Eng. Math.* 18, 7-22.

McIVER, P. 1988 Sloshing frequencies for cylindrical and spherical containers filled to an arbitrary depth. *Private communication.*

MEI, C.C. & BLACK, J.L. 1969 Scattering of surface waves by rectangular obstacles in waters of finite depth. *J. Fluid Mech.* 38, 449-511.

MEI, C.C. 1978 Numerical methods in water wave diffraction and radiation. *Annual Review of Fluid Mechanics* 10, 393-416.

MEI, C.C. 1983 The applied dynamics of ocean surface waves. *Wiley-Interscience, New York.*

MEI, C.C., TETSU HARA & MAMOUN NACIRI 1988 Note on Bragg scattering of water waves by parallel bars on the sea bed. *J. Fluid Mech.* 186, 147-162.

MOISEEV, N.N. 1964 Introduction to the theory of oscillations of liquid-containing bodies. *Advances in Appl. Mech.* 8, 233-289.

MOISEEV, N.N. & PETROV, A.A. 1965 The calculation of free oscillations of a liquid in a motionless container. *Advances in Appl. Mech.* 9, 91-154.

MORISON, J.R., O'BRIEN, M.P., JOHNSON, J.W. & SCHAAF, S.A. 1950 The force exerted by surface waves on piles. *Petroleum Transactions A.I.M.E.* 189, 149-154.

NAFTZGER, R.A. & CHAKRABARTI, S.K. 1979 Scattering of waves by two-dimensional circular obstacles in finite water depths. *J. Ship Res.* 21, No. 1, 32-42.

NEWMAN, J.N. 1965 Propagation of water waves past long two-dimensional obstacles. *J. Fluid Mech.* 23, 23-29.

NEWMAN, J.N. 1975 Interaction of waves with two-dimensional obstacles: A relation between the radiation and scattering problems. *J. Fluid Mech.* 71, 273-282.

NEWMAN, J.N. 1976 The interaction of stationary vessels with regular waves. *Proc. 11th Symp. Naval Hydrodyn. ONR, London*, pp 491-501.

NEWMAN, J.N. 1977 Marine Hydrodynamics. *MIT Press.*

OGILVIE, T.F. 1963 First and second order forces on a cylinder submerged under a free surface. *J. Fluid Mech.* 16, 451-472

PEREGRINE, D.H. 1972 Equations for water waves and the approximations behind them. *Waves on beaches, Academic Press,* pp 95-121.

PIERSON, W.J.Jr. & MOSKOWITZ, L. 1964 A proposed spectral form for fully developed wind seas based on the similarity theory of S.A. Kitaigoradskii. *J. Geophys. Research* 69 (24), 5181-5190.

SCHNUTE, J.T. 1971 The scattering of surface waves by two submerged cylinders. *Proc. Camb. Phil. Soc.* 69, 201-215.

SHAW, R. 1982 Wave energy, a design challenge. *Ellis Horwood Ltd.*

SROKOSZ, M.A. 1979 The submerged sphere as an absorber of wave power. *J. Fluid Mech.* 95, 717-741

TAKANO, K. 1960 Effects d'un obstacle parallélépipédique sur la propagation de la houle. *Houiile blanche,* 15, 247.

THOMAS, J.R. 1981 The absorption of wave energy by a three-dimensional submerged duct. *J. Fluid Mech.* 104, 189-215.

THORNE, R.C. 1953 Multipole expansions in the theory of surface waves. *Proc. Camb. Phil. Soc.* 49, 709-716.

TUCK, E.O. 1976 Some classical water-wave problems in varying depth. *IUTAM Symposium on Waves on Water of Varying Depth, Canberra.*

URSELL, F. 1947 The effect of a fixed vertical barrier on surface waves in deep water. *Proc. Camb. Phil. Soc.* 43, 374-382.

URSELL, F. 1949 On the heaving motion of a circular cylinder on the surface of a fluid. *Quart. J. Mech. Appl. Math.* 2, 218-231.

URSELL, F. 1950 Surface waves on deep water in the presence of a submerged circular cylinder. I. *Proc. Camb. Phil. Soc.* 46, 141-152.

URSELL, F. 1968 The expansion of water-wave potentials at great distances. *Proc. Camb. Phil. Soc.* 64, 811-826.

WANG, S. & WAHAB, R. 1971 Heaving oscillations of twin cylinders in a free surface. *J. Ship Res.* 15, 33-48.

WANG, S. 1981 Wave radiation due to oscillation of two parallel spaced cylinders. *Ocean Eng.* 8, No. 6, 559-621.

WHITHAM, G.B. 1974 Linear and non linear waves. *Wiley Interscience, New York.*

YU, Y.S. & URSELL, F. 1961 Surface waves generated by an oscillating circular cylinder on water of finite depth : Theory and Experiment. *J. Fluid Mech.* 11, 529-551.